On the Construction of Control Lyapunov-Barrier Function

Romdlony, Muhammad Zakiyullah; Jayawardhana, Bayu

34^{th} Benelux Meeting

on

Systems and Control

March 24 – 26, 2015

Lommel, Belgium

Book of Abstracts

The 34^{th} Benelux meeting on Systems and Control is sponsored by

and supported by the

Belgian Programme on Interuniversity Poles of Attraction DYSCO
(Dynamic Systems, Control and Optimization), initiated by the Belgian State,
Prime Minister's Office for Science.

Oscar Mauricio Agudelo Manozca, Amélie Chevalier, Bart De Moor, Geert Gins, Clara Ionescu, Filip Logist, Ivan Markovsky, Wim Michiels, Goele Pipeleers, Wannes Van Loock (eds.)

Book of Abstracts 34^{th} Benelux Meeting on Systems and Control

KU Leuven - Departement Werktuigkunde
Celestijnenlaan 300B, B-3001 Heverlee (Belgium)

D/2015/5769/1
ISBN 9789073802926

Programmatic Table of Contents

Tuesday, March 24, 2015

Plenary: P0 **Les Arcades**
Welcome and Opening
Chair: Wim Michiels **11.25–11.30**

Plenary: P1 **Les Arcades**
PID: Past, present and perspectives
Tore Hägglund
Chair: Clara Ionescu **11.30–12.30**

TuP01 **Les Arcades**
Optimization I
Chair: Julien Hendrickx **14.00–16.05**

TuP01-1 **14.00–14.25**

Adrien B. Taylor Université catholique de Louvain
François Glineur Université catholique de Louvain
Julien M. Hendrickx Université catholique de Louvain

TuP01-2 **14.25–14.50**

Wen Huang Université catholique de Louvain
Kyle A. Gallivan FSU Florida
Xiangxiong Zhang Purdue University

TuP01-3 **14.50–15.15**

Maguy Trefois Université catholique de Louvain
Jean-Charles Delvenne Université catholique de Louvain
Paul Van Dooren Université catholique de Louvain

TuP01-4 **15.15–15.40**

Franck Iutzeler Université catholique de Louvain
Julien M. Hendrickx Université catholique de Louvain

TuP01-5 **15.40–16.05**

Bhagyashri Telsang TU Delft

TuP02 **Emanuel**
Mechanical Engineering I
Chair: Robain De Keyser **14.00–16.05**

TuP02-1 **14.00–14.25**

Muhammad Zakiyullah Romdlony Rijksuniversiteit Groningen
Bayu Jayawardhana Rijksuniversiteit Groningen

TuP02-2 **14.25–14.50**

Amélie Chevalier Ghent University
Clara M. Ionescu Ghent University
Robin De Keyser Ghent University

TuP02-3 **14.50–15.15**

Sebastian Trip Rijksuniversiteit Groningen
Mathias Bürger Robert Bosch GmbH
Claudio De Persis Rijksuniversiteit Groningen

TuP02-4 **15.15–15.40**

Luis D. Couto Université Libre de Bruxelles
Julien Schorsch Université Libre de Bruxelles
Michel Kinnaert Université Libre de Bruxelles

TuP02-5 **15.40–16.05**

Iurii Kapitaniuk Rijksuniversiteit Groningen

TuP03 **Impresario**
Identification I
Chair: Roland Tóth **14.00–16.05**

TuP03-1 **14.00–14.25**

Dieter Verbeke Vrije Universiteit Brussel
Egon Geerardeyn Vrije Universiteit Brussel
Johan Schoukens Vrije Universiteit Brussel

TuP03-2 **14.25–14.50**

M.A.H.Darwish TU Eindhoven
R.Tóth TU Eindhoven
P.M.J. Van den Hof TU Eindhoven

TuP03-3 **14.50–15.15**

Gabriel Hollander Vrije Universiteit Brussel
Philippe Dreesen Vrije Universiteit Brussel
Mariya Ishteva Vrije Universiteit Brussel
Johan Schoukens

TuP03-4 **15.15–15.40**

Harm H.M. Weerts TU Eindhoven
Paul M.J. Van den Hof TU Eindhoven
Arne G. Dankers University of Calgary

TuP03-5 **15.40–16.05**

Jean-Philippe Noël Vrije Universiteit Brussel
Johan Schoukens Vrije Universiteit Brussel
Gaetan Kerschen Université de Liège

TuP04 **Bloemen**
Model Reduction
Chair: Geert Gins **14.00–16.05**

TuP04-1 **14.00–14.25**
Model Reduction of Networked Systems 32
H.J. Jongsma Rijksuniversiteit Groningen
H.L. Trentelman Rijksuniversiteit Groningen
M.K. Camlibel Rijksuniversiteit Groningen

TuP04-2 **14.25–14.50**
Reducing truncation errors by low order augmentation of the observer model for flexible systems . 33
Koen Verkerk TU Eindhoven

TuP04-3 **14.50–15.15**
A linear systems perspective for clustering of complex networks 34
Michael T. Schaub Université catholique de Louvain & UNamur
Jean-Charles Delvenne Université catholique de Louvain
Renaud Lambiotte UNamur
Mauricio Barahona

TuP04-4 **15.15–15.40**
ADM1 Model Reduction and Parameter Estimation 35
Giannina Giovannini UMons
Mihaela Sbarciog UMons
Gonzalo Ruiz-Filippi PUCV Valparaiso
Alain Vande Wouwer

TuP04-5 **15.40–16.05**
Model reduction for greenhouse climate control . 36
Simon van Mourik Wageningen UR
Irineo Lopez-Cruz Chapingo University
Peter van Beveren Wageningen UR
Eldert van Henten

TuE01 **Les Arcades**
Games & Agents I
Chair: Jean-Charles Delvenne **16.30–18.35**

TuE01-1 **16.30–16.55**
Denial of Service in Distributed Control and Communication Systems 37
Danial Senejohnny Rijksuniversiteit Groningen
Pietro Tesi Rijksuniversiteit Groningen
Claudio De Persis Rijksuniversiteit Groningen

TuE01-2 **16.55–17.20**
Diffusion Efficiency on temporal networks 38
Martin Gueuning UNamur & Université catholique de Louvain
Renaud Lambiotte UNamur
Jean-Charles Delvenne Université catholique de Louvain

TuE01-3 **17.20–17.45**
Game-theoretic approach for optimal contract design in railway networks 39
Zhou Su TU Delft
Bart De Schutter TU Delft
Simone Baldi TU Delft

TuE01-4 **17.45–18.10**
New approaches of Černý's Conjecture 40
François Gonze Université catholique de Louvain
Raphaël M. Jungers Université catholique de Louvain

TuE01-5 **18.10–18.35**
A Centrality-Based Security Game for Multi-Hop Networks 41
James Riehl Rijksuniversiteit Groningen
Ming Cao Rijksuniversiteit Groningen

TuE02 **Emanuel**
Biochemical Engineering
Chair: Anne Richelle **16.30–18.35**

TuE02-1 **16.30–16.55**
Off-line optimization of baker's yeast production process 42
Anne Richelle Université Libre de Bruxelles
Philippe Bogaerts Université Libre de Bruxelles

TuE02-2 **16.55–17.20**
Metabolic flux analysis using a convex analysis approach 43
Sofia Fernandes UMons
Georges Bastin Université catholique de Louvain
Alain Vande Wouwer UMons

TuE02-3 **17.20–17.45**
Mathematical modelling of overflow metabolism in hybridoma cell cultures by Flux Balance Analysis 44
Khadija Mhallem Gziri Université Libre de Bruxelles
Anne Richelle Université Libre de Bruxelles
Philippe Bogaerts Université Libre de Bruxelles

TuE02-4 **17.45–18.10**
Dynamic metabolic flux analysis in metabolic networks: a non-linear dynamic optimization approach 45
Philippe Nimmegeers KU Leuven
Filip Logist KU Leuven
Jan Van Impe KU Leuven
Dominique Vercammen

TuE02-5 **18.10–18.35**
On biological feasibility of solutions in a novel mathematical model for testosterone regulation . 46
Hadi Taghvafard Rijksuniversiteit Groningen
Anton V. Proskurnikov Rijksuniversiteit Groningen
Ming Cao Rijksuniversiteit Groningen

TuE03 **Impresario**
Identification II
Chair: Anna Marconato **16.30–18.35**

TuE03-1 **16.30–16.55**
Identification of Linear Time Varying Systems using 2D Regularization 47
Péter Zoltán Csurcsia Vrije Universiteit Brussel
Johan Schoukens Vrije Universiteit Brussel
John Lataire Vrije Universiteit Brussel

TuE03-2 **16.55–17.20**
Identification for Control of High-Tech Motion Systems 48
Robbert Voorhoeve TU Eindhoven
Tom Oomen TU Eindhoven

TuE03-3 **17.20–17.45**

Measuring nonlinear distortions: from test case to an F-16 Fighter 49

M. Vaes Vrije Universiteit Brussel
J. Schoukens Vrije Universiteit Brussel
Y.Rolain Vrije Universiteit Brussel
B. Peeters, J. Debille, T. Dossigne, J.P. Noël, C. Grappasonni, G. Kerschen

TuE03-4 **17.45–18.10**

Study of the control of a UAV/UGV cooperative system manipulating an object 50

Tam Nguyen Université Libre de Bruxelles
Emanuele Garone Université Libre de Bruxelles

TuE03-5 **18.10–18.35**

Compact representations of large dynamical systems based on low-rank tensor approximations . 51

Martijn Boussé KU Leuven
Otto Debals KU Leuven
Lieven De Lathauwer KU Leuven

TuE04 **Bloemen**

Control I

Chair: Benjamin Biemond **16.30–18.35**

TuE04-1 **16.30–16.55**

A switched systems approach to (de-)stabilization of predator-prey tumor dynamics 52

Alina Doban TU Eindhoven
Mircea Lazar TU Eindhoven

TuE04-2 **16.55–17.20**

Synchronization of Goodwin-type oscillators under saturated control 53

Anton V. Proskurnikov Rijksuniversiteit Groningen
Ming Cao Rijksuniversiteit Groningen

TuE04-3 **17.20–17.45**

Estimation of basins of attraction for controlled systems with input saturation and time-delays . . 54

J.J.B. Biemond KU Leuven
W. Michiels KU Leuven

TuE04-4 **17.45–18.10**

Design of periodic event-triggered control for nonlinear systems using overapproximation techniques 55

D.P. Borgers TU Eindhoven
R. Postoyan Univ-Lorraine
W.P.M.H. Heemels TU Eindhoven

TuE04-5 **18.10–18.35**

On delta-sampling verification for discrete-time systems 56

Ruxandra Bobiti TU Eindhoven
Mircea Lazar TU Eindhoven

Meet the Experts: Session 1 **Les Arcades**

Panel of Professors:
Hägglund, Kienle, Scherpen, De Keyser, Hendrickx, Absil, Pintelon, Schoukens, Steinbuch

18.35–19.00

Wednesday, March 25, 2015

WeM01 **Les Arcades**
Optimization II
Chair: Michel Kinnaert **09.00–11.05**

WeM01-1 **09.00–09.25**
About the latest complexity bounds for Policy Iteration 57
Romain Hollanders Université catholique de Louvain
Balázs Gerencsér Université catholique de Louvain
Jean-Charles Delvenne Université catholique de Louvain
Raphaël M. Jungers

WeM01-2 **09.25–09.50**
Mixing time speedup by some added edges and non-reversibility 58
Balázs Gerencsér Université catholique de Louvain
Julien Hendrickx Université catholique de Louvain

WeM01-3 **09.50–10.15**
Robust Gradient Learning with Application to Nonlinear Variable Selection 59
Yunlong Feng KU Leuven
Yuning Yang KU Leuven
Johan A.K. Suykens KU Leuven

WeM01-4 **10.15–10.40**
Influence of uncertainty on temporal stabilizability and compensatability of linear systems with white stochastic parameters 60
L.G. Van Willigenburg Wageningen UR
Willem de Koning

WeM01-5 **10.40–11.05**
Online semi-supervised clustering regularized by Kalman filtering 61
Siamak Mehrkanoon KU Leuven
Oscar Mauricio Agudelo KU Leuven
Johan A. K. Suykens KU Leuven

WeM02 **Emanuel**
MPC
Chair: Jacquelien Scherpen **09.00–11.05**

WeM02-1 **09.00–09.25**
Data driven MPC based on OBF model structures 62
Ahmad Alrianes Bachnas TU Eindhoven
Siep Weiland TU Eindhoven
Roland Tóth TU Eindhoven
A.A. Bachnas

WeM02-2 **09.25–09.50**
Distributed Model Predictive Control of Aquifer Thermal Energy Storage Smart Grids 63
Vahab Rostampour TU Delft
Tamas Keviczky TU Delft

WeM02-3 **09.50–10.15**
Distributed MPC in the Universal Smart Energy Framework 64
D. Bao Nguyen Rijksuniversiteit Groningen
Jacquelien M.A. Scherpen Rijksuniversiteit Groningen

WeM02-4 **10.15–10.40**
Energy-optimal point-to-point motions with high positioning accuracy using offset-free energy-optimal MPC 65
Xin Wang KU Leuven
Jan Swevers KU Leuven

WeM02-5 **10.40–11.05**
Anticipative linear parameter-varying model predictive control 66
J. Hanema TU Eindhoven
R. Tóth TU Eindhoven
M. Lazar TU Eindhoven
S. Weiland

WeM03 **Impresario**
Identification III
Chair: Johan Schoukens **09.00–11.05**

WeM03-1 **09.00–09.25**
Modeling Circadian Rhythm using Coupled Semi-passive Systems 67
Isaac Castanedo Guerra TU Eindhoven
Henk Nijmeijer TU Eindhoven

WeM03-2 **09.25–09.50**
Optimizing Inputs for Nonlinear Systems with Infinite Memory in the Time Domain 68
Alexander De Cock Vrije Universiteit Brussel
Johan Schoukens Vrije Universiteit Brussel

WeM03-3 **09.50–10.15**
A MATLAB toolbox for optimizing splines 69
Wannes Van Loock KU Leuven
Goele Pipeleers KU Leuven
Jan Swevers KU Leuven

WeM03-4 **10.15–10.40**
Modeling and control of heat networks with storage: the single-producer multiple-consumer case . 70
T.W. Scholten Rijksuniversiteit Groningen
C. De Persis Rijksuniversiteit Groningen
P. Tesi Rijksuniversiteit Groningen

WeM03-5 **10.40–11.05**
Design of experiment approach for optimizing the characteristics of the excitation signal for discriminating the internal structure 71
Alireza F. Esfahani Vrije Universiteit Brussel
Johan Schoukens Vrije Universiteit Brussel
Laurent Vanbeylen Vrije Universiteit Brussel

WeM04 **Bloemen**
Systems Theory I
Chair: Geert Gins **09.00–11.05**

WeM04-1 **09.00–09.25**
A Tensor-based Framework for Blind Identification of Linear MIMO FIR Systems 72
Frederik Van Eeghem KU Leuven
Otto Debals KU Leuven
Lieven De Lathauwer KU Leuven

WeM04-2 **09.25–09.50**
Applications of the greatest common divisor in system theory and signal processing 73
Ivan Markovsky Vrije Universiteit Brussel
Mayank Saxena Vrije Universiteit Brussel

WeM04-3 **09.50–10.15**
A survey on stochastic and deterministic tensorization for blind signal separation 74
Otto Debals KU Leuven Kulak
Lieven De Lathauwer KU Leuven Kulak

WeM04-4 **10.15–10.40**
Identifying Parameters with Pre-Specified Accuracies in Linear Physical Systems: Part I 75
Max Potters TU Delft
Xavier Bombois TU Delft
Paul M.J. Van den Hof TU Eindhoven

WeM04-5 **10.40–11.05**
Identifying Parameters with Pre-Specified Accuracies in Linear Physical Systems: Part II 76
Max Potters TU Delft
Mehdi Mansoori TU Delft
Xavier Bombois TU Delft
Paul M.J. Van den Hof

WeM05 **Seaside**
Control Applications I
Chair: Goele Pipeleers **09.00–11.05**

WeM05-1 **09.00–09.25**
Distributed supply coordination for Power-to-Gas facilities embedded in the energy grids 77
Desti Alkano Rijksuniversiteit Groningen
Ilco Kuiper Rijksuniversiteit Groningen
Jacquelien M.A. Scherpen Rijksuniversiteit Groningen

WeM05-2 **09.25–09.50**
Handling uncertainties in balancing short-term and long-term objectives in water-flooding optimization 78
Muhammad Mohsin Siraj TU Eindhoven
Paul M.J. Van den Hof TU Eindhoven
Jan Dirk Jansen TU Delft

WeM05-3 **09.50–10.15**
Analysis and Synthesis of Interconnected Systems: Application to Tuned Vibration Absorber Design for a Flexible Beam 79
Ruben Van Parys KU Leuven
Goele Pipeleers KU Leuven

WeM05-4 **10.15–10.40**
State-Dependent Virtual Hierarchization of Batteries and Its Application to Energy Management Systems 80
Hitoshi Yanami Fujitsu Ltd.
Tomotake Sasaki Fujitsu Ltd.
Junji Kaneko Fujitsu Ltd.
Shinji Hara

WeM05-5 **10.40–11.05**
Extended and unscented Kalman filter designs for hybridoma cell fed-batch cultures 81
Sofia Fernandes UMons
Anne Richelle Université Libre de Bruxelles
Zakaria Amribt Université Libre de Bruxelles
Laurent Dewasme

Plenary: P2 **Les Arcades**
Dynamics and control of particulate processes
Achim Kienle
Chair: Filip Logist **11.30–12.30**

Dynamics and control of particulate processes . . 180
Achim Kienle

WeP01 **Les Arcades**
Control over Networks
Chair: Maurice Heemels **14.00–16.05**

WeP01-1 **14.00–14.25**
Correct-by-Design Control of Physical Systems, Separating Estimation and Control 82
Sofie Haesaert TU Eindhoven
Paul Van den Hof TU Eindhoven
Alessandro Abate Oxford University

WeP01-2 **14.25–14.50**
Complete Vehicle Energy Management with Large Horizon Optimization 83
T.C.J. Romijn TU Eindhoven
M.C.F. Donkers TU Eindhoven
S. Weiland TU Eindhoven
J.T.B.A. Kessels

WeP01-3 **14.50–15.15**
Enterprise-wide Optimization: Graph Constrained Scheduling 84
M. Bahadir Saltik TU Eindhoven
Nikolaos Athanasopoulos TU Eindhoven
Leyla Özkan TU Eindhoven

WeP01-4 **15.15–15.40**
Feedback Control Design for Systems with Data-Intensive Sensing 85
E.P. van Horssen TU Eindhoven
D.J. Antunes TU Eindhoven
W.P.M.H. Heemels TU Eindhoven

WeP01-5 **15.40–16.05**
Sub-Optimal Strategies for Output-Based Event-Triggered Control 86
B. Asadi Khashooei TU Eindhoven
D.J. Antunes TU Eindhoven
W.P.M.H. Heemels TU Eindhoven

WeP02 **Emanuel**
Optimal Control
Chair: Wannes Van Loock **14.00–16.05**

WeP05-4 **15.15–15.40**
Counterweight synthesis for time-optimal robotic path following 105
Frederik Debrouwere KU Leuven
Goele Pipeleers KU Leuven
Jan Swevers KU Leuven

WeP05-5 **15.40–16.05**
Approximate Bisimulation Relations for Linear Systems 106
Noorma Yulia Megawati Rijksuniversiteit Groningen
Arjan van der Schaft Rijksuniversiteit Groningen

WeE01 **Les Arcades**
Games & Agents II
Chair: Bayu Jayawardhana **16.30–18.35**

WeE01-1 **16.30–16.55**
Global asymptotic stability in multi-agent systems 107
Filip Koerts Rijksuniversiteit Groningen
A.J. van der Schaft Rijksuniversiteit Groningen
C. de Persis Rijksuniversiteit Groningen
M. Bürger

WeE01-2 **16.55–17.20**
Predicting on-line opinion dynamics using consensus models 108
Corentin Vande Kerckhove Université catholique de Louvain
Samuel Martin Univ-Lorraine

WeE01-3 **17.20–17.45**
Stability analysis for repeated snowdrift games . 109
Pouria Ramazi Rijksuniversiteit Groningen
Ming Cao Rijksuniversiteit Groningen

WeE01-4 **17.45–18.10**
Local mean field analysis of the Linear Threshold Model 110
Wilbert Samuel Rossi UTwente
Giacomo Como Lund University
Fabio Fagnani Politecnico di Torino

WeE01-5 **18.10–18.35**
New Applications of Tensors to Graphs 111
Paul Smyth KU Leuven
Johan Suykens KU Leuven
Lieven De Lathauwer KU Leuven Kulak

WeE02 **Emanuel**
Mechanical Engineering II
Chair: Maarten Steinbuch **16.30–18.35**

WeE02-1 **16.30–16.55**
Iterative Feedforward Control with Application to a Wafer Stage 112
L.L.G. Blanken TU Eindhoven
F.A.J. Boeren TU Eindhoven
D.J.H. Bruijnen Philips
T.A.E. Oomen

WeE02-2 **16.55–17.20**
Hybrid Potential Bacterial Foraging Optimization Algorithm with Robot Swarm Obstacle Avoidance 113
Thoa Mac Thi Ghent University
Cosmin Copot Ghent University
Robin De Keyser Ghent University
Trung Tran Duc

WeE02-3 **17.20–17.45**
An experimental comparison of control architectures for bilateral teleoperation 114
Ruud Beerens TU Eindhoven
Dennis Heck TU Eindhoven
Henk Nijmeijer TU Eindhoven

WeE02-4 **17.45–18.10**
A waterbed effect in disturbance feedforward control with application to a vibration isolator . . . 115
Michiel A. Beijen TU Eindhoven
Marcel F. Heertjes TU Eindhoven
Hans Butler TU Eindhoven
Maarten Steinbuch

WeE02-5 **18.10–18.35**
Iterative Learning Control for Varying Tasks . . 116
Jurgen van Zundert TU Eindhoven
Joost Bolder TU Eindhoven
Sjirk Koekebakker Océ Technologies
Tom Oomen

WeE03 **Impresario**
Identification VI
Chair: John Lataire **16.30–18.35**

WeE03-1 **16.30–16.55**
Woofer-tweeter adaptive optics for EUV lithography 117
Michel Habets TU Eindhoven
Ruben Merks TU Eindhoven
Siep Weiland TU Eindhoven
Wim Coene

WeE03-2 **16.55–17.20**
RF identification and filter synthesis: a happy marriage? 118
Evi Van Nechel Vrije Universiteit Brussel
Yves Rolain Vrije Universiteit Brussel

WeE03-3 **17.20–17.45**
Tensor-based reduced order adjoints for water flooding optimization 119
Edwin Insuasty TU Eindhoven
Paul Van den Hof TU Eindhoven
Siep Weiland TU Eindhoven
Jan Dirk Jansen

WeE03-4 **17.45–18.10**
Identifying a Multi-tapped Lossless Transmission Line 120
Maral Zyari Vrije Universiteit Brussel
Yves Rolain Vrije Universiteit Brussel

WeE03-5 **18.10–18.35**
Two different approaches to dynamic modeling of hot-melt extrusion processes 121
Jonathan Grimard UMons
Laurent Dewasme UMons
Alain Vande Wouwer UMons

WeE04 **Bloemen**
LPV
Chair: Rik Pintelon **16.30–18.35**

WeE04-1 **16.30–16.55**
Identification of a static LPV differential equation in the continuous time and frequency domain . . 122
Jan Goos Vrije Universiteit Brussel
John Lataire Vrije Universiteit Brussel
Rik Pintelon Vrije Universiteit Brussel

WeE04-2 **16.55–17.20**
Parametric estimation of LPV partial differential equation 123
Julien Schorsch Université Libre de Bruxelles

WeE04-3 **17.20–17.45**
Estimation of LPV-SS Models with Static Dependency 124
P. B. Cox TU Eindhoven
R. Tóth TU Eindhoven
P. M. J. Van den Hof TU Eindhoven

WeE04-4 **17.45–18.10**
A combined global and local identification approach for LPV systems 125
Dora Turk KU Leuven
Goele Pipeleers KU Leuven
Jan Swevers KU Leuven

WeE04-5 **18.10–18.35**
Description of the cyclostationary processes in Linear Periodically Time-Varying (LPTV) systems 126
Vladimir Lazov Vrije Universiteit Brussel
Ebrahim Louarroudi Vrije Universiteit Brussel
Gerd Vandersteen Vrije Universiteit Brussel

WeE05 **Seaside**
Nonlinear Control
Chair: Joseph Winkin **16.30–18.35**

WeE05-1 **16.30–16.55**
Time-Delay Pre-Filter Design for Periodic Signal Tracking of Lightly-Damped Multivariable Systems 127
Rick van der Maas TU Eindhoven
Tarunraj Singh University at Buffalo

WeE05-2 **16.55–17.20**
Output agreement problem with unmatched disturbances 128
Nima Monshizadeh Rijksuniversiteit Groningen
Claudio De Persis Rijksuniversiteit Groningen

WeE05-3 **17.20–17.45**
Asynchronous event-triggered implementation with a lower bound for global event intervals . . . 129
Anqi Fu TU Delft
Manuel Mazo Jr. TU Delft

WeE05-4 **17.45–18.10**
Energy Dissipation in Preisach and Duhem Hysteresis Models for Damage Estimation 130
J.J. Barradas-Berglind Aalborg University
B. Jayawardhana Rijksuniversiteit Groningen
R. Wisniewski Aalborg University

WeE05-5 **18.10–18.35**
Distributed control design for nonlinear output agreement in convergent systems 131
Erik Weitenberg Rijksuniversiteit Groningen
Claudio De Persis Rijksuniversiteit Groningen

Meet the Experts: Session 2 **Les Arcades**
Panel of Professors:
Hägglund, Kienle, Van den Hof, Kinnaert, Hendrickx, Van Dooren, Absil, Pintelon, Schoukens, Steinbuch
18.35–19.00

Thursday, March 26, 2015

ThM01 **Les Arcades**
Games & Agents III
Chair: Paolo Frasca **09.00–11.05**

ThM01-1 **09.00–09.25**
Constrained proportional integral control of dynamical distribution networks with state constraints 132
Jieqiang Wei Rijksuniversiteit Groningen
Arjan van der Schaft Rijksuniversiteit Groningen

ThM01-2 **09.25–09.50**
Average consensus over unreliable networks: an improved compensation method 133
Francesco Acciani UTwente
Geert Heijenk UTwente
Paolo Frasca UTwente

ThM01-3 **09.50–10.15**
Properties of feedback Nash equilibria in scalar LQ differential games 134
J.C. Engwerda Tilburg University

ThM01-4 **10.15–10.40**
Consensus and Automata 135
Pierre-Yves Chevalier Université catholique de Louvain
Julien Hendrickx Université catholique de Louvain
Raphaël Jungers Université catholique de Louvain

ThM01-5 **10.40–11.05**
Robustness Issues with Directed Formations . . . 136
Hector Garcia de Marina Rijksuniversiteit Groningen
Miguel Martinez University of Alcala
Ming Cao Rijksuniversiteit Groningen
Bayu Jayawardhana

ThM02 **Emanuel**
ILC & Adaptive Control
Chair: Jan Swevers **09.00–11.05**

ThM02-1 **09.00–09.25**
Model Inversion-based Iterative Learning Control: Optimal Performance Trade-offs 137
Tong Duy Son KU Leuven
Goele Pipeleers KU Leuven
Jan Swevers KU Leuven

ThM02-2 **09.25–09.50**
Optimal Control of Uncertain Switched Systems Based on Model Reference Adaptive Control . . . 138
Shuai Yuan TU Delft
Simone Baldi TU Delft
Bart De Schutter TU Delft

ThM02-3 **09.50–10.15**
An Adaptive Online Game-theoretic Approach for Complete Vehicle Energy Management 139
H. Chen TU Eindhoven
J.T.B.A. Kessels TU Eindhoven
S. Weiland TU Eindhoven

ThM02-4 **10.15–10.40**
Wave form replication using combined Adaptive and Iterative Learning Control 140
Sikandar Moten KU Leuven
Goele Pipeleers KU Leuven
Jan Swevers KU Leuven
Wim Desmet

ThM02-5 **10.40–11.05**
Combustion Control with Multiple Fuel Injections for Clean and Fuel Efficient Diesel Engines . . . 141
Xi Luo TU Eindhoven
Frank Willems TU Eindhoven

ThM03 **Impresario**
Identification VII
Chair: Amélie Chevalier **09.00–11.05**

ThM03-1 **09.00–09.25**
Initial estimates for Wiener-Hammerstein dynamics using phase-coupled multisines 142
Koen Tiels Vrije Universiteit Brussel
Maarten Schoukens Vrije Universiteit Brussel
Johan Schoukens Vrije Universiteit Brussel

ThM03-2 **09.25–09.50**
Dynamic berth and quay crane allocation for complex berthing process in container terminals . . . 143
R. T. Cahyono Rijksuniversiteit Groningen
E. J. Flonk Rijksuniversiteit Groningen
B. Jayawardhana Rijksuniversiteit Groningen

ThM03-3 **09.50–10.15**
Filter interpretation of the cost function in regularized FIR modeling 144
Anna Marconato Vrije Universiteit Brussel
Johan Schoukens Vrije Universiteit Brussel

ThM03-4 **10.15–10.40**
Towards an assistive drug delivery system for general anesthesia 145
Dana Copot Ghent University
Clara Ionescu Ghent University
Robin De Keyser Ghent University

ThM03-5 **10.40–11.05**
Nonconvex Sorted l1 Minimization for Compressed Sensing 146
Xiaolin Huang KU Leuven
Lei Shi Fudan University
Johan A.K. Suykens KU Leuven

ThM04 **Bloemen**
Systems Theory II
Chair: Geert Gins **09.00–11.05**

ThM04-1 **09.00–09.25**
Cayley-Hamilton and Hilbert's function for nD systems theory 147
Antoine Vandermeersch KU Leuven
Bart De Moor KU Leuven

Contributed Lectures

First-order Methods for Convex Optimization through Smooth Convex Interpolation

Adrien B. Taylor, François Glineur, Julien M. Hendrickx
Institute of Information and Communication
Technologies, Electronics and Applied Mathematics
Université catholique de Louvain, Belgium
Email: {adrien.taylor, francois.glineur, julien.hendrickx}@uclouvain.be

1 Introduction

We have developed a method allowing to build smooth (possibly strongly) convex interpolating functions from a set of points with their corresponding (sub)gradients and function values. We use this procedure on two different applications from the convex optimization framework. The first application is concerned with the recovery of the exact worst-case behaviour of fixed-step first-order methods using the ideas developed in [1, 2]. The second application is the development of a new bundle-like optimization method.

2 Smooth strongly convex interpolation

We consider the problem of interpolating a set $\{(x_i, g_i, f_i)\}_{i\in I}$ by a smooth convex function. That is, we look for a smooth convex function f satisfying

$$f(x_i) = f_i, \quad g_i \in \partial f(x_i),$$

where $\partial f(x_i)$ denotes the subdifferential of f at x_i. In the case of L-smooth convex interpolating functions, the existence condition is given by:

$$f_i \geq f_j + g_j^\top (x_i - x_j) + \frac{1}{2L}||g_i - g_j||_2^2, \quad \forall i, j \in I, \qquad (1)$$

and an interpolating function can be found using standard tools from convex analysis. We developed those results in [1] for the general case of L-smooth μ-strongly convex interpolation.

3 Applications in convex optimization

Consider the standard unconstrained optimization problem

$$\min_{x\in\mathbb{R}^d} f(x), \qquad (2)$$

where f is a L-smooth $\mu-$strongly convex function.

3.1 Performance estimation problems

It is established in [1, 2] that the worst-case performance of any fixed-step first-order method on (2) for the class of functions $\mathscr{F}$ and the criterion $\mathscr{C}$ is exactly given by the infinite dimensional optimization problem PEP.

$$\max_{f, x_0, \ldots, x_N, x^*} \mathscr{C} \qquad \text{(PEP)}$$
$$\text{s.t.} f \in \mathscr{F},\ x^* \text{ optimal for } f,\ ||x_0 - x^*||_2^2 \leq R^2,$$
$$x_1, \ldots x_N \text{ generated by method } \mathscr{M},$$

Interpolation conditions (1) allow reformulating this problem into a convex semidefinite program [3] for all fixed-step first-order methods for the class of convex (possibly smooth and strongly convex) with a concave worst-case criterion. Tight worst-case results for the gradient and fast-gradient methods will be provided in the presentation.

3.2 A new bundle-like optimization method

Bundle and cutting plane algorithms are roughly based on the idea of restricting the search area to the possible positions of the optimal points, and to choose the next iterates among this restricted area.

In this context, the use of our exact interpolation conditions allows obtaining the exact — in the sense that every point of this area may be optimal — area containing the optimal solution, and hence to use more of the information harvested through the previous iterations.

Advances in this topic will be treated in the presentation.

Acknowledgments

This text presents research results of the Belgian Network DYSCO (Dynamical Systems, Control, and Optimization), funded by the Interuniversity Attraction Poles Program, initiated by the Belgian Science Policy Office. The scientific responsibility rests with its authors. A.B.T. is a FRIA fellow (F.R.S.-FNRS).

References

[1] A.B. Taylor, J.M. Hendrickx, F. Glineur. "Convex Interpolation and Exact Worst-case Performances of First-order Methods.", to be submitted.

[2] Y. Drori, M. Teboulle. "Performance of first-order methods for smooth convex minimization: a novel approach." Mathematical Programming 145.1-2 (2014).

[3] L. Vandenberghe and S. Boyd. "Semidefinite Programming. SIAM Review." 1994.

Solving PhaseLift by low-rank Riemannian optimization methods for complex semidefinite constraints

Wen Huang
ICTEAM Institue
Université catholique de Louvain
Avenue G. Lemaître 4
B-1348 Louvain-la-Neuve
Belgium
wen.huang@uclouvain.be

Kyle A. Gallivan
Department of Mathematics
Florida State University
208 Love Building
1017 Academic Way
Tallahassee FL 32306-4510
USA
kgallivan@fsu.edu

Xiangxiong Zhang
Department of Mathematics
Purdue University
150 N. University Street
West Lafayette IN 47907-2067
USA
zhan1966@purdue.edu

1 Abstract

The phase retrieval problem concerns recovering a signal given the modulus of its Fourier transform. It is a key problem for many important applications (see [2] and the references therein). In recent years, a framework called PhaseLift was proposed in [2] to solve the phase retrieval problem. In this framework, the problem is solved by optimizing a convex cost function over the set of complex Hermitian positive semidefinite matrices and the desired minimizer is rank one.

This approach to phase retrieval motivates a more general consideration of optimizing cost functions on semidefinite Hermitian matrices where the desired minimizers are known to have low rank, i.e.,

$$\min_{X \in \mathscr{D}_n} H(X),$$

where $H : \mathscr{D}_n \to \mathbb{R} : X \mapsto H(X)$ and $\mathscr{D}_n = \{X \in \mathbb{C}^{n\times n} | X = X^*, X \geq 0\}$. We consider an approach based on an alternative cost function F defined on a union of appropriate quotient manifolds $\cup_{i=1}^{n} \mathbb{C}_*^{n\times i}/\mathscr{O}_i$, where $\mathbb{C}_*^{n\times i}$ denotes the complex noncompact Stiefel manifold and $\mathscr{O}_i$ denotes the group of i-by-i unitary matrices. The alternative cost function F restricted on $\mathbb{C}_*^{n\times p}/\mathscr{O}_p$ is

$$F_p : \mathbb{C}_*^{n\times p}/\mathscr{O}_p \to \mathbb{R} : \pi(Y_p) \mapsto H(Y_p Y_p^*),$$

where $Y_p \in \mathbb{C}_*^{n\times p}$ and $\pi(Y_p) \in \mathbb{C}_*^{n\times p}/\mathscr{O}_p$ can be represented by Y_p. The function F is related to the function H in a manner that preserves the ability to find a stationary point of H and optimizing F is significantly more efficient computationally. A rank-based optimality condition for stationary points is given and optimization algorithms based on state-of-the-art Riemannian optimization, including trust-region Newton [1] and quasi-Newton methods [3, 4], and dynamically reducing rank are proposed. An approach of using same alternative cost function for problems defined on real positive semidefinite matrices has been given in [6].

Empirical evaluations are performed using the PhaseLift problem. Note that since the cost function H in PhaseLift is convex, finding a stationary of H is equivalent to finding its global minimizer. The new approach is shown to be an effective method of phase retrieval with computational efficiency increased substantially compared to the algorithm used in original PhaseLift paper. The full version of this paper has been submitted [5].

2 Acknowledgements

This paper presents research results of the Belgian Network DYSCO (Dynamical Systems, Control, and Optimization), funded by the Interuniversity Attraction Poles Programme initiated by the Belgian Science Policy Office. This work was supported by grant FNRS PDR T.0173.13.

References

[1] P.-A. Absil, C. G. Baker, and K. A. Gallivan. Trust-region methods on Riemannian manifolds. *Foundations of Computational Mathematics*, 7(3):303–330, 2007.

[2] E. J. Candès, Y. C. Eldar, T. Strohmer, and V. Voroninski. Phase retrieval via matrix completion. *SIAM Journal on Imaging Sciences*, 6(1):199–225, 2013. arXiv:1109.0573v2.

[3] W. Huang, P.-A. Absil, and K. A. Gallivan. A Riemannian symmetric rank-one trust-region method. *Mathematical Programming*, February 2014. doi:10.1007/s10107-014-0765-1.

[4] W. Huang, K. A. Gallivan, and P.-A. Absil. A Broyden class of quasi-Newton methods for Riemannian optimization. *Submitted for publication*, 2014.

[5] Wen Huang, K. A. Gallivan, and X Zhang. Solving Phaselift by low-rank Riemannian optimization methods for complex semidefinite constraints. *Submitted for publication*, 2014.

[6] M. Journée, F. Bach, P.-A. Absil, and R. Sepulchre. Low-rank optimization on the cone of positive semidefinite matrices. *SIAM Journal on Optimization*, 20(5):2327–2351, 2010.

Solving SDD linear systems in nearly-linear time

Maguy Trefois Jean-Charles Delvenne Paul Van Dooren

Dept. of Applied Mathematics
Université catholique de Louvain
Avenue G. Lemaître, 4-6
1348 Louvain-La-Neuve
Belgium
Email: maguy.trefois, jean-charles.delvenne, paul.vandooren@uclouvain.be

1 Introduction

Symmetric and diagonally-dominant (SDD) linear systems appear in many applications of computer science. These systems are usually of important size and solving them is the main computational task. Direct methods for solving linear systems are much too slow in the case of huge systems. In 2013, Kelner *et al.* [1] proposed a new approach for solving SDD systems in time which is nearly-linear in the number of nonzero entries. The original paper [1] presents this method using a physical interpretation of the problem. From this approach, it is unclear how this method works in a matrix theoretic point of view. In this talk, we explain Kelner's algorithm using only matrix theoretic arguments.

2 Problem Formulation

A particular case of linear system is when the coefficient matrix is the Laplacian matrix of an undirected graph with positive weights along the edges. The Laplacian matrix of such a graph is defined as

$$L = D - A,$$

where D is the diagonal matrix of the vertex degrees and A is the weighted adjacency matrix. These particular systems are called Laplacian systems and are SDD linear systems. They are of particular interest since it has been shown that if one can solve any Laplacian system in nearly-linear time, then one can solve any SDD system in nearly-linear time as well.

Consequently, we consider a Laplacian system

$$Lv = b.$$

This system is supposed to have an exact solution v_{opt}.

The goal is finding an ε-approximate solution v_K, namely v_K satisfies

$$||v_K - v_{opt}||_L \leq \varepsilon \cdot ||v_{opt}||_L,$$

in nearly-linear time, i.e. in time

$$\mathcal{O}(m \log^c n),$$

where n is the number of vertices (or the size of the system) and m is the number of edges (or the number of nonzero entries in L).

In this talk, we explain the Kelner algorithm through matrix theoretic arguments.

3 The Kelner algorithm

The method is based on the usual factorization of the Laplacian matrix through an incidence matrix $B \in \mathbb{R}^{m \times n}$:

$$L = B^T R^{-1} B,$$

where $R^{-1} \in \mathbb{R}^{m \times m}$ is the diagonal matrix of the weights along the edges.

We use the variable change $f = R^{-1}Bv$. The method is made up of the two following steps:

1. Solve the Laplacian system in variable f, namely solve
   $$B^T f = b$$
   and compute an ε-approximation f_K of the minimal R-norm solution f_{opt} to $B^T f = b$.
   In order to find f_K, a coordinate descent method is used.
2. Given f_K, use the variable change $f_K = R^{-1}Bv$ to find an ε-approximate solution to $Lv = b$.

In our talk, we explain the Kelner method in details and we show how to perform the crucial steps in order to get a running time in

$$\mathcal{O}(m \log^2 n).$$

References

[1] J.A. Kelner, L. Orecchia, A. Sidford, Z. Allen Zhu, A simple, combinatorial algorithm for solving SDD systems in nearly-linear time, in Proceedings of the 45th annual ACM Symposium on Theory Of Computing (STOC), pp. 911-920, New York, NY, USA, 2013.

Online Relaxation Method for Improving Linear Convergence Rates of the ADMM

Franck Iutzeler[1]
ICTEAM Institute
Université Catholique de Louvain
Belgium
franck.iutzeler@uclouvain.be

Julien Hendrickx
ICTEAM Institute
Université Catholique de Louvain
Belgium
julien.hendrickx@uclouvain.be

1 Introduction

The Alternating Direction Method of Multipliers (ADMM) is a very popular optimization technique, notably used nowadays in distributed optimization and learning [1]. It aims at solving problems of the form $\min_x f(x)+g(Mx)$ where f,g are convex functions and M is a matrix, by performing iterations of the form

$$x^{k+1} = \operatorname*{argmin}_x \left\{ f(x) + \frac{\rho}{2}\left\| Mx - z^k + \frac{\lambda^k}{\rho}\right\|^2 \right\} \quad (1a)$$

$$z^{k+1} = \operatorname*{argmin}_z \left\{ g(z) + \frac{\rho}{2}\left\| Mx^{k+1} - z + \frac{\lambda^k}{\rho}\right\|^2 \right\} \quad (1b)$$

$$\lambda^{k+1} = \lambda^k + \rho(Mx^{k+1} - z^{k+1}). \quad (1c)$$

In quite a large number of cases (when the functions are locally strongly convex, projections, polyhedral, etc.), it is possible to prove that the ADMM converges linearly (*i.e* exponentially) to the sought minimum [2, 3]. In these works, the choice of the ADMM parameter ρ was shown to be critical for the obtained rate. Unfortunately, no simple closed form expression for the optimal ρ are available in general.

Relaxation is a technique that consists in replacing the term Mx^{k+1} in Eqs. (1b) and (1c) by $\eta^k Mx^{k+1} + (1-\eta^k)z^k$ where $\eta^k \in]0,2[$ is a *relaxation parameter*. This method enables to improve convergence in both sub-linear and linear cases, in which choosing a fixed relaxation $\eta^k = \eta \in [1.5, 1.8]$ has been advocated to improve convergence rates [4].

In the recent linear convergence analyses [2, 5], it was shown that, as for ρ, the value of η had a great impact on the rate but again, finding the optimal relaxation parameter is about as hard as solving the whole problem.

2 Contribution

In this paper, we propose an Online Relaxation Method (ORM) for choosing good values of the relaxation parameter for a very moderate additional complexity, thus improving the convergence rate.

In order to warrant this technique, we conduct an analysis of the ADMM linear convergence rate through monotone operators theory. This formalism advocates the study of a variable $\zeta^k = \lambda^k + \rho z^k$ to analyze the convergence of the algorithm. Indeed, the operator, say T, linking ζ^{k+1} to ζ^k when an ADMM iteration is performed is known to have a contraction property called *Firm Non-Expansiveness (FNE)* [4] which suffices to prove convergence. Then, as remarked in [3], in some cases where the ADMM converges linearly, the operator T is linear. It is thus interesting to perform spectral analysis on this operator as the convergence rate the ADMM then depends on the eigenvalues of T.

First, we exploit the FNE property to conclude on the eigenvalues distribution of a linear operator with this property. Then, we explicit the effects of relaxation on these eigenvalues. This enables us to conclude on optimal relaxation parameters in this case and gives us a good insight to derive our Online Relaxation Method for ADMM. Finally, numerical simulations illustrate the performance of ORM in a variety of situations.

[1] This work is supported by the Belgian Network DYSCO (Dynamical Systems, Control, and Optimization), funded by the Interuniversity Attraction Poles Program, initiated by the Belgian Science Policy Office.

References

[1] S. Boyd, N. Parikh, E. Chu, B. Peleato, and J. Eckstein. Distributed optimization and statistical learning via the alternating direction method of multipliers. *Foundations and Trends in Machine Learning*, 2011.

[2] E. Ghadimi, A. Teixeira, I. Shames, and M. Johansson. Optimal parameter selection for the alternating direction method of multipliers (admm): Quadratic problems. *arXiv preprint arXiv:1306.2454*, 2013.

[3] F. Iutzeler, P. Bianchi, Ph. Ciblat, and W. Hachem. Explicit convergence rate of a distributed alternating direction method of multipliers. *accepted to IEEE Transactions on Automatic Control*, 2014.

[4] J. Eckstein and D. P. Bertsekas. On the douglas – rachford splitting method and the proximal point algorithm for maximal monotone operators. *Mathematical Programming*, 1992.

[5] F. Iutzeler. On the effects of relaxation on linear averaged operators and applications to distributed optimization. *Submitted*, Dec. 2014.

A New Perspective of Percentage Calculation

Bhagyashri Telsang
DCSC, TU Delft
b.telsang@student.tudelft.nl

1 Abstract

Percentage is an elemental tool in our daily life; it helps us compare different quantities which would otherwise be difficult to compare directly. The usage of percentages is extremely wide; it is used in every application from representing demographic data to indicating oxygen levels in the blood. This paper merely attempts to demonstrate an alternate approach to calculating percentages which are specific to the practical situations in which they are used.

One of the factors which the current method of calculation of percentages does not emphasize on is the sample size. While in many situations this helps Percentage represent varied type of data in a uniform and readable fashion, it also raises certain ambiguities. Consider two independent scenarios having different values of numerator and denominator quantities with ratio of numerator to denominator being the same in both cases. On calculation of percentage for both cases, it is seen that the same percentage value is obtained, owing to the same ratio. This is a direct indication that the value of the sample size is not given importance, which might be of practical relevance in various applications. For example, a person winning 50 of 60 chess matches will have the same win rate as a person who won 500 of 600 chess matches. However, in common perspective, the second person is more skilled at chess.

When quality of the games played is considered, the answer does not remain obvious. A person winning 500 out of 600 matches against a neophyte in chess might not deserve the same win rate as a person winning 50 out of 60 matches against a Grandmaster. The use of percentage tool in such cases, does not reveal much information. This example simply helps demonstrate some modifications that can be made to percentage tool to suit the situations better. Although there are various tools[1] in mathematics and statistics, like Percentiles, this paper shows that by minor modification to the current method of percentage calculation, it can be made a more powerful tool than it already is.

The two modifications that this paper takes up are : Size of the sample space (i.e., value of the denominator quantity in the current formula for Percentage calculation) and Quality of the sample space. The new formula that is proposed in the paper addresses these two issues and gives a subjective insight into percentage calculation. The mathematical function will incorporate ratio of the quantities, sample size and user selected weights so that emphasis to be placed on the sample space is free to be decided. The formula contains two extra terms; one term houses the modification regarding the size of the sample space and the other term regarding the quality factor.

Analysis of the modification in the current percentage formula is carried out for generic cases and further a comparison is drawn between the new formula and percentiles, weighted percentage and other variations of the percentage tool.

Using the new formula for calculation of percentage, various applicative tools like Percent of increase(or decrease) and Winning Percentage reveal more information about the situation in hand. The paper shows how the usage of the new formula will make evaluation of results easier and more efficient in cases like Testing of a new drug for a particular disease or in cases like Income tax payment calculation. Various such applications which benefit from the modification in percentage formula are also discussed in the paper.

In the last section of the paper, limitations of the modification are touched upon and analysis of situations in which the modifications do not lead to appropriate results is performed. The paper ends by shedding light on future scope of the elements of modification in the current percentage formula, for example, the new formula can be further modified to make data-based algorithms like Least Squares more efficient.

Keywords: Percentage, Sample size, Weighting factor

References

[1] Richard Courant, Herbert Robbins, *What Is Mathematics? An Elementary Approach to Ideas and Methods.* Oxford University Press; 2 edition, 1996.

On the Construction of Control Lyapunov-Barrier Function

Muhammad Zakiyullah Romdlony
Engineering and Technology Institute Groningen
Faculty of Mathematics and Natural Science
University of Groningen
The Netherlands
m.z.romdlony@rug.nl

Bayu Jayawardhana
Engineering and Technology Institute Groningen
Faculty of Mathematics and Natural Science
University of Groningen
The Netherlands
b.jayawardhana@rug.nl

1 Control Lyapunov-Barrier Function

One of the modern control design tools for the stabilization of affine nonlinear systems is the so-called Control Lyapunov Function (CLF) method. Artstein in [1] has given necessary and sufficient conditions for the existence of such CLF, which has been used to design a universal control law for affine nonlinear systems in [6].

Similar with the CLF method, Wieland and Allgöwer in [8] have proposed the construction of Control Barrier Functions (CBF), where the Lyapunov function is interchanged with the Barrier certificate studied in [3]. Using a CBF as in [8], one can design a universal feedback law for steering the states from the set of initial conditions to the set of terminal conditions, without violating the set of unsafe states.

In this paper, we will recall our previous works in [4, 5]. For gaining the stabilization property of CLF and the safety aspect from the CBF, we propose a simple control design procedure for merging a CLF with a CBF. Some previous relevant works, where a barrier function is incorporated explicitly in the CLF control design method, have been proposed in [2] and [7]. In these papers, a stabilization control problem with state saturation is considered which is solved by incorporating explicitly a "barrier function" in the design of a CLF. The resulting CLF has a strong property of being unbounded on the boundary of the state's domain. While in our paper, we consider a more general problem where the unsafe set can be any form of open and bounded set in the domain of the state. It is solved by combining a CLF and CBF(s) that results in a Control Lyapunov-Barrier Function (CLBF) control design method which does not impose unboundedness condition on the boundary of the unsafe set. Hence we admit a larger class of functions than the former approaches.

2 Simulation

The efficacy of the proposed control law is verified by simulation. Two examples, i.e., the nonlinear mechanical systems and the navigation of mobile robot (in Figure 1) are provided. Simulation results show that our proposed approach can guarantee the stability of the closed-loop systems, whilst guarantee its safety.

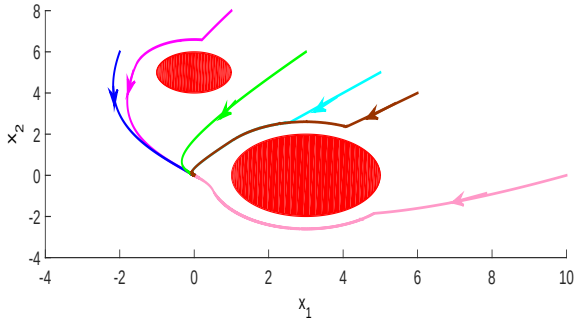

Figure 1: The simulation result of the closed-loop system CLBF approach. The set of unsafe states is shown in red and the plot of closed-loop trajectories are based on six different initial conditions (1 8), (-2 6), (5 5), (3 6), (10 0), and (6 4).

References

[1] Z. Artstein, "Stabilization with relaxed controls," Nonlinear Analysis, vol. 7, pp. 1163-1173, 1983.

[2] K. B. Ngo, et al, "Integrator backstepping using barrier functions for systems with multiple state constraints", Proc. IEEE CDC & ECC, pp. 8306-8312, Sevilla, 2005.

[3] S. Prajna, *Optimization-based Methods for Nonlinear and Hybrid Systems Verification*, PhD thesis, California Institute of Technology, 2005.

[4] M. Z. Romdlony, B. Jayawardhana, "Uniting Control Lyapunov and Barrier Function," Proc. IEEE CDC, Los Angeles, 2014.

[5] M. Z. Romdlony, B. Jayawardhana, "Stabilization with Guaranteed Safety Using Control Lyapunov-Barrier Function", Submitted, 2014.

[6] E.D. Sontag, "A universal construction of Artstein's theorem on nonlinear stabilization," Syst. Contr. Lett., vol. 13, pp. 117-123, 1989.

[7] K. P. Tee, S. S. Ge, E. H. Tay, "Barrier Lyapunov Functions for the Control of Output-Constrained Nonlinear Systems" Automatica, vol. 45, no. 4, pp. 918-927, 2009.

[8] P. Wieland, F. Allgöwer, "Constructive safety using control barrier functions," Proc. IFAC Symp. Nonl. Contr. Syst., pp. 473-478, Pretoria, 2007.

Control of knee joint motion in a dynamic knee rig

Amélie Chevalier, Clara M. Ionescu and Robin De Keyser
Department of Electrical energy, Systems and Automation
Ghent University
Sint-Pietersnieuwstraat 41, 9000, Gent, Belgium
{amelie.chevalier, claramihaela.ionescu, robain.dekeyser}@ugent.be

1 Introduction

The biomechanics of the knee joint have been a focus of extensive research with a twofold reason [1]. Firstly, knee injuries account for 15 to 50% of all sports injuries and secondly, there is a considerable aging in the population which coincides with a high number of knee injuries caused by wear. Total knee replacement, i.e. replacing the knee by a prosthesis, is a common used treatment. To test the performance of newly designed prostheses, the orthopedic surgeons can use a knee rig where natural movements are imposed on the prosthesis. Controlling the motions and forces applied is not an easy task to do. Designing a control strategy for this application is the main focus of this research.

2 System description

The dynamic knee rig is shown in the left part of figure 1 and consists of 3 linear actuators: one which mimics the quadriceps (B) and two on the ankle joint (A and C) which mimic the resulting forces of the hamstrings and the rectus femoris which flexes the thigh at the hip. Both mechanical knees and cadaver knees can be placed in the knee rig in order to evaluate prosthetics. The system is an unstable multi-variable with 3 inputs, i.e. the 3 voltages to the linear actuators and 3 outputs: the x- (horizontal) and y- position (vertical) of the ankle and the quadriceps force.

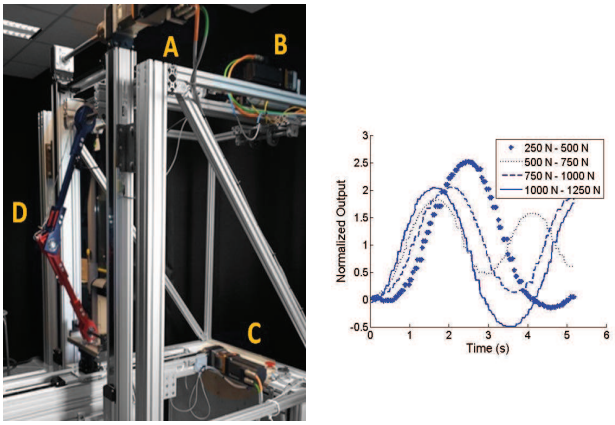

Figure 1: Left: Dynamic knee rig with 3 linear actuators (A,B and C) and a mechanical knee (D). Right: Capturing the system's nonlinear dynamics.

The system has an nonlinear oscillatory behavior which can be seen in the right part of figure 1. A step of 250 N has been applied in each range of the quadriceps force and the normalized force output has been plotted.

3 Controller design and results

In order to improve control of the quadriceps force, the x-position of the ankle and the y-position of the ankle in the system, two PD controllers have been designed based on specifications such as settling time and overshoot. In a first step the PD controller for the x-position and the y-position have been taken the same with a K_p value of 1 and a T_d value of 0,05. The resulting PD controller for the quadriceps force has a K_p value of 1 and a T_d value of 0,02. In figure 2 we can see an experiment where the quadriceps force is gradually increased in steps while maintaining a constant x- and y-position for the ankle. The newly designed controller is compared to the original situation in order to visualize the enhancement.

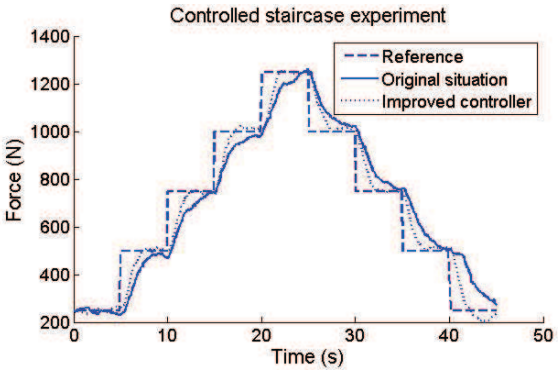

Figure 2: Closed loop control.

4 Conclusion

Initial work for controller design in a dynamic knee rig is presented in order to obtain implementation of natural movements on a knee prosthesis.

References

[1] M. R. Pitkin, "Biomechanics of Lower Limb Prosthetics" Springer, 2010.

An internal model approach to frequency regulation in power grids

S.Trip and C. De Persis
Engineering and Technology institute Groningen
Faculty of Mathematics and Natural Sciences
University of Groningen
Nijenborgh 4, 9747 AG Groningen
the Netherlands
{s.trip, c.de.persis}@rug.nl

M. Bürger
Cognitive Systems
Corporate Research
Robert Bosch GmbH
Robert-Bosch-Str. 2, 71701 Schwieberdingen
Germany
mathias.buerger@de.bosch.com

1 Introduction

We regard the power grid as an interconnected network of different control area's. In order to guarantee reliable operation the frequency is regulated around its nominal value, e.g. 50 Hz. Automatic regulation of the frequency in power grid is traditionally achieved by primary proportional control (droop-control) and a secondary PI-control on the generators, where economic considerations are largely neglected. In our work [1] we formulate the problem within the framework of output agreement on networks presented in [2]. By doing so we are able to regulate the frequency in the presence of unknown and time-varying demands and we can apply the design, based on passivity properties of the system, in a natural way to higher order models including e.g. voltage dynamics. By coordinating the different controllers utilizing communication links we can furthermore realize the minimization of generation costs.

2 Dynamics and problem formulation

The dynamics of the network are described by the following nonlinear equations,

$$\begin{aligned} \dot{\delta}_i &= \omega_i^b - \omega^n \\ M_i\dot{\omega}_i^b &= u_i - \textstyle\sum_{j\in\mathcal{N}_i} V_i V_j B_{ij} \sin\left(\delta_i - \delta_j\right) \\ &\quad -A_i\left(\omega_i^b - \omega^n\right) - P_i^l \\ \frac{T_{doi}}{(X_{di}-X'_{di})}\dot{V}_i &= \frac{E_{fi}}{(X_{di}-X'_{di})} - \frac{1+B_{ii}(X_{di}-X'_{di})}{(X_{di}-X'_{di})}V_i \\ &\quad +\textstyle\sum_{j\in\mathcal{N}_i} V_i B_{ij}\cos\left(\delta_i - \delta_j\right). \end{aligned} \tag{1}$$

where δ_i, ω_i^b and V_i are the voltage angle, frequency and voltage respectively. The unknown time-varying and uncontrollable demand is indicated by P_i^l, whereas u_i is the controllable power generation. In this work we aim at designing a controller that asymptotically regulates the frequency ω_i^b to its nominal value ω^n and at the same time solves $\min \sum_i q_i u_i^2$, s.t. $u_i - \sum_{j\in\mathcal{N}_i} V_i V_j B_{ij}\sin[\delta_i - \delta_j] - P_i^l = 0$, for all i, i.e. minimizes the total generation costs at steady state where $\omega_i^b = \omega^n$.

3 Distributed control

We move along the lines of [2], where an approach to deal with nonlinear output agreement and optimal flow problems for dynamical networks has been proposed. In that paper internal-model-based dynamic controllers have been designed to solve output agreement problems for networks of incrementally passive systems ([3]) in the presence of time-varying perturbations. In [1] we prove that the controller

$$\begin{aligned} \dot{\theta}_{1i} &= \textstyle\sum_{j\in\mathcal{N}_i^{comm}}(\theta_{1j} - \theta_{1i}) - q_i^{-1}\omega_i \\ \dot{\theta}_{2i} &= S_i\theta_{2i} - q_i^{-1}R_i^T\omega_i \\ u_i &= q_i^{-1}\theta_{1i} + q_i^{-1}R_i\theta_{2i}, \end{aligned} \tag{2}$$

achieves both frequency regulation and minimizes the generation costs, where S_i and R_i describe the dynamics of the exosystem generating P_i^l. Figure 1 demonstrates the performance of (2) on a 4-area network in a cycle topology, with a sudden change in demand.

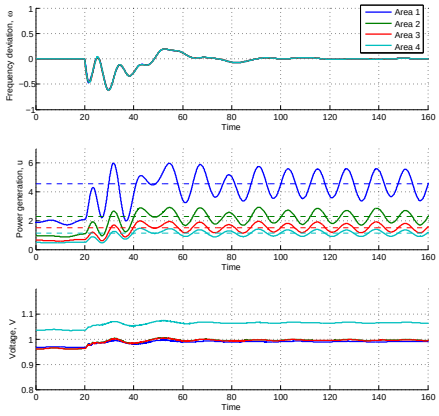

Figure 1: Frequency response and control input using controller (2). The time-varying demand is increased at timestep 20, whereafter the frequency deviation is regulated back to zero.

References

[1] Trip, Bürger and De Persis, "An internal model approach to frequency regulation in power grids," *arxiv.org/abs/1403.7019*, 2014.

[2] M. Bürger and C. De Persis, "Dynamic coupling design for nonlinear output agreement and time-varying flow control," *Automatica*, vol 51, pp. 210–222, 2015.

[3] A. Pavlov and L. Marconi, "Incremental Passivity and Output Regulation," *Systems and Control Letters*, vol. 57, pp. 400–409, 2008.

Management System for Paintable Batteries

Luis D. Couto, Julien Schorsch and Michel Kinnaert
Department of Control Engineering and System Analysis
Université libre de Bruxelles (ULB)
Email: lcoutome@ulb.ac.be, julien.schorsch@ulb.ac.be, michel.kinnaert@ulb.ac.be

The increase in the global energy demand in recent years, the limitation of fossil fuels and the climate change have all contributed to a greater interest in energy saving, as well as distributed energy generation and environmental protection. In this sense, the renewable energies show up as a cornerstone for the development of a sustainable future society. The main issues with renewable energies are that they are unpredictable and there exists a mismatch between supply and consumption periods. A key point to solve the latter problem is energy storage.

The present project is focused on lithium-ion batteries. They are the most promising electrochemical accumulator of energy due to their high energy density and high efficiency. More precisely paintable batteries [1] are considered, in which each component of the battery is made of a thin layer of a specific paint. Such batteries would facilitate the integration of energy storage devices with the energy conversion devices like solar cells for instance.

The objective is to develop a battery-management system (BMS) for such lithium-ion batteries in order to improve their lifetime and performance. This system should on the one hand ensure a proper balancing of the state of charge (SOC) of the different battery cells within a battery pack, and on the other hand detect and localize any malfunctions.

There are two main approaches for developing a BMS: using an equivalent circuit model vs an electrochemical model. To ensure proper operation of the BMS over the entire working range of the battery, the second one will be considered. The focus of the presentation will be the description of the electrochemical model and the challenges to be addressed both for parameter estimation and for exploitation of the model in on-line battery supervision.

The main electrochemical model reported in the literature is the so-called Doyle-Fuller-Newman (DFN) model [2, 3]. It is based on porous electrode and concentrated solution theories, and it consists of three regions: two electrodes (one negative and one positive) and a separator (Figure 1). Each electrode region contains two phases: the porous solid electrode and the electrolyte gel, while the separator region only contains the electrolyte gel. The electrodes active material is assumed to be made up of spherical particles of uniform size, with diffusion being the transport mechanism inside the particle. Diffusion and migration are the transport mechanisms assumed to take place for the ionic species through the electrolyte phase. One dimensional transport of lithium ions is considered. The kinetics follows Butler-Volmer equation.

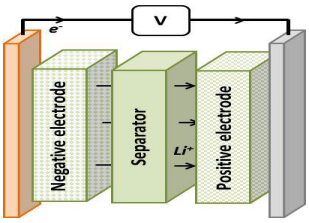

Figure 1: Main components of a battery cell.

The above described physical model consists of a system of coupled non-linear partial differential equations (PDEs). Each phase is described by a set of three PDEs, which yields six PDEs for the electrode regions and three PDEs for the separator region. The applied current and the voltage are the system input and output, respectively.

Regarding control applications, the electrochemical model is difficult to implement due to its complexity. Therefore some reduced models have been proposed to try to estimate SOC and state of health (SOH). SOC and SOH estimation is a challenging problem because the available measurements coming from the battery are limited to current and voltage. Simultaneous SOC and SOH estimation remains as an open problem.

Acknowledgement

This research is funded by the Walloon Region, in the framework of the BATWAL project.

References

[1] Singh, N., et al., Paintable Battery. Sci. Rep., 2012. 2.

[2] Doyle, M., T. Fuller, and J. Newman, Modeling of galvanostatic charge and discharge of the lithium/ polymer/insertion cell. Journal of the Electrochemical Society, 1993. 140(6): p. 1526-1533.

[3] Fuller, T.F., M. Doyle, and J. Newman, Simulation and Optimization of the Dual Lithium Ion Insertion Cell. Journal of the Electrochemical Society, 1994. 141(1): p. 1-10.

Geometric path following control in a moving frame

Iurii Kapitaniuk
Engineering and Technology institute Groningen
University of Groningen
i.kapitaniuk@rug.nl

The design of guidance laws for the unmanned vehicles is an important problem for the researchers in the field of motion control. One of the most interesting task is the moving path following control [1]. In this case the desired path is attached to a movable frame. This is a natural extension of the classical approaches for stationary frames. An application example of this task is the following by UAV of a moving ground vehicles [2]. In this work I would like to demonstrate the method of solution the similar tasks using the geometric path following framework based on the stabilization of sets.

Consider a point mass dynamic model. For this work was selected the simplest model to illustrate the main idea of the proposed approach, but the the method can be extended to more complex model trivially.

$$m\ddot{q} = F_u, \tag{1}$$

where $q \in R^3$ is the Cartesian position vector of the plant in the inertial reference frame, $m \in R$ is a total mass, $F_u \in R^3$ is the vector of the control forces in the inertial reference frame. The description of a moving frame is presented below.

$$\ddot{q}_T = 0,\ \dot{q}_T = Rv_T,\ \dot{\omega}_T = 0,\ \dot{R} = RS(\omega_T), \tag{2}$$

where $q_T \in R^3$ is the Cartesian position vector of the center of a moving frame in the inertial reference frame, $v_T in R^3$ and $\omega_T \in R^3$ are the vectors of velocities in the moving frame, $R \in SO(3)$ is the rotation matrix from the moving frame to the inertial frame, $S(\omega_T)$ is the skew symmetric matrix. Now define position, velocity and acceleration of the plant in the moving frame as

$$r = R^\top (q - q_T), \dot{r} = R^\top (\dot{q} - \dot{q}_T) - S(\omega_T)r, \tag{3}$$

$$\ddot{r} = R^\top \ddot{q} - 2S(\omega_T)\dot{r} - S^2(\omega_T)r. \tag{4}$$

The desired path is a smooth space curve P. It is described as an intersection of two implicit surfaces in the moving frame $\varphi_1(r)$ and $\varphi_2(r)$. The implicit representation of surfaces determines levels of sets in the space. We will use this property for the calculation of the instant position deviation e_1 and e_2 of the plant with respect to the desired surfaces.

$$P:\ e_1(r) = \varphi_1(r) = 0 \cap e_2(r) = \varphi_2(r) = 0. \tag{5}$$

Additional determine the Jacobian matrix in the form

$$\begin{bmatrix} \dot{\tau} \\ \dot{e}_1 \\ \dot{e}_2 \end{bmatrix} = J(r)\dot{r} = \begin{bmatrix} \nabla e_1(r) \times \nabla e_2(r) \\ \nabla e_1(r) \\ \nabla e_2(r) \end{bmatrix} \dot{r}, \tag{6}$$

where $\dot{\tau}$ is the vector of tangential velocity along the curve and ∇f is the gradient of the vector field f. Assume that Jacobian is not singular. This assumption is always true for the smooth curve. Path following control problem is posed as a problem of maintaining the holonomic relationships between the system outputs set in (5). It is augmented by the description of desired longitudinal motion along the path P. We are using the reference tangential velocity vector of longitudinal motion $\dot{\tau}^*$. The simple way to design the control is using of cascade approach. On the first step we shape the inner loop with respect to velocities. Consider Lyapunov function V_1 in the form

$$V_1 = \frac{1}{2}(\dot{r} - u)^\top (\dot{r} - u), \tag{7}$$

where $u \in R^3$ is the vector of the desired velocities. With the control F_u which is represented below $\dot{V}_1 < 0$.

$$F_u = mR\left(2S(\omega_T)\dot{r} + S^2(\omega_T)r + \dot{u} - k_1(\dot{r} - u)\right),$$

where k_1 - is the vector of positive constants. Now we can rewrite original model (1) − (4) in the reduced form

$$\dot{r} = u. \tag{8}$$

For the next step consider the Lyapunov function V_2 as

$$V_2 = \frac{k_2}{2}e_1^2(r) + \frac{k_3}{2}e_2^2(r) \tag{9}$$

With the control

$$u = J^{-1}(r)\begin{bmatrix} \dot{\tau}^* & 0 & 0 \end{bmatrix}^\top + [k_2 e_1(r)\nabla e_1(r) + k_3 e_2(r)\nabla e_1(r)],$$

where k_2 and k_3 are positive constants, the derivative of the Lyapunov function $V_2 < 0$ and the resulting systems is asymptotically stable. This control consist of two terms. First term is the feed-forward part to maintain the vector of desired tangential velocities. It does not affect on the stability due to orthogonality of $\dot{\tau}$ in the expression (6). The second term is used for the elimination of the deviations (5).

References

[1] Oliveira, T.; Encarnacao, P.; Aguiar, A.P., "Moving path following for autonomous robotic vehicles," Control Conference (ECC), 2013 European , vol., no., pp.3320,3325, 17-19 July 2013

[2] Regina, N.; Zanzi, M., "UAV guidance law for ground-based target trajectory tracking and loitering," Aerospace Conference, 2011 IEEE , vol., no., pp.1,9, 5-12 March 2011

The local polynomial method applied to a lightly damped mechanical MIMO system

Dieter Verbeke, Egon Geerardeyn, Johan Schoukens
Department of Electrical Engineering (ELEC)
University of Brussels (VUB)
1050, Brussels
dieter.verbeke@vub.ac.be

1 Introduction

This presentation discusses the estimation of nonparametric noise and frequency response matrix (FRM) models for multiple-input-multiple-output(MIMO) systems. [1] introduced the local polynomial method (LPM) for dynamic multivariable systems excited by arbitrary signals. [2] extended this work to MIMO systems excited by periodic signals in presence of both input and output noise (i.e. an errors-in-variables framework). The local polynomial methods result in a nonparametrical suppression of the noise and system transients (leakage errors) in the frequency response matrix and noise (co-)variance estimates. For lightly damped systems they can either significantly reduce the measurement time or, for a given experiment duration, significantly increase the frequency resolution of the FRM estimate. Although the objective is to apply the methodology to an experimental set-up, namely an active vibration isolation system (AVIS), the discussion here is limited to a series of simulations dealing with critical features.

2 The local polynomial method

The LPM builds on the assumption that the input-output discrete Fourier transform (DFT) spectra $U(k)$, $Y(k)$ of the input-output signals $u(t)$ and $y(t)$ are related as

$$\begin{aligned} U(k) &= U_0(k) + N_U(k) \\ Y(k) &= G(\Omega_k)U_0(k) + N_Y(k) \end{aligned}$$

$$\begin{aligned} N_U(k) &= H_U(k)E_U(k) + T_U(\Omega_k) \\ N_Y(k) &= H_Y(k)E_U(k) + T_Y(\Omega_k) \end{aligned}$$

$$T_Z(\Omega_{kP}) = \begin{bmatrix} T_Y(\Omega_{kP}) \\ T_U(\Omega_{kP}) \end{bmatrix},$$

where $\Omega = e^{-j\omega T_s}$ is the frequency variable in discrete time with $\Omega_k = 2\pi k f_s$, and $f_s = 1/T_s$ is the sampling frequency.

Both G, and T_Z are rational functions in Ω_k that can be approximated locally at DFT frequencies $kP+m$ for $k = 0, 1, ..., N/2-1$ and $m = 1, 2, ...P-1$:

$$T_Z(\Omega_{kP+m}) = T_Z(\Omega_{kP}) + \sum_{r=1}^{R} t_r(k)m^r + \frac{1}{\sqrt{PN}}O(N_1^{-(R+1)})$$

with P the number of periods of the periodic signals, N the number of samples per period, and $N_1 = NP/m$.

3 Objectives

The simulations will provide insight into critical aspects of the methodoly for the particular case of a lightly damped mechanical MIMO system . This includes the design of appropriate input signals, and the choice of the parameters in the local polynomial method. Of particular interest is the impact these decision variables will have on the quality of the obtained FRF estimates around the resonance frequencies. As such, this work is the first stage in the process of using the LPM for the identification of the benchmark example of an industrial AVIS [3] with 8 inputs and 6 outputs..

Acknowledgement

This work was supported in part by the Fund for Scientific Research (FWO-Vlaanderen), by the Flemish Government (Methusalem), and the Belgian Government through the Inter university Poles of Attraction (IAP VII) Program.

References

[1] R. Pintelon, J. Schoukens, G. Vandersteen, K. Barbé, "Estimation of nonparametric noise and FRF models for multivariable systems - Part I: Theory," *Mechanical Systems and Signal Processing*, vol. 24, no. 3, pp.573-595, 2010.

[2] R. Pintelon, K. Barbé, G. Vandersteen, J. Schoukens, "Improved (non-) parametric identification of dynamic systems excited by periodic signals - the multivariate case," *Mechanical Systems and Signal Processing*, vol. 25, no. 8, pp.2892-2922, 2011.

[3] T. Oomen, R. van der Maas, C. Rojas and H. Hjalmarsson, "Iteratively learning the $\mathcal{H}_\infty$ norm of multivariable systems applied to model-error-modeling of a vibration isolation system," Proc. of the 2013 American Control Conference, Invited paper, Washington DC, USA, 2013.

Selecting Shaping Kernels in Bayesian Identification of LTI Systems: An Orthonormal Basis Functions Approach

M.A.H. Darwish[1,2], R. Tóth[1] and P.M.J. Van den Hof[1]
[1]Control Systems Group, Department of Electrical Engineering, Eindhoven University of Technology
[2]Electrical Engineering Department, Faculty of Engineering, Assiut University, 71515 Assiut, Egypt
m.a.h.darwish@tue.nl

1 Introduction

A Bayesian paradigm based approach for LTI system identification has been introduced recently [1], in which, instead of postulating finite-dimensional parameterizations of models of the system, the system impulse response estimation is dealt with as a function estimation problem. This estimation approach corresponds to a particular regularized least-squares methodology that achieves favorable bias/variance trade-off compared to standard Prediction Error Methods and Maximum Likelihood estimators (PEM/ML). A particular feature of this methodology is that the unknown impulse response function is assumed to be a realization of a zero-mean Gaussian stochastic process with certain auto-covariance (Bayesian prior or kernel) function. This function encodes information not only on smoothness but also on BIBO-stability. It is shown that the optimal covariance matrix can be expressed as

$$P = \theta_0 \theta_0^\top, \tag{1}$$

where, θ_0 is the true impulse response. Although, (1) is impossible to be used in practice as the true impulse response is unknown, it provides a guideline to design the optimal kernel function for nonparametric identification. In the literature, there are many choices for kernels, e.g., DC, TC and SS, but, the performance of those single kernels can be further improved especially for systems with widely spread time constants. One approach to handle such complicated systems is by a conic combination of those single kernels. Alternatively, orthonormal basis functions (OBFs) can be introduced which offer a more suitable selection of the kernel function. Next, two different approaches will be discussed.

2 Regularization of the impulse response with OBFs based kernel

OBFs provide bases for the Hilbert space $\mathscr{H}_2$ (space of real-valued functions, i.e., transfer functions, that are squared integrable on the unit circle and analytic outside of it) and are generated by a cascaded network of stable inner transfer functions, i.e., all-pass filters. These inner functions are completely determined, modulo the sign, by their poles [2]. This means that in the context of kernel-based regularization, a positive-definite kernel function can be expressed in terms of OBFs; this kernel function is associated with a RKHS that corresponds to the Hilbert space spanned by the OBFs. An OBFs kernel is parameterized in terms of the generating poles and the tuning of these poles are performed in a Bayesian setting with maximizing the marginal likelihood. To illustrate the usefulness of OBFs generated kernels, see Fig. 1 for the realization of a Gaussian Processes with OBFs kernel. It can be seen from the figure that OBFs kernels generate stable realizations with a wide range of possible dynamics.

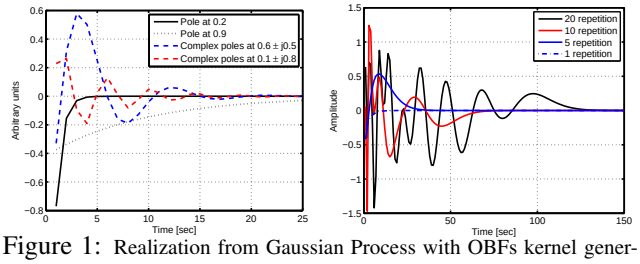

Figure 1: Realization from Gaussian Process with OBFs kernel generated with different pole locations, (left) and with various number of pole repetitions, (right).

3 Regularization of the coefficients of an OBFs based expansion model

Consider a single-input-single-output (SISO), asymptotically stable and linear time-invariant (LTI) discrete-time system, then the following series expansion structure is available

$$y(k) = \sum_{i=1}^{n} h_i \phi_i(q) u(k) + v(k),$$

where, q is the forward time shift operator, y and u are the output and the input of the system respectively. $v(t)$ is a zero-mean quasi-stationary noise process, independent of the input u, and $\phi_i(q)$'s are the basis functions. LTI system expansion in terms of such basis offers a much more compact representation of the system compared to FIR representation, i.e., expansion in terms of pulse basis q^{-i}, especially for slow systems. This representation capability leads to the reduction of the number of the expansion coefficients that are needed to capture the system dynamics. Therefore, regularizing the estimation of the OBFs expansion coefficients instead of the Markov parameters will result in better results, i.e., a better bias/variance trade-off.

4 Acknowledgments

This research has benefited from the financial support of the Student Mission, Ministry of Higher Education, Government of Egypt.

References

[1] G. Pillonetto and G. De Nicolao, A new kernel-based approach for linear system identification, Automatica, vol. 46, no. 1, pp. 81-93, 2010.
[2] P. S. Heuberger, P. M. Van den Hof, and B. Wahlberg, Modelling and identification with rational orthogonal basis functions. Springer, 2005.

Decoupling noisy multivariate polynomials in nonlinear system identification

Gabriel Hollander, Philippe Dreesen, Mariya Ishteva, Johan Schoukens
Dept. ELEC, Vrije Universiteit Brussel, Pleinlaan 2, 1050 Brussels, Belgium
gabriel.hollander@vub.ac.be

1 Introduction

In the field of system identification, the last few decades have witnessed a shift from linear to nonlinear system identification. One special type of nonlinear models are the so-called block-oriented models, and more specifically the Wiener-Hammerstein models. When identifying parallel Wiener-Hammerstein systems based on measurements, a noisy coupled multiple input-multiple output polynomial should be decoupled. However, this decoupling problem has solely been studied for the noiseless case, and not yet for the more involved noisy case. By using the covariance matrix of the polynomial coefficients, we have developed a first step towards the decoupling of noisy multivariate polynomials. This overview describes our contribution to the existing algorithm in the noisy case. For small noise levels (up to 10% of the output level), the covariance matrix method gives a reduction in error up to 10 dB between model and simulation. We expect better results after solving a remaining problem in the covariance matrix algorithm.

2 The algorithm

Let $\mathbf{f}\colon \mathbb{R}^m \to \mathbb{R}^n$ be a multivariate polynomial function. We wish to decouple this function by finding transformation matrices $\mathbf{V} \in \mathbb{R}^{m\times r}$ and $\mathbf{W} \in \mathbb{R}^{n\times r}$ for a certain number of branches r, such that $\mathbf{f}$ can be expressed as $\mathbf{f}(\mathbf{u}) = \mathbf{W}\cdot\mathbf{g}(\mathbf{V}^T\cdot\mathbf{u})$, where the internal vector function $\mathbf{g}\colon \mathbb{R}^r \to \mathbb{R}^r$ is a set of univariate functions: every component g_i of $\mathbf{g}$ is only dependent on one variable x_i, which is the i-th component of the internal variable $\mathbf{x} = \mathbf{V}^T\cdot\mathbf{u}$.

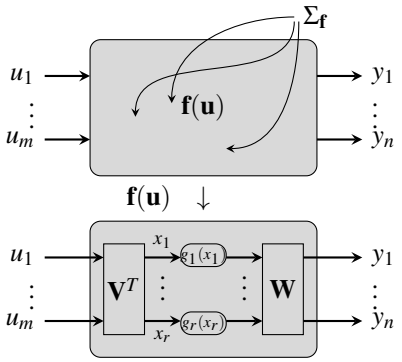

Decoupling of the multivariate function $\mathbf{f}$ *by taking the covariance matrix* $\Sigma_\mathbf{f}$ *into account.*

In [1], an algorithm to compute the matrices $\mathbf{V}$ and $\mathbf{W}$ and the internal functions $g_i(x_i)$ is described using first-order derivative information of the function $\mathbf{f}$. This algorithm involves the so called Canonical Polyadic (CP) Decomposition of a tensor, which is, loosely spoken, a generalization of the singular value decomposition for two-dimensional matrices to multidimensional arrays of numbers.

It is possible to add a weighting tensor to the CP decomposition [3], and this was chosen as follows. This weighting tensor has the same dimensions as the tensor used in [1] and uses covariances between the coefficients of $\mathbf{f}$. For small noise levels in simulations, this decreases the error between model and simulated system up tot 10 dB.

However, the current weighting tensor only uses the covariance matrices between the coefficients of one single input function f_i, and not between two input functions f_i and f_j. We will investigate how to use the full covariance matrix in future work.

3 Conclusions

Taking the covariance matrix of the polynomial coefficients into account decreases the error between model and simulated data, for small noise levels. However, the current method uses a fraction of the covariance matrix due to the dimensions of the weighting tensor. In future work, we will investigate how this restriction in dimensions of the weighting tensor could be relaxed.

References

[1] P. Dreesen, M. Ishteva, J. Schoukens, *Decoupling Multivariate Polynomials in a Parallel Wiener-Hammerstein System Using First-Order Information*, at Xiv preprint arXiv:1410.4060, 2014

[2] T. G. Kolda and B. W. Bader, *Tensor decompositions and applications*, SIAM Rev., vol. 51, no. 3, pp. 455—500, September 2009

[3] Rasmus Bro, *The N-way Toolbox*, www.mathworks.com/matlabcentral/fileexchange/1088-the-n-way-toolbox, 2012

[4] M. Schoukens, K. Tiels, M. Ishteva, J. Schoukens, *Identification of parallel Wiener-Hammerstein systems with a decoupled static nonlinearity*, In *The 19th World Congress of the International Federation of Automatic Control (IFAC WC 2014)*, Cape Town, South Africa, pp. 505—510

System identification in dynamic networks

Harm H.M. Weerts
Control Systems Group,
Dept. of Electrical Engineering,
Eindhoven University of Technology,
h.h.m.weerts@tue.nl

Paul M.J. Van den Hof
Control Systems Group,
Dept. of Electrical Engineering,
Eindhoven University of Technology,
p.m.j.vandenhof@tue.nl

Arne G. Dankers
Dept. of Electrical Engineering,
University of Calgary,
adankers@hifieng.com

1 Introduction

Systems considered in science are becoming more and more complex and of an interconnected nature. Fields where interconnected systems, from now on called networks, are studied include but are not limited to engineering, biology and finance. In these fields modeling the network will generate additional understanding of the underlying system, in engineering in particular the model can be used for control design. We focus on black-box modeling since first principles modeling becomes increasingly complex in networks. A network identification framework was introduced in [1] which allows for consistent identification of modules in the network. In the framework it is assumed that the topology of the network is known, while in practice this assumption might not hold. We work on extending the network identification framework by making less restrictive assumptions. For example in this work we focus on topology detection.

2 Network identification

Consider the network given by the equation

$$w(t) = G^0(q)w(t) + R^0(q)r(t) + H^0(q)e(t) \qquad (1)$$

with $w(t)$ a vector of L internal variables, $G^0(q)$ an $L \times L$ transfer matrix with 0 diagonal, $r(t)$ a vector of K external variables, $e(t)$ a vector of L independent stochastic variables and $R^0(q)$ and $H^0(q)$ transfer matrices of appropriate dimension. A network model structure $\mathscr{M}(\theta)$ is used to define a network predictor as

$$\varepsilon(t,\theta) := H^{-1}(q,\theta)\{(I - G(q,\theta))^{-1} - R(q,\theta)\}. \qquad (2)$$

We do not make assumptions on the structure, hence model $G(q,\theta)$ is fully parametrized with zero diagonal, but also $R(q,\theta)$ and $H(q,\theta)$ are fully parametrized. Consistent estimates of the dynamics are obtained under similar conditions as in [1] when some elements of the network model structure are restricted. The network model structure $\mathscr{M}(\theta)$ is flexible enough to have a model set that contains infinite models that can represent the network equally well, which can be classified as an identifiability problem. Identifiability was addressed in [3] and we continue in a similar reasoning. Restricting the model flexibility using a-priori knowledge is a way to reduce the amount of models in the model set that fit the network. Conditions under which the model structure has been restricted enough and is therefore identifiable are such that each node either has an independent input or the interconnections coming from that node are not parametrized [2]. A special case is the assumption that all noises are independent ($H^0(q)$ diagonal), which leads to a diagonal noise model $H(q,\theta)$ and ensures identifiability.

3 Topology detection

The estimated network models are consistent, however due to variance all the transfer functions will be parametrized as non-zero and as a result no topology detection has been performed then. We would like to see transfer functions be identified as 0 in some measure when there is no interconnection. Parameters or transfer functions are dragged to 0 by adding L1 or mixed L1-L2 regularization to the identification criterion. The regularized estimate is still consistent, and it is sparse such that the topology has been detected.

4 Conclusions

We relaxed assumptions in network identification by allowing noises to be correlated and investigated the consequences for identifiability. Relaxing the assumptions even further could be done by letting the noises be represented by less than L independent noise sources, which leads to interesting mixed stochastic/deterministic problems. Other interesting questions include the tuning of the regularization and making an analysis of the variance.

References

[1] P.M.J. Van den Hof, A. Dankers, P. Heuberger and X. Bombois (2013). Identification of dynamic models in complex networks with prediction error methods - basic methods for consistent module estimates. *Automatica,* Vol. 49, no. 10, pp. 2994-3006.

[2] H.H.M. Weerts (2014). Topology detection in dynamic networks. *M.Sc. thesis*

[3] J. Goncalves and S. Warnick, "Necessary and sufficient conditions for dynamical structure reconstruction of LTI networks", *IEEE Transactions on Automatic Control, 53, 2008.*

A comparison of grey-box and black-box approaches in nonlinear state-space modelling and identification

J.P. Noël, J. Schoukens
ELEC Department
Vrije Universiteit Brussel, Brussels, Belgium
jp.noel@ulg.ac.be, johan.schoukens@vub.ac.be

G. Kerschen
Space Structures and Systems Lab
Aerospace and Mechanical Engineering Department
University of Liège, Liège, Belgium
g.kerschen@ulg.ac.be

1 Abstract

Nonlinear system identification constantly faces the compromise between the flexibility of the fitted model and its parsimony. Flexibility refers to the ability of the model to capture complex nonlinearities, while parsimony is its quality to possess a low number of parameters. In this regard, a nonlinear state-space representation [1]

$$\begin{cases} \dot{\mathbf{x}}(t) &= \mathbf{A}\,\mathbf{x}(t)+\mathbf{B}\,\mathbf{u}(t)+\mathbf{E}\,\mathbf{g}(\mathbf{x},\mathbf{u}) \\ \mathbf{y}(t) &= \mathbf{C}\,\mathbf{x}(t)+\mathbf{D}\,\mathbf{u}(t)+\mathbf{F}\,\mathbf{h}(\mathbf{x},\mathbf{u}) \end{cases} \tag{1}$$

can be classified as very flexible but little parsimonious, two features typically shared by black-box models. In Eqs. (1), $\mathbf{A}\in\mathbb{R}^{n_s\times n_s}$, $\mathbf{B}\in\mathbb{R}^{n_s\times m}$, $\mathbf{C}\in\mathbb{R}^{l\times n_s}$ and $\mathbf{D}\in\mathbb{R}^{l\times m}$ are the linear state, input, output and direct feedthrough matrices, respectively; $\mathbf{x}(t)\in\mathbb{R}^{n_s}$ is the state vector; $\mathbf{y}(t)\in\mathbb{R}^{l}$ and $\mathbf{u}(t)\in\mathbb{R}^{m}$ are the output and input vectors, respectively. The linear-in-the-parameters expressions $\mathbf{E}\,\mathbf{g}(\mathbf{x},\mathbf{u})\in\mathbb{R}^{n_s}$ and $\mathbf{F}\,\mathbf{h}(\mathbf{x},\mathbf{u})\in\mathbb{R}^{l}$ are the nonlinear model terms coupling the state and input variables. The order of the model, *i.e.* the dimension of the state space, is noted n_s.

In the present contribution, it is shown that, in the case of mechanical systems where nonlinearities are physically localised, the model structure in Eqs. (1) can be drastically simplified. Assuming localised nonlinearities, the vibrations of a n_p-degree-of-freedom mechanical system obey Newton's second law written in the form

$$\mathbf{M}\,\ddot{\mathbf{q}}(t)+\mathbf{C}_v\,\dot{\mathbf{q}}(t)+\mathbf{K}\,\mathbf{q}(t)+\sum_{a=1}^{s} c_a\,\mathbf{g}_a(\mathbf{q}_{nl}(t),\dot{\mathbf{q}}_{nl}(t))=\mathbf{p}(t), \tag{2}$$

where $\mathbf{M}$, $\mathbf{C}_v$, $\mathbf{K}\in\mathbb{R}^{n_p\times n_p}$ are the mass, linear viscous damping and linear stiffness matrices, respectively; $\mathbf{q}(t)$ and $\mathbf{p}(t)\in\mathbb{R}^{n_p}$ are the generalised displacement and external force vectors, respectively; the nonlinear restoring force term is written using s basis function vectors $\mathbf{g}_a(t)\in\mathbb{R}^{n_p}$ associated with coefficients c_a. The subset of generalised displacements and velocities involved in the construction of the basis functions are denoted $\mathbf{q}_{nl}(t)$ and $\dot{\mathbf{q}}_{nl}(t)$, respectively.

The dynamics governed by Eq. (2) is conveniently interpreted by moving the nonlinear restoring force term to the right-hand side, *i.e.*

$$\mathbf{M}\,\ddot{\mathbf{q}}(t)+\mathbf{C}_v\,\dot{\mathbf{q}}(t)+\mathbf{K}\,\mathbf{q}(t)=\mathbf{p}(t)-\sum_{a=1}^{s} c_a\,\mathbf{g}_a(\mathbf{q}_{nl}(t),\dot{\mathbf{q}}_{nl}(t)). \tag{3}$$

The feedback structure of Eq. (3) suggests that localised nonlinearities in mechanical systems act as additional inputs applied to the underlying linear system. This, in turn, reveals that black-box nonlinear terms in a state-space model, such as $\mathbf{E}\,\mathbf{g}(\mathbf{x},\mathbf{u})$ and $\mathbf{F}\,\mathbf{h}(\mathbf{x},\mathbf{u})$ in Eqs. (1), are overly complex to address mechanical vibrations. A more parsimonious description of nonlinearities is achieved by translating Eq. (3) in state space, which provides the grey-box model

$$\begin{cases} \dot{\mathbf{x}}(t) &= \mathbf{A}\,\mathbf{x}(t)+\mathbf{B}\,\mathbf{u}(t)+\mathbf{E}\,\mathbf{g}(\mathbf{y}_{nl}(t),\dot{\mathbf{y}}_{nl}(t)) \\ \mathbf{y}(t) &= \mathbf{C}\,\mathbf{x}(t)+\mathbf{D}\,\mathbf{u}(t)+\mathbf{F}\,\mathbf{g}(\mathbf{y}_{nl}(t),\dot{\mathbf{y}}_{nl}(t)), \end{cases} \tag{4}$$

where $\mathbf{g}(t)\in\mathbb{R}^{s}$ is a vector concatenating the nonzero elements in the basis function vectors $\mathbf{g}_a(t)$, and $\mathbf{E}\in\mathbb{R}^{n_p\times s}$ and $\mathbf{F}\in\mathbb{R}^{l\times s}$ are the associated coefficient matrices; $\mathbf{y}_{nl}(t)$ and $\dot{\mathbf{y}}_{nl}(t)$ are the subsets of the measured displacements and velocities located close to nonlinearities, respectively.

For demonstration purposes, black-box and grey-box state-space models of the Silverbox benchmark, *i.e.* an electrical mimicry of a single-degree-of-freedom mechanical system with cubic nonlinearity, are identified using a maximum likelihood estimator. It is found that the grey-box approach allows to reduce markedly modelling errors with respect to a black-box model with a comparable number of parameters. It is also suggested that the greater accuracy of the grey-box model lends itself to the computation of reliable confidence bounds on the model parameters.

References

[1] J. Paduart *et al.*, Identification of nonlinear systems using Polynomial Nonlinear State-Space models, Automatica, 46:647-656, 2010.

Model Reduction of Networked Systems

H.J. Jongsma[1]
h.jongsma@rug.nl

H.L. Trentelman
University of Groningen
h.l.trentelman@rug.nl

M.K. Camlibel
m.k.camlibel@rug.nl

Abstract

Even with the increase in computing power and the availability of numerical tools, analysis and control of large-scale interconnected systems remain complicated tasks. One way to simplify these procedures is to look at less complex approximations that closely model the behavior of the original system. When directly applying existing reduction techniques to networked systems, important properties such as the spatial structure of the network may be lost in the process. In this abstract we investigate a class of networked systems called leader-follower based *multi-agent systems*. We use *clustering* based model reduction techniques that preserve some of the network topology. We show that the reduced systems retain the *consensus* properties of the original system and give an a priori upper bound on the modeling error.

A multi-agent system consists of interconnected identical dynamical systems called *agents*. The interconnections are modeled by a *weighted graph* $G = (V, E, \mathcal{A})$, where the *nodes* $V = \{1, 2, \ldots, p\}$ represent the agents of the network and the *edges* E represent the communication links. The matrix $\mathcal{A} = (a_{ij})$ is the adjacency matrix of G. The set of *neighbors* of agent i is denoted N_i. Each agent has state $x_i \in \mathbb{R}^n$ and dynamics

$$\dot{x}_i = \begin{cases} Ax_i + B\sum_{j\in N_i} a_{ij}(x_j - x_i) & \text{if } i \in V_{\mathrm{F}} \\ Ax_i + B\sum_{j\in N_i} a_{ij}(x_j - x_i) + Eu_i & \text{if } i \in V_{\mathrm{L}} \end{cases}$$

where $V_{\mathrm{L}} = \{v_1, v_2, \ldots, v_m\}$ is the set of leaders, which have an external input, and $V_{\mathrm{F}} = V \setminus V_{\mathrm{L}}$ is the set of followers. The input $u_l \in \mathbb{R}^q$ is applied to the leader $i = v_l$. The overall network dynamics with $x = \mathrm{col}(x_1, x_2, \ldots, x_p)$ and $u = \mathrm{col}(u_1, u_2, \ldots, u_m)$ is then given by

$$\dot{x} = (I \otimes A - L \otimes B)x + (M \otimes E)u, \quad y = (W^{\frac{1}{2}} R^T \otimes I)x, \quad (1)$$

where L is the *Laplacian matrix* of the graph G and the matrix M encodes the leaders, with $M_{ij} = 1$ if $i = v_j$ and 0 otherwise. The output of the system is the *weighted edge disagreement* where R is the incidence matrix and of the graph G, and W is a diagonal matrix with the corresponding edge weights on its diagonal, satisfying $L = RWR^T$. We assume that the graph is *connected* and *undirected*. We further assume that the network reaches consensus for zero input, i.e. that the state of each agent converges to a common trajectory. This is the case if and only if $A - \lambda_i B$ is Hurwitz for all nonzero eigenvalues λ_i of L.

A *nonempty subset* of the set of nodes V is called a *cell*. A collection of cells $\pi = \{C_1, C_2, \ldots, C_k\}$ is called a *partition* of G if $\cup_{j=1}^{k} C_j = V$ and $C_i \cap C_j = \emptyset$ if $i \neq j$. The *characteristic matrix* P of a partition π satisfies $P_{ij} = 1$ if $i \in C_j$ and zero otherwise. A partition π is called *almost equitable* if for any $p, q \in \{1, 2, \ldots, k\}$ with $p \neq q$ it holds that

$$\sum_{v\in N_i \cap C_q} a_{iv} = \sum_{v\in N_j \cap C_q} a_{jv}$$

for all $i, j \in C_p$. This means that the sum of the weights of the edges connecting an agent in a cell C_p to agents in the cell C_q is equal for all agents in C_p.

Given a partition π with characteristic matrix P, the reduced order system obtained by *clustering* the agents according to π is given by

$$\begin{aligned} \dot{\hat{x}} &= (I \otimes A - (P^T P)^{-1} P^T L P \otimes B)x + ((P^T P)^{-1} P^T M \otimes E)u, \\ \hat{y} &= (W^{\frac{1}{2}} R^T P \otimes I)\hat{x}, \end{aligned} \quad (2)$$

where $\hat{L} = (P^T P)^{-1} P^T L P$ is the Laplacian of a *reduced order*, *weighted*, and *directed* graph $\hat{G}$ with node set $\hat{V} = \{1, 2, \ldots, k\}$. The main result of this abstract now follows.

Theorem. *Let π be an almost equitable partition of G, let S be the transfer matrix of the original system* (1) *and $\hat{S}$ that of the reduced system* (2)*. The reduced system then reaches consensus and the* relative model reduction error *satisfies*

$$e(\pi) = \frac{||S - \hat{S}||_2^2}{||S||_2^2} = \frac{||S||_2^2 - ||\hat{S}||_2^2}{||S||_2^2} \leq \frac{S_{\max}}{S_{\min}} \frac{\sum_{i=1}^{m}(1 - \frac{1}{|C_{v_i}|})}{m(1 - \frac{1}{p})}$$

where $|C_{v_i}|$ is the number of nodes in the cell of leader i, $S_{\max} = \max_{\lambda\in\sigma(L)\setminus\sigma(\hat{L})} ||\bar{S}_\lambda||_2^2$, and $S_{\min} = \min_{\lambda>0\in\sigma(L)} ||\bar{S}_\lambda||_2^2$, where $\bar{S}_\lambda$ is the transfer matrix of the auxiliary system

$$\dot{\bar{x}} = (A - \lambda B)\bar{x} + Eu, \quad y = \sqrt{\lambda}\bar{x}.$$

References

[1] N. Monshizadeh H.L. Trentelman and M.K. Camlibel, "Projection based model reduction of multi-agent systems using graph partitions", *IEEE Transactions on Control of Network Systems*, vol. 1, no. 2, pp. 145-154, 2014.

[1]Johann Bernoulli Institute for Mathematics and Computer Science, University of Groningen, P.O. Box 407, 9700 AK Groningen, The Netherlands

Reducing truncation errors by low order augmentation of the observer model for flexible systems

K.W. Verkerk
Department of Electrical Engineering - Control Systems group
Eindhoven University of Technology
P.O. box 513, 5600 MB Eindhoven, The Netherlands
k.w.verkerk@tue.nl

1 Introduction

An observer can be used in high precision control of flexible systems to increase the achievable feedback control bandwidth [1]. As the real flexible system contains a large amount of modes, it is required to truncate the model used in the observer. This truncation will introduce model mismatch which increases the estimation error, specifically during acceleration trajectories. This abstract describes a method to reduce the model mismatch in the frequency region of interest with a minimum increase in the order of the observer model.

The flexible systems considered are assumed to be in modal state space form,

$$\Sigma \left\{ \begin{array}{rcl} \dot{\eta} & = & \begin{bmatrix} \mathbf{0} & \mathbf{I} \\ -\Omega^2 & -2\zeta\Omega \end{bmatrix} \eta + \begin{bmatrix} \mathbf{0} \\ \Phi_a^T \end{bmatrix} u \\ y & = & \begin{bmatrix} \Phi_s & \mathbf{0} \end{bmatrix} \eta \end{array} \right. \tag{1}$$

Here, $\eta = \begin{bmatrix} \eta_1 & \dots & \eta_N & \dot{\eta}_1 & \dots & \dot{\eta}_N \end{bmatrix}^T$ denotes the modal state vector, Ω is a diagonal matrix containing the N modal frequencies in ascending order, $\Phi_s \in \mathbb{R}^{p\times N}$ describes the mapping from each mode to each of the p outputs, $\Phi_a \in \mathbb{R}^{m\times N}$ describes the mapping from each of the m inputs to each mode, $\zeta \in \mathbb{R}^{N\times N}$ is the modal damping matrix, and $\mathbf{0}$ and $\mathbf{I}$ are respectively zero and identity matrices of appropriate dimensions.

The limiting factor on feedback bandwidth stems from the first few flexible modes and thus one would like to use an observer model containing only $n < N$ modes. The structure of (1) can be easily truncated to the appropriate number of modes. Unfortunately the higher modes, that are discarded by the truncation, do affect the system transfer function at low frequencies too, thereby introducing model error in the observer. By suitably selecting augmentation dynamics for the truncated model this mismatch can be reduced.

2 Augmentation dynamics

For low frequencies the $n_d = N - n$ discarded modes can be described by a constant gain. The dynamics of the discarded modes are given by,

$$\Sigma_d \left\{ \begin{array}{rcl} \dot{\eta}_d & = & \begin{bmatrix} \mathbf{0} & \mathbf{I} \\ -\Omega_d^2 & -2\zeta_d\Omega_d \end{bmatrix} \eta_d + \begin{bmatrix} \mathbf{0} \\ \Phi_{ad}^T \end{bmatrix} u \\ y_d & = & \begin{bmatrix} \Phi_{sd} & \mathbf{0} \end{bmatrix} \eta_d \end{array} \right. \tag{2}$$

where all matrices are truncations of the system matrices in (1). The DC gain, K, of (2) is given by,

$$\begin{aligned} K &= \begin{bmatrix} \Phi_{sd} & \mathbf{0} \end{bmatrix} \left(- \begin{bmatrix} \mathbf{0} & \mathbf{I} \\ -\Omega_d^2 & -2\zeta_d\Omega_d \end{bmatrix} \right)^{-1} \begin{bmatrix} \mathbf{0} \\ \Phi_{ad}^T \end{bmatrix} \\ &= \begin{bmatrix} \Phi_{sd} & 0 \end{bmatrix} \begin{bmatrix} 2\left(\Omega_d^2\right)^{-1}\zeta_d\Omega_d & \left(\Omega_d^2\right)^{-1} \\ -I & 0 \end{bmatrix} \begin{bmatrix} 0 \\ \Phi_{ad}^T \end{bmatrix} \\ &= \Phi_{sd}\left(\Omega_d^2\right)^{-1}\Phi_{ad}^T \end{aligned} \tag{3}$$

where $\Phi_{sd} \in \mathbb{R}^{p\times n_d}$, $\Phi_{ad} \in \mathbb{R}^{m\times n_d}$, and $\Omega_d \in \mathbb{R}^{n_d\times n_d}$.

The matrix K can be added as a direct feedthrough term to the truncated model. Alternatively, a low pass structure can be used to keep the observer model strictly proper. From the matrix dimensions in (3) it follows that rank $(K) = r \leq \min(n_d, m, p)$. By taking the singular value decomposition (SVD) of K one obtains $K = U\Sigma V^T$, where $U \in \mathbb{R}^{p\times r}$, $V \in \mathbb{R}^{r\times m}$ are both unitary and $\Sigma \in \mathbb{R}^{r\times r}$ is a diagonal matrix containing the singular values. The resulting low pass augmentation dynamics of order $r \ll 2n_d$ are then given by,

$$\Sigma_z \left\{ \begin{array}{rcl} \dot{z} & = & -\omega_c \mathbf{I} z + \omega_c V^T u \\ y_z & = & U\Sigma z \end{array} \right. \tag{4}$$

where $\omega_c > \omega_n$ is the cut-off frequency of the low pass filters.

When parameter dependency is present in the system (2) this method can still be applied. The DC gain (3) will become parameter dependent as well. By grouping the known parameter dependencies at the input or output matrices it is possible to take the SVD and obtain parameter independent low pass augmentation dynamics that are pre or post multiplied by a parameter dependent matrix.

References

[1] K.W. Verkerk, H. Butler, P.P.J. v.d. Bosch, “Improved tracking accuracy for high precision systems through estimation of the flexible dynamics”, submitted for the European Control Conference, Linz 2015

A linear systems perspective for clustering of complex networks

Michael T. Schaub
Department of Mathematics
University of Namur
5000 Namur
Belgium
michael.schaub@uclouvain.be

Jean-Charles Delvenne
ICTEAM
Université catolique de Louvain
1348 Louvain-la-Neuve
Belgium

Renaud Lambiotte
Department of Mathematics / naXys
University of Namur

Mauricio Barahona
Department of Mathematics
Imperial College London

1 Introduction

The problem of network clustering, or community detection, has received large interest over recent years. Given a network, the task is to partition this system into modules (or communities) of nodes which are 'quasi-decoupled' such there are few interactions between nodes of different groups. For networks generated from high-dimensional, relational datasets this task is akin to clustering the data into meaningful subgroups. For networked systems of dynamical units, the hope is further that by finding such a decomposition one can gain additional insight into the behavior of the system in terms of a reduced, simplified description based on the found modules. Given the prevalence of system descriptions in form of networks, applications of this problem exist in a variety of different areas, cutting through disciplines.

2 Network Clustering from a linear systems perspective.

Community Detection and graph clustering methods have been mainly defined from a structural (combinatorial) point of view. Popular methods to find modular structure include Newman's and Girvan's modularity [1], which aims to find modules in (static) graphs which have a high density of internal links (compared to some expected density described by a null model), or spectral methods which arise when minimizing some form of (normalized) cut in the network (see for instance Ref. [2]).

Here we develop a dynamical perspective on community detection based on assessing the time-evolution of a (marginally) stable linear time invariant system, exemplified by a consensus dynamics, taking place on the network. We show how by comparing the transient responses of the system to localized impulses applied at the nodes, we can effectively decompose the system into groups of nodes which dynamically affect the system in a similar way. Our derivations emphasize a geometric picture in the state space, in which nodes are clustered together if the trajectories resulting from the localized impulse inputs at these nodes are close in state space after a given time horizon.

Interestingly, this dynamical viewpoint can be shown to generalize a number of community detection algorithms proposed in the literature. Notably, Modularity [1] (and variants thereof) and spectral clustering [2] arise as special cases of this formalism for a particular time scale. We can thus give an interpretation of these methods in terms of a consensus dynamics, or its dual random walk based process.

While diffusion based approaches on network clustering have already received some attention in the literature (see e.g. [3, 4]), our generic linear systems perspective provides an increased flexibility for the construction of specific quality functions for network clustering as it can be constructed from any (marginally) stable linear dynamics and can thus be adapted to the specific problem under investigation. In particular, we highlight how using a consensus-like linear dynamics enables us to naturally define a dynamical network clustering measure for signed graphs, containing both positive and negative edge-weights.

References

[1] Newman, M. E. J. & Girvan, M. "Finding and evaluating community structure in networks", (2004), *Phys. Rev. E*, 69, 026113.

[2] Shi, J. & Malik, J. "Normalized cuts and image segmentation", (2000), *IEEE Transactions on Pattern Analysis and Machine Intelligence*, 22, 888-905

[3] Delvenne, J.-C., Yaliraki, S. N. & Barahona, M. "Stability of graph communities across time scales", (2010), *Proceedings of the National Academy of Sciences*, 107, 12755-12760

[4] Nadler, B., Lafon, S., Coifman, R. R. & Kevrekidis, I. G. "Diffusion maps, spectral clustering and reaction coordinates of dynamical systems", (2006), *Applied and Computational Harmonic Analysis*, 21, 113 - 127

ADM1 model reduction and parameter estimation

Giannina Giovannini[1,2], Mihaela Sbarciog[1], Gonzalo Ruiz-Filippi[2], Alain Vande Wouwer[1]
[1]Service d'Automatique, Université de Mons, B-7000, Mons, Belgium.
[2]Escuela de Ingeniería Bioquímica, Pontificia Universidad Católica de Valparaíso, Valparaíso, Chile.
giannina.giovannini, mihaelaiuliana.sbarciog, alain.vandewouwer@umons.ac.be, gonzalo.ruiz@ucv.cl

1 Introduction

Recent increases in environmental pollution and regulations for pollutant minimization have raised the need for new and effective methods to treat waste. In this context, Anaerobic Digestion (AD) is an environmentally sustainable technology of great interest since it converts a variety of wastes into energy in the form of biogas. In spite of the many advantages the AD technology provides, it is still not used at its full potential, due to the high complexity of the process. Therefore, an important step towards an optimal operation is a better understanding of the interplay between the process dynamics and the operational conditions, which may be achieved by means of a reliable model. In this study we obtain a simple model for AD processes using model reduction techniques and maximum likelihood method for identification. A prerequisite in the model development is the inclusion of widely available measurements in real waste treatment plants. Moreover, this study proposes a simplified model which includes the hydrogen gas concentration as a key variable, which can give important information about the stability of the reactor in fast and effective way.

2 Model Development

One of the most detailed model available for AD processes is the ADM1 model, which may be customized for a wide variety of wastes and plant configurations. From a control and optimization viewpoint however, ADM1 is not practical due to its complexity. Therefore it is used as a virtual reactor to generate data. In this study, the Maximum Likelihood Principal Component Analysis (MLPCA) [1] method is used to develop a simplified model of the ADM1. MLPCA is a systematic, optimization-based, model reduction procedure, which takes into account the noise corrupting the data. Firstly, it provides the minimum number of macroscopic reactions necessary to represent at best a given data set. Secondly, it provides an estimate of the stoichiometric matrix. Kinetics parameters are estimated using maximum likelihood method for identification procedure. The developed model describes the dynamics of 7 state variables: two substrates, the organic matter S_1 and the volatile fatty acids S_2; two biomasses, the acid-forming bacteria X_1 and the methane producing bacteria X_2; three biogases, methane CH_4, hydrogen H_2 and carbon dioxide CO_2.

In order to preserve the greatest possible variability and consequently obtain a model which is able to work on a wide range of operational conditions, the data is obtained from simulations with the ADM1 model exposed to changes in dilution rate (D) and influent organic matter S1_in. Moreover, each variable was corrupted with an independent, normally distributed, additive white noise.

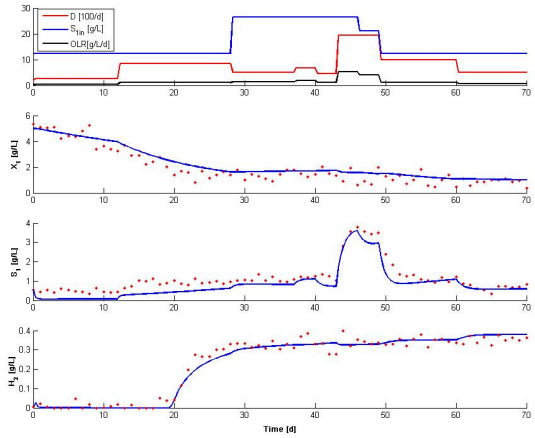

Figure 1: Noisy-experimental data (dots) and reduced-model simulated variables (solid lines). Upper graph shows the changes in the applied S1_in, dilution rate (D), and the applied organic loading rate (OLR). Due to space limitation only three state variables are shown.

3 Conclusion

The results obtained with MLPCA technique shows that the complex dynamics of the ADM1 model can be approximated with only 7 state variables and 2 growth-associated reactions. Hence, a reasonable sized model for optimization and control was obtained. In addition, a good estimation of the kinetic and stoichiometric parameters leads to an accurate prediction of the process state variables.

4 Acknowledgments

This paper presents research results of the Belgian Network DYSCO (Dynamical Systems, Control, and Optimization), funded by the Interuniversity Attraction Poles Programme, initiated by the Belgian State, Science Policy Office.

References

[1] J. Mailier, M. Remy, and A. Vande Wouwer. Stoichiometric identification with maximum likelihood principal component analysis. *Journal of mathematical biology*, 67(4):739–765, 2013.

Model reduction for greenhouse climate control

Simon van Mourik
Farm Technology Group
Wageningen University
P.O. Box 16 6700 AA Wageningen
The Netherlands
simon.vanmourik@wur.nl

Irineo Lopez-Cruz
Dept. of Agricultural Engineering
Chapingo University
Mexico
irineo.lopezcruz@wur.nl

Peter van Beveren
Farm Technology Group
Wageningen University
The Netherlands
peter.vanbeveren@wur.nl

Eldert van Henten
Farm Technology Group
Wageningen University
The Netherlands
eldert.vanhenten@wur.nl

1 Introduction

Predictive climate models are widely used to study climate control of greenhouse and storage rooms [1, 2]. A wide range of models can be used to describe climate spatiotemporal behavior, such as Computational Fluid Dynamics [3], partial differential equation models [4], and differential equation models [5, 6]. A general problem for control design is model complexity, either causing computational troubles, or resulting in a model format that is not suitable for classic controller design [7]. Model reduction techniques such as time scale decomposition, linearization, transfer function approximation, and LQG balancing are well known, but their effect on model predictive power is hard to foresee.

2 Material and methods

We investigated the opportunities of model reduction for greenhouse climate control by comparing a dynamic nonlinear mechanistic model against a severely reduced static linear regression model, in order to predict temperature, humidity, and carbon-dioxide concentration as a function of 16 variables related to outdoor climate and control actions. The prediction error (mean squared error weighted with sensor noise) of both models was assessed using a data set containing a one year time series of measurements of climate and inputs in 5 minute intervals. The parameters of both models were optimized using training data.

3 Results

With 100 days of training data, the linear regression model had poorer predictions on average over a 30 day period. With 200 days of training data, the prediction accuracy of both models was comparable. Surprisingly, the number of severe prediction errors was smaller for the reduced model. Changing the sample time from 5 to 30 minutes did not alter these results.

4 Discussion

These preliminary findings do not invalidate elaborate mechanistic modelling, but merely indicate that model simplification does not necessarily result in loss of predictive power, especially when online sensor measurements are available for parameter calibration.

References

[1] Gerrit Van Straten, Gerard van Willigenburg, Eldert van Henten, and Rachel van Ooteghem. *Optimal control of greenhouse cultivation*. CRC press, 2010.

[2] Simon van Mourik. *Modelling and control of systems with flow*. PhD thesis, University of Twente, 2008.

[3] Davide Piscia, Juan I Montero, Esteban Baeza, and Bernard J Bailey. A CFD greenhouse night-time condensation model. *Biosystems Engineering*, 111(2):141–154, 2012.

[4] S van Mourik, H Zwart, and KJ Keesman. Switching input controller for a food storage room. *Control Engineering Practice*, 18(5):507–514, 2010.

[5] PJM Van Beveren, J Bontsema, G Van Straten, and EJ Van Henten. Minimal heating and cooling in a modern rose greenhouse. *Applied Energy*, 137:97–109, 2015.

[6] BHE Vanthoor, C Stanghellini, EJ Van Henten, and PHB De Visser. A methodology for model-based greenhouse design: Part 1, a greenhouse climate model for a broad range of designs and climates. *Biosystems Engineering*, 110(4):363–377, 2011.

[7] Hans Zwart, Simon van Mourik, and Karel Keesman. Switching control for a class of non-linear systems with an application to post-harvest food storage. *European Journal of Control*, 16(5):567–573, 2010.

Denial of Service in Distributed Control and Communication Systems

Danial Senejohnny
d.senejohnny@rug.nl

Pietro Tesi
p.tesi@rug.nl.

Claudio De Persis
Faculty of Mathematics and Natural Sciences, University of Groningen, The Netherlands
c.de.persis@rug.nl

1 Abstract

Recent years have witnessed a growing interest towards cyber-physical systems (CPSs), i.e. systems with a tight conjoining of computational and physical resources. Their field of application is immense, ranging from autonomous vehicles and supply chains to power and transportation networks. Many of these applications are safety-critical. This has triggered considerable attention to networked systems in the presence of attacks, bringing the question of cyber-security into filtering and control theories [1], [2].

As argued in [1], [2] security in CPSs drastically differs from security in general-purpose computing systems. In CPSs, attacks can in fact cause disruptions that transcend the cyber realm and affect the physical world. For instance, if a critical process is open-loop unstable, failures in the plant-controller communication network can result in environmental damages.

In a networked control system, malicious attacks to the communication links can be classified as either false data injection attacks or denial-of-service (DoS) attacks. The former affects the integrity of data by manipulating the packets transmitted over the network, while the latter affects the availability of data by causing packet losses.

This work is concerned with DoS attacks in networked control systems. Specifically, we consider a consensus-like control network [3], in which the communication medium is vulnerable to attack; the attacker objective is to prevent consensus by denying communication among the agents. The problem of interest is that of finding conditions under which consensus can be preserved.

Inspired by [4], [5], we consider a general attack model that only constrain the attacker action in time by posing limitations on the frequency of DoS attacks and their duration. This makes it possible to capture many different types of DoS attacks, including trivial, periodic, random and protocol-aware jamming [6]-[8].

By introducing the notion of Persistence of Communication (PoC), we provide an explicit characterization of the frequency and duration of DoS attacks under which consensus is not destroyed.

In addition to generalizing the conclusions of [4], [5] to a distributed setting of practical relevance, the results provide several insights into the design of control policies that achieve robustness against failures of the communication medium. An example is finally provided to substantiate the analysis.

References

[1] A. Cardenas, S. Amin, and S. Sastry, Secure control: towards survivable cyber-physical systems, Proc. of The 28-th International Conference on Distributed Computing Systems Workshops, 2008.

[2] Y. Mo, T. Hyun-Jin Kim, K. Brancik, D. Dickinson, H. Lee, A. Perrig, and B. Sinopoli, Cyber-physical security of a smart grid infrastructure, Proceedings of the IEEE, vol. 100, pp. 195-209, 2012.

[3] C. De Persis and P. Frasca, Robust self-triggered coordination with ternary controllers, IEEE Trans. on Automatic Control, vol. 58, pp. 3024-3038, 2013.

[4] C. De Persis and P. Tesi, Resilient control under denial-of-service, in Proceedings of the IFAC World Congress, Cape Town, South Africa, 2014.

[5] C. De Persis and P. Tesi, On resilient control of nonlinear systems under denial-of-service, in Proceedings of the IEEE Conference on Decision and Control, Los Angeles, CA, USA, 2014.

[6] D. Thuente and M. Acharya, Intelligent jamming in wireless networks with applications to 802.11b and other networks, Proc. 25th IEEE Communications Society Military Communications Conference, Washington, DC, USA, 2006.

[7] W. Xu, W. Trappe, Y. Zhang, and T. Wood, The feasibility of launching and detecting jamming attacks in wireless networks, ACM International Symposium on Mobile Ad-Hoc Networking & Computing, 2005.

[8] B. De Bruhl and P. Tague, Digital filter design for jamming mitigation in 802.15.4 communication, in Int. Conf. on Computer Communications and Networks, Maui, Hawaii, 2011.

Diffusion Efficiency on temporal networks

Martin Gueuning
Naxys / ICTEAM
University of Namur / UCLouvain
Rempart de la Vierge 8, 5000 Namur
Belgium
Email: martin.gueuning@unamur.be

Renaud Lambiotte
Department of Mathematics / naXys
University of Namur
Rempart de la Vierge 8, 5000 Namur
Belgium
Email: renaud.lambiotte@unamur.be

Jean-Charles Delvenne
Ecole Polytechnique de Louvain/ ICTEAM
Universite Catholique de Louvain
Avenue George Lemaitre 4-6 , 1348 Louvain-la-Neuve
Belgium
Email: jean-charles.delvenne@uclouvain.be

1 Introduction

In this work, we are looking at an epidemic-like propagation process on a network of agents. We suppose that the time between two consecutive meetings is random and described by a given inter-meeting time probability distribution, which is typically a power-law for human-related networks ([1]), and that at each meeting an infected individual transmits the disease to his/her neighbours with some probability p.
The goal is to determine the effective inter-event time distribution of the underlying process, that is the distribution of the time it takes for an individual to transmit the disease/information to his/her neighbour once he/she is infected. Knowing this allows us to compare different behaviour showing same characteristics such as the mean time between two successful transmissions but driven by different inter-meeting time distribution, leading to an optimal trade-off between single message-efficiency and sending activity.

2 Results

Working in the Laplace domain and with probability generating function, one can analytically determine the first and second moments of the inter-event time distribution, that directly give the mean and variance of this process, in function of p and the moments $\langle \tau^k \rangle$ of the inter-meeting time distribution.
From these results, we obtain some important values of this diffusion process such as the average relay time, which is a standard measure of the burstiness of a process ([2]):

$$\bar{\tau} \quad = \quad 1 + p\left(\frac{\langle \tau^2 \rangle}{2\langle \tau \rangle^2} - 1\right).$$

Once recovery is taken into account, we can find the transmissibility $\mathbb{P}$ of the diffusion, which is the overall probability that individual transmits the infection before recovery. In the case of a tree-network, relevant to study the early-phase of diffusion for instance, the reproduction number R_0, giving the epidecmic treshold for the diffusion, equals to $\mathbb{P}\langle n \rangle$, where $\langle n \rangle$ is the mean degree of the nodes. We also find that for a given average time $\frac{\langle \tau \rangle}{p}$ between two infectious contacts, rarer (high $\langle \tau \rangle$) but more 'efficient' contacts (high p) lead to less bursty (low relay time) but more transmissible contacts, that is higher probability of transmitting the disease before recovery once infected.
Ongoing work indicates that optimal trade-off between single-message efficiency and sending intensity may be determined analytically given some arbitrary cost function.

3 Conclusion

In this work, we could determine important values such a average relay time or transmissibility of an epidemic-like propagation process taking place on a network of agents. We find that the mean time between two successful transmissions is not sufficient to characterize the diffusion speed of the epidemics, as between two agents with the same mean time of successful transmission, the one with fewer but more efficient contacts has a higher transmissibility for the disease, that is a higher probability of transmitting the disease to his/her neighbours before recovery.

References

[1] A. L. Barabasi (2005). "The origin of bursts and heavy tails in human dynamics", Nature, 435(7039), 207-211.

[2] M. Kivela *et al.* (2012). "Multiscale analysis of spreading in a large communication network," Journal of Statistical Mechanics: Theory and Experiment, 2012(03), P0300

[3] R. Lambiotte *et al.*, "Burstiness and spreading on temporal networks," European Physical Journal B. Condensed Matter and Complex Systems, (2013).

Game-theoretic approach for optimal contract design in railway networks

Zhou Su, Bart De Schutter, Simone Baldi
Delft Center for Systems and Control
Delft University of Technology
2628 CD, Delft
the Netherlands
z.su-1@tudelft.nl

1 Introduction

Since the privatisation of Dutch railways, the maintenance of the railway infrastructure is performed by private contractors, whose short-term objectives are not always fully aligned with the long-term objectives of the infrastructure manager, ProRail, and conflicts arise from such misalignment of interests. Game theory provides mathematical analysis techniques for situations in which two or more decision makers, called players, make decisions that influence the objective of the other player(s) [1].
A particular setting, the principal-agent model [2], considers situations with conflicting objectives and asymmetric information, which is suitable to investigate the interactions between ProRail and the contractors under a performance-based maintenance contract. The overall aim of this work is to develop new methodologies for optimal contract design that can also be applied to other situations similar to the maintenance of Dutch railways, i.e. large infrastructure networks like road and water networks.

2 Problem formulation

As a starting point, we focus on the bilateral contractual relationship between ProRail and one contractor, resulting in a single-principal-single-agent model. We view all the maintenance activities of a contractor within one maintenance period as a single maintenance task, and consider no repetitions of the maintenance task at the moment, so the situation is modelled as a one-shot game.
The primary concern of the principal, also the contract designer in the context, is how to design incentives to induce the agent to align its objectives to that of the principal. The incentive considered in our problem takes the form of a payment scheme, which specifies the monetary transfer from the principal to the agent according to a quantitative performance output, i.e. a payment scheme can be fully represented by the pair of performance output and monetary transfer. Under this context, the principal's decision is the value of the monetary transfer to the agent, while the agent's decision is the effort level applied to achieve a desired performance output. Uncertainty, i.e. the performance achieved by an agent subjects to random effects imposed by nature, is also considered by applying a Bayesian-game approach to the problem.
The principal suffers from information asymmetry due to inaccessibility to the agent's private information relevant to the outcome of the game, e.g. cost structure; this game-relevant private information of an agent is called "type" in principal-agent literature. It is also assumed that the principal has an a priori estimation of the probability distribution of the agent's type. Under assumption on the finiteness of the type space and of the decision space of both the principal and the agent, the optimal contract design problem can be reduced to a linear programming problem.

3 Conclusions and future work

This work presents an initial game-theoretic modelling framework to tackle the real world problem of optimal contract design in railway networks that is able to capture the essence of the relationship between ProRail and the contractor under a performance-based contract. However, the static one-shot setting suppresses the rich dynamics typical to large networks like railways, so the next step would be to apply a dynamic setting, e.g. combing the principal-agent framework with a Markov decision process. Another extension is to consider multi-agent setting.

Acknowledgement

Research sponsored by the NWO/ProRail project "Multi-party risk management and key performance indicator design at the whole system level (PYRAMIDS)", project 438-12-300, which is partly financed by the Netherlands Organisation for Scientific Research (NWO).

References

[1] R.B. Myerson, "Game Theory: Analysis of Conflict," Harvard University Press, 1997.

[2] J.J. Laffont, and D. Martimort, "The Theory of Incentives: The Principal-Agent Model," Princeton University Press, 2009.

New approaches of Černý's Conjecture

François Gonze
ICTEAM, UCLouvain
1348, Louvain la Neuve
Belgium
francois.gonze@uclouvain.be

Raphaël M. Jungers
ICTEAM, UCLouvain
1348, Louvain la Neuve
Belgium
raphael.jungers@uclouvain.be [1] [2]

1 Introduction

We present results about *synchronizing automata*. This subject appeared in computers and relay control systems in the 60s. The aim was to restore control over these devices without knowing their current state. It later found applications in industry and biology. A complete introduction and a survey of the recent developments is given in [1].

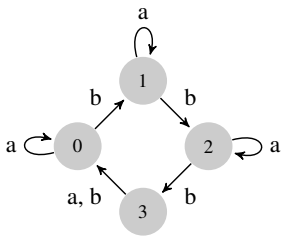

Figure 1: A synchronizing automaton.

In a few words, a (deterministic, finite state, complete) automaton (DFA) is composed by a set of *states* Q, an alphabet of *letters* Σ and a *transition function* $\delta : Q \times \Sigma \to Q$. A *word* is a sequence of letters. This word is called *synchronizing* if it maps any state onto a single one. An automaton having such a word is called *synchronizing automaton*. Figure 1 gives an example of such an automaton with $Q = \{0,1,2,3\}$, $\Sigma = \{a,b\}$ and transition function shown by the edges. The word *abbbabbba* maps any state onto state 0.

More than 40 years ago, Jan Černý's conjectured in [2] that any synchronizing automaton with n states has a synchonizing word of length not higher than $(n-1)^2$. Although it has a simple formulation, this conjecture remains open. We analyse here a game theoretical approach of the problem, and propose an easier concept, the *triple rendezvous time*.

2 Synchronizing Probability Function

In [3], the synchronization of an automaton is reformulated as a two-player game with the following rules. A length t is chosen beforehand. Player Two chooses the states of the automaton and keeps it secret. Player One then chooses a word of length at most t, which is applied to the automaton, and guesses what the final state is. If he is right, he wins, otherwise Player Two wins. Choosing a synchronizing word would ensure him the win. Thereby, the *synchronizing probability function* $k(t)$ is defined as the best probability of Player One to win the game, depending on the length t.

It turns out that the synchronizing probability function can be computed using a linear program. From linear programming properties, many new results regarding synchronizing automata were deduced (see [3]).

3 Triple Rendezvous Time

The *triple rendezvous time* T_3 is defined as the length of the shortest word mapping three of the states of the automaton onto a single one. It is an intermediate step toward synchronization, and a good indication of the length of a synchronizing word. In the example of Figure 1, the word *abbba* maps states 0, 3 and 2 to state 0, and $T_3 = 5$. We are going to search for bounds on T_3 depending on the number of states of the automaton.

When $t < T_3$, the synchronizing probability function $k(t)$ of the automaton can only take some particular values. Using this property, we obtained in [4] the following upper bound on the triple rendezvous time for an automaton with n states:

$$T_3 \leq \frac{n(n+4)}{4} - \frac{n \bmod 2}{4}.$$

On the other hand, in [4], we present a family of automata such that $T_3 = n+3$, which provides a lower bound for the maximal triple rendezvous time.

References

[1] Volkov, M. V., Synchronizing Automata and the Černý Conjecture, Proceedings of LATA'08, 11-27, Springer-Verlag, 2008.

[2] Černý, J. and Pirická, A. and Rosenauerova, B., On directable automata, Kybernetica, 7, 289-298, 1971

[3] Jungers, R. M., The synchronizing probability function of an automaton, SIAM Journal on Discrete Mathematics, 26, 177-192, 2012

[4] F. Gonze and R. M. Jungers, On the Synchronizing Probability Function and the Triple Rendezvous Time for Synchronzing Automata, ArXiv preprint. http://arxiv.org/abs/1410.4034, 2014

[1] R. M. Jungers is a F.R.S.-FNRS Research Associate

[2] This work was also supported by the communauté francaise de Belgique - Actions de Recherche Concertées and by the Belgian Program on Interuniversity Attraction Poles initiated by the Belgian Federal Science Policy Office.

A Centrality-Based Security Game for Multi-Hop Networks

James R. Riehl and Ming Cao
University of Groningen
{j.r.riehl, m.cao}@rug.nl

1 Introduction

We present a new analysis of multi-hop network security in the form of a game played between an attacker who tries to disrupt a network by disabling one or more nodes, and the nodes of the network who must allocate limited resources in defense of the network.

Using social network analysis to improve the performance and robustness of physical networks is a relatively new area of research. In [1], the authors studied the effects of coordinated attacks on wireless mesh networks and showed that targeting and disabling the nodes with the highest betweenness centrality results in a more effective attack than targeting based on degree. However, this strategy might easily be predicted and thwarted by a smart defender. Game theory offers solutions that are best-suited to such competitive settings and for this reason has become a valuable tool in the study of network security [2]. We formulate here a topological network security problem as a two-player zero-sum game and present fast algorithms to compute Nash equilibrium strategies for both the attacker and defender.

2 Problem Setup

Consider a multi-hop network with n nodes and a possibly time varying edge set where an attacker tries to disrupt a network and the nodes must coordinate to defend such an attack. We begin by observing that in general both attack and defense of a network require some finite amount of resources. For example, a distributed denial of service (DDoS) attack requires energy and bandwidth from multiple coordinating attackers in an effort to deplete the memory or bandwidth resources of the targeted system. Similarly, such an attack can be defended by adding memory or bandwidth capacity to vulnerable nodes in the network [3]. Initially, we assume the attacker has enough resources to disable one undefended node of the network and the defender has enough resources to defend one node against such an attack.

The strategies for the attacker and defender thus correspond to attack and defense of each node in the network: $\mathcal{A} = \mathcal{D} = \{1, 2, \ldots, n\}$. An undefended attack results in removal of that node from the network, while a defended attack results in no change to the network. The cost of node removals can be modeled by various network performance metrics, which often correspond to centrality measures. For example, an attacker who wants to disrupt the most paths in a network using a shortest-path routing protocol should attack the node with the highest betweenness centrality. Likewise, the defender should defend this node. However, it is not quite that simple because the attacker knows the defender is likely to defend that node and vice versa. These competitive dynamics are modeled nicely by a two-person zero-sum game with the following payoff matrix:

$$A = \begin{bmatrix} 0 & -a_1 & \cdots & -a_1 \\ -a_2 & 0 & \cdots & -a_2 \\ \vdots & \vdots & \ddots & \vdots \\ -a_n & -a_n & \cdots & 0 \end{bmatrix} \tag{1}$$

where a_i denotes the performance loss to the network resulting from the disabling of node i, and the attacker and defender are row and column players, respectively.

3 Nash Equilibrium Strategies

Let $\mathbf{y}$ and $\mathbf{z}$ denote the mixed strategies of the attacker and defender, respectively. The strategy pair forming a saddle-point or Nash equilibrium of the zero-sum game is given by the solution to the following minimax problem:

$$v^* = \min_{\mathbf{y} \in \mathcal{A}} \max_{\mathbf{z} \in \mathcal{D}} \mathbf{y}^T A \mathbf{z}. \tag{2}$$

By the minimax theorem, a unique saddle-point equilibrium v^* always exists and the corresponding strategies can be computed by solving a pair of linear programming problems for the attacker and defender. However, exploiting the structure of the payoff matrix allows us to construct an algorithm that runs in near linear time in the size of the network.

4 Current Work

Both the centrality and minimax computations require information exchange between nodes which may be subject to constraints or time delays, and the attacker may also not have perfect information. We now seek equilibrium strategies based purely on local information. We are also considering the case of multiple-node attacks, which scales exponentially in computation with the number of nodes.

References

[1] M. Kas, S. Appala, C. Wang, K. M. Carley, L. R. Carley, and O. K. Tonguz, "What if wireless routers were social?" *Wireless Communications, IEEE*, vol. 19, no. 6, pp. 36–43, 2012.

[2] Z. Han, D. Niyato, W. Saad, and A. Hjørungnes, *Game theory in wireless and communication networks: theory, models, and applications*. Cambridge University Press, 2011.

[3] S. Arunmozhi and Y. Venkataramani, "A new defense scheme against ddos attack in mobile ad hoc networks," in *Advanced Computing*. Springer, 2011, pp. 210–216.

Off-line optimization of baker's yeast production process

Anne Richelle
3BIO-BioControl
Université Libre de Bruxelles
1050, Brussels
Belgium
arichell@ulb.ac.be

Philippe Bogaerts
3BIO-BioControl
Université Libre de Bruxelles
1050, Brussels
Belgium
philippe.bogaerts@ulb.ac.be

1 Introduction

In a fed-batch production context, the determination of optimum operating conditions consists of the definition of a feeding time profile optimizing a cost function (optimization criterion) while taking into account all the constraints of the process. Dynamic optimization allows the computation of this profile by solving an optimization problem formulated as a pre-defined performance index (e.g. yield, productivity). When the process model is known and relatively simple, this problem can be solved analytically by applying the principle of the Pontryagin minimum. But for more complex models, the dynamic optimization problems continue to present a challenge to researchers today.

In this study, a macroscopic model [2] was used for the determination of optimal feeding time profiles in carbon and nitrogen sources for a fed-batch baker's yeast production process in the sense of a production criterion. To this end, two different approaches were used and compared with numerical and experimental data: a control vector parameterization approach with mesh refinement and an approach based on the mathematical analysis of optimal operating policy (semi-analytical approach) [3].

2 Optimization criterion

In this work, the optimization criterion is the total amount of biomass obtained at the end of the culture ($J_{VX}(F^{in}) = V(t_f)X(t_f)$) under the following constraints: the duration of the culture t_f is fixed, the initial operating conditions are known, the total amount of available substrates for the culture is fixed and the feeding rate F^{in} is bounded.

3 Control parameterization approach with mesh refinement

To solve this dynamic optimization problem, a vector parameterization method of the control variable was used to approximate the feed rate. The infinite dimensional optimization problem is then approximated as a problem with a finite set of control actions:

$F^{in}(t) = F^{in}(j), t_j \leq t \leq t_{(j+1)}$where $j = 1 : N$ and N is the number of partitions of the feeding rate $F^{in}(t)$. In order to approximate the feeding profile with the greatest accuracy possible while reducing the number of parameters for which an initial value must be provided, a mesh refinement was considered. This refinement is an increasing discretization on an iterative way allowing a multiple repetition of optimization steps with an increasing number of partitions N.

4 Approach based on the mathematical analysis of optimal operation

In general, it is theoretically possible to define the optimization problem by simpler sub-problems that can be solved analytically. This approach allows the determination of a feeding profile close to the optimum and, also, often limits the number of parameters characterizing the optimization problem [1]. In this work, feeding profile sequences similar to [1] are defined in order to cause an ethanol peak during the culture while ensuring maximum process efficiency.

5 Conclusions

The results of the two approaches lead to the determination of similar optimal operation conditions which are very similar to the profiles obtained by industrial manufacturers through an empirical optimization of the process (trial-and-error method). The feeding time profiles in nitrogen and glucose found through optimization have been applied experimentally. In accordance with the optimization goal, the final biomass has been increased. Moreover, the model predictions are in good accordance with experimental data.

References

[1] J.M. Modak, H.C. Lim, and Y.J. Tayeb, Y.J. General characteristics of optimal feed rate profiles for various fed-batch fermentation processes. Biotechnology and Bioengineering, 28(9):1396-407, 1986.

[2] A. Richelle, P. Fickers and Ph. Bogaerts. Macroscopic modelling of baker's yeast production in fed-batch cultures and its link with trehalose production. Computers and Chemical Engineering, 61:220-233, 2014.

[3] A. Richelle and Ph. Bogaerts. Off-line optimization of baker's yeast production process. Chemical Engineering Science, 119:40-52, 2014.

Metabolic flux analysis using a convex analysis approach

Sofia Fernandes[1], Georges Bastin[2], Alain Vande Wouwer[1]
[1]Service d'Automatique, Université de Mons,
31 Boulevard Dolez, 7000 Mons, Belgium
(sofia.afonsofernandes and alain.vandewouwer@umons.ac.be)
[2]Cesame, Université catholique de Louvain,
av. G. Lemaitre 4, B1348 Louvain-La-Neuve, Belgium
(Georges.Bastin@uclouvain.be)

1 Introduction

Metabolic flux analysis (MFA) has been a subject of intense research for almost two decades. It is a useful tool to estimate *in vivo* metabolic fluxes in, among others, mammalian cell cultures [1].

In this study, a metabolic network with 72 biochemical reactions and $m = 45$ internal metabolites is considered and MFA is applied in order to determine the intracellular fluxes. Due to an insufficient number of extracellular measurements, the classical pseudo-steady state assumption (no accumulation of internal metabolites) leads to an underdetermined system of algebraic equations and a unique solution cannot be computed. To overcome this problem, a convex analysis approach can be used [2], which considers a mass balance system around intracellular metabolites and for the measured extracellular species, as follows:

$$\begin{pmatrix} N_i & 0 \\ N_m & -v_m \end{pmatrix} \times \begin{pmatrix} v \\ 1 \end{pmatrix} = 0 \qquad (1)$$

In this expression, v is the flux distribution, N_i is the stoichiometric matrix deduced from the metabolic network, N_m is the matrix connecting the fluxes to the available measurements and v_m represents the specific uptake and excretion rates of the measured extracellular species.

2 Results

In our study, system (1) is not redundant ($rank(N_i) = m = 45$), and with the information provided by 23 extracellular measurements from experiments with hybridoma HB58 cells in batch/perfusion cultures [4], it is underdetermined with a degree of freedom of 4. The solution set is a polytope in the positive orthant and each admissible flux distribution v can be expressed as a positive interval $v_i^{min} \leq v_i \leq v_i^{max}$, which can be calculated using the toolbox METATOOL [3].

The objective of our study is to investigate the influence of the batch and perfusion operating modes on the metabolic flux intervals. Figure 1 shows a sample of the results, e.g., the bounded flux intervals obtained over the perfusion phase for the tricarboxylic acid cycle.

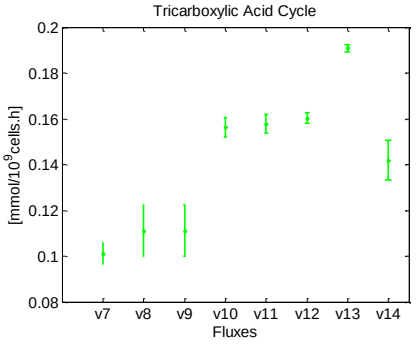

Figure 1: TCA bounded fluxes over perfusion phase.

Acknowledgements

This paper presents research results of the Belgian Network DYSCO (Dynamical Systems, Control, and Optimization), funded by the Interuniversity Attraction Poles Programme initiated by the Belgian Science Policy Office. The authors are very grateful to Dr. Niu Hongxing for providing the experimental data.

References

[1] G.Stephanopoulos, A.A.Aristidou, J.Nielsen. Metabolic Engineering: Principles and Methodologies. Academic Press, San Diego, 1998.

[2] A. Provost and G. Bastin. Dynamic metabolic modelling under the balanced growth condition. *Journal of Process Control*, 14(7):717-728, 2004.

[3] T. Pfeiffer, I. Sánchez-Valdenebro, J. C. Nuño, F. Montero, S. Schuster. Metatool: for studying metabolic networks. *Bioinformatics*, 15(3):251-257, 1999.

[4] N. HongXing, Z. Amribt, P. Fickers, W. Tan, P. Bogaerts. Metabolic pathway analysis and reduction for mammalian cell cultures_Towards macroscopic modeling. *Chemical Engineering Science*, 102:467-473, October 2013.

Mathematical modelling of overflow metabolism in hybridoma cell cultures by Flux Balance Analysis

Khadija Mhallem Gziri, Anne Richelle and Philippe Bogaerts
Unit of Biomodelling and Bioprocesses
Université Libre de Bruxelles
Department of General Chemistry and Biosystems
Av. F.-D. Roosevelt 50 C.P. 165/61
B-1050 Brussels
kmhallem@ulb.ac.be; arichell@ulb.ac.be; Philippe.Bogaerts@ulb.ac.be

1 Abstract

To legitimate overflow metabolism modelling in hybridoma cell cultures, a Flux Balance Analysis (FBA) model is developed. It is based on the assumption that the cells behave so as to maximize biomass growth. Based on a limited number of reactions and measurements, and using three linear constraints, the resulting intracellular fluxes are in agreement with the overflow metabolism [1, 2].

2 Introduction

Many popular models describe cell cultures are with macroscopic kinetics of extracellular subtrates and products, ignoring the intracellular metabolism. Others models have been developed the last decades to take this into account. These models, metabolically structured, include the FBA approach. The original contribution of FBA is based on an evolutionnary hypothesis. Indeed it assumes that the cells evolve to respond to a certain objective function [3, 4].
Among all the pharmaceutical cell cultures, the mammalian ones are widely used for production of complex protein pharmaceuticals and viral vaccines. Their highest benefit stay in their ability of complex post-translational modifications on the produced protein unlike microbial systems [1].
Hybridoma cells are mammalian cells used for production of very specific monoclonal antibodies. Their energy metabolism is a substrate-concentration-dependent overflow metabolism. Indeed the overflow concentrations of carbon and nitrogen substrates increase by-product formation and very little carbon enters the energy metabolism, also known as the tricarboxylic acid cycle (TCA). Moreover, these by-products are often inhibitory for the cell culture [1, 2].
This contribution aims at better understanding the intracellular behaviour of hybridoma cell cultures in overflow metabolism.

3 Contribution

In this study, data of four fed-batch cultures of hybridoma cell line HB-58 producing IgG1 monoclonal antibodies are used. It is composed of the measurements of the biomass, two substrates (glucose and glutamine) and two products concentrations (lactate and ammonia). The same data have already been used to develop a macroscopic model [1].
In accordance with the literature on mammalian cells, the metabolic network takes into account the following metabolisms: a central metabolism constituted of glycolysis, glutaminolysis pathway and TCA cycle, the pentose phosphate and the nucleotide synthesis pathways. It involves 24 reactions and 21 metabolites [4].
Based on this metabolic network, the proposed FBA model assumes that the cells evolve to maximise the biomass production. This latter is deduced from the nucleotide synthesis. The constraints are the two input fluxes of substrates and also an upper bound on the flux of oxaloacetate in the TCA cycle. The results show, more interestingly, the production of by-products and very small entry in the TCA cycle during the overflow metabolism. It also shows the shift of cell metabolism once glucose and glutamine are depleted. Moreover, the profiles of extracellular metabolites are well simulated in direct and cross-validation. These results are obtained without any a priori information about the different phases of the culture and without using any indicator of overflow.

References

[1] Z. Amribt, H. Niu, P. Bogaerts, "Macroscopic modelling of overflow metabolism and model based optimization of hybridoma cell fed-batch cultures," A Biochemical Engineering Journal, vol. 70, pp. 196-209, 2013.

[2] M. Doverskog, J. Ljunggren, L. Ohman, L. Häggström, "Physiology of cultured animal cells," Journal of Biotechnology, vol. 59, pp. 103-115, 1997.

[3] E. P. Gianchandani, A. K. Chavali, J. A. Papin, "The application of flux balance analysis in systems biology," Wiley Interdiscip Rev Syst Biol Med, vol. 2, pp. 372-382, 2010.

[4] A. Provost, G. Bastin, S. N. Agathos, Y.-J. Schneider, "Metabolic design of macroscopic bioreaction models: application to Chinese hamster ovary cells," Bioprocess and Biosystems Engineering, vol. 29, pp. 349-366, 2006.

Dynamic metabolic flux analysis in metabolic networks: a non-linear dynamic optimization approach

P. Nimmegeers, D. Vercammen, F. Logist and J.F.M. Van Impe
BioTeC, Department of Chemical Engineering, KU Leuven
W. de Croylaan 46 PB 2423, B-3001 Heverlee (Leuven), Belgium
{philippe.nimmegeers, filip.logist, jan.vanimpe}@cit.kuleuven.be

1 Introduction

Micro-organisms play an important role in industry, e.g. food industry (avoid growth of pathogens and food spoilage) and industrial biotechnology (stimulate growth for production of high added value products). Therefore a good insight in the biochemical reactions (fluxes) inside micro-organisms enables model based monitoring, control and optimization of bioprocesses.

An important tool in systems biology are metabolic reaction networks in which the knots represent the metabolites (chemical substances produced or/and consumed in the micro-organisms) and the connections indicate the reaction fluxes between those metabolites.

2 Problem statement

The analysis of the metabolic fluxes in steady state conditions is already well known in literature [3, 4]. *Metabolic Flux Analysis (MFA)* and *Flux Balance Analysis (FBA)* are two well-known methods that are used for the estimation and prediction respectively of the intracellular fluxes. However, these techniques are mainly developed for steady state conditions.

When considering transient phenomena, it is needed to grasp the dynamic behavior of the fluxes. Therefore techniques of *dynamic Metabolic Flux Analysis (dMFA)* [6] and *dynamic Flux Balance Analysis (dFBA)* [2] are developed. For these methods data from dynamic experiments are needed for the estimation of these fluxes. These data can originate from measurements of exchange fluxes between the cell and its environment or from measurements from ^{13}C labelling experiments.

Recent *dMFA* approaches [1, 2] have some drawbacks, i.e.: *(i)* the obtained flux profiles are not smooth, *(ii)* chemically relevant constraints (e.g. irreversibility constraints) cannot be taken into account and a basis for the null space of the stoichiometric matrix has to be chosen [1, 6].

In this paper an alternative *dMFA* approach [6] for the estimation of the intracellular fluxes, is adopted and validated with example metabolic networks.

3 Results

The presented method in this work is based on a B-spline parameterization of the fluxes. State-of-the-art methods and tools are used for the dynamic optimization problems that are encountered in this *dMFA* approach, i.e., automatic differentiation with CasADi, interior point optimization with IPOPT and an orthogonal collocation scheme. For the validation of this method, several case studies involving (des)activation in metabolic networks are investigated in an ideal theoretical setting without noise and in a more realistic setting with randomly sampled noise for which Monte Carlo simulations are used.

Acknowledgements. Work supported in part by Project PFV/10/002 (OPTEC Optimization in Engineering Center) of the Research Council of the KU Leuven, KU Leuven Knowledge Platform SCORES4CHEM (www.scores4chem.be), FWO KAN2013 1.5.189.13, FWO-G.0930.13 and the Belgian Program on Interuniversity Poles of Attraction initiated by the Belgian Federal Science Policy Office. The authors assume scientific responsibility.

References

[1] M.R. Antoniewicz, "Dynamic metabolic flux analysis: tools for probing transient states of metabolic networks," Current Opinion in Biotechnology, 24(6): 973-978, 2013.

[2] R.W. Leighty, and M.R. Antoniewicz, "Dynamic metabolic flux analysis (DMFA): a framework for determining fluxes at metabolic non-steady state," Metabolic Engineering, 13(6):745-755, 2011.

[3] F. Llaneras, and J. Picó, "Stoichiometric modelling of cell metabolism," Journal of Bioscience and Bioengineering, 105(1):1-11 2008.

[4] J.D. Orth, I. Thiele, and B.Ø. Palsson, "What is flux balance analysis?," Nature Biotechnology, 28(3):245-248, 2010.

[5] J.F. Van Impe, D. Vercammen and E. Van Derlinden, "Toward a next generation of predictive models: a systems biology primer," Food Control, 29(2):336-342, 2013.

[6] D. Vercammen, F. Logist, and J. Van Impe, "Dynamic estimation of specific fluxes in metabolic networks using non-linear dynamic optimization," BMC Systems Biology, 8:132-154, 2014.

On Biological Feasibility of Solutions in a Novel Mathematical Model for Testosterone Regulation

Hadi Taghvafard, Anton V. Proskurnikov and Ming Cao
ENTEG, Faculty of Mathematics and Natural Sciences,
University of Groningen, The Netherlands
{h.taghvafard, a.v.proskurnikov, m.cao}@rug.nl

1 Introduction

The study of hormonal regulatory processes and their mathematical modeling is essential to identify the culprits in their dysfunction and elaborate effective prophylaxis and medical treatment against them. In this paper, we deal with a model for testosterone regulation, important to understand mechanisms of the prostate cancer and reproductive failures. This model was originally proposed in [1]; in the recent paper [2], it was demonstrated that the real hormonal concentrations in a patient during a day really obey this model, replacing the continuous Hill-type nonlinearity with a pulse modulator.

The model from [1] involves concentrations of three hormones: testosterone (Te), produced in testes, and the luteinizing hormone (LH) and gonadotropin-releasing hormone (GnRH), produced in different parts of the brain. The secretion of GnRH stimulates that of LH which, in turn, stimulates the production of Te, while Te inhibits the secretion of GnRH. There is, however, experimental evidence that testosterone also inhibits the production of LH [3], for which direct negative feedback was not taken into account in [1, 2]. The models of biochemical oscillators usually employ Hill-type nonlinearities to express the negative feedback. At the same time, presence of multiple nonlinearities in Goodwin-type models dramatically complicates their dynamics; the applicability of many criteria for the stability and the existence of cycles (e.g. those from [2]) remains open problem. This motivates us to introduce a novel model for testosterone regulation, employing a *linear* negative feedback from Te to LH. This feedback, however, breaks the positivity of the system and gives rise to the question which solutions are biologically feasible, staying in the positive octant. In this paper, we give sufficient conditions for such feasibility.

2 The Mathematical Model in Question

Like the models from [1, 2], our model involves three variables $R(t), L(t), T(t)$ standing for the serum concentrations of the GnRH, LH and testosterone, respectively. These concentrations obey the following differential equations:

$$\begin{cases} \dot{R} = f(T) - b_1 R, \\ \dot{L} = g_1 R - b_2 L - cT, \\ \dot{T} = g_2 L - b_3 T. \end{cases} \tag{1}$$

The constants $b_1, b_2, b_3 > 0$ describe clearing rates of the hormones; the constants $g_1, g_2 > 0$ and the positive and non-increasing function $f(\cdot)$ determine the rates of their secretion. The mapping $f(\cdot)$ may be smooth, piecewise-smooth or even generalized function describing the pulse modulator [2], assuming the solution exists and unique for any initial conditions. The crucial difference between the model (1) and those from [1, 2] is the term $-cT$ in the second equation, where $c \geq 0$. For $c = 0$ our model coincides with Smith's model, whereas $c > 0$ corresponds to the additional negative feedback from Te to LH and makes the system non-positive.

3 Solution Feasibility

Since functions $R(t), L(t), T(t)$ stand for the chemical concentrations, the minimal feasibility requirement for them is to be positive and bounded. Whereas positivity is easily proved for any initial conditions, since $f(T)$ is bounded (see [2] for similar proof), the positivity can no longer be guaranteed for arbitrary initial conditions. In this paper, we outline the class of solutions that remains bounded and thus biologically feasible. Our main result is as follows.

Theorem. Assume that $R(0), L(0), T(0) > 0$ and

$$b_2 < b_3; c < \frac{(b_3 - b_2)^2}{4g_2}; \frac{T(0)}{L(0)} < \min\left\{ \frac{2g_2}{b_3 - b_2}, \frac{b_3 - b_2}{2c} \right\}.$$

Then $R(t), L(t), T(t) > 0$ for any $t > 0$. Thus for any compact $D \subset (0, +\infty)^3$, all the solutions emanating from D are positive, provided $b_2 < b_3$, $g_2 > 0$ is large and $c > 0$ is small.

References

[1] W.R. Smith. "Hypothalamic regulation of pituitary secretion of luteinizing hormone-II. feedback control of gonadotropin secretion". *Bull. Math. Biol.*, 42(1980) 57-78.

[2] A. Churilov, A. Medvedev, A. Shepeljavyi, "Mathematical model of non-basal testosterone regulation in the male by pulse modulated feedback", *Automatica*, 45(2009) 78-85.

[3] C.B. Scheckter, A.M. Matsumoto, W.J. Bremner, "Testosterone administration inhibits gonadotropin secretion by an effect directly on the human pituitary", *J. of Clin. Endocrinology and Metabolism*, 68 (1989) 397-401.

Identification of Linear Time Varying Systems using 2D Regularization

Péter Zoltán Csurcsia, Johan Schoukens, John Lataire
Vrije Universiteit Brussel, Pleinlaan 2, 1050 Elsene, Belgium
Email: peter.zoltan.csurcsia@vub.ac.be

1 Introduction

This paper presents a methodology to obtain an impulse response function ($h_{LTV}[t][\tau]$) estimate of a time varying system using 2D regularization . Unlike the linear time invariant systems where the impulse response function is unique, the time varying impulse response is not restricted to only one solution. Assume that the length of input and output is N, then the possible variations for the impulse response function are N^2. Hence there is no unique impulse response function that relates the input to the output, because there are only N linear relations for $O(N^2)$ unknowns. The user can impose additional constrains to decrease this freedom. In the proposed case smoothness and exponential decaying are used over the system time t (direction of the impulse responses, referring to the behavior) and smoothing constraint is used over the global time τ (referring to the system memory). The excess degrees of freedom can be removed using these constains [1][3].

2 An example

In this Section a measurement example is observed. A second order slowly time varying band-pass filter is examined with sampling frequency (denoted by f_s) of 625 kHz. A frequency domain representation is shown in Fig.1. The total length of the measurement consists of 62520 samples. The filter is excited by a frequency limited odd random phase multisine [2]. The input and output signals are band limited. Fig. 2. shows the results of this method compared with the frequency domain approach using FDTVident (Frequency Domain Time Varying identification) toolbox [4] and B-splines [3], respectively. This comparison is also made for the ordinary least squares estimation considering that the underlying system is LTI (the selected model order is L=200). This can give an idea about what happens if the time variations are not taken into account.

3 Summary

In this work a powerful time domain estimation method is developed for smooth LTV systems. This technique is illustrative, flexible, user friendly.
With respect to the system dynamics using the proposed method, it is possible 1) to reduce the model order 2) to decrease the effect of the disturbing noise.

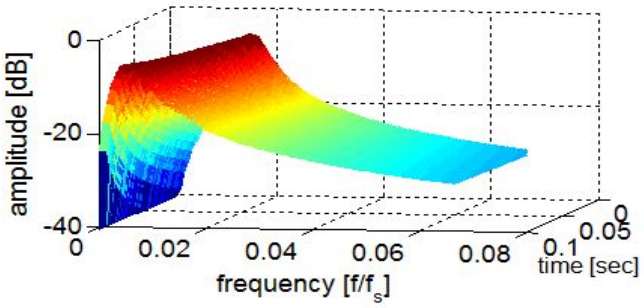

Figure 1: Representation of the measured systems frequency response function.

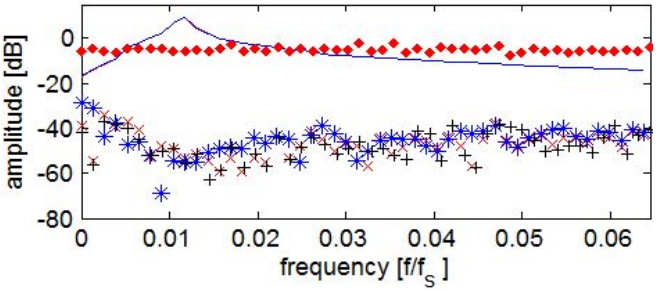

Figure 2: The solid lines shows the measurement output in the frequency domain. The crosses (x) are the modeling errors between the FDTVident and the measured outputs, the asterisks (*) are the modeling error for the B-spline fitting, the plus signs (+) are the modeling errors for the regularized estimation fitting, the rhombuses (♦) are the Least Squeares modeling errors.

References

[1] G. Pillonetto, F. Dinuzzo, T. Chen, G. De Nicolao, and L. Ljung, "Kernel methods in system identification, machine learning and function estimation: A survey," Automatica, vol. 50, no. 3, pp. 657-682, 2014

[2] R. Pintelon, J. Schoukens: "System identification, a frequency domain approach, second edition" New Jersey, 2012

[3] P.Z. Csurcsia, J. Schoukens: "Nonparametric Estimation of a Time-variant System: an Experimental Study of B-splines and the Regularization Based Smoothing," I2MTC, accepted for publication, 2015

[4] J. Lataire, R. Pintelon, E. Louarroudi: "Nonparametric estimate of the system function of a time-varying system," Automatica, pp. 666-672, April 2012

Identification for Control of High-Tech Motion Systems

Robbert Voorhoeve, Tom Oomen
Eindhoven University of Technology, Department of Mechanical Engineering, Control Systems Technology group,
PO Box 513, 5600MB Eindhoven, The Netherlands, e-mail: r.j.voorhoeve@tue.nl

1 Background

In the near future the requirements for motion control will become much tighter. To meet these future demands, it is envisaged that active control of flexible dynamics is required, including the use of additional actuators and sensors. This implies that the number of inputs and outputs is likely to increase, as well as the order of the relevant flexible dynamics. As a result, a model-based approach based on parametric models is a natural approach for a systematic design of controllers for such complex systems.

Although the theory and design of model-based controllers for motion systems is well-developed, the modeling task still poses a major challenge in practice. System identification is the natural approach for the modeling of such systems, since it is inexpensive, fast, and accurate. However, the identification of parametric models, as is typically required for model-based control, remains rather challenging for these high-precision motion systems.

One of the challenging aspects is the numerical reliability of the identification algorithms. This is evidenced by the fact that a significant number of approaches to address numerical implementation have been developed, including frequency scaling, amplitude scaling and the use of orthonormal basis functions. More recently, a numerically reliable identification approach was proposed based on the use of orthonormal basis functions with respect to a discrete, data-dependent inner product [1]. In this work, an extension of this approach is investigated and showcased on a high quality dataset of a vibration isolation system.

2 Approach

A recently introduced algorithm for frequency domain parametric system identification is the IV-algorithm [2]. Essentially, the computational aspect of this algorithm involves solving linear equations of the form $C^H A\theta = C^H b$. The matrices C and A, and their conditioning, depend on the choice of basis functions used to parameterize the model. Recently the use of a bi-orthonormal basis has been introduced [3], which is bi-orthonormal with respect to the bi-linear form

$$\langle \psi_i(\xi),\, \phi_j(\xi) \rangle := \sum_{k=1}^{m} \psi_j^H(\xi_k) w_{2k}^H w_{1k} \phi_i(\xi_k), \qquad (1)$$

where the weights w_{1k} and w_{2k} are the weights in C and A. Theoretically, this basis leads to optimal numerical conditioning of the system of equations, i.e., $\kappa(C^H A) = 1$. In this work we implemented and experimentally investigated this technique as well several pre-existing solutions for the identification of a high tech motion system.

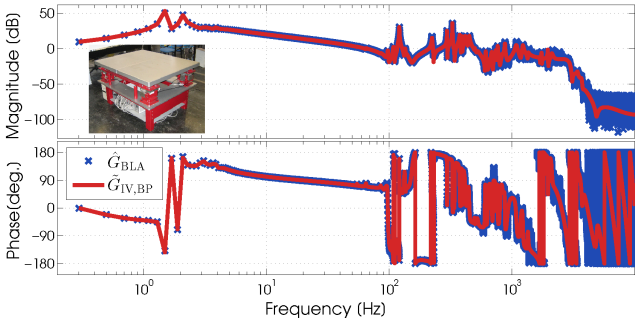

Figure 1: Non-parametric estimate of $G_{\mathrm{BLA}\,1,1}$ (blue) and the fitted model (red)

3 Results

An extensive MIMO dataset has been measured on an active vibration isolation system using full random orthogonal multisines to measure the best linear approximation [4].

Figure 1 shows the non-parametric estimate of $G_{\mathrm{BLA}\,1,1}$ as well as a 100^{th} order model, identified using the approach described in section 2. As can be seen in this Figure, the identified model is in good agreement with the non-parametric data. The geometric mean condition number during iterations, using the bi-orthonormal basis, was $\overline{\kappa} = 2$, indicating good numerical reliability. For reference, the IV algorithm using a monomial basis yields $\overline{\kappa} = 1 \cdot 10^{154}$, or $\overline{\kappa} = 2 \cdot 10^{18}$ for a scaled monomial basis. For these reference solutions, the algorithm did not converge and sub-optimal results were obtained. That these numerical issues are already present in the SISO case, shows the relevance and challenge of numerically reliable identification.

4 Ongoing work

Related to the work presented here, further research is currently being done on the following topics:

- position dependent modal modeling,
- control relevant modeling, and
- further extensions of the bi-orthormal basis function implementation (MIMO) and theory.

References

[1] Bultheel, A., van Barel, M., Rolain, Y., and Pintelon, R. (2005). Numerically robust transfer function modeling from noisy frequency domain data. *IEEE Transactions on Automatic Control*, 50(11), 1835-1839.

[2] Blom, R. and van den Hof, P. (2010) Multivariable frequency domain identification using iv-based linear regression. In *Proc. of the 49th IEEE Conference on Decision and Control*, 1148-1153.

[3] van Herpen, R., Oomen, T., and Steinbuch, M. (2014). Optimally conditioned instrumental variable approach for frequency-domain system identification. *Automatica*, 50(9), 2281-2293.

[4] Pintelon, R. and Schoukens, J. (2012). System Identification: A Frequency Domain Approach. *Wiley-IEEE press*, second edition.

Measuring nonlinear distortions: from test case to an F-16 Fighter

M. Vaes[1], J. Schoukens[1], Y. Rolain[1], B. Peeters[2], J. Debille[2], T. Dossigne[3], J.P Noël[3], C. Grappasonni[3], G. Kerschen[3]

[1] Vrije Universiteit Brussel (VUB), Dept. ELEC [2] Siemens Industry Software, Leuven, Belgium

[3] Space Structures and Systems Lab, Aerospace and Mechanical Engineering Department University of Liège, Belgium

mark.vaes@vub.ac.be

1 Introduction

What are the similarities and differences between the behavior of a small vibrating test system and an F-16 fighter? To find it out, we compare measurements of the test system to measurements from the bolted connection of the wing and the missile of a F-16 Fighter Falcon from the Belgian air force. These measurements were done during a ground vehicle test (GVT) campaign. Essentially, the behavior of these systems match, even though the test system is only the heart of a self-study kit for nonlinear system identification and the F-16 is a complex real life mechanical structure. This clearly shows the added value of an experiment driven nonlinear educational system identification package. It provides safe small-scale toy examples for hands-on exercises that react like real systems. We believe that this practical approach lowers the gap between learning system identification concepts and applying it on real systems.

2 Methodology

The mechanical systems are first excited by a multisine signal with a low measured amplitude. The frequency response function (FRF) is a rather smooth curve with resonance frequencies. When the amplitude is slightly increased, the FRF does not change. The system behaves like a typical linear time invariant (LTI) system (Figure 1, dark grey).
Increasing the amplitude of the input signal further makes the FRF depart from this value for both systems as the nonlinear distortions pop up.

In Figure 1 the resonance frequency of the FRF is shifting to the left for both systems. This shows a softening effect. Note also the increased noise and amplitude change.
Adapting the input signal empowers detection, quantification, and qualification of nonlinear distortions and the measurement noise [1][2]. What is the gain? Interpretation of these FRF's leads to a better understanding of both systems and can be of great importance for the practitioner. Odd nonlinear distortion can be detected which lies at the origin of the changes in both dynamics of the system (Figure 2).

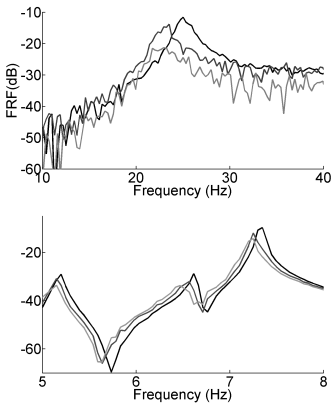

Figure 1: FRF Measurement with increasing amplitude (Dark to light grey). Up: Test case system ; Down: F-16 fighter

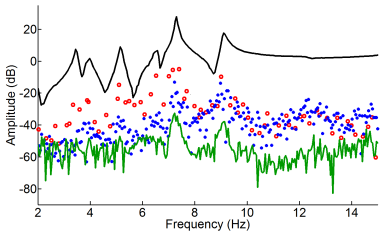

Figure 2: Detect, quantify and qualify nonlinear distortions of an F-16 Fighter: black: FRF, blue: even NL, red: odd NL, Green:noise

3 Application

An example where this knowledge is of great importance is in the case of GVT campaigns. In GVT mostly, LTI-based methods are used to identify the resonance frequencies and predict flutter of an aircraft. If the system contains odd nonlinear distortions, this becomes very dangerous to asses damping as the dynamics of the system is changed.
An F-16 and the test system look pretty much alike indeed, the kit prepares practitioners to tackle real-world problems.

References

[1] R. Pintelon and J. Schoukens, *System Identification, A Frequency Domain Approach.*, IEEE Press, New York (2012).

[2] J. Schoukens, R. Pintelon and Y. Rolain, *Mastering System Identification in 100 Exercises*, IEEE Press, New York (2012).

Study of the Control of a UAV/UGV Cooperative System Manipulating an Object

Tam Nguyen
Université Libre de Bruxelles
tanguyen@ulb.ac.be

Emanuele Garone
Université Libre de Bruxelles
egarone@ulb.ac.be

1 Abstract

This contribution focuses on the control of a heterogeneous system composed of an Unmanned Aerial Vehicle (UAV) and an Unmanned Ground Vehicle (UGV). The two units need to cooperate to manipulate an object (see Figure 1). The UAV and UGV are both subject to saturation constraints. The objective is to design a control law able to steer the system to a configuration of equilibrium. It is assumed that no communication is exchanged between the two vehicles and that only angle sensors are used.

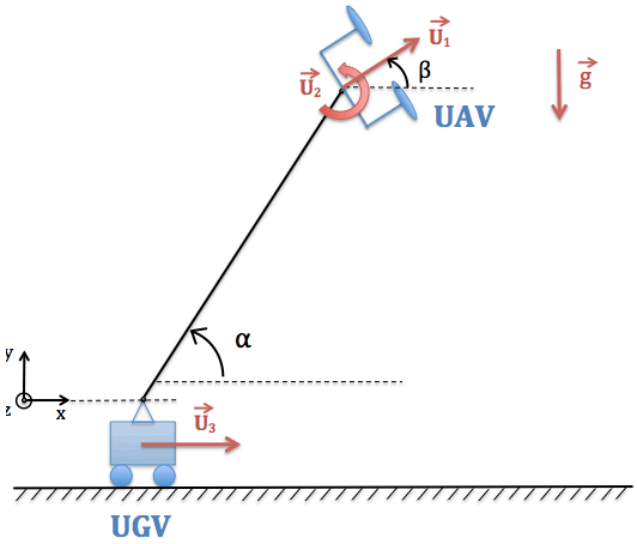

Figure 1: 2D-planar model. $\vec{U}_1, \vec{U}_2$ and $\vec{U}_3$ are the actuated forces. x, α and β are the generalized coordinates.

To study the system, the first step consists in developing a model using the Euler-Lagrange approach. Then, the attainable points of equilibrium of the system are determined by taking into account the saturation of the actuators. This set of points depends on the maximum thrust of the UAV, its mass and the mass of the beam. On the basis of this analysis, a control strategy is proposed. Such strategy is based on three main ideas:

1. The reference attitude of the UAV is fixed and is a function of the beam angle
2. The energy consumption of the UAV is minimized
3. The beam is moved to the desired angle using U_1 and U_3

Points 1 and 2 are achieved by defining a continuous function $\beta_{ref} = f(\alpha)$. The boundaries of this function must satisfy the following conditions on U_1:

- Its tangential component is zero when the beam is vertical
- Its normal component is zero when the beam reaches its limit angles

A PD controller is used to control the attitude. Point 3 is achieved using a PD controller with gravity compensation and assuming that the attitude loop is fast enough.

The stability of the automated system is proven using ISS arguments and the small gain theorem. The use of a reference governor is proposed to ensure constraints satisfaction during the transients.

References

[1] Nonlinear Systems, Second Edition, Hassan K. Khalil

Compact representations of large dynamical systems based on low-rank tensor approximations

Martijn Boussé*† martijn.bousse@esat.kuleuven.be

Otto Debals*†‡ otto.debals@esat.kuleuven.be

Lieven De Lathauwer*†‡ lieven.delathauwer@kuleuven-kulak.be

*Department of Electrical Engineering (ESAT) STADIUS Center for Dynamical Systems, Signal Processing and Data Analytics, KU Leuven, Kasteelpark Arenberg 10, 3001 Leuven, Belgium. †Group Science, Engineering and Technology, KU Leuven Kulak, E. Sabbelaan 53, 8500 Kortrijk Belgium. ‡iMinds Medical IT, KU Leuven, Kasteelpark Arenberg 10, 3001 Leuven, Belgium.

Large dynamical systems appear in many applications, e.g., home monitoring systems in biomedical sciences based on wireless body area networks, electroencefalography (EEG) or electrocorticography (ECoG) with high spatial resolution and more recently neural probes/dust. Other applications can be found in wireless communications, e.g., large-scale sensor array processing and massive MIMO systems. In all of these cases, many sensors are located closely together, resulting in possibly very smooth system coefficients. Consequently, the coefficients exhibit some (approximate) low-rank structure, which becomes increasingly present in the data as the sensor density grows. This structure can be exploited to obtain a compact system representation.

Higher-order tensors provide remarkable possibilities in this context. They are higher-dimensional arrays of numbers; as such, they are natural generalizations of vectors (first order) and matrices (second order) [1, 2]. Recently, the domain of multilinear algebra has received increasing attention, mostly because of the powerful tensor decompositions. These decompositions are promising models that are more powerful than linear models, but are less complex to deal with than nonlinear models. Furthermore, they have several properties that are not present in conventional matrix methods, which makes them the proper tools for a variety of applications. Moreover, multilinear algebra provides a powerful framework for the compact representation and analysis of large and possibly high-dimensional datasets, as well as alleviating or even breaking the curse of dimensionality [3].

We propose to exploit the underlying compactness of large dynamical systems by tensorizing the system coefficients and subsequently applying a low-rank approximation. As such, the system can be represented with a drastically reduced number of coefficients. A comparably strategy has proven to be very successful in the field of tensor-based scientific computing [4]. This strategy is particularly interesting in blind system identification (BSI); here, one tries to identify an unknown system based only on the measured outputs. This problem occurs in a variety of applications, such as signal processing (e.g., speech dereverberation and digital communications), image processing (e.g., astronomical or medical image restoration) and sensor array processing (e.g., (non-)uniform linear arrays, wireless communications, wireless body area networks). By applying the above strategy, the BSI problem boils down to the computation of a tensor decomposition, which can for instance be done with Tensorlab [5]. As such, we can uniquely identify large-scale systems under mild conditions. The method is deterministic; hence, it even works well when only a small number of samples are available. Moreover, only mild conditions are imposed on the inputs. Finally, the same strategy can be applied to the more simpler problem of blind source separation (BSS); here, one wants to separate unknown sources from observed signals which are unknown instantaneous mixtures of the sources, i.e., a BSI problem with no memory.

References

[1] T.G. Kolda and B.W. Bader, "Tensor decompositions and applications," *SIAM Review*, 51(3):455–500, 2009.

[2] A. Cichocki, C. Mandic, A. Phan, C. Caifa, G. Zhou, Q. Zhao, and L. De Lathauwer, "Tensor decompositions for signal processing applications. From two-way to multiway component analysis," *IEEE Signal Processing Magazine*, March 2015. (to appear).

[3] N. Vervliet, O. Debals, L. Sorber, and L. De Lathauwer, "Breaking the curse of dimensionality using decompositions of incomplete tensors: Tensor-based scientific computing in big data analysis," *IEEE Signal Processing Magazine*, 31(5):71–79, 2014.

[4] L. Grasedyck, D. Kressner, and C. Tobler, "A literature survey of low-rank tensor approximation techniques," *GAMM-Mitteilungen*, 36(1):53–78, 2013.

[5] L. Sorber, M. Van Barel, and L. De Lathauwer, "Tensorlab v2.0," 2014. Available online at http://www.tensorlab.net/.

A switched systems approach to (de–)stabilization of predator-prey tumor dynamics

Alina Doban
Eindhoven University of Technology
a.i.doban@tue.nl

Mircea Lazar
Eindhoven University of Technology
m.lazar@tue.nl

1 Abstract

In this work we consider the problem of destabilizing an undesired given equilibrium of a continuous–time predator–prey model such that the trajectories of the system converge to a desired one. The considered predator–prey model was proposed in [1] to model the competition between malignant and immune cells in cancer development and has three equilibria whose stability character depends on the parameter values of the model. The three equilibria have a direct clinical interpretation and they correspond to extinction of the normal cell population, extinction of the invading (tumor) population and to a stable co-existence of the malignant cells with the normal cells, i.e. tumor dormancy, respectively.

If the problem of maintaining a certain stable equilibrium, i.e. maintaining a stable tumor, is of interest, then this is equivalent to maintaining the tumor model states in the domain of attraction (DOA) of the tumor dormancy equilibrium. Furthermore, the trajectories of the considered system can be driven away from the DOA of an unwanted equilibrium to the DOA of the equilibrium of interest. *More specifically, in this work it will be investigated under which conditions the tumor dynamics will converge or can be steered by therapy to a stable tumor dormancy equilibrium. This will be done by means of switching between different DOA approximations.*

The predator–prey model is defined by

$$\begin{aligned} \dot{N_N} &= R_N N_N - \frac{R_N}{K_N} N_N^2 - \frac{R_N \alpha_{NT}}{K_N} N_T N_N \\ \dot{N_T} &= R_T N_T - \frac{R_T}{K_T} N_T^2 - \frac{R_T \alpha_{TN}}{K_T} N_T N_N, \end{aligned} \quad (1)$$

where N_T represents tumor cells population which interacts with the normal cells population N_N. The most relevant parameters are α_{TN}, which represents the effect of the immune response on the tumor, and α_{NT}, which represents the negative effect of the tumor on normal tissue.

Computing an estimate of the DOA for general nonlinear systems is a very complex problem. In the approach of this work Rational Lyapunov Functions (RLFs) as proposed in [2], will be used to approximate maximal Lyapunov functions. These functions tend to infinity as the system trajectories approach the DOA boundary, thus the level sets of RLFs provide the best DOA approximation [3].

We consider the problem of controlling an invasive tumor dynamics to a dormant tumor dynamics. This can be formulated as de–stabilization of an undesired equilibrium and stabilization of a different, desired equilibrium. To achieve this, we will assign a sequence of parameters that corresponds to a sequence of equilibria and we will switch among them.

A possible application of the developed stabilization strategy is therefore, treatment of an invasive tumor to achieve a dormant tumor. To this end, the model parameters used for DOA computation and switching should be linked with the effect of drugs prescribed to the patient by medical doctors.

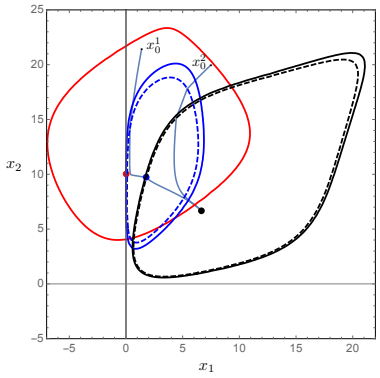

Figure 1: Estimation of the DOAs of E_1–red, E_2–blue and E_3–black together corresponding equilibrium values and two switched systems trajectories.

In Figure 1 an illustration of the proposed strategy for the considered problem is shown, where E_1, E_2 and E_3 are the three possible equilibria of the tumor model with their corresponding domains of attraction computed using RLFs. As shown in the figure, the switch is triggered whenever the trajectory initiated in the DOA corresponding to current parameter values hits the boundary of the DOA corresponding to the next parameter values in the sequence.

References

[1] R. A. Gatenby, "Models of tumor-host interaction as competing populations: Implications for tumor biology and treatment," *Journal of Theoretical Biology*, vol. 176, no. 4, pp. 447 – 455, 1995.

[2] A. Vannelli and M. Vidyasagar, "Maximal Lyapunov functions and domains of attraction for autonomous nonlinear systems," *Automatica*, vol. 21, no. 1, pp. 69–80, 1985.

[3] A. I. Doban and M. Lazar, "Domain of attraction computation for tumor dynamics," in *53rd IEEE Conference on Decision and Control (CDC)*, Los Angeles, 2014, pp. 6987–6992.

Synchronization of Goodwin-type oscillators under saturated control

Anton V. Proskurnikov and Ming Cao
ENTEG institute at the University of Groningen
a.v.proskurnikov@rug.nl; m.cao@rug.nl

Many processes in living organisms, including circadian clocks and hormonal regulation, are controlled by ensembles of biochemical oscillators, synchronized via some physical coupling. Study of these synchronization mechanism is extremely important, for instance, to understand how the stable 24h rhythm the "biological clock", or the main circadian pacemaker, is maintained by the network of intracellular genetic oscillators with periods spread between 20h and 28h; the entrainment of the circadian rhythms by the daylight cycle is also facilitated by synchronization [2].

In the recent paper [1] a first important step in examining synchronization phenomenon for biochemical oscillators has been done. A criterion for synchronization of *identical* oscillators of cyclic structure under linear diffusive couplings was proposed based on the notion of *incremental passivity*. It was shown that if the oscillator is constituted by incrementally output passive blocks, then it is incrementally feedback passive [1] (considered as whole system); the system of such oscillators renders synchronized by a static diffusive couplings, provided that its "strength" (the algebraic connectivity of the network) is sufficiently large.

The application of the criterion from [1] to most of real biochemical oscillators may, however, be troublesome, since it in fact assumes implicitly that solutions are bounded. Furthermore, to design a synchronizing protocol, one has to know passivity gains of the constituent blocks, that are to be finite and involved in the formula for the critical coupling strength. However, *finite* passivity gains may be guaranteed only in a finite domain; to choose a linear protocol, providing the solutions to stays in such a domain, is a quite nontrivial problem. Instead, we suggest another type of protocols, obtained via superposition of linear protocols from [1] with special globally bounded "saturating" nonlinearities. This allows to separate two goals: boundedness of the solution (achieved due to saturated control) and synchronization (achieved via sufficiently strong couplings). Unlike [1], the margin for the coupling strength may be found explicitly.

We confine ourselves to Goodwin-type oscillators of cyclic structure with external input.

$$\begin{array}{rclcrcl} \dot{x}_1 &=& -f_1(x_1)+g_{n+1}(y_n)+u_{ext}, & & y_1 &=& g_1(x_1), \\ \dot{x}_2 &=& -f_2(x_2)+y_1, & & y_2 &=& g_2(x_2), \\ \vdots & & & & & & \\ \dot{x}_n &=& -f_n(x_n)+y_{n-1}, & & y_n &=& g_n(x_n). \end{array} \tag{1}$$

For simplicity, we assume that all $f_i(x), g_i(x)$ are Mikhaelis-Menten nonlinearities (functions of the form $ax/(bx+c)$, where $a,c>0, b\geq 0$, which become linear for $b=0$), $g_{n+1}(x)$ is a smooth decreasing function with $g_{n+1}(+\infty)=0$.

Consider the functions h_i, given by the recursion $h_1=f_1^{-1}$, $h_2=f_2^{-1}\circ g_1\circ h_1,\ldots,\ h_n=f_n^{-1}\circ g_{n-1}\circ h_{n-1}$. We assume that $h_i(\cdot)$ are defined on $[0; g_n(0)+m_0]$, $m_0>0$. Consider a network of N identical systems (1), their state variables and inputs denoted by x_i^p, u_{ext}^p ($p=1,\ldots,N$), coupled as follows:

$$u_{ext}^j(t)=g_0(cv^j(t)),\quad v^j(t)=\sum_{k=1}^{N}a_{jk}(y_1^k(t)-y_1^j(t)). \tag{2}$$

We assume the network is undirected: $a_{jk}=a_{kj}$. Here we intentionally introduce the coupling strength c, included into a_{jk} in [1]. We adopt the following assumptions on g_0.

Assumption. The function g_0 is smooth and bounded: $0\leq g_0(-\infty)\leq g_0(+\infty)\leq m_0$. Furthermore, $g_0'(x)>0$ decreases at infinity sufficiently slowly: $c\min\limits_{|y|\leq c}g_0'(y)\to+\infty$ as $c\to+\infty$.

Theorem 1. All the solutions with $x_i^p(0)>0$ (where $i=1,\ldots,n,\ p=1,\ldots,N$) remain positive ($x_i^p(t)>0$) and bounded; their ultimate bounds are given by

$$\overline{\lim_{t\to\infty}}\,x_i^p(t)\leq \bar{x}_i^*:=h_i(g_n(0)+m_0)\ \forall i,p.$$

Furthermore, the protocol (2) synchronizes the network if $c>\bar{c}$, where $\bar{c}$ depends only on $\bar{x}_i^*$ and may be found explicitly, see the full version [3] for details.

Theorem 1 shows that for sufficiently strong couplings the protocol (2) synchronizes the network of identical oscillators (1). The crucial difference with the result in [1] is that the minimal threshold for the couplings strength $\bar{c}$ may be explicitly found and does not depend on the concrete trajectory thanks to a priori ultimate bounds for the solution.

References

[1] A. Hamadeh, G.-B. Stan, R. Sepulchre, and J. Gonçalves. Global state synchronization in networks of cyclic feedback systems. *IEEE TAC*, 2012, 57(2):478–483.

[2] D. Gonze, S. Bernard, C. Waltermann, A. Kramer, and H. Herzel, Spontaneous synchronization of coupled circadian oscillators, *Biophys. Journal*, 2005, 89, p.120–129

[3] A.V. Proskurnikov, M. Cao, Synchronization of biochemical oscillators under boundedness and nonnegativeness constraints for solutions, *IEEE TAC* (under review).

Estimation of basins of attraction for controlled systems with input saturation and time-delays

J.J. Benjamin Biemond
Department of Computer Science
KU Leuven
3000, Leuven
Belgium
benjamin.biemond@cs.kuleuven.be

Wim Michiels
Department of Computer Science
KU Leuven
3000, Leuven
Belgium
wim.michiels@cs.kuleuven.be

1 Introduction

Basins of attraction are instrumental to study the effect of input saturation in control systems, as these sets characterise the initial conditions for which the control strategy induces attraction to the desired state. We describe these sets when the open-loop system is exponentially unstable and the system is controlled by actuators with both constant time-delays and saturation. Estimates of the basin of attraction are provided and the allowable time-delay in the control loop is determined with a novel piecewise quadratic Lyapunov-Krasovskii functional that exploits the piecewise affine nature of the system.

2 System model and Lyapunov-Krasovskii functional

Consider the class of linear systems with saturating actuators modelled as

$$\dot{x}(t) = Ax(t) + Bu(t), \tag{1}$$

where $x \in \mathbb{R}^n$, $A \in \mathbb{R}^{n\times n}$, $B \in \mathbb{R}^{n\times m}$, and $u \in \mathbb{R}^m$ the inputs of the actuators that experience saturation. The inputs u experience a delay τ and are given by $u(t) = \text{sat}(Kx(t-\tau))$, $K \in \mathbb{R}^{m\times n}$ and $\text{sat}(y)_i := \text{sign}(y_i)\min(|y_i|,1)$, $i = 1,\dots,m$ for $y \in \mathbb{R}^m$. Hence, the closed-loop system is given by the nonsmooth retarded differential equation:

$$\dot{x}(t) = Ax(t) + B\text{sat}(Kx(t-\tau)). \tag{2}$$

We define the function $V_{nd} : \mathbb{R}^n \to \mathbb{R}$ as:

$$V_{nd}(x) = \bar{x}^T \bar{P}(x)\bar{x} \tag{3}$$

with $\bar{x} = \begin{pmatrix} x^T & 1 \end{pmatrix}^T$, $\bar{P}(x) := F(x)^T T F(x)$, with $F(x)$ a piecewise constant function such that $F(x)\bar{x} = \begin{pmatrix} Kx - \text{sat}(Kx) \\ x \end{pmatrix}$. Then, we can analyse the retarded differential equation (2) with the Lyapunov-Krasovskii functional

$$V(x_\tau(t)) = V_{nd}(x(t)) + W(x_\tau(t)), \tag{4}$$

with V_{nd} in (3) and a nonnegative functional, for $R \succ 0$:

$$W(x_\tau(t)) := \int_{-\tau}^{0}\int_{t+\theta}^{t} \dot{x}(\bar{s})^T K^T R K \dot{x}(\bar{s}) d\bar{s} d\theta. \tag{5}$$

3 Basin of attraction estimate

In this presentation, matrix inequality conditions are derived for A, B, K, T, τ such that the sublevelset

$$B_{oa} := \{x_\tau \in AC([-\tau, 0], \mathbb{R}^n) \mid V(x_\tau) \leq \Gamma\} \tag{6}$$

provides a basin of attraction estimate, with Γ selected such that the Lyapunov-Krasovskii functional V decreases along solutions. Then, given a predefined analysis domain D_a which contains B_{oa} in its interior, we provide an algorithm [1] to find T and Γ such that

- $V_{nd}(x) \geq 0, \forall x \in D_a$,
- $\frac{dV(x_\tau)}{dt} \leq 0$, for all x_τ such that $x_\tau(0) \in D_a \cap B_{oa} \wedge \dot{x}_\tau(0) = Ax_\tau(0) + B\text{sat}(Kx_\tau(-\tau))$
- B_{oa} is a 'large' domain.

Hence, B_{oa} is a subset of the basin of attraction.

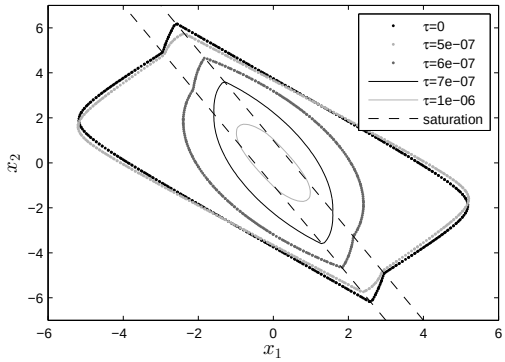

Figure 1: Basin of attraction estimates for varying τ and $A = \begin{pmatrix} 0 & 1 \\ 1 & 0 \end{pmatrix}$, $B = \begin{pmatrix} 0 \\ -5 \end{pmatrix}$, $K^T = \begin{pmatrix} 2 \\ 1 \end{pmatrix}$.

Assuming $u(s) = 0$ for $s \in [0, \tau]$, the set B_{oa} of initial functions is translated to initial conditions for x. Such estimate is shown in Fig. 1. Hence, this procedure computes delay-dependent non-ellipsoidal basins of attraction estimates using LMI-tools.

References

[1] J.J.B. Biemond, W. Michiels, "Estimation of basins of attraction for controlled systems with input saturation and time-delays" IFAC World Congress, Cape Town, 2014.

Design of periodic event-triggered control for nonlinear systems using overapproximation techniques

D.P. Borgers
Eindhoven University of Technology
The Netherlands
d.p.borgers@tue.nl

R. Postoyan
Université de Lorraine, CRAN, UMR 7039
and CNRS, CRAN, UMR 7039, France
romain.postoyan@univ-lorraine.fr

W.P.M.H. Heemels
Eindhoven University of Technology, The Netherlands
m.heemels@tue.nl

1 Introduction

We consider a dynamical system of the form

$$\dot{x} = f(x, u), \tag{1}$$

where $x \in \mathbb{R}^{n_x}$ is the state and $u \in \mathbb{R}^{n_u}$ the control input, with $n_x, n_u \in \mathbb{N}_{>0}$. We assume that a control law $u = k(x)$ is available, such that the closed loop in continuous time satisfies desired stability and performance specifications. However, on a digital platform, the control law cannot be implemented in continuous time. Instead, the input u is only updated at discrete times t_k, $k \in \mathbb{N}$, and held constant between updates, leading to

$$\dot{x}(t) = f(x(t), k(x(t_k))) = f(x(t), k(x(t) + e(t))), \tag{2}$$

for all $t \in [t_k, t_{k+1})$, where $e(t) := x(t_k) - x(t)$ is reset to zero at each sampling instant. We can write (2) as

$$\dot{z}(t) = g(z(t)), \qquad \text{for all } t \in [t_k, t_{k+1}) \tag{3}$$

$$z(t_k^+) = b(z(t_k)), \tag{4}$$

for all $k \in \mathbb{N}$, where z consists of x and e, and g and b are obtained by direct calculations.

In conventional systems, the jump times t_k, $k \in \mathbb{N}$, are determined a priori, purely based on time. In event-triggered control (ETC), the jump times are defined as

$$t_{k+1} = \min\{t > t_k \mid \Gamma(z(t)) \geq 0\}. \tag{5}$$

where Γ is chosen such that ensuring $\Gamma(z(t)) \leq 0$ guarantees the required performance for the closed loop. The updates based on (5) are typically less frequent than those based on conventional time-triggered control, which saves valuable computation and communication resources.

2 From ETC to PETC

In (5), the function $\Gamma(z(t))$ has to be monitored continuously, which is also hard to accomplish on digital platforms. Therefore, a periodic event-triggered controller (PETC) [1] is of interest that will only carry out periodic time-triggered checks of a different event-triggering condition of the form $\tilde{\Gamma}(z(t))$ but still ensures that $\Gamma(z(t)) \leq 0$ for all times $t \in \mathbb{R}_{\geq 0}$, where $\tilde{\Gamma}$ has to be designed. To be precise, the jump times in the envisioned PETC implementation are given by

$$t_{k+1} = \min\{t = t_k + nh \mid \tilde{\Gamma}(z(t)) \geq 0, n \in \mathbb{N}_{>0}\}, \tag{6}$$

where $h > 0$ is the sampling period. The problem of designing h and $\tilde{\Gamma}$ that achieve this goal has been addressed in [1], where a design methodology is presented to *approximately* preserve the non-positivity of Γ along the system's solution. The objective of this work is to provide design guidelines for $\tilde{\Gamma}$ and h to *exactly* preserve $\Gamma(z(t)) \leq 0$ along the solutions to the corresponding PETC system. The proposed construction exploits ideas from [1], which show that under certain assumptions on differentiability of g and Γ, the evolution of $\Gamma(z(t))$ can be upper bounded by a linear system. Using these results from [1] we can construct $\tilde{\Gamma}$ by exploiting ideas from convex overapproximation [2], resulting in a systematic design procedure for PETC strategies for nonlinear systems.

3 Acknowledgements

This work is supported by the Innovational Research Incentives Scheme under the VICI grant "Wireless control systems: A new frontier in automation" (No. 11382) awarded by NWO (The Netherlands Organization for Scientific Research) and STW (Dutch Science Foundation).

References

[1] W.P.M.H. Heemels, R. Postoyan, M.C.F. Donkers, A.R. Teel, A. Anta, P. Tabuada, and D. Nešić, "Periodic event-triggered control," in "Event-based control and signal processing, M. Miskowicz (Ed.)," 2015.

[2] W.P.M.H. Heemels, N. van de Wouw, R.H. Gielen, M.C.F. Donkers, L. Hetel, S. Olaru, M. Lazar, J. Daafouz, and S.I. Niculescu, "Comparison of overapproximation methods for stability analysis of networked control systems," Hybrid Systems: Computation and Control (HSCC), 181–191, 2010.

On δ–sampling verification for discrete–time systems

Ruxandra Bobiti and Mircea Lazar
Department of Electrical Engineering
Technische Universiteit Eindhoven
P.O. Box 513, 5600 MB Eindhoven
The Netherlands
Email: r.v.bobiti@tue.nl, m.lazar@tue.nl

1 Introduction

The problem of safety verification for discrete–time, possibly discontinuous dynamical systems is considered. Typical solutions rely on finding invariant sets or Lyapunov functions and require solving optimization problems, which suffer from scalability and numerical solvers issues. Recently, an alternative method for verifying invariance for Lipschitz–continuous dynamics was proposed in [1], which does not make use of optimization. This method allows verification of the invariance of a set by verification for only a finite number of points in the set, called a δ–sampling of the set.

Here, a δ–sampling verification result is proposed for extending the previous result to general discrete–time, possibly discontinuous dynamics. This opens up the application of δ–sampling verification to hybrid systems.

2 Main result

We will present a result that reduces verification of an inequality of the type $F(x) \leq 0$ for all $x \in \mathcal{S}$, where F is a function and $S \subset \mathbb{R}^n$ is a set, to verification of the inequality in a finite number of points of $\mathcal{S}$ generated using δ–sampling. Our result is building upon Theorem 1 in [1], where F was assumed to be Lipschitz continuous on $\mathcal{S}$. In what follows we consider the more general case when F can be discontinuous on $\mathcal{S}$.

Consider the following problem setting. Let $\mathcal{S}$ be a compact subset of $\mathbb{R}^n$. Let $F : \mathcal{S} \to \mathbb{R}$ and $F_i : \overline{\mathcal{S}_i} \to \mathbb{R}$ be real valued functions for all $i \in \mathcal{I} := \{1, \dots, N\}$ for some $N \in \mathbb{N}$. Here $\overline{\mathcal{S}_i}$ denotes the closure of $\mathcal{S}_i$ and the sets $\mathcal{S}_i$ satisfy $\cup_{i\in\mathcal{I}}\mathcal{S}_i = \mathcal{S}$. We assume that the following property holds:

$$\forall x \in \mathcal{S}, \quad \exists_1 i \in \mathcal{I} \; : \; F(x) = F_i(x), \tag{1}$$

where $\exists_1$ denotes that there exists a unique element. We assume that F_i is continuous on $\overline{\mathcal{S}_i}$ for all $i \in \mathcal{I}$, but note that this does not imply that F is continuous on $\mathcal{S}$. For example, F could be constructed by switching among the different F_i functions depending if $x \in \mathcal{S}_i$. Next, define the set–valued regularization map $\overline{F} : \mathcal{S} \rightrightarrows \mathbb{R}$ as

$$\overline{F}(x) := \bigcap_{\rho>0} \overline{\bigcup_{\epsilon\in\rho\mathcal{B}} F(x+\epsilon)},$$

where $\mathcal{B}$ denotes a unit–radius ball in $\mathbb{R}^n$. For all $x \in \mathcal{S}$ define the index set:

$$I(x) := \{i \in \mathcal{I} \; : \; F_i(x) \in \overline{F}(x)\}.$$

Furthermore, define the real–valued function $\varepsilon : \mathbb{R}^n \to \mathbb{R}_+$,

$$\varepsilon(x) := \max\{|F_i(x) - F_j(x)| \; : \; (i,j) \in \mathcal{I}(x) \times \mathcal{I}(x)\}.$$

Observe that ε yields the maximum absolute jump that can occur in the value of the function F at a point x, due to discontinuity. If F is continuous at x clearly $I(x)$ is a singleton and consequently $\varepsilon(x) = 0$. As such, if F is continuous on $\mathcal{S}$, then $\varepsilon(x) = 0$ for all $x \in \mathcal{S}$.

Since for all $i \in \mathcal{I}$, F_i is continuous on the compact set $\overline{\mathcal{S}_i}$, there exist functions $\sigma_i \in \mathcal{K}$ such that:

$$|F_i(x) - F_i(y)| \leq \sigma_i(\|x-y\|), \quad \forall (x,y) \in \overline{\mathcal{S}_i} \times \overline{\mathcal{S}_i}. \tag{2}$$

By defining $\sigma(s) := \max_{i\in\mathcal{I}} \sigma_i(s) \in \mathcal{K}$ we are ready to state the δ–sampling verification theorem.

Theorem. *Suppose that the above assumptions regarding the compact set $\mathcal{S} \subset \mathbb{R}^n$ and the functions F and $\{F_i\}_{i\in\mathcal{I}}$ hold. Let $\delta \in \mathbb{R}_{>0}$ be the sampling density and let $\mathcal{S}_\delta$ be the δ–sampling of the set $\mathcal{S}$. If there exists a $\gamma \in \mathbb{R}_{>0}$ such that* (i) *$\sigma(\delta) < \gamma$ and* (ii) *for all $x_\delta \in \mathcal{S}_\delta$ it holds that $F(x_\delta) \leq -\gamma - \varepsilon(x_\delta)$, then $F(x) \leq 0$ holds for all $x \in \mathcal{S}$.*

Observe that any property which can be posed through a function F with the above properties can be verified with this result. In this work we show how δ–sampling can be used to verify invariance of a set, finite–step invariance, but also Lyapunov conditions, for nonlinear, possibly discontinuous systems.

References

[1] J. Kapinski, and J. Deshmukh, "Discovering Forward Invariant Sets for Nonlinear Dynamical Systems.," In Proceedings of the International Conference on Applied Mathematics, Modeling and Computational Science, Waterloo, Ontario, Canada, 2013

About the latest complexity bounds for Policy Iteration[1]

Romain Hollanders, Balázs Gerencsér, Jean-Charles Delvenne and Raphaël M. Jungers[2]
UCLouvain, Avenue Georges Lemaître 4, 1348 Louvain-la-Neuve, Belgium

1 Markov Decision Processes and Policy Iteration

Markov Decision Processes (MDPs) are a successful state model to solve many decision problems from engineering. The idea is to discretize the system of interest into a set of possible states and identify the possible actions (or decisions) in each state, as well as their effect on the system. To make good decisions in our system, we aim for the most rewarding choice of actions which can be found efficiently using, e.g., the Policy Iteration algorithm (PI). Although the above definition is rather abstract, the talk will provide a good intuitive idea of how MDPs work as well as several perspectives on how their structure can be viewed. We will focus on the question of the complexity of Policy Iteration, a major challenge in complexity theory, with close relations to the study of the Simplex algorithm for Linear Programming.

2 How many steps for Policy Iteration?

Policy Iteration has been shown to require an exponential number of steps to converge in some pathological cases. Nevertheless, we are interested in general upper bounds on this number of steps. Using some structural properties of PI, we obtain the following bound [2], thereby improving over a fifteen years old bound from Mansour and Singh [3].

Theorem 1. *If $m^{PI}(n)$ is the number of steps of PI on an n-states MDP, then $m^{PI}(n) \leq (2+o(1))\frac{2^n}{n}$.*

3 Could the Fibonacci sequence be a valid bound?

The following definition allows new perspectives.

Definition 1. *A matrix $A \in \{0,1\}^{m\times n}$ is Order-Regular (OR) whenever for every pair of rows i, j of A with $1 \leq i < j \leq m$, there exists a column k such that*

$$A_{i,k} \neq A_{i+1,k} = A_{j,k} = A_{j+1,k}. \tag{1}$$

Whenever we have $j+1 = m+1$, we use the convention that $A_{m+1,k} = A_{m,k}$.

To see the link with MDPs, the number of columns and rows of an OR matrix respectively relate to the number of states of an MDP and the number of iterations of PI to solve that MDP. The following result is known [4].

Proposition 1. *Let $m^*(n)$ be an upper bound on the number of rows of any n-column OR matrix. Then $m^{PI}(n) \leq m^*(n)$.*

[1] Research supported by the *Poles d'Attraction Interuniversitaires* (PAI) and the *Actions de Recherches Concertées* (ARC).

[2] J.-C. D. is with CORE and NAXYS and R. M. J. is with F.R.S./FNRS.

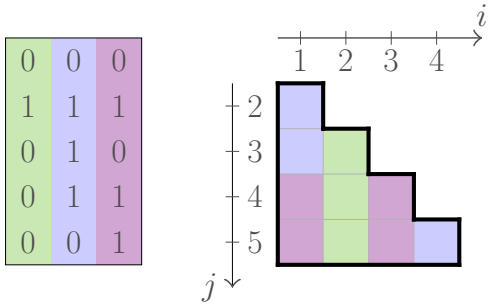

Figure 1: Each column of this Order-Regular matrix satisfies some of the (i, j) constraints, here graphically represented by squares on the 2D plane.

Simulations have shown the following results:

n	1	2	3	4	5	6	7
$m^*(n)$	2	3	5	8	13	21	≥ 33

Based on these observations, Hansen and Zwick conjectured the following [4]:

Conjecture 1 (Hansen & Zwick [4])**.** *$m^*(n) = F_{n+2} = O(1,618^n)$, where F_{n+2} is the $(n+2)^{nd}$ Fibonacci number.*

In our recent paper, we first develop a code capable of performing an exhaustive search for $n = 7$ and we thereby invalidate Conjecture 1 by showing that $m^*(7) = 33$. We also show the following bound [1], improving over the previous $\Omega\left(\sqrt{2}^n\right)$ bound from Schurr and Szabó [5].

Theorem 2. $m^*(n) \geq \Omega\left(1.4269^n\right)$.

References

[1] B. Gerencsér, R. Hollanders, J.-C. Delvenne and R.M. Jungers, "A complexity analysis of Policy Iteration through combinatorial matrices arising from Unique Sink Orientations", arXiv preprint arXiv:1407.4293, 2015.

[2] R. Hollanders, B. Gerencsér, J.-C. Delvenne and R.M. Jungers, "Improved bound on the worst case complexity of Policy Iteration", arXiv preprint arXiv:1410.7583, 2014.

[3] Y. Mansour and S. Singh, "On the Complexity of Policy Iteration", Proceedings of the 15th Conference on Uncertainty in Artificial Intelligence, UAI, 1999.

[4] T.D. Hansen, "Worst-case Analysis of Strategy Iteration and the Simplex Method", Ph.D. Thesis, Aarhus University, 2012.

[5] I. Schurr and T. Szabó, "Jumping doesn't help in abstract cubes", Integer Programming and Combinatorial Optimization, pp. 225–235, Springer, 2005.

Mixing time speedup by some added edges and non-reversibility

Balázs Gerencsér
UC Louvain
Avenue Georges Lematre, 4
B-1348 Louvain-la-Neuve (Belgium)
balazs.gerencser@uclouvain.be

Julien Hendrickx
UC Louvain
Avenue Georges Lematre, 4
B-1348 Louvain-la-Neuve (Belgium)
julien.hendrickx@uclouvain.be

1 The aim for fast mixing

Throughout several applications, we often arrive to the task of randomly sampling a node of a complicated graph or to average some values appearing at the nodes of this graph. In both cases, the corresponding mathematical problem is to find a Markov chain on this graph with good mixing properties.

Whenever the Markov chain is reversible (e.g., symmetric), there is a reliable way to find the fastest mixing chain [1]. But what happens if we do not require reversibility? Even more, what do we expect if we add a few new edges to the graph? In this work, we show on a simple example how the interplay of these two modifications can subsantially speed up the mixing of the Markov chain.

2 Definitions and models

First of all, we have to quantify the speed of mixing. Given a Markov chain transition matrix P with stationary distribution π we define

$$\lambda = \sup_{x \in \mathscr{P}} \limsup \|xP^k - \pi\|^{1/k},$$

where $\mathscr{P}$ is the set of all possible starting distributions.

We now describe the set of Markov chains we consider. Given a graph G, we allow Markov chains where transitions happen with positive probability only along the edges of G. Moreover, we require the stationary distribution to be uniform.

Reversibility means that on each edge of G, transitions happen with the same frequency in the two directions. In our case, where the stationary distribution is uniform, this is equivalent to P being symmetric.

The random graph model with which we work is the following: The model depends on a parameter $0 < \alpha < 1$. We start with a cycle graph of n nodes, and uniformly select a subset A of them such that $|A| = \lceil n^\alpha \rceil$. We then add the complete graph on A.

3 Results

Based on the tools of [2] we can get general bounds on the mixing rate.

Theorem 1. *For a fixed $0 < \alpha < 1$ and a Markov chain on a random graph corresponding to the definitions above, we have*

$$1 - c_1 \frac{n^{\alpha-1}}{\log n} < \lambda < 1 - c_2 \frac{n^{2\alpha-2}}{\log^3 n}.$$

Moreover, for reversible chains on the same graph, λ matches the upper bound (up to a $\log n$ factor in the fraction), that is, it is the slowest possible. The novelty in the current work is to show a strong speedup in the non-reversible case. We fix the transition probabilities as follows. All counter-clockwise steps are given $1/2$ probability, all clockwise steps are prohibited. All long-range edges are given the same, $1/(2\lceil n^\alpha \rceil)$ probability.

Theorem 2. *For the non-reversible Markov-chain described above, we have*

$$\lambda < 1 - c \frac{n^{\alpha-1}}{\log^5 n}.$$

The interpretation of these somewhat complicated formulas is that the asymmetric, non-reversible version of the Markov chain mixes to a certain precision in square root of the time needed for the reversible Markov chain.

4 Outlook

The speedup we see is already impressive, but it also leads to a range of new questions. First, we might want to generalize our results when clockwise steps are also allowed (while keeping the asymmetry). Intuitively we should see the same phenomenon, but we have to face new technical difficulties. We might also change the random graph model. Simulations show that we do not need a complete graph on A to achieve the speedup. In fact, if only a random matching is added to A, we already experience the same type of fast mixing.

References

[1] Stephen Boyd, Persi Diaconis, and Lin Xiao. Fastest mixing Markov chain on a graph. *SIAM Rev.*, 46(4):667–689 (electronic), 2004.

[2] Balázs Gerencsér. Mixing times of Markov chains on a cycle with additional long range connections. arXiv:1401.1692, Submitted for Publication, 2014.

Robust Gradient Learning with Application to Nonlinear Variable Selection

Yunlong Feng
ESAT-STADIUS
KU Leuven
3001, Leuven, Belgium
yfeng@esat.kuleuven.be

Yuning Yang
ESAT-STADIUS
KU Leuven
3001, Leuven, Belgium
yyang@esat.kuleuven.be

Johan A.K. Suykens
ESAT-STADIUS
KU Leuven
3001, Leuven, Belgium
johan.suykens@esat.kuleuven.be

1 Introduction

The gradient learning (GL) model proposed in [2] aims at learning the gradients of the regression function, which is directly driven by variable selection and coordinate covariance problems. However, in real-life applications, data sets might be contaminated by outliers or heavy-tailed noise, which may appear in both response or the predictors. In this case, the GL model cannot help in learning gradients. In our study, we present a framework of robust gradient learning (RGL) model to learn the gradients of the regression function robustly [1].

2 The Proposed RGL Model

Let $\mathscr{K} : \mathscr{X} \times \mathscr{X} \to R$ be a kernel function which is not restricted to be a positive definite kernel. We denote $\mathscr{H}_{\mathscr{K},\mathbf{z}}$ as a linear span over the instance-based kernelized dictionary $\{\mathscr{K}(\mathbf{x},\mathbf{x}_i)\}_{i=1}^m$ with coefficients $\{\alpha_i\}_{i=1}^m$. More explicitly, $\mathscr{H}_{\mathscr{K},\mathbf{z}}$ is defined as the following function set

$$\left\{ g : g(\mathbf{x}) = \sum_{i=1}^{m} \alpha_i \mathscr{K}(\mathbf{x}_i,\mathbf{x}),\ \alpha_i \in R, i = 1,\ldots,m, \mathbf{x} \in \mathscr{X} \right\}.$$

Let $\overrightarrow{g} = (g_1, g_2, ..., g_n)^T \in \mathscr{H}_{\mathscr{K},\mathbf{z}}^n$ with the coefficient $A = (\alpha_1, ..., \alpha_m)$, where $\alpha_i = (\alpha_{1,i}, ..., \alpha_{n,i})^T$ for $i = 1, ..., m$ and $\mathscr{H}_{\mathscr{K},\mathbf{z}}^n$ is an n-fold $\mathscr{H}_{\mathscr{K},\mathbf{z}}$ defined by

$$\mathscr{H}_{\mathscr{K},\mathbf{z}}^n = \left\{ (g_1,\ldots,g_n)^T \,|\, g_j \in \mathscr{H}_{\mathscr{K},\mathbf{z}}, j = 1,\ldots,n \right\}.$$

We denote $\mathscr{E}_{\mathbf{z}}^{\rho}(\overrightarrow{g})$ as the empirical risk when taking $\overrightarrow{g}$ as an empirical estimator of $\nabla f^{\star}$. Denote ω_{ik} values as weights which are given by $\omega_{ik} = \exp\{-\frac{\|\mathbf{x}_i - \mathbf{x}_k\|^2}{2s^2}\}$ with some $s > 0$.

In the regression setting, $\mathscr{E}_{\mathbf{z}}^{\rho}(\overrightarrow{g})$ is defined as

$$\mathscr{E}_{\mathbf{z}}^{\rho}(\overrightarrow{g}) = \frac{1}{m^2} \sum_{i,k=1}^{m} \omega_{ik} \rho\left((y_i - y_k) + \overrightarrow{g}(\mathbf{x}_i) \cdot (\mathbf{x}_k - \mathbf{x}_i) \right),$$

where $\rho(\cdot)$ is a robust distance-based regression loss.

Based on the above notations, our RGL model takes the following form

$$\overrightarrow{g_{\mathbf{z}}} = \arg\min_{\overrightarrow{g} \in \mathscr{H}_{\mathscr{K},\mathbf{z}}^n} \left\{ \mathscr{E}_{\mathbf{z}}^{\rho}(\overrightarrow{g}) + \lambda \|A\|_{p,q}^q \right\}, \qquad (1)$$

where $\lambda > 0$ is a regularization parameter, and

$$\|A\|_{p,q}^q := \sum_{i=1}^{n} \left(\sum_{j=1}^{m} |\alpha_{i,j}|^p \right)^{q/p}$$

with $p \geq 1$ and $q \geq 1$.

With a positive constant σ, the following robust regression loss ℓ_σ is used: $\ell_\sigma(t) = \sigma^2 \left(1 - \exp\left(-t^2/\sigma^2\right)\right)$, $t \in R$.

3 Algorithms and Applications

Although the proposed RGL model enjoys its robustness from the robust loss ℓ_σ, the nonconvexity of ℓ_σ also leads to computational difficulty. To tackle this problem, in our study, we propose a gradient descent based iterative soft thresholding algorithm to solve the proposed RGL model. The algorithm is simple and easy to implement and we also give explicit proof of its convergence.

The proposed RGL model associated with different regularizers can be applied to many applications, such as nonlinear variable selection, supervised dimension reduction and coordinate covariance estimation. In our study, we carry out simulation studies with the RGL model on both synthetic and real data sets in the nonlinear variable selection problem. Numerical results indicate that the proposed model can outperform the existing gradient learning methods in the presence of outliers and give comparable performance in the absence of outliers.

Acknowledgement

This works was supported by GOA/10/09 MaNet, CoE PFV/10/002(OPTEC), FWO: G.0377.12, G.088114N, BIL12/11T, IUAP P7/19 (DYSCO, 2012-2017), ERC AdG A-DATADRIVE-B.

References

[1] Y. Feng, Y. Yang, J. A.K. Suykens, "Robust Gradient Learning with Applications," *Internal Report, ESAT-SISTA, KU Leuven, Leuven, Belgium*, 2014.

[2] S. Mukherjee and D.-X. Zhou, "Learning Coordinate Covariances via Gradients," *The Journal of Machine Learning Research*, 7:519–549, 2006.

Influence of uncertainty on temporal stabilizability and compensatability of linear systems with white stochastic parameters

Gerard van Willigenburg
Biobased Chemistry & Technology Group
(former Systems & Control Group)
Wageningen University
P.O. Box 17, 6700 AA Wageningen
The Netherlands
Email: gerard.vanwilligenburg@wur.nl

Willem de Koning
Kroeskarper 6
2318 NG Leiden
The Netherlands
Email: wilros@planet.nl

1 Introduction

Apart from changes of system structure vital system properties such as stabilizability and compensatability may be lost *temporarily* due to the stochastic nature of system parameters. To demonstrate this very recently new system properties called temporal mean-square stabilizability (tms-stabilizability) and temporal mean-square compensatability (tms-compensatability) for time-varying linear discrete-time systems with white stochastic parameters (multiplicative white noise) were developed. When controlling such systems by means of (optimal) state feedback, tms-stabilizability identifies intervals where mean-square stability (ms-stability) is lost temporarily. This is vital knowledge to both control engineers and system scientists. Similarly, tms-compensatability identifies intervals where ms-stability is lost temporarily in case of full-order (optimal) output feedback. Tests explicit in the system matrices were provided to determine each temporal system property. Here an illustrative example concerning the practical application is presented together with the associated references.

2 Illustrative example

Example 1 from [1]
Consider the digital optimal perturbation feedback control of the "Goddard Rocket" around its optimal trajectory as presented in [2], example 2. The example considered here is identical except for the parameters of the equivalent discrete time-varying linearised system (EDTVLS) used for digital optimal perturbation feedback design. These are turned into *stochastic parameters* using a possibly time-varying *parameter uncertainty measure* $\beta_i \geq 0$, where i denotes discrete-time. When $\beta_i = \beta = 0$ the parameters are deterministic at each time i and the results of example 2 presented in [2] are obtained. With increasing β_i, parameter uncertainty at time i increases. □

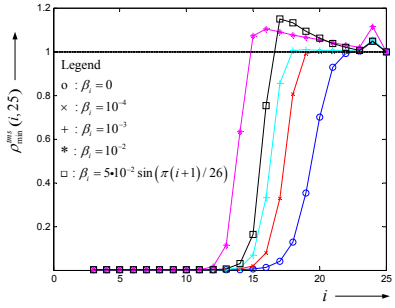

Fig. 1: tms-stabilizability measures Example 1 for different values of β_i

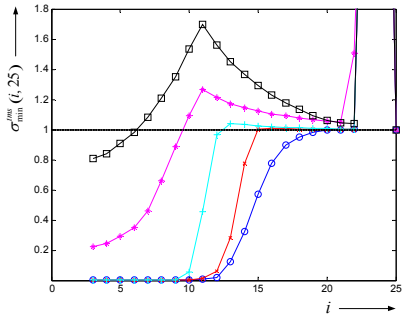

Fig. 2: tms-compensatability measures Example 1 for different values of β_i

Fig. 1 presents values of the temporal mean-square stabilizability measure $\rho_{\min}^{tms}(i,25)$, i=0,1,..,24 of the closed loop system with full state feedback over time-interval $(i,25)$. If the value falls below one, the system is temporal mean-square stabilizable (tms-stabilizable) over time-interval $(i,25)$. Similarly Fig. 2 presents values of the temporal mean-square compensatability measure $\sigma_{\min}^{tms}(i,25)$, i=0,1,..,24 of the closed loop system with full-order output feedback over time-interval $(i,25)$. Again if the value falls below one, the system is temporal mean-square compensatable (tms-compensatable) over time-interval $(i,25)$. As expected, with increasing constant values of β, i.e. with increasing parameter uncertainty at each time i, tms-stabilizability and tms-compensatability become worse because their measures increase. Also observe that tms-stabilizability is far better than tms-compensatability. This represents the well-known fact that full state feedback is to be preferred over full-order output feedback.

References

[1] L.G. Van Willigenburg, W.L. De Koning, 2015, "Temporal stability, stabilizability and compensatability of time-varying linear discrete-time sytems with white stochastic parameters". European Journal of Control, doi: 10.1016/j.ejcon.2015.01.005.

[2] L.G. Van Willigenburg, W.L. De Koning, 2013, "Temporal and one-step stabilisability and detectability of discrete time linear systems", IET Control Theory & Applications, 7, 1, 151-159.

Online semi-supervised clustering regularized by Kalman filtering

Siamak Mehrkanoon, Oscar Mauricio Agudelo and Johan A. K. Suykens
KU Leuven, ESAT-STADIUS, Kasteelpark Arenberg 10, B-3001 Leuven (Heverlee), Belgium.
Email: Siamak.Mehrkanoon@esat.kuleuven.be

1 Introduction

An on-line semi-supervised learning algorithm formulated as a regularized kernel spectral clustering (KSC) approach is proposed. Given a few user-labeled data points the initial model is learned and then the class membership of the remaining data points in the current and subsequent time instants are estimated and propagated in an on-line fashion. Furthermore we show how the tracking capabilities of the Kalman filter can be used to provide the labels of objects in motion and thus regularizing the solution obtained by the MSS-KSC algorithm.

2 Formulation of the method

Consider training data points $\mathscr{D} = \{x_1, \ldots, x_{n_u}, x_{n_u+1}, .., x_n\}$, where $\{x_i\}_{i=1}^n \in \mathbb{R}^d$. The first n_u data points do not have labels whereas the last $n_L = n - n_u$ points have been labeled. Assume that there are Q classes, then the label indicator matrix $Y \in \mathbb{R}^{n_L \times Q}$ is defined as follows: $Y_{ij} = +1$, if the ith point belongs to the jth class and -1 otherwise. The formulation of Multi-class semi-supervised KSC (MSS-KSC) in primal is given as follows [1]:

$$\begin{aligned} \min_{w^{(\ell)}, b^{(\ell)}, e^{(\ell)}} \quad & \frac{1}{2}\sum_{\ell=1}^{Q} w^{(\ell)T} w^{(\ell)} - \frac{\gamma_1}{2}\sum_{\ell=1}^{Q} e^{(\ell)T} V e^{(\ell)} + \\ & \frac{\gamma_2}{2}\sum_{\ell=1}^{Q} (e^{(\ell)} - c^{(\ell)})^T \tilde{A} (e^{(\ell)} - c^{(\ell)}) \\ \text{subject to} \quad & e^{(\ell)} = \Phi w^{(\ell)} + b^{(\ell)} 1_n, \; \ell = 1, \ldots, Q, \end{aligned} \tag{1}$$

where c^{ℓ} is the ℓ-th column of the matrix C defined as

$$C = [c^{(1)}, \ldots, c^{(Q)}]_{n \times Q} = \left[\frac{0_{n_u \times Q}}{Y}\right]_{n \times Q}, \tag{2}$$

where $0_{n_u \times Q}$ is a zero matrix of size $n_u \times Q$ and Y is defined as previously. The matrix $\tilde{A}$ is defined as follows:

$$\tilde{A} = \left[\begin{array}{c|c} 0_{n_u \times n_u} & 0_{n_u \times n_L} \\ \hline 0_{n_L \times n_u} & I_{n_L \times n_L} \end{array}\right],$$

where $I_{n_L \times n_L}$ is the identity matrix of size $n_L \times n_L$. V is the inverse of the degree matrix. In the dual the solution is obtained by solving a system of linear equations [1]:

$$\gamma_2 \left(I_n - \frac{R 1_n 1_n^T}{1_n^T R 1_n}\right) c^{(\ell)} = \alpha^{(\ell)} - R\left(I_n - \frac{1_n 1_n^T R}{1_n^T R 1_n}\right) \Omega \alpha^{(\ell)}, \tag{3}$$

where $R = \gamma_1 V - \gamma_2 \tilde{A}$. The proposed on-line MSS-KSC consists of two stages [2]. In the first stage, one trains the MSS-KSC algorithm to obtain the initial solution vectors α_i and the cluster memberships. Assuming that N_c clusters are detected, the initial cluster representatives are then obtained. The aim of the second stage is to predict the membership of the new arriving data points using the updated solution vectors α_i. The score variables of the arrived batch of new data points is estimated by means of the out-of-sample extension property of the MSS-KSC method. Then the estimation of the projection of the points in the α-space and calculating the membership of the points are carried out. Finally the cluster representatives in both α and original spaces are updated. The interaction between Kalman filter and I-MSS-KSC algorithm is shown in Fig. 1.

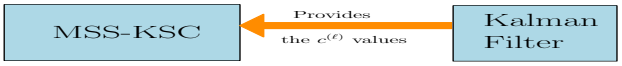

Figure 1: Kalman filter acts as a regularizer for the MSS-KSC algorithm

The applicability of the approach for online video segmentation are shown in the Fig. 2.

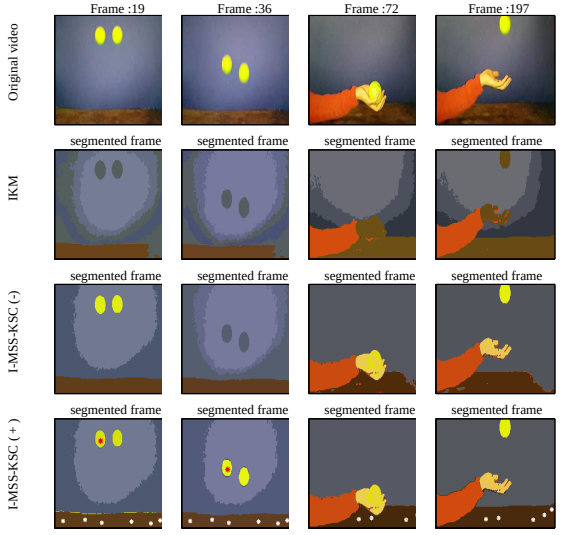

Figure 2: Bouncing balls and Siamak's hand video. **First row:** Original video, **Second row:** IKM, **Third row:** I-MSS-KSC(-), **Fourth row:** I-MSS-KSC(+)

Acknowledgments. This work was supported by: • Research Council KUL: GOA/10/09 MaNet, PFV/10/002 (OPTEC), several PhD/postdoc & fellow grants • Flemish Government: ○ IOF: IOF/KP/SCORES4CHEM; ○ FWO: PhD/postdoc grants, projects: G.0377.12 (Structured systems), G.083014N (Block term decompositions), G.088114N (Tensor based data similarity); ○ IWT: PhD Grants, projects: SBO POM, EUROSTARS SMART; ○ iMinds 2013 • Belgian Federal Science Policy Office: IUAP P7/19 (DYSCO, Dynamical systems, control and optimization, 2012-2017) • IBBT • EU: FP7-SADCO (MC ITN-264735), ERC ST HIGHWIND (259 166), ERC AdG A-DATADRIVE-B (290923) • COST: Action ICO806: IntelliCIS. Johan Suykens is a professor at the KU Leuven, Belgium.

References

[1] S. Mehrkanoon, C. Alzate, M. Raghvendra, R. Langone, and J. A. K. Suykens, *Multi-class semi-supervised learning based upon kernel spectral clustering*, IEEE Transactions on Neural Networks and Learning Systems, In press,2014.

[2] S. Mehrkanoon, M. Agudelo, J. A. K Suykens, *Incremental multi-class semi-supervised clustering regularized by Kalman filtering*, Internal Report 14-154, ESAT-SISTA, KU Leuven (Leuven, Belgium), 2014., Lirias number.

Data driven MPC based on OBF model structures

A. A. Bachnas, S.Weiland and R. Tóth
Dept. of Electical Engineering
Control System group, TU/e
a.a.bachnas@tue.nl, s.weiland@tue.nl, r.toth@tue.nl

1 Introduction

Model Predictive Control (MPC) is widely applied in the field of process control. The aforementioned control scheme is able to realize control objectives while obeying safety constraint on the input side. However, desired performance of the controller can only be sustained in small time periods after its commissioning. The performance degradation is usually caused by the change of disturbance characteristics and/or growing plant-model mismatch. These phenomena have led to numerous proposed solutions to prolong the lifetime of an MPC controller.

In this work, a novel solution is proposed by employing a flexible model structure, namely an *orthonormal basis function* (OBF) model structures into the MPC scheme. Due to its model characteristics, structured model updates can be conducted iteratively in a closed loop setting via latest measured input-output data. Small updates towards model coefficients are done iteratively to fine tune the prediction part of the control scheme. If the change of the plant and/or disturbances persist for a long period, model overhaul is conducted by re-updating the basis functions. This will reduce the modeling uncertainty to ensure that the plant can still be accurately described by the selected basis functions. Moreover, since OBF model structures can be seen as a generalization of FIR model structures, the wide application of FIR model in the industrial MPC scheme is another appealing reason for the proposed solution.

2 Formulation

The OBF model structure utilizes a broader selection of orthonormal basis functions $\{\phi_i(z)\}_{i=1}^{n_g}$ instead of just the pulse basis $\{z^{-i}\}_{i=1}^{n}$ which are used in FIR model structures. The formulation of an OBF model of an LTI system is:

$$y(k) = \sum_{i=1}^{n_g} w_i \phi_i(q) u(k) + v(k), \tag{1}$$

with $w \in \mathbb{R}^{n_y \times n_g}$ being the collection of expansion coefficients, and $v(k)$ is the noise process which is assumed to be white. The output error noise structure provides consistent estimation in the close loop setting. With appropriately selected basis functions, the plant dynamics can be described by a small amount model coefficients. This leads to a parsimonious model of the system.

2.1 Coefficient estimation

Data-driven estimation is conducted iteratively to re-estimate expansion coefficients w by minimizing the least square prediction error criterion. The size of the measured data as well as possible weighting on the criterion, will be a design parameter to mitigate or adept any changes in the plant behavior. Lastly, the OBF model and the identification criterion can be easily formulated a state-space description which is better suited for the standard MPC problem formulation.

2.2 MPC formulation

The proposed scheme uses standard MPC formulation with quadratic cost function to penalize deviations of the predicted outputs $y(k+i|k)$ from a reference trajectory $r(k+i|k)$

$$V(k) = \sum_{i=0}^{Hp} \| y(k+i|k) - r(k+i|k) \|_Q^2 + \sum_{j=0}^{Hu} \| \Delta u(k+j|k) \|_R^2$$

where Δu is the input increment, and H_p, H_u is the prediction and control horizon respectively. Expression $\| x \|_Q^2$ is equivalent with $x^\top Q x$ where Q is the symmetric tuning matrix. The task of the control scheme is to compute the optimal input sequence that minimizes the cost function while satisfying operational constraint on input and output.

2.3 Joint data-driven scheme

Since $y(k+i|k)$ is the future prediction of a model which is iteratively updated from measured input-output data (in a least square fashion), the quadratic cost function $V(k)$ can be formulated solely based on the collection of measured data. Thus, the computation of the optimal input sequence and model coefficient can be done in one single formulation. Besides of the data-driven case, the performance level of the whole scheme can be monitored periodically. In case the level dropped below some threshold, model overhaul by re-optimizing the selected basis functions can be conducted to adapt the model towards major changes in the system or disturbance characteristics.

3 Ackonowledgments

This research is financially supported by the SMART project which is a joint consortium of TU Eindhoven, KU Leuven, and IPCOS.

References

[1] Heuberger, P.S.C.,Van den Hof, P.M.J.,Wahlberg, B. *Rational Orthonormal Basis Functions*, Springer, Heidelberg, 2005.

[2] Maciejowski, J. *Predictive control with constraints*, Prentice Hall, 2002.

Distributed Model Predictive Control of Aquifer Thermal Energy Storage Smart Grids [1]

Vahab Rostampour
Delft Center for Systems and Control
Delft Univeristy of Technology
v.rostampour@tudelft.nl

Tamas Keviczky
Delft Center for Systems and Control
Delft Univeristy of Technology
t.keviczky@tudelft.nl

Abstract

Aquifer Thermal Energy Storage (ATES) systems are used to store large quantities of thermal energy in underground aquifers enabling the reduction of energy usage and CO_2 emissions of the heating and cooling systems in buildings. In dense urban environments, the proximity of hot and cold wells in nearby ATES systems installations may lead to undesired interactions between such energy storage systems leading to suboptimal operation or conservative design choices [1, 5]. The interactions between ATES systems are dynamically time-varying and plagued by uncertainty due to the absence of detailed underground models and cooperation between operators regarding the influence of nearby systems. ATES systems interact via the aquifer in a way comparable to how distributed sources and sinks of electricity are interacting via the electricity smart grid [3].

In a smart grid setting, every agent represents an ATES system and has the potential to contribute to the local thermal balance of the grid. A single ATES system is linked to the neighboring agents via the aquifer that is defined as a complicating constraint. Therefore, coordination is expected to provide improvements in the local and system-wide thermal energy cost and efficiency, while fulfilling all coupling constraints. Thus the motivation for ATES smart grids can be both economical and environmental.

When designing controllers for the underlying interconnected dynamical system, distributed solutions are sought in order to reduce the computational complexity, and allow individual operators to operate their installations locally without the need for a central entity to determine the system-wide optimal pumping schedules. The proposed distributed approach should provide performance close to that of a centralized one, while being robust to uncertainties in the subsystem models and their interactions, and relying only on a limited amount of information exchange. Distributed MPC (DMPC) is a promising methodology in this context since it is able to fulfill local and complicating constraints between subsystems while striving for economically and environmentally optimal operation (see [2, 4] and the references therein).

[1] Research supported by the Netherlands Organization for Scientific Research (NWO) under the project Aquifer Thermal Energy Storage Smart Grids (ATES-SG) with grant number 408-13-030.

In this work, we propose a price-based (Lagrangian) coordination scheme that is based on solving a local agent problem subject to the local constraints in parallel. Each ATES system optimizes its own objective function that is modified according to a set of prices assigned for the thermal energy resource. The goal of this price-based method is to coordinate agents by finding equilibrium resource prices which lead to a globally optimal ATES smart grid state. Due to the fact that ATES system operates in various modes in each season, the optimization problem becomes a mixed integer program.

We first introduce a mathematical model for a single ATES system, based on the physical description and limitations, that is suitable for an optimal control problem formulation. Subsequently, we extend the single system model to an interconnected grid by introducing the complicating constraints. As part of our future work, we will develop a methodology that ensures tractability while providing convergence and performance guarantees with respect to the centralized optimum of the whole networked system. The efficiency and practical feasibility of the theoretical results will be investigated by applying them to a real case study.

References

[1] M. Bloemendal, T. Olsthoorn, and F. Boons. How to achieve optimal and sustainable use of the subsurface for aquifer thermal energy storage. *Energy Policy*, 66, 2014.

[2] Minh Dang Doan, Pontus Giselsson, Tamás Keviczky, Bart De Schutter, and Anders Rantzer. A distributed accelerated gradient algorithm for distributed model predictive control of a hydro power valley. *Control Engineering Practice*, 21(11):1594–1605, 2013.

[3] V. Rostampour, K. Margellos, M. Vrakopoulou, M. Prandini, G. Andersson, and J. Lygeros. Reserve requirements in ac power systems with uncertain generation. In *ISGT IEEE/PES EUROPE*. IEEE, 2013.

[4] Riccardo Scattolini. Architectures for distributed and hierarchical model predictive control–a review. *Journal of Process Control*, 2009.

[5] W. Sommer, J. Valstar, I. Leusbrock, T. Grotenhuis, and H. Rijnaarts. Optimization and spatial pattern of large-scale aquifer thermal energy storage. *Applied Energy*, 2015.

Distributed MPC in the Universal Smart Energy Framework

D.B. Nguyen, J.M.A. Scherpen
Faculty of Mathematics and Natural Sciences, University of Groningen
Nijenborgh 4, 9747 AG Groningen, The Netherlands
E-mail: {d.b.nguyen, j.m.a.scherpen}@rug.nl

Abstract

Environmental concerns have prompted a shift towards the usage of renewable energy resources, such as wind or solar energy. Windmills and solar panels are, however, often spatially distributed, hence the energy production itself also becomes distributed. This presents a paradigm shift from the traditional, centralized generation. Furthermore, renewable energy resources depend on weather conditions which results in a fluctuating production and creates an imbalance between supply and demand. The problem can be addressed by demand response, in which the consumer side is also playing an active role in the balancing process.

To facilitate the development of smart energy services, the Smart Energy Collective (SEC) is setting up a standardized platform in the Netherlands, called the Universal Smart Energy Framework [1]. USEF introduces flexible households that are equipped with appliances capable of moving their load demand and thus change their energy consumption in time.

We describe a model predictive control scheme to balance between supply and demand in a network of flexible households. The households can communicate and share their imbalance information with local neighbors. The network topology is represented by a weighted adjacency matrix, where the weights express the importance of imbalance information from a particular neighbor. An example is given below with corresponding information sharing matrix $\mathbf{A}$.

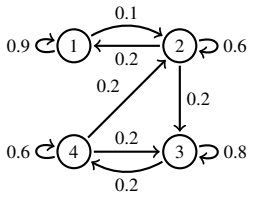

$$\mathbf{A} = \begin{bmatrix} 0.9 & 0.2 & 0 & 0 \\ 0.1 & 0.6 & 0 & 0.2 \\ 0 & 0.2 & 0.8 & 0.2 \\ 0 & 0 & 0.2 & 0.6 \end{bmatrix}$$

We denote the flexible (eg., washing machines, refrigerators) and fixed (eg., TVs, radios) loads of household i at time-step k by $f_i[k]$ and $g_i[k]$, respectively. We also set the day-ahead forecast of its energy consumption as $\text{goal}_i[k]$. Then, the MPC formulation of the problem is given by:

$$x_i[k+1] = \mathbf{A}_{ii}x_i[k] + \sum_{j\neq i} \mathbf{A}_{ij}x_j[k] + \\ + u_i[k] + d_i[k] - \Delta\text{goal}_i[k],$$

where $x_i[k]$ is the imbalance of household i, $u_i = f_i[k+1] - f_i[k]$, $d_i = g_i[k+1] - g_i[k]$ and $\Delta\text{goal}_i[k] = \text{goal}_i[k+1] - \text{goal}_i[k]$, for all k. The objective is to minimize the total imbalance in the network:

$$\min_u \sum_k \sum_i x_i^2[k]$$

This (centralized) MPC formulation can be rewritten in a distributed fashion using dual decomposition. Larsen *et al.* [2] applied the approach to avoid peak loads in a network of flexible washing machines by "flattening" the load patterns.

We extend the idea to embed it into the USEF hierarchical setting and show that the algorithm succesfully matches demand with supply to minimize the imbalance. We demonstrate the large-scale feasibility of the method via MATLAB simulation. Our current implementation is capable of handling 10.000 households and can scale up well with additional computing power. Moreover, we study how specific parameters influence the performance of the controller.

Our next step is to incorporate the role of the Distribution System Operator (DSO) into the model. DSOs are responsible for staying within the transmission line capacity limits and for invoking the flexibility of households in case of overloads.

Acknowledgements

The research project is supported by the "TKI Switch2SmartGrids", with DNV GL (member of the SEC) as the project leader. We also thank J. Pons* and L. Doddema† for their contribution to the MATLAB simulation.

References

[1] Smart Energy Collective, "An Introduction to the Universal Smart Energy Framework", 2014

[2] G.K.H. Larsen, J. Pons, S. Achterop, and J.M.A. Scherpen, "Distributed MPC applied to power side control", In *Proceedings of the 12th European Control Conference (ECC13)*, pages 3295–3300, 2013

*J. Pons, "Distributed Model Predictive Control – As Control Method in the Universal Smart Energy Framework", Master's thesis, University of Groningen, 2013

†Master's thesis in progress

Energy-optimal point-to-point motions with high positioning accuracy using offset-free energy-optimal MPC

Xin Wang[1], Jan Swevers
Department of Mechanical Engineering, KU Leuven, Celestijnenlaan 300B, B-3001 Heverlee, Belgium
Xin.Wang@mech.kuleuven.be, Jan.Swevers@mech.kuleuven.be

1 Introduction

Offset-free Energy-optimal Model Predictive Control (offset-free EOMPC) is developed based on our previous research - Energy-optimal Model Predictive Control (EOMPC) [1] to improve its positioning accuracy in the presence of unmodelled disturbances. This is realized by augmenting the system state with disturbance variables such that the disturbances are estimated and the effects of which are cancelled. Experimental validation of the offset-free EOMPC is implemented on a linear motor with coulomb friction and cogging disturbances.

2 Offset-free energy-optimal MPC

EOMPC [1] is a MPC approach for time-constrained energy-optimal point-to-point motion control of LTI systems. The EOMPC approach guarantees the two conflicting time- and energy- requirements by solving a *two-layer* optimization problem. The top layer has the highest priority and aims to guarantee the request motion time. The bottom layer aims to minimize the energy consumed during P2P motions. However, EOMPC cannot achieve high positioning accuracy in the presence of unmodelled disturbances. In order to cope with this problem, a disturbance model strategy is adopted: the system state is augmented with disturbance variables. Based on the disturbance model, the disturbances are estimated using a state estimator. Then, the reference of the input is determined such that the steady-state condition is satisfied with the estimated disturbance. Thus, the effects of the disturbance can be cancelled. The EOMPC approach adopting the disturbance model yields the offset-free energy-optimal MPC (offset-free EOMPC).

3 Test setup

The test setup is a current-controlled permanent-magnet linear motor. The control input to the system is motor current $[A]$, and the output is the position of the carriage $[m]$. The main disturbances in this test setup are Coulomb friction and cogging and are expressed in $[A]$ because they are input disturbances. Coulomb friction is a constant which depends on the sign of the velocity. Cogging, which is independent of motion velocity, is more or less a periodic function of the position and the period corresponds to the distance between the magnetic poles of the linear motor.

[1]**Acknowledgement** This work benefits from KU Leuven-BOF PFV/10/002 Center-of- Excellence Optimization in Engineering (OPTEC), the Belgian Programme on Interuniversity Attraction Poles, initiated by the Belgian Federal Science Policy Office (DYSCO) and KU Leuven's Concerted Research Action GOA/10/11.

4 Experimental Results and conclusion

The following motion is validated on the linear motor with sampling rate $f_s = 100Hz$. The system is initially at rest at position $0m$, and $y_{ref} = 0.12m$ is requested at time $t = 0.4s$. The required motion time $T = 0.6s$, the prediction horizon $N_{max} = 80$. Figure 1 shows that time-constrained energy-optimal point-to-point motion with high positioning accuracy is achieved using offset-free EOMPC.

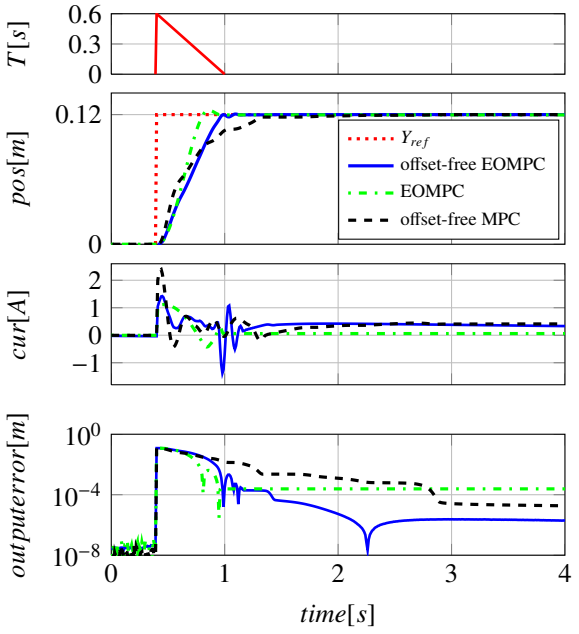

Figure 1: Experimental results

Methods	$u^2[A^2]$	error	motion time
offset-free EOMPC	27.88	$5\mu m$	guaranteed
EOMPC	24.33	0.5mm	guaranteed
offset-free MPC	40.88	$5\mu m$	approximately (Q_y)

References

[1] Xin Wang, Julian Stoev, Gregory Pinte and Jan Swevers, Energy Optimal Point-to-point Motion Using Model Predictive Control,DSCC, vol.2, October 17, 2012, pp. 267-273.

Anticipative linear parameter-varying model predictive control

J. Hanema, R. Tóth, M. Lazar and S. Weiland
Control Systems Group, Department of Electrical Engineering
Eindhoven University of Technology
P.O. Box 513, 5600 MB, The Netherlands
j.hanema@tue.nl

1 Introduction

To achieve sub-nanometer level positioning accuracy in high-tech systems advanced control design approaches are necessary. On this scale a wide range of physical phenomena leading to e.g. position-dependent system behaviour becomes relevant, and a controller has to account for these effects to obtain the required accuracy. In a wafer scanner for instance, deformations in the mechanical structure caused by a non-uniform temperature can lead to unacceptable errors. To develop controllers which take into account all relevant phenomena causing dynamical variations, a design procedure based on *linear time-invariant* (LTI) models is no longer adequate. The use of highly accurate first-principle models on the other hand is unsuitable for real-time applications.

The framework of *linear parameter-varying* (LPV) systems offers a promising trade-off between model accuracy and complexity. In an LPV system the relations between input and output signals are assumed to be linear, but these linear relations depend on a time-varying and on-line measurable variable: the so called scheduling signal $p : \mathbb{Z} \to \mathbb{P}$. This approach provides the capability to capture the behaviour of complex non-linear systems, while control design can be addressed in a unified framework which can be regarded as an extension to the powerful results of the existing LTI theory [1].

2 MPC for LPV systems

In *model predictive control* (MPC) the N future control inputs $u(k), \ldots, u(k+N)$ to a system are determined by minimizing on-line, at each sampling instant k, a predefined cost function. In general, this cost function depends on the future inputs and on the *predicted* outputs $y(k+1), \ldots, y(k+N)$. An advantage of using MPC for complex system is that it can explicitly account for physical limitations such as actuator saturation.

The central problem in MPC for LPV systems is that the future values of the parameter p – which are required to predict the future outputs – can be unknown. Theoretically this can be handled by considering a min-max optimization where the worst-case value of a cost function over all possible variations of p within the set $\mathbb{P}$ is minimized. Unfortunately, this approach is not computationally tractable as uncertainty propagates over time. Existing proposed solutions either introduce limitations on control performance or do not manage to sufficiently decrease the computational burden.

3 Towards anticipative LPV-MPC

To overcome the aforementioned issues, it is proposed to use knowledge on the future trajectory of p in the controller. In this way it *anticipates* upon future parameter variations, improving performance and reducing computational complexity. When the values of p are known exactly for all instants in the prediction horizon the LPV predictive control law can be reduced to a quadratic program, such that computational issues are eliminated and closed-loop stability can be guaranteed [2]. This setting is physically interesting because in the wafer scanner context p is dependent on the route (chip layout) to be followed, which is known. This route may, however, not be exactly realized due to positioning errors and disturbances.

In view of the challenging application requirements, it is proposed to carry out fundamental research on the achievable levels of performance of LPV-MPC algorithms which

- Use exact or partial knowledge on the behaviour of p;
- Are robust against modelling mismatch and unmeasured disturbances;
- Are computationally simple to allow for real-time implementation.

The results of the research will be applied for thermal control of the wafer table in a lithography machine.

References

[1] Tóth, R. (2010). Modeling and Identification of Linear Parameter-Varying Systems. Berlin, Heidelberg: Springer.

[2] Hanema, J. (2014). Data-driven linear parameter-varying predictive control for process systems. MSc thesis, Eindhoven University of Technology.

Modeling Circadian Rhythm using Coupled Semipassive Systems

Isaac T. Castanedo-Guerra
Department of Mechanical Engineering
Eindhoven University of Technology
5600 MB, Eindhoven
The Netherlands
i.t.castanedo.guerra@tue.nl

Prof.dr. Henk Nijmeijer
Department of Mechanical Engineering
Eindhoven University of Technology
5600 MB, Eindhoven
The Netherlands
h.nijmeijer@tue.nl

1 Introduction

The biological clock regulates 24-h rhythms in our body. This clock is located in the suprachiasmatic nucleus (SCN). The output entails a 24-h rhythm in electrical impulse frequency with a higher frequency during the day and a lower frequency during the night. There is evidence that individuals neurons within the SCN act as circadian oscillators. Due to local coupling the oscillators synchronize and an overall rhythm emerges [1].

2 Neural Oscillators

As an example of a neural oscillator, we use the Hindmarsh-Rose model which is a semipassive system [2]. We aim to model the SCN as a population of coupled oscillators, hence the model is given by

$$\begin{aligned} \dot{z}_{i,1} &= -y_i^2 - 2y_i - z_{i,1} \\ \dot{z}_{i,2} &= 0.005(4(y_i + 1.1180) - z_{i,2}) \\ \dot{y}_i &= -y_i^3 + 3y_i - 8 + 5z_{i,1} - z_{i,2} + I + u_i \end{aligned}$$

Where y is the output potential of the neuron, I is the bifurcation parameter, which regulates the behavior of the neuron, and u is the coupling between neurons, defined as,

$$u_i = \sigma \sum_{j \in \epsilon_i} a_{ij}(y_j - y_i),$$

and, σ is the coupling strength between cells.

3 Contribution

Our targets are to analyze the network topology, and external inputs (such as sunlight).

3.1 Network Topology

The interconnection between neurons inside the SCN is not well defined, neither the coupling strength. We aim to investigate the best way to represent this internal structure of the SCN, such as line, ring, mesh, or combination of them. Moreover, it is pertinent to analyze the way a small sample of neurons can resemble a large scale network.

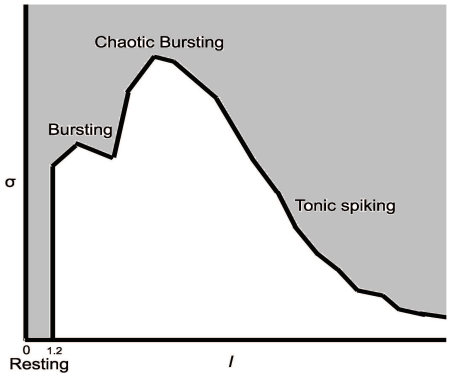

Figure 1: Region of sync

3.2 Exogenous Inputs

Early researches have shown that synchronization of neural behavior is closely related to many biological features. For the proper functioning of circadian systems, they have to be synchronized, or trained, to the daily external cycle. The most important synchronizing stimulus in the environment is light, rather than the change of temperature or other environmental stimuli. Such a thing can lead to appealing regions of synchronization or weak coupling limits, see Fig. 1.

References

[1] Rohling, J., "Simulation of Day-Length Encoding in the SCN: From Single-Cell to Tissue-Level Organization". J. of B. R., 2006.

[2] Steur, E. "Synchronous behavior in network of coupled systems", PhD Thesis, TU/e, 2011.

Optimizing Inputs for Nonlinear Systems with Infinite Memory in the Time Domain

Alexander De Cock
Vrije Universiteit Brussel
1050, Pleinlaan 2
Belgium
adecock@vub.ac.be

Johan Schoukens
Vrije Universiteit Brussel
1050, Pleinlaan 2
Belgium
Johan.Schoukens@vub.ac.be

1 Introduction

The quality of system models obtained through identification largely depends on the experimental conditions under which the measurement data was obtained. Therefore experimental design is an important step in the identification process. One aspect of the experiment that can be optimized is the input signal that is used to excite the system. For linear dynamic systems and nonlinear static systems the problem of optimal input design is well understood and well covered in literature. However, no general solution is known for nonlinear dynamical systems [1].

2 Problem Statement

Instead of considering the whole class of nonlinear systems, we will limit ourselves to Wiener systems consisting of an infinite impulse response filter (IIR) followed by a static differentiable nonlinearity. Notice that this is a subclass of the nonlinear infinite memory systems.

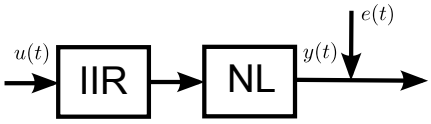

Figure 1: IIR filter followed by a polynomial nonlinearity

3 Solution Method

Our goal is to obtain a better understanding of what makes an input informative in the case of nonlinear infinite memory systems. However, unlike linear dynamic systems or nonlinear finite memory systems [2], no global or convex solver is known for this problem. Therefore, a brute force optimization will be performed where we optimize the time samples of the input with the help of numerical nonlinear solvers. In order to avoid local maxima, the settings of the optimization problem need to be carefully chosen. Three important settings will be considered: the total signal length, the sampling frequency and the initial values of the optimization. Once the correct settings are known, different systems for the system class will be considered and their optimal inputs designs will be compared in order to detect which aspects of the design influence the information content.

4 Revisiting the Linear Case

To obtain an insight in how to choose the settings of the problem, we will revisit the linear case. It should be noted that for linear systems, direct optimization of the time samples is not very common due to the existence of convex optimization methods in the frequency domain. Therefore, investigating the behavior of nonlinear optimization methods in the time domain for linear systems has its own scientific merits.

5 Results

Successful optimization of the input samples for linear systems has been performed in the time domain with performance comparable to the state of the art designs obtained with the existing convex optimization methods. Rules of thumbs have been derived for the choice of the signal length and sampling frequency based on the behavior of a second order system. Extensions of these rules to the nonlinear case are still in progress.

6 Acknowledgments

This work was supported in part by the Fund for Scientific Research (FWO-Vlaanderen), by the Flemish Government (Methusalem), the Belgian Government through the Interuniversity Poles of Attraction (IAP VII) Program, and by the ERC advanced grant SNLSID, under contract 320378.

References

[1] H.Hjalmarsson, J.Martensson, and B.Ninness, "Optimal input design for identification of non-linear systems: Learning from the linear case," in *American Control Conference*, 2007.

[2] C.A.Larsson, H.Hjalmarsson, and C.R.Rojas, "On optimal input design for nonlinear FIR-type systems," in *49th IEEE Conference on Dicision and Control*, 2010.

A MATLAB toolbox for optimizing splines

Wannes Van Loock, Goele Pipeleers and Jan Swevers
KU Leuven, BE-3001 Leuven, Belgium
Depertment of Mechanical Engineering, Division PMA
Wannes.VanLoock@kuleuven.be

1 Introduction

This work presents a new MATLAB toolbox for modeling and solving optimization problems of the following form

$$\begin{aligned} \underset{x}{\text{minimize}} \quad & f(x) \\ \text{subject to} \quad & h(x,\theta) \geq 0, \forall \theta \in \Theta \end{aligned}$$

where x are the coefficients of a (polynomial) spline

$$s(x,\theta) = \sum_{\alpha} x_\alpha b_\alpha(\theta),$$

with basis b_α and labeled by the (multi-)index α.

The main challenge when solving these problems lies in transforming the constraints that should hold for infinitely many values of θ, so-called *semi-infinite* constraints, to a (conservative) finite set of constraint. For spline representable $h(x,\cdot)$, this toolbox implements an efficient novel relaxation scheme based on the partition of unity of the basis functions and using knot insertion.

Spline solutions of the problem can be interpreted as an approximation to the solution of the more general *infinite* dimensional problem in which a function $s(\cdot)$ is searched for without preset parameterization. For these problems, splines are a particularly interesting parameterization as it can be shown that splines are a good approximation of smooth functions [1]. The toolbox therefore enables solving many practical that arise in engineering, physics, economics, and so on. In control engineering applications, one can think of optimal control problems, explicit model predictive controllers, the design of $\mathscr{H}_\infty/\mathscr{H}_2$ gain scheduling controllers and combined structure and control design. A spline

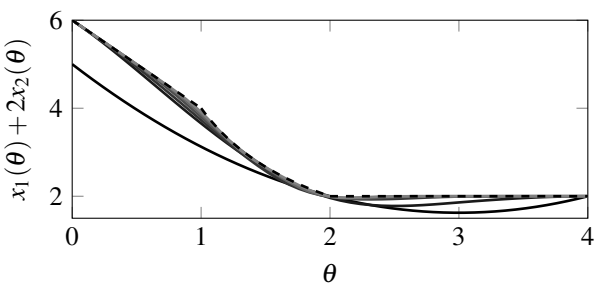

Figure 1: The approximation (solid) converges to the exact solution (dashed) for an increasing number of knots

2 A software toolbox

This research develops a MATLAB based software tool that aids the engineer in defining and solving his own spline optimization problems. The aim is to provide a simple syntax, similar to YALMIP's and to relax the semi-infinite constraints automatically. To this end, a spline class that overloads many of MATLAB's built-in methods has been developed. Consider following optimization problem

$$\begin{aligned} \underset{x_1(\cdot),x_2(\cdot)}{\text{maximize}} \quad & \int_0^4 x_1(\theta) + 2x_2(\theta) d\theta \\ \text{subject to} \quad & 0 \leq x_1(\theta), \forall \theta \in [0,4] \\ & 0 \leq x_2(\theta) \leq 2, \forall \theta \in [0,4] \\ & x_1(\theta) + \theta x_2(\theta) \leq 2, \forall \theta \in [0,4]. \end{aligned}$$

The solution to this problem is approximated by a cubic spline with degree d and n equally distributed knots:

```
Bl = BSplineBasis([0, 4], n, d);
theta = parameter(1);
x = BSpline.sdpvar(Bl, [1, 2]);
obj = x(1) + 2 * x(2);
con = [x(1) >= 0, x(2) >= 0, x(2) <= 2,
       x(1) + theta * x(2) <= 2];
sol = optimize(con, -obj.integral);
```

In Figure 1 the dashed line illustrates the exact solution for $x_1 + 2x_2$ and the solid lines the spline approximation for an increasing number of knots. It is clear that the approximation converges to the exact solution. The presentation will analyze two more involved examples from the field of optimal control and combined structure and control design.

Acknowledgment

IWT ICON project Sitcontrol: Control with Situational Information, IWT SBO project MBSE4Mechatronics: Model-based Systems Engineering for Mechatronics, FWO project G0C4515N: Optimal control of mechatronic systems: a differential flatness based approach. This work also benefits from KU Leuven-BOF PFV/10/002 Center-of-Excellence Optimization in Engineering (OPTEC), from the Belgian Programme on Interuniversity Attraction Poles, initiated by the Belgian Federal Science Policy Office, and from KU Leuven's Concerted Research Action GOA/10/11 "Global real-time optimal control of autonomous robots and mechatronic systems". Goele Pipeleers is partially supported by the Research Foundation Flanders (FWO Vlaanderen).

References

[1] de Boor, Carl. 2001. *A Practical Guide to Splines*. Springer.

Modeling and control of heat networks with storage: the single-producer multiple-consumer case

Tjardo Scholten
Department of ENTEG
University of Groningen
Nijenborgh 4
9747 AG Groningen
t.w.scholten@rug.nl

Claudio De Persis
Department of ENTEG
University of Groningen
Nijenborgh 4
9747 AG Groningen
c.de.persis@rug.nl

Pietro Tesi
Department of ENTEG
University of Groningen
Nijenborgh 4
9747 AG Groningen
p.tesi@rug.nl

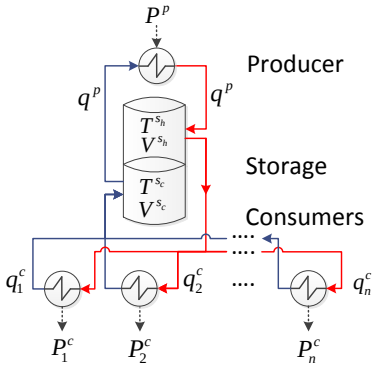

Figure 1: Topology of a district heating network.

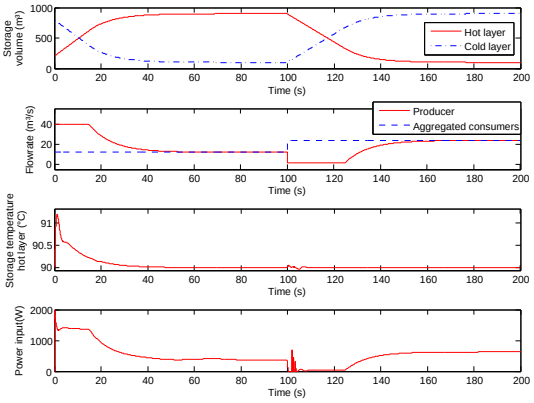

Figure 2: Simulation results of three consumers with time varying demand.

1 Introduction

In heat networks, energy storage is a viable approach to balance demand and supply. In such networks, a heat carrier is used in the form of water, where heat is injected and extracted through heat exchangers. The network can transport heated water and store it in stratification tanks. We define a setpoint tracking problem in which a desired amount of energy is stored in the storage tank while satisfying a, possible time varying, demand. A setup is considered which includes a single producer with a storage tank and multiple consumers as is depicted in Figure 1.

2 Controller

In order to solve the tracking problem a model consisting of differential equations is derived. This model is based on general modeling principles of thermodynamical systems which can be found in [1], while the heat exchanger models are adopted from [2]. In contrast to [3] where pressures and flows are considered this model describe the dynamics of the temperatures and volumes. In order to store a desired amount of energy we formulate the control problem as an output regulation problem where both the volume and temperature should converge to the prescribed setpoints. Using the internal model principle as in [4], a controller is derived for which it is proven that the tracking error converges asymptotically to zero.

3 Simulation and conclusion

In order to illustrate the performance of the proposed controller a simulation is conducted, where the thermal storage device has a fixed temperature setpoint of $90°C$. By regulating the volume in the storage a desired amount of stored energy is achieved. We aim to store $900m^3$ in the first time interval to and drain it to $100m^3$ in the second time interval. Figure 2 shows that the proposed controller is able to regulate the energy level in the storage device when consumers extract their time varying heat demand.

References

[1] S. Skogestad, *Chemical and energy process engineering*. CRC press Boca Raton, 2009.

[2] K. M. Hangos, J. Bokor, and G. Szederkényi, *Analysis and control of nonlinear process systems*. Springer, 2004.

[3] C. De Persis and C. Kallesoe, "Pressure regulation in nonlinear hydraulic networks by positive and quantized controls," *Control Systems Technology, IEEE Transactions on*, vol. 19, pp. 1371–1383, Nov 2011.

[4] A. Isidori, L. Marconi, and A. Serrani, *Robust autonomous guidance: an internal model approach*. Springer, 2003.

Design of experiment approach for optimizing the characteristics of the excitation signal for discriminating the internal structure

Alireza Fakhrizadeh Esfahani afakhriz@vub.ac.be
Johan Schoukens Johan.Schoukens@vub.ac.be
Laurent Vanbeylen LVbeylen@vub.ac.be
Vrije Universiteit Brussel, Dept. ELEC

1 Introduction: objectives

Nonlinear (NL) system identification is a high demanding field. Several NL system identification algorithms require very high quality frequency response functions (FRFs). These are used to generate an initializing estimate of the model in the optimization stage. In this work a practical method, based on design of experiment (DOE) is proposed to generate optimal quality FRFs. The proposed method tunes the DC and standard deviation (STD) levels of the excitation signal in a sense, to have an FRF (BLA, the best linear approximation) with minimum distortion level [1].

2 Problem and Methodology

For discriminating the internal structure it is proposed to excite the system with varying STD levels and looking at the BLAs behavior and trend [2]. But, increasing the STD level of the input signal, usually increases the NL distortion of the input (right side of Fig.1) which results in a decrease of the quality of the BLAs. Another approach is to introduce, a DC content to the signal. By varying the DC level it is seen that the BLAs have superior quality (left side of Fig.1). This raises the question what is the optimal selection of the STD and DC level settings in a 2-dimensional plane? This work proposes an answer to this question.

The method of central composite design (CCD) [3] is used to minimize the mean square error (MSE), which is defined on the total distortion of the BLA. Based on this method, at least 10 experiments are done on the system, with different DC and STD levels. The BLAs are calculated. By using periodic excitations, it is possible to calculate the total distortion. It is assumed, that the MSE of the distortions is a quadratic function of DC and STD levels of the excitation signal. It gives a convex surface for the MSEs, that facilitates the optimization procedure.

The coefficients of the quadratic function are estimated. The signal to noise ratio (SNR) of the coefficients is calculated by using the noise information of the multiple experiments on the center point. The coefficients with low SNR are dropped. The direction associated with the lowest eigenvalue of the final quadratic function shows the best experiment strategy.

3 Results

Fig.1 shows the BLAs of the silverbox device (NL mass-spring damper system) by either varying the DC (left side) or STD (right side). By using the DOE, the total distortion and the NL distortion are decreased but the noise distortion

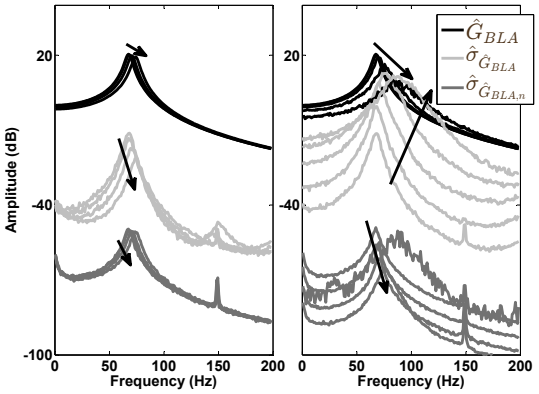

Figure 1: BLAs of silverbox (black), total distortion (light gray), and noise distortion (dark gray). The left side by varying the DC and the right side by varying the STD levels of the excitation.

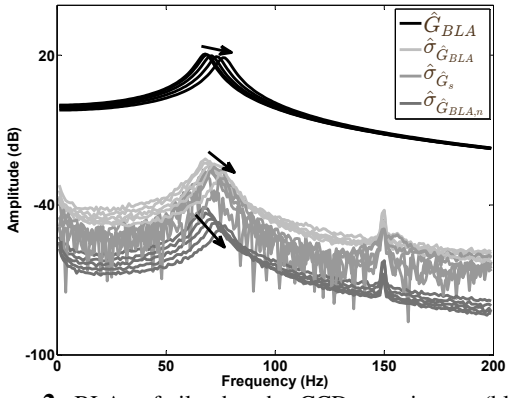

Figure 2: BLAs of silverbox by CCD experiments (black), total distortion (light gray), NL distortion (medium gray), and noise distortion (dark gray).

is increased with a small value (see Fig.2). The quality of the BLAs are superior to the approach where the DC level varied.

References

[1] R. Pintelon, and J. Schoukens, *System Identification a Frequency Domain Approach,* John Wiley & Sons, Inc., 2012.

[2] L. Lauwers, J. Schoukens, R. Pintelon, and M. Enqvist, A nonlinear block structure identification procedure using frequency response function measurements, IEEE Trans. Instrum. Meas., vol. 57, pp. 2257 2264, 2008.

[3] W.G.H. George, E.P. Box, and J. Stuart Hunter, *Statistics for experimenters: design, discovery, and innovation,* John Wiley & Sons, Inc., 2005.

A tensor-based framework for blind identification of linear MIMO FIR systems

Frederik Van Eeghem ⋆ † ‡
Frederik.VanEeghem@kuleuven.be

Otto Debals ⋆ † ‡
Otto.Debals@kuleuven.be

Lieven De Lathauwer ⋆ † ‡
Lieven.DeLathauwer@kuleuven-kulak.be

⋆ Department of Electrical Engineering (ESAT), STADIUS Center for Dynamical Systems, Signal Processing and Data Analytics, KU Leuven. Kasteelpark Arenberg 10, 3001 Leuven, Belgium.
† Group Science, Engineering and Technology, KU Leuven Kulak.
Etienne Sabbelaan 53, 8500 Kortrijk, Belgium.
‡ iMinds Medical IT, KU Leuven.
Kasteelpark Arenberg 10, 3001 Leuven, Belgium.

1 Blind system identification

Contrary to classical identification, blind system identification (BSI) attempts to estimate a system using output measurements only. This is especially useful when the input data are expensive or impossible to measure, as is the case in several medical applications, wireless communications, and the processing of seismographic data [1]. However, it is not possible to blindly identify systems without making some extra assumptions. Here, the inputs are assumed to be statistically independent, which is done often and has proven to be a good approximation in several applications [2]. This assumption bridges the gap between BSI and independent component analysis (ICA).

In its most basic form, ICA tries to estimate signals from an instantaneous mixture. The convolutive extension of ICA strongly resembles the blind identification of linear FIR systems, which are characterized by a convolution. The only difference in both approaches lies in the goal: BSI tries to identify the system itself, whereas ICA is mainly interested in estimating the input signals.

2 A tensor-based framework

Datasets are frequently surfacing as multi-way arrays, making tensors a natural tool for data representation. As a higher-dimensional generalization of vectors and matrices, tensors possess favorable properties lacking in their lower-dimensional counterparts. One of the key properties is the uniqueness under mild conditions of several decompositions, motivating why tensors have been increasingly studied during the past decades [3].

Tensor methods for instantaneous ICA have already been well established and mostly make use of second- and higher-order statistics [2]. Here, the focus lies on expanding these tensor-based methods to blind MIMO FIR identification and convolutive ICA, which has only been studied little so far [4, 5]. A tensorial framework is developed which allows to blindly identify linear FIR systems with either i.i.d. or temporally coherent inputs, assumed mutually independent. The framework not only comprises existing methods but has new variants as well. By relating each method to a tensor decomposition, we can tap into the theory developed for the latter. This allows us to formulate uniqueness conditions. Moreover, the performance of several methods is improved by fusing both second- and higher-order statistics in coupled decompositions.

References

[1] Abed-Meraim, K., Qiu, W., and Hua, Y., "Blind system identification." Proceedings of the IEEE 85.8 (1997): 1310-1322.

[2] Comon, P., and Jutten, C., eds. Handbook of Blind Source Separation: Independent component analysis and applications. Academic press, 2010.

[3] Cichocki, A., Mandic, C., Phan, A., Caifa, C., Zhou, G., Zhao, Q., De Lathauwer, L., "Tensor Decompositions for Signal Processing Applications. From two-way to multiway component analysis." IEEE Signal Processing Magazine (accepted). 2014.

[4] Bousbia-Salah, H., Belouchrani, A., and Abed-Meraim, K., "Jacobi-like algorithm for blind signal separation of convolutive mixtures." Electronics Letters 37.16 (2001): 1049-1050.

[5] Fernandes, C. E., Favier, G. A. and Mota, J. C., "PARAFAC-based blind identification of convolutive MIMO linear systems." System Identification. Vol. 15. No. 1. 2009.

Applications of the greatest common divisor in system theory and signal processing

Ivan Markovsky and Mayank Saxena
Department ELEC, Vrije Universiteit Brussel (VUB)
{ivan.markovsky,mayank}@vub.ac.be

1 Introduction

Finding the *greatest common divisor (GCD)* of a set of univariate polynomials is a classic problem in algebra, which is still an active research topic. Numerically it is an ill-conditioned problem: small perturbations in the input data (the polynomials' coefficients) may result in large changes in the solution (the GCD coefficients). This makes the problem computationally challenging. For a recent overview of computational approaches, we refer the reader to [3].

Applications of the GCD in systems, control, and signal processing, however, are surprisingly missing from the broad literature on the theoretical and computational aspects of the problem. We present here three applications that are directly solvable by a GCD computation. Subsequently existing GCD methods, algorithms and software can be used in the applications. Vice verse, methods, algorithms and software developed for the applications can be viewed as and used for GCD computation.

2 Blind FIR system identification

The indeterminate of a polynomial is denoted by z, as a reminder to the Z-transform that maps finite duration time domain signals to polynomials.

Problem 1 (GCD)**.** Given polynomials $a^1(z),\dots,a^g(z)$, find a maximal degree polynomial $c(z)$ that divides all $a^i(z)$'s, *i.e.*, there are $b^i(z)$, such that $a^i(z) = c(z)b^i(z)$, for all i.

We denote the GCD of $a^1(z),\dots,a^g(z)$ by $\mathrm{GCD}(a^1,\dots,a^g)$.

Problem 2. Given output observations $y^1,\dots,y^N$ of a *finite impulse response (FIR)* system, generated by unknown signals $u^1,\dots,u^N$, find the impulse response h of the system.

The Z-transform of a finite duration signal y^i is a polynomial $y^i(z)$. (With some abuse of notation, we use the same lower case letter for both the time-domain and Z-domain signals.)

Theorem 3. *Assuming that 1) $N \geq 2$, 2) $u^1,\dots,u^N$ have finite support, 3) $GCD\big(u^1(z),\dots,u^N(z)\big) = 1$, and 4) $y^1,\dots,y^N$ are the full responses of the filter, including the transients, $h(z)$ can be obtained up to a scaling factor α as*

$$h(z) = \alpha GCD\big(y^1(z),\dots,y^N(z)\big).$$

3 GCD applications in systems theory

An application of GCD for computing the distance of a linear time-invariant system to the set of uncontrollable system is described in [1]. A related problem, described next, is reduction of a non-minimal kernel representation to a minimal one [2]. For simplicity, we restrict to the case of scalar autonomous systems. A (non-minimal) kernel representation is defined by a $g \times 1$ vector polynomial $R(z)$, such that the solutions of differential/difference equation $R(\frac{\mathrm{d}}{\mathrm{d}t}) = 0$ / $R(\sigma) = 0$, where σ is the shift operator, are the set of all trajectories (the behavior) of the system. The representation is minimal if g is as small as possible. In the scalar autonomous case, a minimal representation is a scalar polynomial $R_{\min}$, which is given by

$$R_{\min}(z) = \mathrm{GCD}\big(R_1(z),\dots,R_g(z)\big). \qquad (*)$$

Other applications of the GCD computation in system theory are: finding the intersections of two (autonomous) behaviors, detecting spurious poles in operational modal analysis, and separation of the disturbance shaping filter from the system's dynamics. Current work is focus on generalization of $(*)$ to multivariable systems. The solution tools are based on low-rank Hankel and Sylvester structured matrix computations.

Acknowledgments

The research leading to these results has received funding from the European Research Council under the European Union's Seventh Framework Programme (FP7/2007-2013) / ERC Grant agreement number 258581 "Structured low-rank approximation: Theory, algorithms, and applications".

References

[1] N. Guglielmi and I. Markovsky. Computing the distance to uncontrollability: the SISO case. Technical report, Vrije Univ. Brussel, 2014.

[2] J. Polderman and J. C. Willems. *Introduction to Mathematical Systems Theory*. Springer-Verlag, New York, 1998.

[3] K. Usevich and I. Markovsky. Variable projection methods for approximate (greatest) common divisor computations. Technical report, Vrije Univ. Brussel, 2013.

A survey on stochastic and deterministic tensorization for blind signal separation

Otto Debals*†‡
otto.debals@esat.kuleuven.be

Lieven De Lathauwer*†‡
lieven.delathauwer@kuleuven-kulak.be

*Department of Electrical Engineering (ESAT) STADIUS Center for Dynamical Systems, Signal Processing and Data Analytics, KU Leuven, Kasteelpark Arenberg 10, 3001 Leuven, Belgium;
†Group Science, Engineering and Technology, KU Leuven Kulak, E. Sabbelaan 53, 8500 Kortrijk Belgium; ‡iMinds Medical IT, KU Leuven, Kasteelpark Arenberg 10, 3001 Leuven, Belgium;

Introduction Given a mixture of some source signals, the Blind Signal Separation (BSS) problem consists of the identification of both the mixing matrix and the original sources. Specifically, one tries to determine $\mathbf{M}$ and $\mathbf{S}$ in $\mathbf{X} = \mathbf{MS}$ with only $\mathbf{X}$ known. The source signals, mixing vectors and sensor signals are contained in $\mathbf{S}$, $\mathbf{M}$ and $\mathbf{X}$, respectively. One can see that the problem consists of a matrix factorization of $\mathbf{X}$. The solution is not unique (except for a single source), and scaling and permutation of the mixing part and source signals are two insurmountable indeterminacies.

Solutions for BSS The eigenvalue decomposition, the QR/LQ decomposition and the singular value decomposition are the most well known matrix factorization techniques. However, the constraints defining these (such as triangularity and/or orthogonality) are too restrictive for BSS. More suitable techniques have been introduced in recent history, e.g., Non-negative Matrix Factorization (NMF), Sparse Component Analysis (SCA) and Independent Component Analysis (ICA).

The possibility of obtaining a single unique solution is an desirable quality of a BSS-technique. Proving this is a hard task. For example, NMF needs additional constraints (such as sparsity) to enforce uniqueness of the solution. Tensors (as higher-order generalizations of vectors and matrices [1]) provide a solution for a lot of techniques for BSS. Decompositions of tensors, such as the Canonical Polyadic Decomposition (CPD) and Block Term Decomposition (BTD), are very powerful as they are unique under only mild conditions. They can be used for BSS after the observation matrix is mapped to a tensor through tensorization, translating the assumptions made on the sources and/or mixing vectors. The decomposition afterwards ensures the uniqueness.

Tensorization Different tensorization techniques have recently appeared but in a disparate manner. Also, the link to tensor decompositions has been omitted in many existing techniques for BSS despite it being inherently present. The multilinear setting however provides a comprehensive framework. We will present tensorization as an important concept by itself.

We shall discuss the following tensorization techniques:

- Higher-Order Statistics, useful for ICA [2];
- the stacking of matrices depending on a single (or multiple) parameters. Stacked covariance matrices are an example also suitable for ICA [2];
- 'Hankelization', useful for a separation into exponential polynomials [3];
- 'Loewnerization', useful for a separation into rational functions [4];
- 'Segmentation', useful for big data with compact representations through low-rank approximations [5].

The first item is a stochastic tensorization technique, together with the example in the second item. The latter three are purely deterministic techniques. They work well for a low number of samples. There are other techniques such as Taylor/McLaurin series coefficients, constant modulus & constant power constraints and time-frequency & wavelet representations, which we omit for brevity.

References

[1] Cichocki, A., et al. "Tensor Decompositions for Signal Processing Applications. From Two-way to Multiway Component Analysis." *IEEE Signal Processing Magazine*, March 2015, accepted.

[2] Comon, P. and Jutten, C., eds. *Handbook of Blind Source Separation: Independent Component Analysis and Applications.* Academic press, 2010.

[3] De Lathauwer, L. "Blind Separation of Exponential Polynomials and the Decomposition of a Tensor in Rank-$(L_r, L_r, 1)$ Terms." *SIAM Journal on Matrix Analysis and Applications* 32.4 (2011): 1451-1474.

[4] Debals, O., Van Barel, M., De Lathauwer, L. "Blind Signal Separation of Rational Functions using Löwner-based Tensorization." *Proceedings of ICASSP 2015*, accepted.

[5] Boussé, M., Debals, O., De Lathauwer, L. "A Novel Deterministic Method for Large-Scale Blind Source Separation." Internal Report 15-07, ESAT-STADIUS, KU Leuven (Leuven, Belgium), 2015

Identifying Parameters with Pre-Specified Accuracies in Linear Physical Systems: Part I

Max Potters, Xavier Bombois
Delft Centre for Systems and Control
Delft University of Technology
Mekelweg 2
2628 CD Delft
The Netherlands
M.G.Potters@tudelft.nl

Paul M.J. Van den Hof
Department of Electrical Engineering
Eindhoven University of Technology
Den Dolech 2
P.O. Box 513, 5600 MB Eindhoven
The Netherlands
P.M.J.VandenHof@tue.nl

Introduction

Estimation of key parameters in physical systems is an important problem in many fields of science. For instance, materials can be characterised by their conductivity and diffusivity parameters [1], groundwater contamination simulations require estimates of diffusivity and advection constants [2], and permeability and porosity estimates are crucial parameters to characterize subsurface reservoirs [3]. In light of the above motivation, we studied the design of least-intrusive input signals that nevertheless result in parameter estimates with variances that do not exceed user-chosen limits. The subject dealing with this problem is referred to as Least-Costly Experiment Design (LCED).

Identification and Experiment Design for linear physical systems involve two aspects that need to be treated carefully. The main differences between a ordinary input-output system are: (i) an irrational infinite-order transfer function, and (ii) input, output and parameter values that differ by many orders of magnitude.

Due to these intrinsic properties of many physical systems we can not straightforwardly apply the classical LCED framework nor identification procedures to physical systems. In part I of a series of two presentations we introduce the classical LCED framework [4]. We discuss two scenarios: LCED for the purpose of control (multi-dimensional ellipsoidal constraints) and for the purpose of accurate parameter estimates (multi-dimensional box constraints). In particular we provide new insight in the numerical solutions. With this background we proceed in Part II with the identification and LCED in physical systems, where we elaborate on issues (i) and (ii). We show how to alleviate both issues and introduce a uniform framework for the identification and LCED procedure. Our results are illustrated on diffusion-advection systems.

The presentations are structured in such a way that they can be followed independently.

Part I: Fundamentals on Least-Costly Experiment Design

In Part I we define the least-costly experiment design problem and show how it is currently solved numerically. We explain the optimization problems of the two scenarios mentioned above and discuss their differences. Furthermore, we show new analytical results for both scenarios which generalize earlier ones [5]. These solutions allow us to (i) interpret the numerical results, (ii) validate the numerical results, (iii) analyse the accuracy of the numerical solution, (iv) analyse the consequences of the so-called chicken-and-egg problem, and (v) solve some problems many times quicker and more accurate than with the numerical method.

References

[1] J. Gabano, and T. Poinot, '*Fractional Modelling Applied to Heat Conductivity and Diffusivity Estiimation*', Physica Scripta (136), 2009.

[2] B. Wagner, and J. Harvey, '*Experimental Design for Estimating Parameters of Rate-Limited Mass Transfer: Analysis of Stream Tracer Studies*', Water Resources Research (33), 1997.

[3] M. Mansoori, P.M.J. Van den Hof, J.D. Jansen, and D. Rashchian, '*Pressure Transient Analysis of Buttonhole Pressure and Rate Measurements using System Identification Techniques*', submitted to SPE Journal, 2014.

[4] X. Bombois, G. Scorletti, M. Gevers, P.M.J. Van den Hof, and R. Hildebrand , '*Least-Costly Identification Experiment for Control*' Automatica (42), 2006.

[5] M. Potters, M. Forgione, X. Bombois, and P.M.J. Van den Hof, '*Least-Costly Experiment Design for Uni-Parametric Linear Models: An Analytical Approach*', submitted to the European Control Conference, 2015.

Identifying Parameters with Pre-Specified Accuracies in Linear Physical Systems: Part II

Max Potters, Mehdi Mansoori, Xavier Bombois
Delft Centre for Systems and Control
Delft University of Technology
Mekelweg 2
2628 CD Delft
The Netherlands
M.G.Potters@tudelft.nl

Paul M.J. Van den Hof
Department of Electrical Engineering
Eindhoven University of Technology
Den Dolech 2
P.O. Box 513, 5600 MB Eindhoven
The Netherlands
P.M.J.VandenHof@tue.nl

Introduction

Estimation of key parameters in physical systems is an important problem in many fields of science. For instance, materials can be characterised by their conductivity and diffusivity parameters [1], groundwater contamination simulations require estimates of diffusivity and advection constants, and permeability and porosity estimates are crucial parameters to characterize subsurface reservoirs [2]. In light of the above motivation, we studied the design of least-intrusive input signals that nevertheless result in parameter estimates with variances that do not exceed user-chosen limits. The subject dealing with this problem is referred to as Least-Costly Experiment Design (LCED).

Identification and Experiment Design for linear physical systems involve two aspects that need to be treated carefully. The main differences between a ordinary input-output system are: (i) an irrational infinite-order transfer function, and (ii) input, output and parameter values that differ by many orders of magnitude.

Due to these intrinsic properties of many physical systems we can not straightforwardly apply the classical LCED framework nor identification procedures to physical systems. In part I of a series of two presentations we introduce the classical LCED framework [3]. We discuss two scenarios: LCED for the purpose of control (multi-dimensional ellipsoidal constraints) and for the purpose of accurate parameter estimates (multi-dimensional box constraints). In particular we provide new insight in the numerical solutions. With this background we proceed in Part II with the identification and LCED in physical systems, where we elaborate on issues (i) and (ii). We show how to alleviate both issues and introduce a uniform framework for the identification and LCED procedure. Our results are illustrated on diffusion-advection systems.

The presentations are structured in such a way that they can be followed independently.

Part II: Parameter Identification in Physical Systems with Optimal Input Signals

To tackle point (i) we have to approximate the infinite-order transfer function. Although several methods exist, see for instance [4], we require that the approximate transfer function is explicit in the physical variables in order to apply LCED. To this end, we discretize the PDE equations with an appropriate numerical scheme to obtain a stable and rational transfer function. This scheme also allows us to simulate the physical system, which is required in the identification procedure. Point (ii) is taken care of by appropriately scaling the system and parameters. This step ensures convergence of the numerical methods. Next, we generalise the LCED framework by introducing an algorithm that also computes optimal actuator and sensor locations.

Lastly, we apply our methodology to a problem in heat transfer studies: estimating conductivity and diffusivity parameters in front-face experiments. We show, among other things, that sensor and actuator locations play a crucial role in the accuracy of the parameter estimates.

References

[1] J. Gabano, and T. Poinot, '*Fractional Modelling Applied to Heat Conductivity and Diffusivity Estimation*', Physica Scripta (136), 2009.

[2] M. Mansoori, P.M.J. Van den Hof, J.D. Jansen, and D. Rashchian, '*Pressure Transient Analysis of Buttonhole Pressure and Rate Measurements using System Identification Techniques*', submitted to SPE Journal, 2014.

[3] X. Bombois, G. Scorletti, M. Gevers, P.M.J. Van den Hof, and R. Hildebrand , '*Least-Costly Identification Experiment for Control*' Automatica (42), 2006.

[4] R. Pintelon, J. Schoukens, L. Pauwels, and E. Van Gheem, '*Diffusion Systems: Stability, Modelling, and Identification*', IEEE Transactions on Instrumentation and Measurement (54), 2005.

Distributed supply coordination for Power-to-Gas facilities embedded in the energy grids

Desti Alkano, Ilco Kuiper, and Jacquelien M.A. Scherpen
Engineering and Technology Institute, University of Groningen
d.alkano@rug.nl, ilcokuiper@gmail.com, j.m.a.scherpen@rug.nl

1 Introduction

Power-to-Gas (PtG) facility is currently an alternative energy storage for a power grid with high penetration of renewable energy. The facility converts excess electricity into a gaseous energy carrier, i.e. hydrogen. The produced hydrogen can be used in different ways, e.g. it can be injected in the gas grid or sold to a mobility sector. Alternatively, it can be stored in a hydrogen buffer and later on reconverted into electrical energy using a fuel cell before selling it to a power grid. The facility overview is shown in Figure 1.

Relying on the fact that a number of PtG facilities embedded in the existing energy grids may increase, it is therefore of interest to study on how to maximize their estimated revenue from the produced hydrogen without exceeding grid capacities. The problem is solved by distributed model predictive control, allowing each PtG facility locally to decide how much hydrogen each PtG facility $i = 1,\ldots,n$ injects into the gas grid g_i, sells to the mobility sector y_i, stores to the hydrogen buffer $u_{s,i}$, and/or reconverts into electricity before injecting it to the power grid e_i, given the estimated predictions of demand patterns and selling prices in the gas grid, the mobility sector, and the power grid. As the energy grids have limited capacities, these decisions need to be coordinated with the operators of the energy grids.

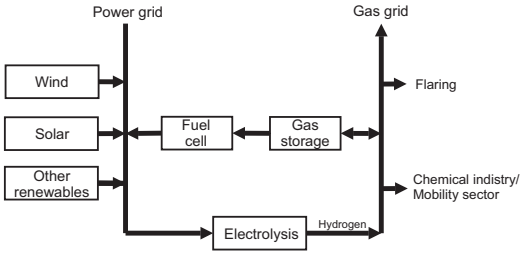

Figure 1: An overview of Power-to-Gas facility equipped with a hydrogen buffer and a fuel cell.

2 Distributed supply coordination through prices

Inspired by [1], a dual decomposition approach combined with the projected sub-gradient method applied in the model predictive control scheme is used to solve our problem in a distributed fashion. With this approach, each operator sets extra fee for energy transport and system service utilized by PtG facilities if overloading grid is detected. In this way, PtG facilities are induced to modify their supply levels. This bidding process is illustrated in Figure 2. We provide results on how the dynamic extra fee is useful to avoid overloading grids, as shown in Figure 3 and Figure 4.

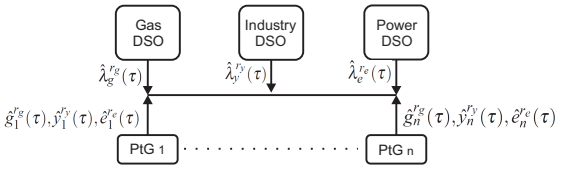

Figure 2: **Interactions among PtG facilities and the operators of energy grids at each iteration r_g, r_y, r_e within a time step τ.** Given extra fees $\lambda_g^{r_g}(\tau), \lambda_y^{r_y}(\tau), \lambda_e^{r_e}(\tau)$, PtG facilities bid their supply levels $g_i^{r_g}(\tau), y_i^{r_y}(\tau), e_i^{r_e}(\tau)$ to the operators of energy grids.

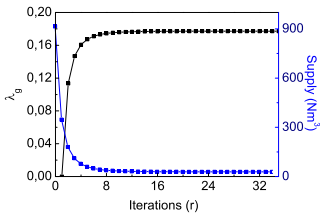

Figure 3: The decrease of supply level when the initial fee set by the operator of the gas grid is at zero level, i.e. $\lambda_g^{r_g=0} = 0$, and the allowable hydrogen in the gas grid is 83 Nm^3.

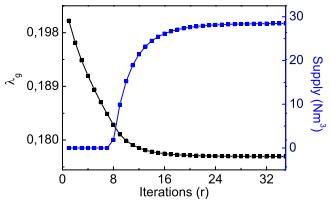

Figure 4: The increase of supply level when the initial fee is set at 0.2, i.e. $\lambda_g^{r_g=0} = 0.2$, and the allowable hydrogen in the gas grid is 28 Nm^3.

References

[1] N. Trichakis, A. Zymnis, and S. Boyd, Dynamic network utility maximization with delivery contracts, in Proc. of the 17th IFAC World Congress, July 2008.

Handling uncertainties in balancing short-term and long-term objectives in water-flooding optimization

M. Mohsin Siraj and Paul M.J. Van den Hof
Electrical Engineering, Control Systems group
Eindhoven University of Technology
m.m.siraj,P.M.J.vandenhof@tue.nl

Jan Dirk Jansen
Department of Geoscience and Engineering
Delft University of Technology
J.D.Jansen@tudelft.nl

1 Introduction

Water-flooding involves the injection of water in an oil reservoir to increase oil production. Dynamic optimization of the water-flooding process has shown significant scope for improvement of the economic life-cycle performance of oil fields [1]. The financial measure, Net Present Value (NPV) used in this optimization, because of its cumulative nature, focuses on the long-term gains while the short-term production is not explicitly addressed. At the same time the achievable NPV is highly uncertain due to the limited knowledge of reservoir model parameters and the varying economic conditions. Different (ad-hoc) methods have been proposed to introduce short-term considerations to balance short-term and long-term objectives in a model-based approach [1]. In this work, we address the question whether through an explicit handling of model and economic uncertainties in NPV (robust) optimization, an appropriate balance between these economic objectives is naturally obtained.

2 Robust optimization

An ensemble of possible realizations of the reservoir models and different oil price scenarios are considered to characterize geological and economic uncertainty respectively. A robust optimization (RO) approach is implemented which maximizes an average NPV over these ensembles. Furthermore, as RO does not attempt to reduce the negative effects of uncertainty, a mean-variance optimization (MVO) approach is used which maximizes the average NPV and minimizes the variance of the NPV distribution [2].

3 Simulation examples

In the first example, only geological uncertainty is considered. The RO, conventional reactive control (RC) and the MVO (with different weighting γ on the variance term in the mean-variance objective) strategies are applied to the geological model ensemble resulting in a set of NPV values for each strategy. The corresponding PDFs, as shown in Fig.1a, show a reduction in variance with increasing value of γ. The maximum and minimum values of the time-evolution of NPV form a tube as shown in Fig. 1b. It can be observed that, due to better uncertainty handling, all MVO strategies provide a faster build-up of NPV over time (high short-term gains) but at the cost of compromising long-term gains. The second example considers an ensemble of varying oil price scenarios with a single geological model realization. The time evolution of the NPV is shown in Fig. 2b. Fig. 2a shows the average NPV values of these bands. With MVO approaches, an improvement in the short-term gains compared to the RO case can also be observed.

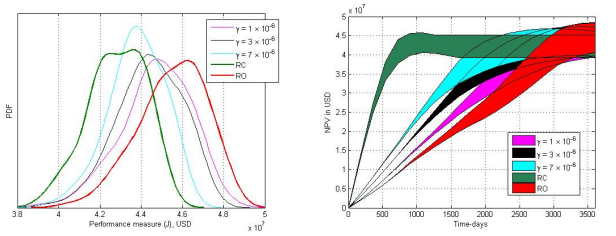

(a) PDF from each strategy (b) Tubes of NPV time buildup

Figure 1: Results comparison with geological uncertainty

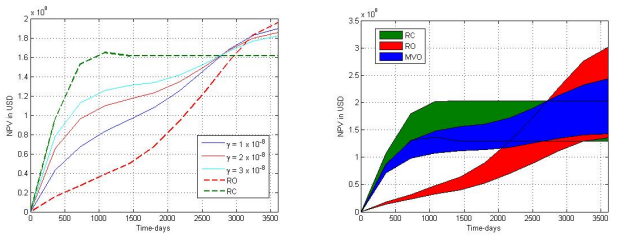

(a) Average values of NPV tubes (b) Tubes of NPV time buildup

Figure 2: Results comparison with economic uncertainty

4 Acknowledgements

The authors acknowledge financial support from the Recovery Factory program sponsored by Shell Global Solutions Internationals.

References

[1] P.M.J. Van den Hof, J.D. Jansen and A.W. Heemink. *Recent developments in model-based optimization and control of subsurface flow in oil reservoirs*. Proc. 1st IFAC Workshop on Automatic Control in Offshore Oil and Gas Production. 31 May-1 June 2012, Trondheim, Norway, pp. 189-200.

[2] M.M. Siraj, P.M.J. Van den Hof and J.D. Jansen. *Handling model and economic uncertainties in balancing short-term and long-term objectives in water-flooding optimization*. Accepted for presentation at the 2015 SPE Reservoir Simulation Symposium, Houston, TX, USA.

Analysis and Synthesis of Interconnected Systems: Application to Tuned Vibration Absorber Design for a Flexible Beam

Ruben Van Parys, Goele Pipeleers
KU Leuven, BE-3001 Heverlee, Belgium
Department of Mechanical Engineering, Division PMA
ruben.vanparys@kuleuven.be

1 Introduction

Since the last decade, substantial research has been devoted to the analysis and synthesis of interconnected systems by addressing techniques from robust systems theory. An important result is the convex reformulation of the distributed controller design problem, for which the controller has the same interconnection scheme as the plant and the controller subunits having the same order as the ones on the plant [1]. However, this controller type is not always applicable. In some cases, it is desired to synthesize controllers with a much lower degree or with a free interconnection topology. In this work, two strategies are explored to solve structured distributed control problems. These are applied on the design of tuned vibration absorbers for a flexible beam.

2 Analysis and Synthesis of Interconnected Systems

The lower part of Figure 1 illustrates an interconnected system with equal subunits G. This system can be addressed as an uncertain one with the time and spatial frequency as uncertainties. Using techniques from robust systems analysis, one obtains an LMI condition, guaranteeing an input-output energy attenuation γ in a given time frequency interval:

$$\begin{bmatrix} I \\ G \end{bmatrix}^T \Theta(P_t, P_s, \gamma) \begin{bmatrix} I \\ G \end{bmatrix} \prec 0 \qquad (1)$$

Θ is a Hermitian matrix which depends linear on respectively the time and spatial related multiplier P_t, P_s and on γ. In order to retrieve the best attenuation in a desired frequency range, appropriate distributed controllers are designed. In this work, the structure of the controller is fixed and by solving problem (1) while minimizing γ, the optimal control parameters are determined. Because G depends on those parameters, the problem is non-convex and currently two approaches are investigated to solve it effectively. As the non-convex matrix inequality can be decomposed in a convex and concave part, it can be solved by sequential convex programming [2]. Secondly, the problem can also be solved as a parametric program. The variables P_t, P_s and γ are parametrized as B-Splines which depend on the control parameters. The problem becomes convex and results in the best performance as a function of the control parameters.

3 Tuned Vibration Control for a Flexible Beam

The synthesis methods are applied on the design of periodically attached tuned vibration absorbers for a flexible beam in order to create a desired frequency stop band which reduces the noise radiation in this frequency range. Because the absorbers are attached periodically, the structure can be modelled as an interconnection of equal subunits (Figure 1), from which the system representation is derived from the finite element model of the beam. The input of the system is a vector containing all nodal forces acting on the beam, the outputs are the nodal displacements. Therefore γ expresses the worst-case compliance seen over all possible spatial force distributions. In order to create a desired frequency stop band, the optimal parameters for the tuned absorber are determined which minimize γ in this frequency interval. A first result is illustrated in Figure 2. Using parametric programming, the worst-case compliance γ in the given frequency range is determined as a function of the damping coefficient of the tuned absorber, for which the mass is fixed and the resonance frequency is tuned in the middle of the desired stop band.

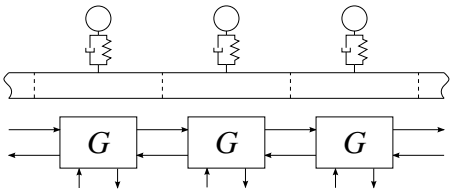

Figure 1: Beam with periodically attached tuned vibration absorbers modelled as an interconnected system.

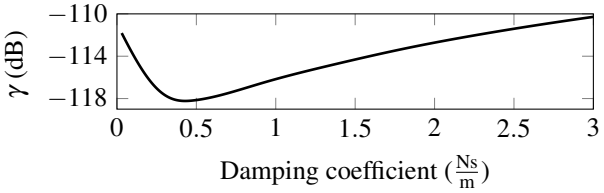

Figure 2: Worst-case compliance γ in a frequency band of 10 rad/s around 1000 rad/s for a beam with periodically attached tuned vibration absorbers with variable damping.

References

[1] R. D'Andrea and G. E. Dullerud, "Distributed control design for spatially interconnected systems.," *IEEE Trans. Automat. Contr.*, vol. 48, no. 9, pp. 1478–1495, 2003.

[2] D. Q. Tran, S. Gumussoy, W. Michiels, and M. Diehl, "Combining convex-concave decompositions and linearization approaches for solving bmis, with application to static output feedback.," *IEEE Trans. Automat. Contr.*, vol. 57, no. 6, pp. 1377–1390, 2012.

Acknowledgement This work benefits from KU Leuven-BOF PFV/10/002 Center-of-Excellence Optimization in Engineering (OPTEC) and the Belgian Programme on Interuniversity Attraction Poles, initiated by the Belgian Federal Science Policy Office (DYSCO). Ruben Van Parys is a PhD fellow of the Research Foundation Flanders (FWO Vlaanderen). Goele Pipeleers is partially supported by the Research Foundation Flanders.

State-Dependent Virtual Hierarchization of Batteries and Its Application to Energy Management Systems

Hitoshi Yanami
yanami@jp.fujitsu.com
Tomotake Sasaki
tomotake.sasaki@jp.fujitsu.com
Junji Kaneko
kaneko.junji@jp.fujitsu.com
Fujitsu Limited, Kawasaki, Japan

Shinji Hara
Shinji_Hara@ipc.i.u-tokyo.ac.jp
Yafei Wang
wang@hori.k.u-tokyo.ac.jp
Satoshi Moriyama
Satoshi_Moriyama@ipc.i.u-tokyo.ac.jp
The University of Tokyo, Tokyo, Japan

Hidenao Iwane
iwane@nii.ac.jp
National Institute of Informatics, Tokyo, Japan

1 Introduction

To control next-generation, large energy network systems, hierarchical and decentralized control methods are needed. We focus on such systems with batteries and examine how they should be controlled for effective use of energy with a model predictive control approach [1, 2]. The present paper is based on the work of the CREST team directed by Shinji Hara to realize glocal control [3] in energy network systems.

2 Problem Setting

We consider energy network systems in a community such as an office or area where a lot of batteries are placed that are available to energy management. We make the following assumptions about batteries and power network: (1) Required power for charging a battery, charge speed, and discharge speed are all constant. (2) Specifications of batteries such as a full charge capacity and required power for charging are all comparable, (3) Each of the total power consumptions of electrical instruments attached to a battery is time-invariant and all of them are comparable, and (4) All batteries are assumed to be supplied with grid power only.

The energy management server forecasts electric energy demand of the whole community based on the past energy demand, ambient temperature and other data. The main task of the server is to create an appropriate charge and discharge plan for each battery to reduce peak power in the community based on the forecast data, each battery's state of charge (SOC) and the like. Each computational device attached to a battery receives signals from the server and controls actual charge and discharge.

3 State-Dependent Virtual Hierarchization

Our control algorithm is based on a three-layered state-dependent virtual hierarchization of the batteries in which the batteries are grouped according to their SOCs, and their data are aggregated. With this structure we split an optimization problem for the whole system formulated by a model predictive control approach with both temporal and spatial scales into smaller ones; the top layer cares about a global objective of peak power reduction only concerning a dimension of time, the middle layer determines battery modes, a spatial optimization with a shorter time-horizon.

Simulation studies on computer show that our algorithm effectively reduces the peak power in a community with up to a million batteries. We also examine a long-term effect on the SOC distribution of the batteries in the system.

4 Acknowledgement

This work is partially supported by a CREST program "Creation of Fundamental Theory and Technology to Establish a Cooperative Distributed Energy Management System and Integration of Technologies Across Broad Disciplines Toward Social Application" of Japan Science and Technology Agency.

References

[1] M. Shinohara, M. Murakami, H. Iwane, S. Takahashi, S. Yamane, H. Anai, T. Sonoda, and N. Yugami, "Development of an integrated control system using notebook PC batteries for reducing peak power demand," *International Journal of Informatics Society*, vol. 5, no. 3, pp. 109–118, Dec. 2013.

[2] H. Yanami, T. Sasaki, J. Kaneko, S. Hara, S. Moriyama, Y. Wang, and H. Iwane, "A glocal control with state-dependent virtual hierarchization and its application to battery mode management for office peak power reduction," in *Proc. the 57th Japan Joint Automatic Control Conference*, Shibukawa, Japan, Nov. 2014, pp. 969–975, (in Japanese).

[3] S. Hara, "Glocal control: Realization of global functions by local measurement and control," in *Proc. the 8th Asian Control Conference*, Kaohsiung, Taiwan, May 2011, keynote Address.

Extended and unscented Kalman filter designs for hybridoma cell fed-batch cultures

Sofia Fernandes[1], Anne Richelle[2], Zakaria Amribt[2],
Laurent Dewasme[1], Philippe Bogaerts[2], Alain Vande Wouwer[1]
[1]Service d'Automatique, Université de Mons,
31 Boulevard Dolez, 7000 Mons, Belgium
(sofia.afonsofernandes, laurent.dewasme and alain.vandewouwer@umons.ac.be)
[2]3BIO-BioControl, Brussels School of Engineering, Universit Libre de Bruxelles,
Av. F.-D. Roosevelt 50 C.P. 165/61, 1050 Brussels, Belgium
(arichell, zakaria.amribt and Philippe.Bogaerts@ulb.ac.be)

1 Introduction

In the present study, both extended (EKF) and unscented (UKF) kalman filters are applied to hybridoma cell cultures to estimate glucose and glutamine concentrations, using a macroscopic model taking account of an overflow metabolism within glycolysis and glutaminolysis [1].

In many study cases, sensitivity of measured model states to unmeasured ones is low, leading to poor estimation quality. This is due to the fact that when using least-squares method to identify model parameters, no guarantee is provided about sensitivity. To overcome this problem, a parameter identification procedure is proposed in [2], which is based on a cost function combining the usual least-squares criterion with a state estimation sensitivity criterion.

The motivation of this work is to show the effectiveness of the parameter identification for state estimation procedure when state observability is limited.

2 Results

Glucose and glutamine concentrations are estimated by the EKF and UKF observers using a set of modified parameters based on a cost function combining the usual least-squares criterion with a state estimation sensitivity criterion, when applied to a structurally comparable model defined by a set of nominal parameters identified by a classical least-squares method.

From fig. 1 it is shown that the use of an exponential feeding can lead to divergent state estimates when the observers are set with the nominal parameters (NP). This phenomenon is observed when the sensitivity of the unmeasured states to the measured ones becomes very low (which happens here when the glutamine is almost depleted) and, simultaneously, the corresponding state estimates are still far from the true values. This phenomenon is not observed with the modified parameters (MP) as they lead to a significantly higher state estimation sensitivity.

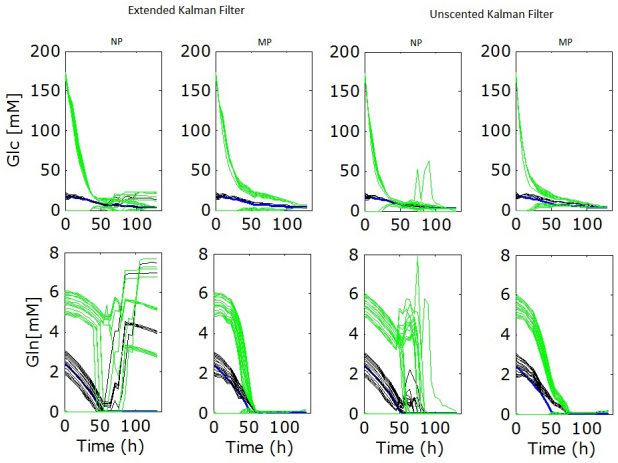

Figure 1: Glucose and glutamine estimations with EKF and UKF using consecutively the nominal and modified parameter values (20 runs are achived for varying initial conditions - black curves) for a fed-batch culture with exponential feeding. In blue: model evolution. In green: Confidence intervals at 95%.

Acknowledgements

This paper presents research results of the Belgian Network DYSCO (Dynamical Systems, Control, and Optimization), funded by the Interuniversity Attraction Poles Programme initiated by the Belgian Science Policy Office.

References

[1] Z. Amribt, H. Niu and P. Bogaerts. Macroscopic modelling of overflow metabolism and model based optimization of hybridoma cell fed-batch cultures. Biochemical engineering journal, 70: 196-209, 2013.

[2] P. Bogaerts and A. Vande Wouwer. Parameter identification for state estimationapplication to bioprocess software sensors. Chemical Engineering Science, 59: 24652476, 2004.

Correct-by-Design Control of Physical Systems Separating Estimation and Control

Sofie Haesaert, Paul Van den Hof
Department of Electrical Engineering
Eindhoven University of Technology
{s.haesaert,p.m.j.vandenhof}@tue.nl

Alessandro Abate
Department of Computer Science
Oxford University
aabate@cs.ox.ac.uk

1 Background

Reliable and autonomous operation of many complex engineered systems demand guaranteed behaviour over the full spectrum of operating conditions. This is for instance the case with systems in avionics, automotive, railway transportation, electronic systems, and semiconductors, where safety is critical and mistakes can lead to heavy economical losses.
Formal methods [1] have arisen to assist in the model based-design and certification of these systems. Using tools from formal methods, specifications of interest can be analyzed and used as an important design tool. Specifications are expressed within a *language* comprising logical expressions, or formulae. Since the underlying formal *language* is built upon sound syntax and semantics it is possible to *mechanize*, or *automatize* analysis methods into a computer-aided set of tools for the verification, and the automated synthesis of the behaviour of the model of interest.

2 Problem Setting

Recently the demand towards robust extensions of automatic synthesis of correct-by-design controllers [2, 3] for applications on (cyber-)physical systems has arisen. Current research strives towards the application of these formal methods in i.a. robotics, symbolic planning of robot motion [4], and in the analysis of biological systems such as genetic networks [5]. However, at this moment these formal methods are incompatible with the uncertainty present in physical systems as they hinge on exact knowledge of the dynamics and full state observability. Whereas in general, no state measurements are available and measurements are distorted by sensor noise.
Classical methods [6] for the control of physical systems based on output measurements include (frequency domain) methods using PID tuning, and robust control methods as in H_∞ control. Alternatively, known techniques for state feedback are often exported to noisy output feedback through a separated approach where an observer, to estimate the state of the system, is designed separately from a state-feedback controller, yielding when combined an output feedback controller. Examples include the standard separation theorem for optimal LQG design.

3 Goals

In this work, we consider the latter approach in the extension of correct-by-design controller synthesis to output-based controllers for cyber-physical systems. We explicitly consider the accuracy of applying this separation for estimation and control in the synthesis of an output-feedback, correct-by-design controller. As a first step, in this talk physical systems are assumed to be linear, time-invariant systems, and disturbed by additive stochastic noise and with additive sensor noise on output measurements.

This work fits within the overall objective of data-based automatic synthesis of controllers and formal verification of physical systems. Recent work considers the data-driven and model-based verification of grey box system from noisy measurements [7]. Future work will consider the influence of modelling errors on correct-by-design controllers. Additionally, we are interested in identification methods tailored to correct-by-design controller synthesis.

References

[1] Clarke, E. M. (2008). The birth of model checking. *25 Years of Model Checking* (p. 1-26). Springer.

[2] Tabuada., P. (2008). An approximate simulation approach to symbolic control. *Autom. Control. IEEE Trans.* 53(6), 1406-1418.

[3] Manuel Mazo Jr, Anna Davitian, and Paulo Tabuada. (2010). PESSOA : towards the automatic synthesis of correct-by-design control software. *Work-in-progress HSCC*.

[4] Belta, C., Bicchi, A., Egerstedt, M., Frazzoli, E., Klavins, E., & Pappas, G. J. (2007). Symbolic planning and control of robot motion [grand challenges of robotics]. *Robotics & Automation Magazine, IEEE*, 14(1), 61-70.

[5] Yordanov, B., Belta, C., & Batt, G. (2007). Model checking discrete-time piecewise affine systems: application to gene networks. *In European Control Conference.*

[6] Skogestad, S., and Postlethwaite,I. (2007) Multivariable feedback control: analysis and design. *New York: Wiley.*

[7] Haesaert, S., Van den Hof, P.M.J., Abate, A., Data-driven Property Verification of Grey-box Systems by Bayesian Experiment Design, ACC 2015 *(To appear)*

Complete vehicle energy management with large horizon optimization

T.C.J. Romijn, M.C.F. Donkers, S. Weiland and J.T.B.A. Kessels
Department of Electrical Engineering, Control Systems Group
Eindhoven University, P.O. Box 513, 5600 MB Eindhoven
Email: T.C.J.Romijn@tue.nl, M.C.F.Donkers@tue.nl, S.Weiland@tue.nl, J.T.B.A.Kessels@tue.nl

1 Introduction

Hybrid vehicle technology has the premise of reducing fuel consumption under various driving conditions. This technology requires an energy management strategy to optimally control the power flow between the internal combustion engine (ICE) and the electric machine (EM), while meeting strict state-of-charge boundaries in the high-voltage battery. Besides an electric machine, heavy-duty vehicles can also be equipped with a refrigerated semi-trailer and many other auxiliaries with the interesting property of having a flexible power demand and/or the ability of storing energy (see Fig. 1). Including these components in the energy management strategy, yielding complete vehicle energy management (CVEM), is attractive for reducing fuel consumption, but requires a new approach to solving the energy management problem [1].

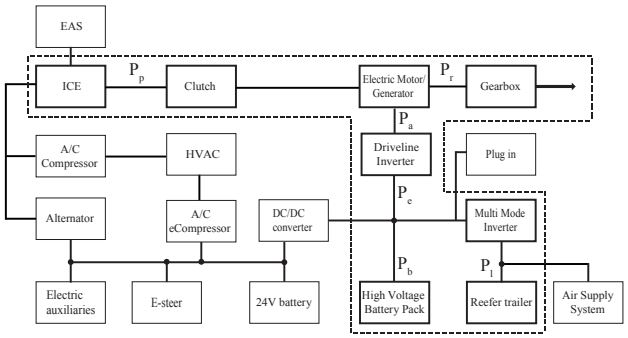

Figure 1: Topology of a hybrid heavy-duty vehicle

2 Approach

The approach taken in [1] is based on the dual decomposition. The CVEM problem is solved for a heavy-duty vehicle with an electric machine, a high-voltage battery and a refrigerated semi-trailer over a short horizon of 800 time steps. As long-haul heavy-duty vehicles easily operate for 10 hours and more, solving the problem for large horizons is necessary to truly establish the benefit of CVEM.
The dual decomposition results in four separated optimization problems, i.e., the dual functions. Each of the dual functions is related to one of the components in the vehicle and all dual functions are coupled by the dual variables. The primal problem is solved by iteratively solving the dual functions and subsequently updating the dual variables with a subgradient method. This approach is not only attractive because of its distributed nature, but also because of the decomposition, which allows each of the dual functions to be solved using any preferred solution method. By selecting the best solution method for each dual function, the decomposed CVEM problem introduced in [1] is solved for large horizons with 53000 time steps (approximately 15 hours).

3 Simulation results

The CVEM problem is solved using different solution methods for each of the dual problems. In particular, the solution of the dual function related to the engine and electric machine is found explicitly. The dual function related to the battery is solved with the Lagrangian method adapted to state constraints. The dual function related to the refrigerated semi-trailer is solved by applying 'the method of multipliers' similar to distributed quadratic programming. The results presented in Fig. 2 show that both, the battery State-of-Energy (SoE) and the temperature inside the refrigerated semi-trailer remain between bounds. Moreover, the computation time for this large-scale optimization problem is only 13.2 minutes on a standard laptop pc and scales linearly with the length of the horizon. In particular, computation time is reduced with a factor 100 for a horizon with 2000 time steps, compared to the approach taken in [1].

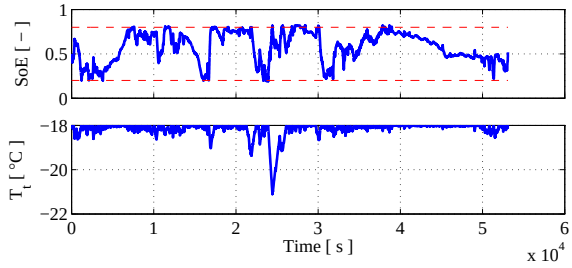

Figure 2: Optimal State-of-Energy and temperature trajectory

4 Acknowledgements

This work has received financial support from the FP7 of the European Commission under the grant CONVENIENT (312314).

References

[1] T.C.J. Romijn, M.C.F. Donkers, J.T.B.A. Kessels and S. Weiland, *A Dual Decomposition Approach to Complete Energy Management for a Heavy-Duty Vehicle,* Proc. 53rd Annu. Conf. on Decision and Control, 2014.

Enterprise-wide Optimization: Graph Constrained Scheduling

M. Bahadir Saltik Nikolaos Athanasopoulos Leyla Özkan
Department of Electrical Engineering
Eindhoven University of Technology
5600 MB, Eindhoven, The Netherlands
{m.b.saltik,n.athanasopoulos,l.ozkan}@tue.nl

1 Introduction

The aim of this work is to introduce graphs to reduce the complexity of scheduling algorithms that are conducted for enterprise-wide optimization, see, e.g., [1]. The scheduling decisions when to turn-on or when to turn-off a so-called unit operation (UO), a subprocess of a large-scale system, will be the main research topic. In order to reduce the inherent complexity, we follow a modeling approach of the scheduling logic rules on labeled directed graphs that allow self-loops. The decision tree is greatly reduced (w.r.t. unconstrained case) by making use of graphs of each UO. Then by utilizing forward reachability algorithms, we find the all possible trajectories, which distinguishes the infeasible (undesired) and feasible schedules. The proposed approach is implemented on a whey processing example.

2 Graph Theory and Scheduling Algorithms

In industries like food or pharmaceuticals, it is common that UOs are turned on or off due to various offline activities, such as cleaning or safety regulations. Due to these on-off time windows, scheduling algorithms are considered to increase the efficiency and throughput. The on-off nature of the problem introduces binary decision variables, hence the optimization problems for scheduling purposes are in the class of integer programming problems (IPPs). The IPPs are inherently difficult to solve. The standard approaches concern either relaxing the IPP or constructing a decision tree, which is effected by *curse of dimensionality*. To reduce the number of possible decisions, we recast the scheduling constraints into a directed graph, making use of ideas from [2]. In this graph, each vertex corresponds to on or off condition of subprocess while carrying the memory information, that is, every time step in either condition creates a new vertex. The edges stand for logical rules inherent to the system, which models the switching between on-off conditions or staying in either condition. For example one can consider the logical rules such as maximal operational time, minimum offline time span, which shapes the graph of that UO.

3 A Case Study and Future Work

We consider the scheduling problem of cleaning times of a simplifies whey processing plant. The process has 2 UOs, which induces 3 binary decision variables α^j constrained to 3 different cyclic digraphs, see Figure 1, and 2 continuous states, denoted as x_i which stands for the mass hold up in the UOs. The simulation result shows that none of the schedules causes an unstable trajectory, as visualized in Figure 2. From this result we deduce that for a process that can be modeled only with cyclic graphs, the scheduling problem reduces to decide the starting node of graphs to select the best schedule, which is simpler than other methods.

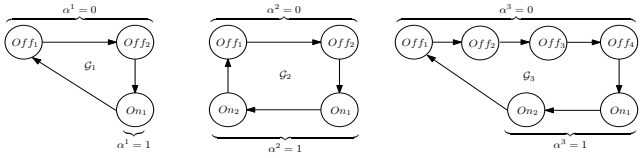

Figure 1: The graphs of considered subsystems.

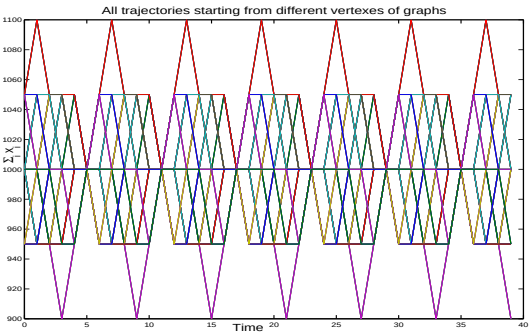

Figure 2: The evolution of the sum of the mass hold ups over time for all possible initial conditions.

Future directions will consider a-priori detection of feasible schedules for an initial condition set and introduction of stochastic variables for extending the deductions to mixed-integer stochastic programming.

References

[1] Michael Pinedo and Xiuli Chao. Operations scheduling. McGraw Hill, 1999.

[2] Nikolaos Athanasopoulos and Mircea Lazar. Stability analysis of switched linear systems defined by graphs. IEEE Conference on Decision and Control, pp.5451-5456, 2014.

Feedback Control Design for Systems with Data-Intensive Sensing

E.P. van Horssen, D.J. Antunes, W.P.M.H. Heemels
Control Systems Technology Group, Department of Mechanical Engineering
Eindhoven University of Technology
P.O. Box 513, 5600 MB Eindhoven, The Netherlands
Email: {e.p.v.horssen, d.antunes, w.p.m.h.heemels}@tue.nl

1 Introduction

Many emergent applications require a tight coupling between computational, communication and control (cyber) devices and physical processes (e.g. mechanical, electrical). These so-called cyber-physical systems (CPS) [1] require engineers and researchers from various disciplines to work together and solve problems that overstep the boundaries of their individual fields. Such an integrated design approach potentially yields better results than a traditional approach building on separation of concerns.

The next development step in this field is the design of tools that are robust to non-ideal situations, so-called robust CPS [2]. Large information flows from sensors can result in such a non-ideal situation. This so-called data-intensive sensing poses challenges in various parts of the systems' control loops, coping with delays in particular. Data-intensive sensing becomes increasingly relevant in many high-tech systems since the number and the complexity of sensors in these systems is continuously increasing.

The aim of this work is first to give an overview of the challenges of data-intensive feedback control. Second, research directions are presented on how these challenges can be handled. Inspiration is drawn from the tools used for hybrid, switched and networked control systems. Third, examples of applications are discussed to show how these methods can be used.

2 Research challenge example

Acquisition of control-relevant data is generally done by data processing. While an application may allow a large time for the post-processing of data to improve results, to improve the quality of the data itself control-relevant data is needed in real-time and typically as fast as possible. The trade-off between the quality of control-relevant data and the processing delay, i.e. small delay and low quality versus large delay and high quality, is evident. Our approach is to cope with this trade-off on-line, as a function of the needs of the system, thus making it more robust to uncertainties and disturbances.

3 Methodology

The case described in the previous section and several other scenarios can be captured in the following model of a discrete-time switched linear system with (stochastic) disturbances:

$$x_{k+1} = A_{\sigma_k} x_k + B_{\sigma_k} u_k + w_{\sigma_k} \quad (1)$$

$$y_k = C_{\sigma_k} x_k + v_{\sigma_k} \quad (2)$$

where x_k, u_k, σ_k, y_k, denote state, control input, switching mode and output, respectively, at discrete time instance $k \in \mathbb{Z}$. Real matrices A_{σ_k}, B_{σ_k} and C_{σ_k} describe the system dynamics in mode σ_k and are dependent on the processing delay. The signals w_{σ_k} and v_{σ_k} are mode-dependent (stochastic) disturbances. In particular, we consider zero-mean Gaussian noise with mode-dependent covariance.

We consider the co-design problem of computing simultaneously the mode σ_k, switching the system configuration, and control input u_k, providing the feedback action. This problem is known to be combinatorial, therefore an approximate approach must be pursued. Our approach uses approximate dynamic programming algorithms such as in [3].

4 Applications

Data-intensive sensing is particularly relevant in vision systems dealing with acquisition and processing of images [4]. An example of a vision system in an industrial application is electron microscopy [5]. Another example is vehicle-to-vehicle (V2V) communication, where using networks of wireless sensors results in data-intensive sensing.

References

[1] *http://cyberphysicalsystems.org/*

[2] *http://www.stw.nl/nl/programmas/robust-design-cyber-physical-systems-cps*

[3] Antunes, D. and Heemels, W.P.M.H. *Rollout Event-Triggered Control: Beyond Periodic Control Performance*, IEEE Transactions on Automatic Control, vol. 59, no. 12, pp. 3296-3311, 2014

[4] *http://www.technolution.eu/nl/technologiedomeinen/18-patterning-imaging-and-acquisition-pia-board.html*

[5] FEI company, "Introduction to electron microscopy", *http://www.fei.com/introduction-to-electron-microscopy*, 2010

Sub-optimal strategies for output-based event-triggered control

B. Asadi Khashooei, D. J. Antunes, W. P. M. H. Heemels
Mechanical Engineering Dept., Eindhoven University of Technology, Eindhoven, The Netherlands
Emails: B.Asadi.Khashooei, D.Antunes, M.Heemels@tue.nl

1 Introduction

Recent research advocates that replacing the periodic communication paradigm by an event-triggered paradigm can have significant benefits for control systems. Here we propose an optimization-based output-feedback event-triggered solution for linear discrete-time systems which guarantees a performance that is within a certain factor of all-time transmission control, while reducing the communication load significantly.

2 Problem Formulation

We consider the control of a linear discrete-time system over a shared network as depicted in Figure 1. We assume that the controller, collocated with the sensors, sends the control inputs to the actuator over a communication network. This controller should not only compute the control inputs but also decide at which times $k \in \mathbb{N}_0$ new control inputs are sent to the actuator. In present work, the controller will be of an event-triggered nature. To model the occurrence of transmissions in the network, we introduce $\sigma_k \in \{0,1\}, k \in \mathbb{N}_0$, as a decision variable indicating if a transmission occurs at time k, in which case $\sigma_k = 1$, or otherwise, in which case $\sigma_k = 0$. We also consider that at the actuator side a standard zero-order hold device holds the previous value of the control action as long as no new control input is received. Let $u_k \in \mathbb{R}^{n_u}$ denote the received value by the actuators at time $k \in \mathbb{N}_0$ when a transmission occurs and have any arbitrary value otherwise. Considering an extended state $\xi_k := (x_k, \hat{u}_{k-1}) \in \mathbb{R}^{n_x} \times \mathbb{R}^{n_u}$, we obtain the model

$$\begin{aligned} \xi_{k+1} &= A_{\sigma_k}\xi_k + B_{\sigma_k}u_k + \omega_k, \quad k \in \mathbb{N}_0 \\ y_k &= C\xi_k + v_k, \end{aligned} \tag{1}$$

where $\omega_k := (s_k^T, 0_{n_u}^T)^T$ and s_k and v_k denote the state disturbance and measurement noise at time $k \in \mathbb{N}_0$, respectively. A_j, B_j are the appropriate matrices and we arbitrate that $\hat{u}_{-1} = 0$. The performance measure is defined to be

$$\mathbb{E}[\sum_{k=0}^{\infty} \alpha^k (1+\theta\sigma_k) g(\xi_k, u_k, \sigma_k)]. \tag{2}$$

where $g(\xi, u, j) = \xi^T Q_j \xi + u^T R_j u + 2\xi^T M_j u$ with Q_j, M_j, R_j are proper cost matrices and $0 < \alpha < 1$ is the discount factor. Moreover, this cost penalizes transmissions with a multiplicative factor $(1+\theta)$ in the stage cost associated with time k if a transmission occurs at time k. We are interested to find the policy $(u_k, \sigma_k) = \mu_k(I_k)$, $I_k := \{y_0, \ldots, y_k, u_0, \ldots, u_{k-1}, \sigma_0, \ldots, \sigma_{k-1}\}$, that improves the quadratic performance index (2) over all-time transmission control where $\sigma_k = 1 \; \forall k \in \mathbb{N}_0$.

3 Proposed Method and Results

The ETC block consists of three functions, namely: (i) the estimator, which computes estimates of the state $\hat{x}_k$ based on the information, I_k available up to time k, (ii) the controller, which computes control actions, and (iii) the scheduler, which makes the transmission decisions also based on information vector. At each time step the scheduler decides whether or not to transmit based on the value of the cost function of the two possible scheduling sequences as shown in Figure 2. In both cases, after the first step, all-time updates are being used. For each of these two fixed possible scheduling sequences, one can compute the value of the cost function (2) associated with transmitting, denoted here by J^1, and the cost function (2) associated with not transmitting, denoted here by J^0, based on the available information at each iteration. If $J^0 < J^1$ no transmission takes place and the actuator holds its current value. Otherwise, the new optimal control value computed for all-time transmission case is sent over the network. The procedure is then repeated at the next iteration.

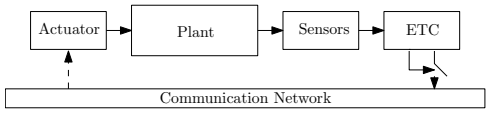

Figure 1: The schematic of the considered structure

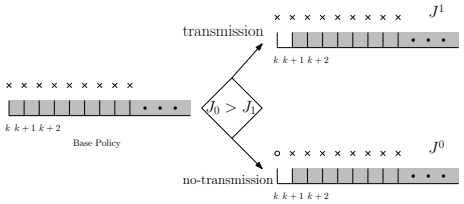

Figure 2: Schematic of the proposed algorithm

The main result of this work is to prove that the proposed output-based ETC algorithm guarantees a performance bound which is within a factor $(1+\theta)$ of the performance obtained with all-time transmission algorithm, while reducing the communication load. Numerical results for an example of two connected masses controlled over a shared network showed that approximately 40% communication reduction is achieved while guaranteeing a performance within 1.1 of the all-time transmission control performance. (See [1])

4 Acknowledgment

This work is supported by the Innovational Research Incentive Scheme under the VICI grant "Wireless control systems: A new frontier in automation" (No. 11382) awarded by NWO (The Netherlands Organization for Scientific Research) and STW (Dutch Technology Foundation)

References

[1] B. Asadi Khashooei, D. J. Antunes, W. P. M. H. Heemels, "Rollout Strategies for Output-Based Event-Triggered Control," submitted to European Control Conference (ECC), 2015.

Bringing optimal feedback controller design to practice

Maarten Verbandt, Goele Pipeleers and Jan Swevers
KU Leuven, BE-3001 Heverlee, Belgium
Department of Mechanical Engineering, Division PMA
maarten.verbandt@kuleuven.be

1 Introduction

Although optimal feedback controller design based on $\mathscr{H}_\infty$ or $\mathscr{H}_2$ criteria [1] has already proven its potential in academia, it has yet to find wide acceptance in industry. One explanation is the lack of software support for practitioners without expertise in optimal control. Matlab's robust control toolbox [2] contains the core tools for $\mathscr{H}_\infty$ and $\mathscr{H}_2$ control, but (i) it doesn't allow for an easy and intuitive control problem formulation; (ii) it doesn't support multi-objective controller designs; (iii) it doesn't allow for unstable [3] or improper weights. To overcome these drawbacks we are developing a Matlab toolbox that combines an intuitive control problem formulation with efficient and numerically stable algorithms that overcome the drawbacks mentioned above.

2 Control problem formulation

In order to simplify multi-objective feedback controller design, a novel intuitive LTI problem parser is being developed. It is intended to be as simple as *sysic* and as flexible as *iconnect*. Moreover, it is designed specifically to easily impose control objectives. Some example code is depicted in figure 1. The generalized plant is constructed by connecting several subsystems. Next the control specifications are expressed in terms of a weight on a certain transfer function. Combining both gives rise to a general multi-objective control problem, which is then analyzed and solved. Future work includes the introduction of even higher level specifications for the controller design, e.g. 'maximize bandwidth' or 'add sufficient damping'.

```
lti_begin()
   % Object declaration
   subsystem G, signal r
   % Connection declaration
   u = Gin; y = Gout; e = r - y;
   % Input-output declaration (GP)
   control_in([u]); control_out([e]);
   exog_in([r]); exog_out([y]);
   % Control problem formulation
   ctrl_begin()
      minimize(WS*(e/r))
      MS*(e/r) <= 1
      WT*(y/r) <= 1
   ctrl_end
lti_end
```

Figure 1: Multi-objective control problem formulation using the new LTI Toolbox' syntax.

3 Control problem solution

Traditional multi-objective controller design uses weights to shape the closed loop behavior of the system. These weights are typically chosen to be proper since it simplifies the construction of the augmented plant. However, if the transfer function of interest is proper and of relative degree d, it is possible to add an improper weight with a zero-pole excess up to d, without making the augmented plant improper. This reduces the order of the resulting controller because poles, intended to make weights proper and typically of high frequency, can be omitted.

Adding an improper weight might result in an improper generalized plant which is modeled using a descriptor form (1):

$$E\dot{x} = Ax + Bu, \quad y = Cx + Du \tag{1}$$

Current solvers cannot deal with the descriptor form, making it impossible to add improper weights with a zero-pole excess larger than d. However, this may be necessary in order to obtain the desired roll-off in e.g. the complementary sensitivity function. To this end, future research will go to the extension of multi-objective feedback controller design to improper generalized plants.

The descriptor form also holds potential to increase the numerical conditioning of the optimization problem. Up till now only systems with unity E were valid. However allowing E to be different from unity and thus making its conditioning worse, may result in a better conditioning of A and a better conditioning of the overall LMI problem. Research will therefore focus on the optimization of the numerical conditioning of the LMI problem through appropriate transformation of A and E.

References

[1] C. Scherer, P. Gahinet and M. Chilali, "Multiobjective output-feedback control via LMI optimization," Automatic Control, IEEE Transactions on, Vol. 42, 7, 896–911, 1997.

[2] http://www.mathworks.com/help/robust/

[3] H. Köroğlu, "$\mathscr{H}_\infty$ synthesis with unstable weighting filters: An LMI solution," Decision and Control (CDC), 2013 IEEE 52nd Annual Conference on, 2429–2434, 2013.

Acknowledgement IWT SBO project MBSE4Mechatronics: Model-based Systems Engineering for Mechatronics, FWO project G091514N: Study and development of an integrated system identification and control design approach for multi-variable nonlinear systems. This work also benefits from K.U.Leuven-BOF PFV/10/002 Center-of-Excellence Optimization in Engineering (OPTEC), from the Belgian Programme on Interuniversity Attraction Poles, initiated by the Belgian Federal Science Policy Office, and from K.U.Leuvens Concerted Research Action GOA/10/11 "Global real-time optimal control of autonomous robots and mechatronic systems". Goele Pipeleers is partially supported by the Research Foundation Flanders (FWO Vlaanderen).

Application of Tensor Decomposition Based Reduction for Dynamic Programming

Julian Stoev
Flanders Make (FMTC)
Celestijnenlaan 300 - bus 4027 B-3001 Heverlee
julian.stoev@flandersmake.be

Steve Vandenplas
Flanders Make (FMTC)
Celestijnenlaan 300 - bus 4027 B-3001 Heverlee
steve.vandenplas@flandersmake.be

1 Introduction

Dynamic programming (DP) is a well known approach with many applications, among them optimal control. It can handle a broad class of systems including nonlinear ones and can incorporate practically relevant constraints including state and input. The results of the DP come in the form of multidimensional look-up tables (LUT), which can be implemented efficiently on real-time control platforms. Unfortunately the big disadvantage of dynamic programming is related with the curse of dimensionality, which results in the size of the look-up tables growing very quickly with the number of states and their discretization. This reduces significantly the class of systems which can be handled. Significant efforts were directed to remove this disadvantage in many different ways and this topic is still very relevant direction for research [3].

This work aims to reduce some of the disadvantages of DP by using tensor decomposition [1, 2] based reduction of the look-up tables. The idea is rather straightforward and simple. The set of look-up tables resulting from DP can be arranged in the form of multidimensional tensor. Higher-order singular value decomposition (also known as Tucker decomposition) is then performed on it, resulting in a reduced core tensor and a set of one-dimensional look-up tables. The memory required to store these is reduced with respect to the original look-up table.

The approach is demonstrated using a simple mechanical system with two states. It represents the moving mass of a linear actuator, which is part of a robot playing badminton. The robot has to intercept the shuttle at particular location and at precise time. The first designs were using time-optimal trajectories, which resulted in successful play of the robot, but wasted a lot of energy due to the unnecessary high velocity and accelerations. Later works [4] concentrated on improving the energy needed for the motion. Optimal trajectories can be designed in different ways, so that the robot arrives at the interception point on time and with required precision. The tracking of the trajectories is performed with a simple PID-like control, which remains the same. We compare the energy needed to move the linear actuator for the same complex trajectory simulating a real play of the robot.

2 Application

The real dynamics has also friction, but we neglect the friction dynamics, which is mostly a low frequency phenomena and model the mass as a pure double integrator. Previous experimental results were used to derive a simple model relating the consumed electrical power needed for the motion and the robot velocity and acceleration. Thus the energy model includes also the energy effects of friction. This is all the information we need to apply DP for this problem. The resulting DP full look-up table (LUT) has dimension 227x227x65 and can be used to generate feed-forward signals for the robot trajectory. The results using experimental measurements are shown in Table 1, where we show both the energy and the missed hits during the play of the robot taking approximately 10 minutes. A hit is missed if the the robot position at the moment of the hit has error of more than 0.05 m. We see that the performance of the full LUT is recovered after the tensor reductions.

	Energy [J]	Miss hit
Time optimal (PTOS)	212.4551	2
Energy optimal (PEOS)	101.3346	6
DP full LUT	97.5798	2
reduced LUT (10 components)	99.3826	2
reduced LUT (20 components)	97.9767	2
reduced LUT (30 components)	97.5007	2

Table 1: Experimental results

References

[1] L. De Lathauwer, B. De Moor, and J. Vandewalle. A multilinear singular value decomposition. *SIAM Journal on Matrix Analysis and Applications*, 21(4):1253–1278, 2000.

[2] T. Kolda and B. Bader. Tensor decompositions and applications. *SIAM Review*, 51(3):455–500, 2009.

[3] W.B. Powell. *Approximate Dynamic Programming: Solving the Curses of Dimensionality*. Wiley Series in Probability and Statistics. Wiley, 2011.

[4] Xin Wang, Julian Stoev, Gregory Pinte, and Jan Swevers. Classical and modern methods for time-constrained energy optimal motion application to a badminton robot. *Mechatronics*, 23(6):669 – 676, 2013.

Optimal tracking gain computation for mechanical systems with unilateral constraints

M.W.L.M. Rijnen, A. Saccon and H. Nijmeijer
Department of Mechanical Engineering
Eindhoven University of Technology
P.O. box 513, 5600 MB Eindhoven, The Netherlands
{m.w.l.m.rijnen, a.saccon, h.nijmeijer}@tue.nl

1 Introduction

We consider the problem of trajectory tracking for mechanical systems with unilateral constraints [1]. These systems can be casted in the framework of hybrid systems with continuous (flow) and discrete (jump) dynamics. In [2] it has been shown how the local behavior about a reference trajectory with state jumps can be described by a specific time-triggered jumping linear system. In this work, we investigate the possibility of employing LQR-like ideas to compute optimal tracking gains for this class of mechanical systems.

2 Problem formulation

Consider a hybrid system where the state x evolves in free motion according to

$$\dot{x} = f(x,u,t) \tag{1}$$

and at impact times $t = \tau_i$, $i = \{1,2,\ldots\}$, the state is reset according to

$$x^+ = x^- + \Delta(x^-,\tau_i). \tag{2}$$

An impact occurs at time $t = \tau_i$ when $g(x^-(\tau_i),\tau_i) = 0$. The aim of this work is to design a control strategy such that this system tracks a given reference state-input trajectory with jumps $(\alpha(t), \mu(t))$ in an optimal sense. The main difficulty here lies in the fact that for the tracking system a slight perturbation from the reference will cause a difference in the event time. A solution to this time difference and introduction of an appropriate error definition is given in [2] and is based on extending the reference trajectories before and after the event to past this impact time.

3 Preliminary results

By linearizing the system about the reference state-control trajectory $(\alpha,\ \mu)$ an optimal control strategy may be constructed inspired by the well-known Linear Quadratic Regulator (LQR). The linearized control input v is found from

$$\min_v \frac{1}{2}\int_0^T \left(z^{\mathrm{T}}Qz + v^{\mathrm{T}}Rv\right) \mathrm{d}s + \frac{1}{2}z(T)^{\mathrm{T}}P_T z(T) \tag{3}$$

$$\begin{aligned} \text{s.t.} \quad \dot{z} &= A(t)z + B(t)v && t \neq \tau_i \\ z^+(\tau_i) &= z^-(\tau_i) + H(\tau_i)z^-(\tau_i) && t = \tau_i \end{aligned} \tag{4}$$

with z the linearized state vector, Q and R weighting matrices, and P_T the terminal cost weighting. Using the linearized system that jumps at the nominal impact times $t = \tau_i$, $i = \{1,2,\ldots\}$ and the linearized jump map $H(\tau_i)$, the matrix Riccati differential equation can be employed to solve the optimal control problem. Given a reference trajectory (Fig. 1) for a controlled bouncing mass (coefficient of restitution 0.8), the corresponding position feedback gain can surprisingly become negative for a short amount of time before the impacts as can be seen in Fig. 2.

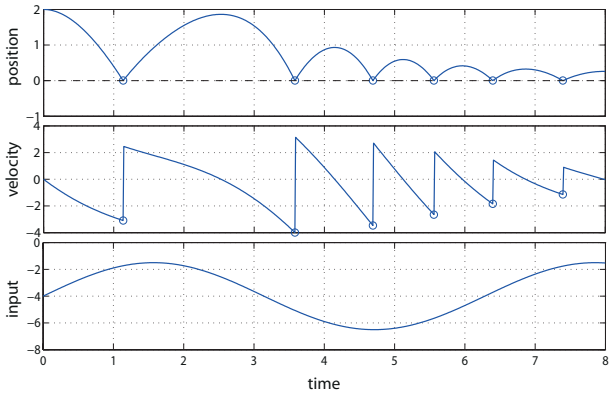

Figure 1: Reference trajectory for an actuated bouncing mass.

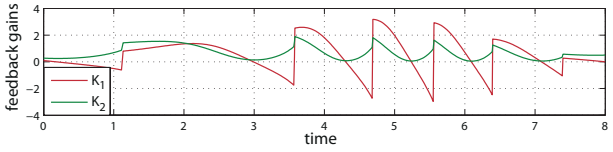

Figure 2: Feedback gains for tracking the reference in Fig.1

References

[1] J.J.B. Biemond, N. van de Wouw, W.P.M.H. Heemels, H. Nijmeijer. Tracking control for hybrid systems with state-triggered jumps. *IEEE Transactions on Automatic Control*, 58(4):876-890, April 2013

[2] A. Saccon, N. van de Wouw, H. Nijmeijer. Sensitivity analysis of hybrid systems with state jumps with application to trajectory tracking. *53rd IEEE Conference on Decision and Control (CDC)*, December 15-17, 2014, Los Angeles

Time-optimal motion planning in the presence of moving obstacles

Tim Mercy, Wannes Van Loock, Goele Pipeleers and Jan Swevers
KU Leuven, BE-3001 Leuven, Belgium
Department of Mechanical Engineering, Division PMA
Tim.Mercy@kuleuven.be

1 Introduction

Autonomous motion systems are becoming more and more popular in industry. Some examples are AGV's, fruit picking robots, welding robots, drones and autonomous cars. To drive these systems, one generally wants to compute the fastest or the most energy efficient motion trajectory to move the system from its current position to its destination while obeying input and state constraints and avoiding collision with obstacles in the environment. This motion trajectory is typically computed by solving an optimization problem. As autonomous systems often operate in environments with moving obstacles of which the motions are not fully known a priori, the trajectory needs to be updated in real time.

This abstract presents a method for calculating a time-optimal motion trajectory in the presence of moving obstacles. The method has two key aspects: (*i*) via a B-spline parametrization of the motion trajectory it is possible to make a trade-off between the complexity of the optimization problem and the optimality of the resulting trajectory; (*ii*) the properties of B-splines allow to transform all constraints to conservative constraints on the B-spline coefficients. This relaxation lowers the amount of constraints. These aspects lead to a small scale optimization problem that is suitable for real-time implementation [2].

The method has been tested extensively by numerical simulations. In addition, it has been validated in an experimental demo where a *KUKA youBot* moved time-optimally from one point to another while avoiding a moving obstacle.

2 Methodology

The time-optimal B-spline trajectory is determined by solving an optimization problem with the motion time as the *objective function*. The *optimization variables* are the motion time and the spline coefficients. Three types of constraints are considered: (*i*) *kinematic constraints*, limiting the speed and acceleration of the vehicle; (*ii*) *initial and final conditions*, imposing the vehicle's initial and final position, speed and acceleration; and (*iii*) *anti-collision constraints*, ensuring the vehicle avoids all obstacles in its environment. Currently, the anti-collision constraints can cope with ellipsoidal and rectangular vehicles and obstacles. For rectangular obstacles and/or vehicles, the constraints are based on the separating hyperplane theorem [1].

In order to deal with moving obstacles, a linear prediction of their future positions, based on the current position, orientation and speed, is added to the anti-collision constraints. To account for uncertainty in this prediction the proposed method re-optimizes the trajectory in each time step by using new initial conditions, and updated obstacle information and velocity estimation.

The developed method allows generating a time-optimal point-to-point trajectory to avoid elliptical, circular and rectangular obstacles with a circular or rectangular vehicle or robot. In future work, more general vehicle and obstacle shapes will be considered, as well as including the vehicle's dynamics.

3 Results

Figure 1 shows an optimal motion trajectory for moving a circular robot from the start point to the marked end point. When the dashed static circular obstacle is also considered the optimal trajectory changes to the dashed trajectory.

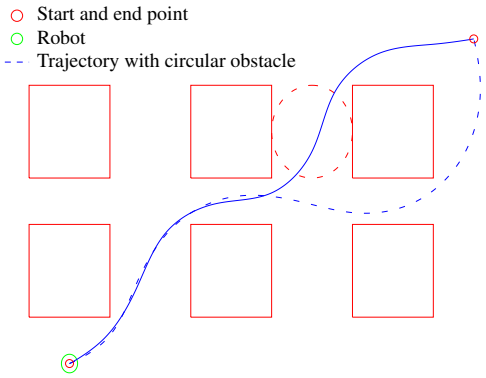

Figure 1: Circular robot moving through a warehouse

Acknowledgement IWT ICON project Sitcontrol: Control with Situational Information, IWT SBO project MBSE4Mechatronics: Model-based Systems Engineering for Mechatronics, FWO project G0C4515N: Optimal control of mechatronic systems: a differential flatness based approach. This work also benefits from K.U.Leuven-BOF PFV/10/002 Center-of-Excellence Optimization in Engineering (OPTEC), from the Belgian Programme on Interuniversity Attraction Poles, initiated by the Belgian Federal Science Policy Office, and from K.U.Leuvens Concerted Research Action GOA/10/11 "Global real-time optimal control of autonomous robots and mechatronic system". Goele Pipeleers is partially supported by the Research Foundation Flanders (FWO Vlaanderen).

References

[1] S. Boyd, L. Vandenberghe, "Convex Optimization" 2004, Cambridge University Press

[2] W. Van Loock, G. Pipeleers, J. Swevers, "Optimal motion planning for differentially flat systems with guaranteed constraint satisfaction", Submitted to the 2015 American Control Conference, July 1-3, Chicago

It's not MPC !
An Explicit Reference Governor for the supervision of constrained nonlinear systems

Marco M. Nicotra, Emanuele Garone
Service d'Automatique et d'Analyse des Systèmes
Université Libre de Bruxelles
Av. Roosevelt 50, CP 165/55, 1050 Brussels, Belgium
Email: mnicotra@ulb.ac.be
This work is supported by a FRIA Scholarship.

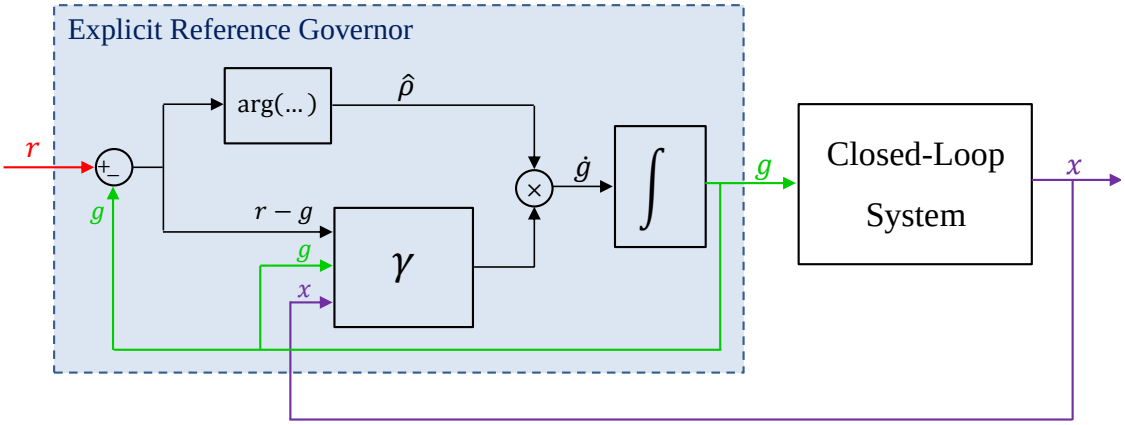

Figure 1: Proposed control architecture.

1 Introduction

This talk introduces a novel control law that dynamically modifies the reference of a pre-compensated nonlinear system so as to ensure the satisfaction of convex constraints without resorting to online optimization. This is done by translating state space constraints into a constraint on the Lyapunov function and limiting its value by modulating the velocity of the applied reference. The theory is introduced for general nonlinear systems subject to convex constraints and is then specialized to the large and highly relevant class of nonlinear systems admitting a Lyapunov function that is lower-bounded by a quadratic form. Some extension and implementation will be discussed as well.

2 Problem Statement

Consider the pre-compensated nonlinear system subject to constraints and let $r(t)$ denote the desired reference signal (not known in advance). The ERG problem is that of generating, at each time instant t, a reference $g(t)$ such that:
1) if $g(t)$ is kept constant, constraints are not violated;
2) $g(t)$ approximates $r(t)$ as much as possible.

3 Basic Idea

By taking advantage of invariance properties of closed-loop systems, it has been shown in [1] that a set of state-space constraints can be translated into a single constraint on the Lyapunov function

$$V_g(x) \leq \Gamma_g.$$

Assuming that $g(0)$ satisfies condition 1) of the problem statement, the Explicit Reference Governor provides a closed-form solution by assigning the applied reference velocity as $\dot{g} = \hat{\rho}\,\gamma$, where $\hat{\rho}$ is the unitary vector that points to the desired reference $r(t)$ whereas γ is a positive scalar.
The problem statement is then solved by choosing

$$\gamma = \kappa(\Gamma_g - V_g(x))$$

with $\kappa > 0$ an arbitrarily large scalar.

References

[1] Elmer G. Gilbert and Ilya Kolmanovsky. Set-point control of nonlinear systems with state and control constraints: A lyapunov function reference governor approach. In *IEEE Conference on Decision and Control (CDC)*, Dec. 1999.

Irradiance Models for Projection Optics

Ruben Merks[1,2], Michel Habets[1], Siep Weiland[1], Wim Coene[1,2]
[1]Department of Electrical Engineering, Eindhoven University of Technology
P.O. Box 513, 5600 MB Eindhoven, The Netherlands
[2]ASML Netherlands B.V., De Run 6501, 5504 DR Veldhoven
P.O. Box 324, 5500 AH Veldhoven, The Netherlands
Email: r.w.h.merks@student.tue.nl

1 Thermal modelling of projection optics

Thermally induced deformations of optical elements influence the performance of high precision optical projection systems. For extreme ultraviolet (EUV) lithography, the mirrors each absorb approximately 35% of the incident power. The thermally induced deformations are for this reason mainly a result of the irradiance on the mirrors. Measuring the temperature distribution and/or the deformations of the mirrors is impractical. In order to determine and predict the induced deformations for design as well as control purposes irradiance models can be utilized.

Propagation of light can be simulated using ray tracing. A full ray tracing approach could be used to determine the irradiance on the elements accurately, but this approach requires hours of calculation time. In this presentation faster approaches are proposed and compared to full ray tracing.

2 Case study

The irradiance models are determined for a projection optics box (POB) with a numerical aperture (NA) at object side $NAO = 0.0625$, a magnification $MA = 0.25$ and with 6 mirrors that each absorb 35% of the incident power. [2]

3 Theory

The irradiance models are created using a method as proposed by Saathof [1]. In this method ray tracing is utilized to determine the projected pupils for each position within the object. These projected pupils are an image of the aperture stop of the POB, which determines the range of angles for each position that will be able to pass through the POB.

The wavelength of EUV light is 13.5 [nm]. The irradiance after the mask is mainly determined by diffraction for feature sizes in the same order as this wavelength. The mirrors of the system are in the far field and for this reason it is possible to use Fraunhofer diffraction. The irradiance per position in the field of the object can be determined by placing the diffraction pattern inside the projected pupils for this position. The total irradiance profile is then a superposition of these projected pupils for a set of positions in the field of the object.

4 Irradiance models

Paraxial approach (1): The paraxial (linear) approximation of ray tracing uses various assumptions. The projected pupils are circular, with the radius r of the pupils independent of the position in the field of the object. The centre positions of these pupils form an image of the object, scaled by a factor s. The projected pupils on each mirror can therefore be parametrised by r and s. These two parameters can be determined by tracing two rays using paraxial ray tracing.

Improved paraxial approach (2): An improvement to the paraxial approach is made by determining r and s using real (nonlinear) ray tracing of at least two rays.

Simplified full ray approach (3): The method could be improved further by assuming circular projected pupils with position dependent parameters. In this way the pupil radii $r(x,y)$ and centre position vectors $\vec{c}(x,y)$ are dependent on the position within the field of the object (x,y). These parameters can be approximated by real ray tracing of at least two rays per object position.

5 Results

The projected pupils for these approaches are compared geometrically to the pupils of the full ray tracing approach. The resulting errors, relative to pupil radius r, are shown in the following table:

Method	Relative pupil projection error [%]	Computational time in MATLAB
1	2.3875	$\sim$ seconds
2	0.6027	$\sim$ seconds
3	0.5504	$\sim$ minutes
Full	0	$\sim$ hours

References

[1] Rudolf Saathof. “Adaptive Optics to Counteract Thermal Aberrations”. PhD thesis. Delft, 2013

[2] R. Hudyma, ”High numerical aperture ring field projection system for extreme ultraviolet lithography,” U.S. Patent 6 033 079, Mar. 7, 2000.

Multi-Tone Synthesis of RF Power Amplifiers

Piet Bronders Gerd Vandersteen
Piet.Bronders@vub.ac.be Gerd.Vandersteen@vub.ac.be
Vrije Universiteit Brussel

1 Introduction

Efficiency enhanced power amplifiers (PA), such as the Doherty PA, the Envelope Tracking (ET) technique and many others [1], are either designed by using exquisite nonlinear models or more generally with the help of a simple one tone excitation that heavily simplifies the PA behaviour, ignoring the dynamical behaviour that such devices demonstrate. This work proposes the use of multi-tone excitations as a trade-off between complexity and oversimplification. This in the hope that a first pass solution is attained that gives a more performing result than classical one tone design techniques and permits a greater extent of control to the designer.

In the following section a possible design proposal for a ET PA, as is shown in Figure 1, using multi-tone excitation signals will be clarified. In the case of a ET PA, the envelope of the Radio Frequency (RF) input signal $u(t)$ is applied to the drain node (V_{DD}). By reducing/increasing this bias voltage in function of the envelope, maximum efficiency can theoretically be preserved. The shaping function that meets this criterion is in most practical cases unknown and must be intelligently chosen by the designer.

2 Preliminary Design Proposal

The main goal of the design is to obtain a supply shaping function dependent on a set of design criteria such as efficiency, power gain, gain compression or a combination of all. At the input port the PA will be excited by a multi-tone signal $u(t)$ that closely mimicks the final operating conditions for which the PA is intended. The extracted envelope $e(t)$ of this bandpass multitone will be used as the drain bias voltage. According to the theoretical framework it is known that the ideal drain bias modulation (satisfying the design criteria) is closily related to the unmodified envelope signal. Needless to say that most of the theoretical assumptions do not apply in practice, such as the hypothesis that the transistor has static behaviour. One of the biggest advantages that the usage of multi-tones allows in contrast to one tone excitation signals is that the dynamical behaviour of the underlying device can be identified as well. In a more theoretical sense we face a common design problem present in a variety of control applications; given a set of constraints, give the required input signal such that the device satisfies all of these constraints.

A small inband multitone perturbation $\delta(t)$, generally called a tickler tone, is now added to the drain node. An important hypothesis is that this additional multitone only evokes a linear response of the device at hand. Using this assumption we can now attempt to linearize the nonlinear impact of the modulation of the drain voltage around the unmodified envelope signal $e(t)$. Fluctuations of the efficiency, power gain and several other figures of merit under influence of this tickler tone can now be analyzed and will give an indication of the wanted supply shaping function.

Important to note is that this approach only results in a correct outcome if the ideal drain bias modulation is assumed to be close to the unmodified envelope signal which might, in disagreement to the theoretical assumptions, not be the case. Even if this condition is not satisfied, the design method might however still result in a superior first iteration of the supply shaping function in comparison to the classical one tone design techniques.

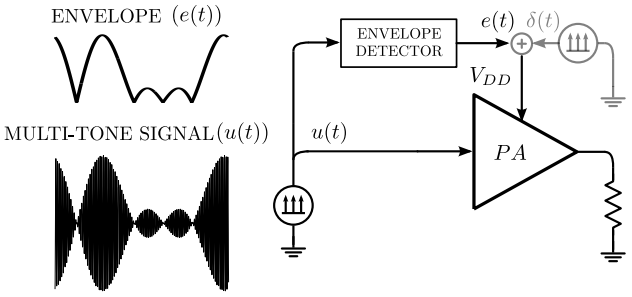

Figure 1: Simplified schematic of a ET PA excited by a multi-tone signal $u(t)$. The extracted envelope signal $e(t)$ and inband tickler multitone $\delta(t)$ are also shown for clarification purposes.

3 Conclusion

The first steps on the path to a potential multi-tone synthesis technique have been taken, hopefully resulting in a feasible design method for the supply shaping of a ET PA.

Acknowledgement

This work is sponsored by the Strategic Research Program of the VUB (SRP-19), Fund for Scientific Research (FWO-Vlaanderen), the Methusalem grant of the Flemish Government (METH-1) and the Belgian Federal Government through the IAP VII/19 DYSCO program

References

[1] S. C. Cripps, *"RF Power Amplifiers for Wireless Communications"*, Artech House, 2006

Kalman filter based reconstruction and robust control of the plasma density in tokamaks

Thomas Blanken
FOM-institute DIFFER
Dutch Institute for Fundamental Energy Research
Association EURATOM-FOM
PO Box 1207, 3430 BE Nieuwegein
The Netherlands
t.c.blanken@tue.nl

Federico Felici
Eindhoven University of Technology
Faculty of Mechanical Engineering
Control Systems Technology group
PO Box 513, 5600 MB Eindhoven
The Netherlands

Marco de Baar
FOM-institute DIFFER
Dutch Institute for Fundamental Energy Research
Association EURATOM-FOM
PO Box 1207, 3430 BE Nieuwegein
The Netherlands

Maurice Heemels
Eindhoven University of Technology
Faculty of Mechanical Engineering
Control Systems Technology group
PO Box 513, 5600 MB Eindhoven
The Netherlands

1 Abstract

An observer and a feedback controller are presented which can reconstruct and control the density profile of a tokamak plasma. A control-oriented, model-based approach is employed to design a Kalman filter and a feedback controller using robust control theory [1]. The framework is generic and can be adapted to different tokamaks, measurement systems and actuators. Observer design is based on a similar approach for the estimation of plasma temperature and current density [2].

The tokamak is a magnetic plasma confinement device and is a promising candidate for reaching controlled nuclear fusion for electricity production. Real-time reconstruction and control of tokamak plasmas is necessary to maintain the desired stable plasma conditions, avoid safety limits and compensate for disturbances.

We present a control-oriented model of the plasma density and the tokamak particle balance. Particle transport in a tokamak plasma is modeled by a 1D partial differential equation. Two additional ordinary differential equations complete the model of the particle balance. We explicitly take the influence of other physical plasma quantities (such as plasma temperature, current and 2D equilibrium) and operational modes of the tokamak into account as exogeneous inputs. We assume these quantities to be available through equilibrium reconstruction and measurements.

Multiple measurement channels of an interferometry system allow to infer the spatio-temporally varying density. A Kalman Filter is designed to estimate the state as well as unknown disturbances. One problem with interferometry systems is the occurence of fringe jumps, which are infrequent but substantial steps in the output signal. A threshold scheme is proposed to detect fringe jumps and correct for them in the state estimation. Offline reconstruction simulations using interferometry measurements from the TCV tokamak indicate accurate density estimation, demonstrate the tuning tradeoffs and show the quality of fringe jump detection.

Existing closed-loop control systems for the plasma density often consist of PI-type controllers [3]. Applying robust control theory can improve the stability and performance of the closed-loop system in the presence of disturbances, nonlinearities and varying operating regimes of the tokamak. Positivity constraints on the actuators complicate the design of a controller. Both SISO and TITO controllers are designed to be robust against uncertainties in model coefficients and exogeneous inputs. Closed-loop simulations for TCV show the controller performance.

References

[1] T. Blanken, “Model-based reconstruction and control of the density in tokamaks,” Master’s thesis, Eindhoven University of Technology, 2014

[2] F. Felici, M. de Baar and M. Steinbuch, “A dynamic state observer for real-time reconstruction of the tokamak plasma profile state and disturbances,” American Control Conference, Portland, USA (2014)

[3] W. Vijvers, F. Felici, H. Le, B. Duval, S. Coda and the TCV team, “Nonlinear digital real-time control in the TCV tokamak,” 39th EPS Conference on Plasma Physics 2012 and the 16th International Congress on Plasma Physics, 2012

Regularized Nonparametric Volterra Kernel Estimation

Georgios Birpoutsoukis
Vrije Universiteit Brussel
Pleinlaan 2, 1050 Brussel
georgios.birpoutsoukis@vub.ac.be

Johan Schoukens
Vrije Universiteit Brussel
Pleinlaan 2, 1050 Brussel
johan.schoukens@vub.ac.be

1 Introduction

One way to describe the nonlinear behavior of a process is by use of the nonparametric Volterra series representation. The major advantage lies in the fact that the problem of choosing the appropriate nonlinear model structure is bypassed. Unfortunately it comes at the cost that the number of parameters to be estimated increases fast for increasing memory of the several impulse responses. This results in a very large variance for the estimated parameters leading to a poor description of the system dynamics, unless very long data records are available. In this work, we present a method to estimate efficiently finite Volterra kernels without the need of long records, based on the regularization methods that have been developed for the one-dimensional (1-D) impulse responses for linear time invariant (LTI) systems.

2 Regularization for the 2^{nd} degree Volterra Kernels

Assume that the dynamics of a true discrete nonlinear process can be described by the following finite second degree Volterra series representation [1]:

$$y_k = \underbrace{\sum_{\tau_1=0}^{n_1-1} g_{\tau_1} u_{k-\tau_1}}_{\text{Linear dynamics}} + \underbrace{\sum_{\tau_1=0}^{n_2-1}\sum_{\tau_2=0}^{n_2-1} h_{\tau_1,\tau_2} u_{k-\tau_1} u_{k-\tau_2}}_{\text{Quadratic dynamics}} + e_k \qquad (1)$$

where u_k denotes the input, y_k represents the measured output signal, e_k is zero mean i.i.d. white measurement noise with variance σ^2, $\tau_i, i = 1,2$ are lag variables and g_{τ_1} and h_{τ_1,τ_2} are the impulse coefficients of the first and second order kernels, respectively. It can be easily shown that, given N input-output measurements, (1) can be transformed into a linear-in-the-parameters problem [2], namely $Y_N = \Phi_N^T \theta + E$, where θ contains g_{τ_1} and h_{τ_1,τ_2}. The regularized least squares problem given a linear-in-the-parameters model is defined as [3]:

$$\hat{\theta}_N^{Reg} = \arg\min_{\theta} \|Y_N - \Phi_N^T \theta\|^2 + \underbrace{[\bar{\theta}_1^T \ \bar{\theta}_2^T]}_{\theta^T} \underbrace{\begin{pmatrix} D_1 & 0 \\ 0 & D_2 \end{pmatrix}}_{D} \underbrace{\begin{pmatrix} \bar{\theta}_1 \\ \bar{\theta}_2 \end{pmatrix}}_{\theta}$$

where D_1 and D_2 are matrices penalizing the parameters of the first ($\bar{\theta}_1$) and the second ($\bar{\theta}_2$) order kernel. In this work we propose a method such that prior information about the smoothness and the exponential decay of the higher dimensional kernels is used during the identification step. The latter is achieved by proper construction of the matrices D_1 and D_2 [2].

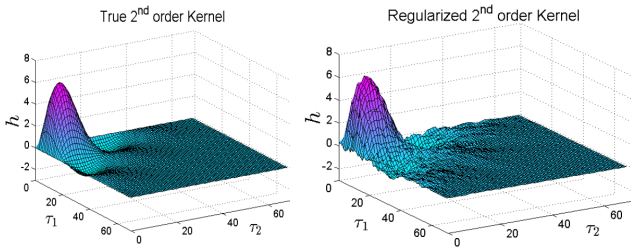

Figure 1: Left: The second order kernel to be estimated. Right: The estimated second order kernel using regularization.

3 Results

It can be clearly observed in Fig.1 that, using the regularization method the properties of exponential decay and smoothness have been effectively reflected on the estimated 2-D impulse response, leading to a precise description of the true dynamics. The method can be easily extended to identification of Volterra kernels of dimension higher than two.

4 Acknowledgments

This work was supported in part by the Fund for Scientific Research (FWO-Vlaanderen), by the Flemish Government (Methusalem), the Belgian Government through the Inter university Poles of Attraction (IAP VII) Program, and by the ERC advanced grant SNLSID, under contract 320378.

References

[1] M. Schetzen, "The Volterra and Wiener theories of nonlinear systems.", Vol. 1, New York: Wiley, 1980.

[2] G. Birpoutsoukis and J. Schoukens, "Regularized nonparametric Volterra kernel estimation", 2015 IEEE International Instrumentation and Measurement Technology Conference (I2MTC), accepted for publication.

[3] G. Pillonetto, F. Dinuzzo, T. Chen, G. De Nicolao, and L. Ljung, "Kernel methods in system identification, machine learning and function estimation: A survey," Automatica, vol. 50, no. 3, pp. 657-682, 2014

Nonlinear System Identification of Hydrostatic Drivetrain

Julian Stoev
Vrije Universiteit Brussel - department ELEC
Pleinlaan 2, Brussels, Belgium
Julian.Stoev@vub.ac.be

Johan Schoukens
Vrije Universiteit Brussel - department ELEC
Pleinlaan 2, Brussels, Belgium
Johan.Schoukens@vub.ac.be

1 Introduction

The engineering community has extensive experience in identification of linear systems. Nonlinear system identification is a more recent and advanced body of knowledge. It is of practical interest to apply nonlinear system identification to diverse industrial cases and gain understanding how it compares with existing linear methods in situations close to real-life.

1.1 Nonlinear state-space model of the system

Polynomial Nonlinear State Space (PNLSS) models are composed of a best linear approximation (BLA) augmented with multi-ivariable polynomial non-linearities dependent on the states and the inputs.

1.2 Subsystem structure preserving identification

The experimental setup consists of several hydraulic and electrical subsystems. It is practically important to preserve the separation of these subsystems and to obtain a model representing each of these subsystems as parts of the bigger model.

2 Experimental setup

The test set-up for this work comprises a relatively large hydrostatic drive train as depicted in Figure 1, available at FladersMake a Strategic Research Centre for Manufacturing Industry in Leuven. The hydraulic motors and pumps in the setup are driven by large induction motors. There are flywheels imitating inertia on the load side, where the motors can also be used to imitate different loads. The setup is controlled with a dSpace system. From control point of view the system is MIMO, time-varying and non-linear, with not fully understood dynamics. Due to the large amount of energy stored in different parts of the system, the safety of the experiments is also of particular concern.

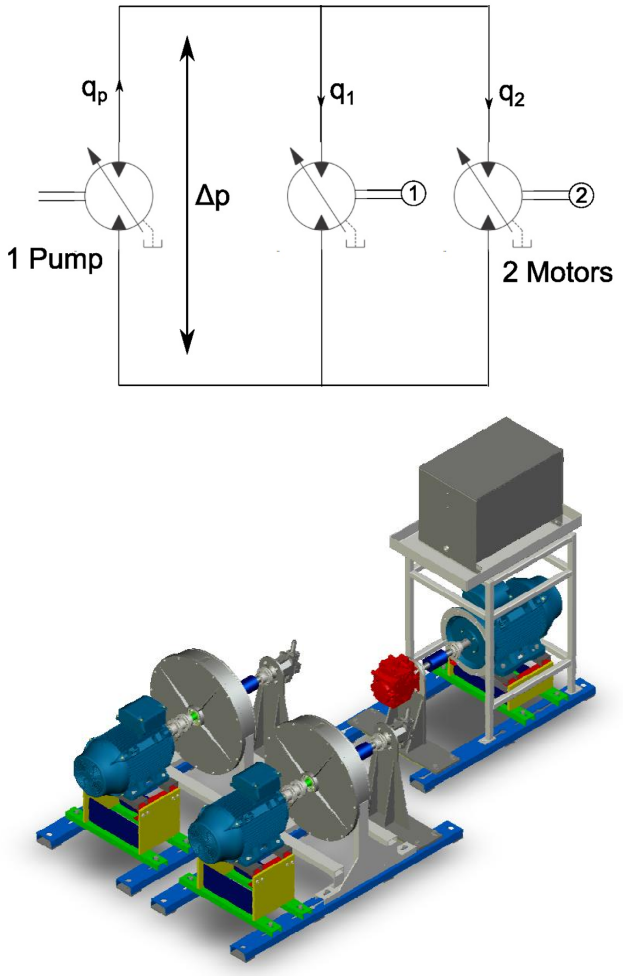

Figure 1: Electro-hydraulic drivetrain

References

[1] M. Jelali and A. Kroll. *Hydraulic Servo-systems: Modelling, Identification and Control*. Advances in Industrial Control. Springer London, 2003.

[2] H.E. Merritt. *Hydraulic Control Systems*. Wiley, 1967.

[3] R.B. Walters. *Hydraulic and Electro-Hydraulic Control Systems*. Springer Netherlands, 1991.

FRF Smoothing Improves the Initial Values for Transfer Function Estimation

Egon Geerardyn, John Lataire
Department ELEC
Vrije Universiteit Brussel (VUB), 1050 Brussels, Belgium
egon.geerardyn@vub.ac.be, john.lataire@vub.ac.be

1 Introduction

Estimating a parametric model based on measured input-output data is a commonly occurring step in e.g. control design. Unfortunately, this often boils down to solving a non-convex optimization problem [1, 2]. Especially for high model orders and/or very noisy data, classical optimization schemes easily get stuck in local optima. To avoid these local optima, a good initial estimate becomes pivotal. Hence, the obtained model quality is strongly influenced by the quality of the initial estimate.

Based on the premise that it is easier to produce initial parametric estimates for a smooth FRF than for a noisy FRF, this presentation proposes to smoothen the measured (non-parametric) frequency response function (FRF) to obtain better initial estimates for a parametric transfer function.

2 Approach

First, a smoothing technique is used to extract a smooth FRF from the measured (noisy) input/output data. In this case study, the time-truncated Local Polynomial Method (LPM) [3], on the one hand, and the regularized finite impulse response (RFIR) [4], on the other hand, are used to this end. Existing initialization schemes, such as generalized total least squares (GTLS) and bootstrapped total least squares (BTLS) [1], are then used to convert the non-parametric FRF into an improved initial parametric estimate. To assess the effectiveness of smoothing the FRF as starting value, the model quality obtained after further optimization is compared for the different initialization strategies (no smoothing, smoothed with the time-truncated LPM or smoothed with RFIR).

3 Results

The FRF smoothing techniques aid in producing better initial estimates as they reduce unwanted phenomena such as noise and leakage. By doing so, the quality of the actual parametric model can be increased considerable as shown in Figure 1 without requiring any additional effort from the user.

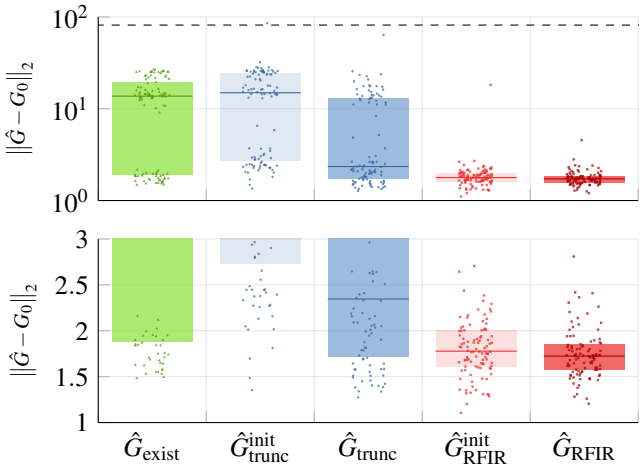

Figure 1: Norm of the model error, determined from a measured validation data record for the different initialization strategies. The estimates obtained using the proposed techniques ($\hat{G}_{\text{trunc}}$ and $\hat{G}_{\text{RFIR}}$) produce models that are (on average) almost an order of magnitude better than the existing techniques (BTLS/GTLS: $\hat{G}_{\text{exist}}$).

References

[1] R. Pintelon and J. Schoukens, *System Identification: a Frequency Domain Approach*, 2nd ed. Wiley-IEEE Press, 2012.

[2] C. T. Kelley, *Iterative Methods for Optimization*. SIAM, 1999. [Online]. Available: http://www.siam.org/books/kelley/fr18/

[3] M. Lumori, E. Geerardyn, J. Schoukens, and J. Lataire, "Smoothing the LPM estimate of the frequency response function via an impulse response truncation technique," *Instrumentation and Measurement, IEEE Transactions on*, vol. 63, no. 1, pp. 214–220, Jan 2014.

[4] T. Chen and L. Ljung, "Implementation of algorithms for tuning parameters in regularized least squares problems in system identification," *Automatica*, vol. 49, no. 7, pp. 2213 – 2220, 2013.

Characterization and Nonlinear modelling of Li-Ion battery

Rishi Relan*, Laurent Vanbeylen*, Yousef Firouz**, Johan Schoukens*
Department ELEC*, Department ETEC-MOBI**, Vrije Universiteit Brussel
[rishi.relan*,laurent.vanbeylen*,Yousef.Firouz**,johan.schoukens*]@vub.ac.be

1 Abstract

Lithium ion (Li-ion) batteries are attracting significant and growing interest because their high energy and high power density render them an excellent option for energy storage, particularly in hybrid and electric vehicles as well as an ideal candidate for a wide variety of applications. Some limitations of existing Li-ion battery technology include underutilization, stress-induced material damage, capacity fade, and the potential for thermal runaway. In order to develop a complete dynamic model of a lithium ion battery that is suitable for virtual-prototyping of portable battery-powered systems, accurate estimation of the state of charge (SOC) and state of health (SOH) is required , which in-turn depends on the quality of the models which are used for the estimation of these quantities. In this paper, a data-driven polynomial nonlinear state-space model (PNLSS) is proposed for the nonlinear regime of the battery's electrical operation based on a non-parametric characterization of the battery's behaviour.

2 Chracterization of the battery electrical behaviour

Generating a control-oriented model e.g. needed by battery management system (BMS), that can describe the input-to-output (Current to Voltage) dynamics of a battery is a challenging problem. A primary reason for this is that battery dynamics vary significantly with operating conditions, and are typically nonlinear in nature. For example, temperature can affect the rate of electrochemical reactions ; SoC determines the available reaction components ; and, current demand (in particular, the direction) determines the types of reactions. Hence, before proceeding to model the battery dynamical behaviour, it is very important to characterize the battery response under varying operational conditions. In this paper, we propose a non-parametric technique in frequency domain [1], which utilises the properties of the random phase multisines signals to characterize the battery's behaviour in different regimes of its operating range. Fig.1(a) shows the result of the non-parametric analysis done on the measurement data acquired from a NMC (EIG, 20Ah) type cell using a PEC tester at room temeperature, 10% SOC. The effect of the even nonlinearities is clearly obsevered at -20 *dB* relative to the output spectrum at excited lines along with the weak odd nonlinearities and also the time variations.

3 Nonlinear modelling

In order to identify the discrete-time nonlinear model for the battery, the polynomial nonlinear state-space model structure [2] is selected :

$$x(t+1) = Ax(t) + Bu(t) + E\zeta(t) \quad (1)$$

$$y(t) = Cx(t) + Du(t) + F\eta(t) \quad (2)$$

The coefficients of the linear terms in $x(t) \in \mathbb{R}^{n_a}$ and $u(t)$ are given by the matrices $A \in \mathbb{R}^{n_a \times n_a}$ and $B \in \mathbb{R}^{n_a \times n_u}$ in the state equation, $C \in \mathbb{R}^{n_y \times n_a}$ and $D \in \mathbb{R}^{n_y \times n_u}$ in the output equation. The vectors $\zeta(t) \in \mathbb{R}^{n_\zeta}$ and $\eta(t) \in \mathbb{R}^{n_\eta}$ contain nonlinear monomials in $x(t)$ and $u(t)$ of degree two up to a chosen degree P . The coefficients associated with these nonlinear terms are given by the matrices $E \in \mathbb{R}^{n_a \times n_\zeta}$ and $F \in \mathbb{R}^{n_y \times n_\eta}$. For the identification, a discrete-time linear model is fitted on non-parametric data and this linear discrete-time model was converted in to a state-space form before optimizing it to identify in least-sqaure sense a nonlinear state-space model. Fig.1(b) clearly shows the improvement in final the PNLSS model output error in the desired frequency band of interest with respect to output measurement and linear model.

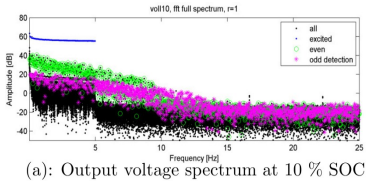

(a): Output voltage spectrum at 10 % SOC

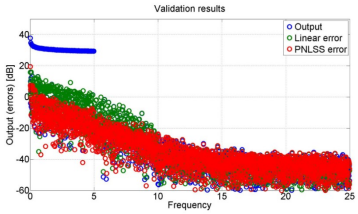

(b):Output Error of PNLSS Model at 10 % SOC

FIGURE 1: Battery Identification

4 Acknowledgements

This work was supported in part by the IWT-SBO BATTLE 639, Fund for Scientific Research (FWO-Vlaanderen), by the Flemish Government (Methusalem), the Belgian Government through the Inter university Poles of Attraction (IAP VII) Program, and by the ERC advanced grant SNLSID, under contract 320378. The authors would also like to acknowledge the support provided by Dr.ir Jean-Marc Timmermans and Dr.ir Noshin Omar of the Department ETEC-MOBI, VUB.

References

[1] Rik. Pintelon, and Johan. Schoukens, " System Identification : A Frequency Domain Approach, 2nd Edition". Wiley-IEEE Press, 2012.

[2] J. Paduart, L. Lauwers, et.al, "Identification of nonlinear systems using polynomial nonlinear state space models", Volume 46, Issue 4, Pages 647-656, Automatica, 2010.

SMA-actuated catheter systems

Rolf Gaasbeek

Eindhoven University of Technology, Department of Mechanical Engineering, P.O. Box 513, 5600 MB Eindhoven, The Netherlands.

Email: R.I.Gaasbeek@tue.nl

1 Introduction

Steerable catheter systems have a dominant role in minimal invasive treatments of cardiovascular diseases. Typically, catheters are steered through simple mechanical pull-wire systems. These systems have the disadvantage that they have restricted directionality and limited shape control. The use of Shape Memory Alloy (SMA) actuators, integrated in the tip of the catheter, enables the realization of extremely accurate and flexible catheters. Thereby, SMA-actuated catheter systems allow for quicker and more advanced minimal invasive surgeries.

2 Shape Memory Alloy for Actuation

Shape Memory Alloy (SMA) is a lightweight material with considerable higher actuation strain and work output than other active materials such as (high strain) piezo-materials [1]. For this reason SMA-actuators have a great potential in micro-robotic systems, such as catheters, and are the point of interest in this work.

SMA is able to recover from large deformation by changing crystallographic structure. This change in structure is stress and temperature dependent and has highly nonlinear contributions to the material dynamics. Additionally, the material suffers from a hysteresis effect [2].

The crystallographic transformation, and thus the actuating movement, is typically controlled by applying Joule heating to a SMA-wire.

3 Physical Modeling of SMA-actuators

A non-linear physical model for SMA-actuators has been derived, characterized and validated. The model accurately describes macroscopic behavior of the material.

By using a suitable class of transformation dynamics, parameters in the model are engineering-based and can be determined with standard material characterization tests [3].

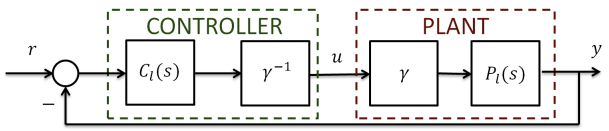

Figure 1: Nonlinearity Compensation

* The research leading to these results is part of INCITE, an Eniac Joint Undertaking project that is co-funded by grants from the Netherlands, Finland, Hungary, France, Ireland, Sweden, Spain, and Poland.

4 Nonlinearity Compensation

As previously stated, the high actuation stroke of SMA-actuators is a result of crystallographic changes in the SMA material. In order to fully address the nonlinear dynamics that dominate this crystallographic change, it is proposed to rewrite the model from Section 3 in a Hammerstein representation with a static nonlinearity γ and a linear part $P_l(s)$. The latter allows for compensation of the non-linearity in the control action, provided that the nonlinearity is invertable. The proposed methodology is depicted in Figure 1. Similar strategies have been successfully implemented for other active materials with alike non-linearities [4] [5].

Note that a Hammerstein description for SMA-actuators also yields a possibility for parametric system identification [6]. Parametric identification provides model parameters and thereby makes extensive material characterization tests redundant. The latter is not only of great value for control engineers, but also for material scientists that are interested in accurate and quick material characterization.

5 Overview

In future work, the possibilities of the proposed framework of Hammerstein-representation and parametric identification have to be investigated. Furthermore, both control design and extension to 3D actuators (multiple wires) have to be addressed in order to allow for multi-directional steering of SMA-based catheter systems.

References

[1] Stéphane Lederlé, "Issues in the design of shape memory alloy actuators," *Master Thesis, Massachusetts Institute of Technology*, 2002.

[2] Dimitris C. Lagoudas, "Shape Memory Alloys: Modeling and Engineering Applications", *Springer*, 2008.

[3] Hassan Sayyaadi, Mohammad Reza Zakerzadeh, Hamid Salehi, "A comparative analysis of some one-dimensional shape memory alloy constitutive models based on experimental tests", *Scientia Iranica B*, vol. 19(2), pp. 249-257, 2012.

[4] Zhenyan Wang, Zhen Zhang, Jianqin Mao and Kemin Zhou, "A Hammerstein-based Model for Rate-dependent Hysteresis in Piezoelectric Actuator," *IEEE Conf. Decis. Control*, pp. 1391 - 1396, 2012.

[5] Micky Rakotondrabe, "Bouc-Wen modeling and inverse multiplicative structure to compensate hysteresis nonlinearity in piezoelectric actuators," *IEEE Trans. Autom. Sci. Eng.*, vol. 8, no. 2, pp. 428 - 431, 2011.

[6] Maarten Schoukens, Rik Pintelon and Yves Rolain, "Parametric Identification of Parallel Hammerstein Systems," *IEEE Trans. Instrum. Meas*, vol. 60, no. 12, pp. 3931 - 3938, 2011.

Separation of breathing signals from respiratory response using regularization

Hannes Maes (hlmaes@vub.ac.be), Gerd Vandersteen (gerd.vandersteen@vub.ac.be)
Department ELEC, VUB

Lung diseases can be monitored by measurement of the respiratory admittance. The forced oscillation technique (FOT) is a widely used measurement technique to obtain respiratory admittance.

The FOT applies small amplitude pressure oscillations p (in the order of 0.1kPa) at the mouth of the patient. A resulting airflow q generated by the patient as a response to the pressure oscillations is measured. The respiratory admittance G is defined as the frequency dependent ratio between the resulting air flow q and the imposed pressure p.

A lot of useful information is contained in the frequency range of spontaneous breathing $(0.1-1$ Hz) [1]. Therefore, a setup is developed that can generate pressure oscillations in this frequency range [2].

To make the measurement technique clinically practical for patients, the setup is designed so that the patient can continue breathing spontaneously during the measurement. This spontaneous breathing br generates a signal in the same frequency range as the respiratory response q. Since the setup does not allow to measure the breathing signal separately, the breathing signal is considered as a disturbance on the response signal as illustrated in Figure 1.

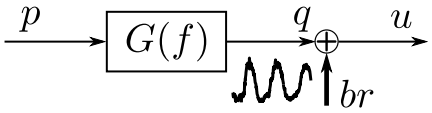

Figure 1: The measured flow signal u contains both the response q of the respiratory admittance to the pressure oscillation p as the breathing disturbance br.

Separating breathing and respiratory response

The measured flow signal u consists of the superposition of br and q (Figure 1). Since the pressure excitation p is known, the respiratory response q needs to be extracted from u in order to obtain the respiratory admittance. Therefore, a model for both q and br needs to be introduced.

The model for q is the linear response to a known excitation signal. The pressure excitation p is a random phase multisine consisting of N_{exc} excitation lines. Therefore the following model is presented for q

$$q(t,\theta_q) = \sum_{k=1}^{N_{exc}} \alpha_k \sin(2\pi k f_0 t) + \beta_k \cos(2\pi k f_0 t)$$

with $f_0 = 1/T$ and T the multisine period.

Spontaneous breathing can vary strongly depending on the patient which demands for a more flexible model. In previous works, nonlinear models with a high number of parameters were used [3]. In this work a simple linear model is proposed for br

$$br(t,\theta_{br}) = \sum_{m=1}^{M} A_m(t)\sin(2\pi m f_{br} t) + B_m(t)\cos(2\pi m f_{br} t)$$

with f_{br} the fundamental breathing frequency, M the number of harmonics and $A_m(t)$ and $B_m(t)$ polynomials of a chosen order. By using this model on multiple short time data segments both amplitude and phase variation can be taken into account.

The parameter vectors θ_q and θ_{br} can be gathered in one vector θ_u. This parameter vector can be obtained using a least square estimator which minimizes the cost

$$V = \|Y - K\theta_u\|^2 \tag{1}$$

with Y the measurement data and K the regression matrix.

The problem which arises is that the regression matrix of the least square estimator K will be ill conditioned due to the overlapping frequncy lines of br and q.
Regularization is used and the following cost function is minimized

$$V = \|Y - K\theta_u\|^2 + \theta_u^T R \theta_u \tag{2}$$

with R the regression matrix.
In this work, several regularization techniques and their influence on the estimation of the respiratory admittance are compared.

Acknowledgement

This work was supported in part by the Fund for Scientific Research (FWO-Vlaanderen), the Methusalem grant of the Flemish Government (METH-1) and by the Belgian Government through the IAP VII/19 DYSCO program.

References

[1] D. W. Kaczka and R. L. Dellaca, "Oscillation mechanics of the respiratory system: applications to lung disease," *Crit Rev Biomed Eng.*, vol. 39, pp. 337–359, 2011.

[2] H. Maes, G. Vandersteen, M. Muehlebach, and C. Ionescu, "A fan-based, low-frequent, forced oscillation technique apparatus," *Instrumentation and Measurement, IEEE Transactions on*, 2013.

[3] H. Maes, G. Vandersteen, and C. Ionescu, "Estimation of respiratory impedance at low frequencies during spontaneous breathing using the forced oscillation technique," in *Engineering in Medicine and Biology Society (EMBC), 2014 36th Annual International Conference of the IEEE*, Aug 2014, pp. 3410–3413.

Estimating the BLA of MIMO sub-networks in simulations

Adam Cooman
ELEC, VUB
acooman@vub.ac.be

Ebrahim Louarroudi
ELEC, VUB
elouarro@vub.ac.be

Gerd Vandersteen
ELEC, VUB
gvanders@vub.ac.be

Complex systems usually consist of an interconnected network of more basic sub-systems. Examples can be found in many different disciplines like electric circuits, biological systems and flexible mechanical systems. Analysis of the sub-systems can give valuable information about how the global system operates. One can, for example, study the way disturbances propagate through the network to find the dominant source of non-linear distortion [1].

In this talk, we consider simulations of such interconnected sub-systems, more specifically: electronic circuits. Due to the port-based representation, classically used in this context, the sub-networks are all Multiple-Input Multiple-Output (MIMO) systems. The global system is excited by a single large signal (See figure below). This signal sets the non-linear operating point of the whole network.

The goal is to determine the Best Linear Approximation (BLA) of the sub-networks. The estimation of the MIMO BLA is a well-studied problem [3]. The classic techniques use orthogonal excitation signals, which require a multisine source for each input of the sub-system. Adding these extra excitation signals to the input of the sub-systems can potentially change the non-linear operating point of the whole network, and with it, the BLA.

We propose to use a different technique which requires no extra large-signal sources in the network. The proposed technique considers the input multisine as a periodic scheduling and linearises the circuit around that scheduling [2]. By studying the linearised behaviour for different phase realisations of the input multisine, we obtain the wanted BLA of the sub-network.

Besides removing the risk of changing the non-linear operating point, the linearisation-based technique has the additional benefit that less phase realisations are required to estimate the BLA. With an efficient implementation, this could lead to a drastic reduction in simulation time.

References

[1] A. Cooman and G. Vandersteen. Distortion contribution analysis by combining the best linear approximation and noise analysis. In *Proc. of the 2014 International Symposium on Circuits and Systems (ISCAS 2014)*, 2014.

[2] E. Louarroudi. *Frequency Domain Measurement and Identification of Weakly Nonlinear Time-Periodic Systems*. PhD thesis, Vrije Universiteit Brussel (VUB), 2014.

[3] R. Pintelon, G. Vandersteen, J. Schoukens, and Y. Rolain. Improved (non-)parametric identification of dynamic systems excited by periodic signals the multivariate case. *Mechanical Systems and Signal Processing*, 25:2892 – 2922, 2011.

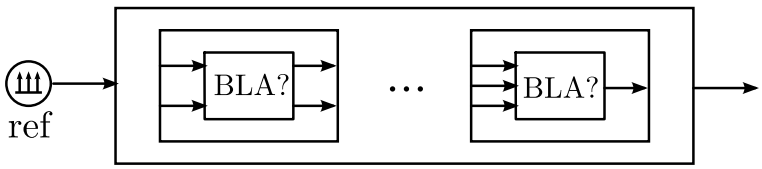

We consider an interconnection of MIMO systems where a single large-signal multisine sets the non-linear operating point. The goal is to determine the MIMO BLA of the sub-systems.

agency for Innovation by Science and Technology

This work is sponsored by the Strategic Research Program of the VUB (SRP-19), Institute for the Promotion of Innovation through Science and Technology in Flanders (IWT-Vlaanderen), Fund for Scientific Research (FWO-Vlaanderen), Flemish Government (Methusalem) and the Belgian Federal Government (IUAP VI/4)

Vrije Universiteit Brussel

Optimal control of greenhouse climate with grower defined bounds

P.J.M. van Beveren[1], J. Bontsema[2], G. van Straten[3], E.J. van Henten[1]

[1]Farm Technology Group, Wageningen University, P.O.Box 16, 6700AA Wageningen, The Netherlands

[2]Wageningen UR Greenhouse Horticulture, P.O. Box 644, 6700AP Wageningen, The Netherlands

[3]Biobased Chemistry & Technology, Wageningen University, P.O. Box 17, 6700AA Wageningen, The Netherlands

peter.vanbeveren@wur.nl, jan.bontsema@wur.nl, gerrit.vanstraten@wur.nl, eldert.vanhenten@wur.nl

1 Introduction

An optimization framework to minimize the total energy input to a greenhouse was developed and analyzed for a modern greenhouse with active cooling and industrial CO_2 injection.

2 Optimization procedure

A dynamic three state model was developed for greenhouse air temperature, humidity, and CO_2 concentration. Given the model, initial conditions $T_{air}(0)$, $\chi_{air}(0)$, and $CO_{2,air}(0)$, external inputs, and constraints on the climate variables and control inputs, the optimal control trajectory that minimizes total energy input over time can be found by minimizing the following functional J:

$$\min_{Q_{E,h},Q_{E,c},g_V,\phi_{c,inj}} J(Q_{E,h},Q_{E,c},g_V,\phi_{c,inj}) = \int_{t_0}^{t_f} \left(Q_{E,h}^2 + Q_{E,c}^2\right) dt \qquad (1)$$

where $Q_{E,h}$ is heating, $Q_{E,c}$ cooling, g_V the specific ventilation, and $\phi_{c,inj}$ the injection of CO_2 . Also the control inputs had constraints. Another constraint was the total amount of CO_2 that could be injected per day. One full year was optimized and compared with data from a 4 ha commercial rose greenhouse. Standard optimization settings, based on grower's operation of the greenhouse were formulated to compare the optimal situation with the grower. By adapting the lower bound for heating to the amount of energy coming from the pipe rail heating system in case of minimum pipe temperature, the effect of settings that growers are familiar with can be made explicit.

3 Results

The daily optimization results with standard settings for the whole year 2012 are shown in Fig. 1 and Table 1.

Table 1: Total heating, cooling, and CO_2 injection of the grower, the optimal situation with standard settings, and the optimal situation with minimum pipe temperature as used by the grower for 2012.

	Heating $GJ\,m^{-2}\,y^{-1}$	Cooling $GJ\,m^{-2}\,y^{-1}$	CO_2 injection $kg\,m^{-2}\,y^{-1}$
Grower	2.08	0.71	95.4
Opt standard settings	1.10	0.60	85.7
Opt minimum pip	1.49	0.71	85.9

Optimization for the whole year resulted in a reduction of 47 % in heating, 15 % in cooling, and 10 % in CO_2 injection

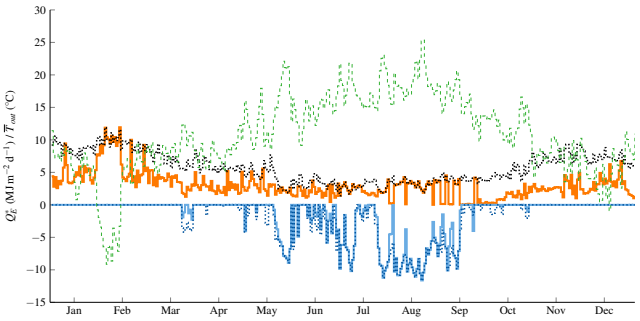

Figure 1: Results of daily optimization with standard settings for the year 2012. Optimal heating (——), optimal cooling (——), heating grower (·····), cooling grower (·····), and mean outside temperature (- - -).

for the year 2012. When the minimum pipe temperature of the grower was implemented, still, a reduction of 28 % in heating, 14 % in cooling, and 10 % in CO_2 injection use was found. The effect of different bounds on the optimal energy input was analyzed. Fig. 2 shows the effect of changing the boundaries for CO_2 on 16 June, 2012. A lower lower bound

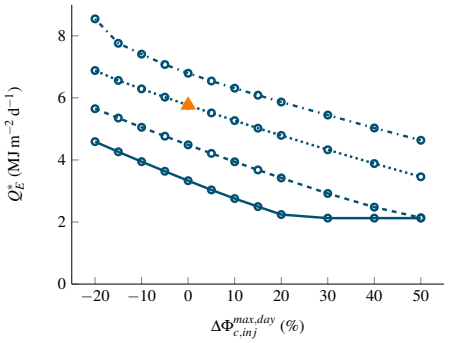

Figure 2: Effect of changing CO_2 bounds for 16 June, 2012. Values for $CO_{2,air}^{min}$ were the standard settings −20 % (—o—), −13 % (- o -), −3 % (·· o ··), and 7 % (· o · -). Other settings were standard optimization settings. ▲is optimization with standard settings.

for the CO_2 concentration leads to lower energy input by heating and cooling, because the windows can be opened more during day time instead of using active cooling. If more CO_2 is available per day, the same effect can occur.

Research supported by Dutch Technology Foundation STW

Robust control of fuel-cell-car-based smart energy systems

Farid Alavi and Bart De Schutter
Delft Center for Systems and Control
Delft University of Technology
Delft, The Netherlands
f.alavi@tudelft.nl

1 Introduction

Any fuel cell car can also be considered as a small power plant that can produce electricity from hydrogen in an efficient and clean way. By considering a large number of fuel cell cars in the future, one can imagine the presence of several locations spread in the city that can provide a safe parking place for these kind of cars and at the same time, may extract electricity from the fuel cells of the cars and inject it into the power grid. Therefore, these kind of installations can be considered as future power plants.
The car as power plant (CaPP) can increase the efficiency of the electricity production. However, there are several challenges in the realization of such a system. Technological challenges, like efficient ways to produce hydrogen and fuel cells, social behavior of fuel cell car owners in presence of such a system, and charging/discharging management of the vehicles are among the most important challenges. In this project, we will develop a robust hybrid model-based predictive control (MPC) approach to determine the optimal time instants to charge or discharge the electrical vehicles in a CaPP installation in order to minimize the overall cost of the system.

2 Fuel-cell-car-based smart energy system

A CaPP installation with several fuel cell cars has the capacity to produce and inject electricity into the power network by using the fuel cells of the cars, and on the other hand, it can consume electricity from the power network and store it in the batteries of the cars. The overall cost of electricity production/consumption of the parking station can be determined by considering the current charge state of the fuel cells and batteries of the cars, production capability of the renewable power sources, energy prices, degradation of the fuel cells when producing electricity, and possibly a reward paid to the car owners. In addition to these factors, every car owner has a desired time to take back the car from the parking station. As a result, several factors should be considered in a parking station in order to determine a charge/discharge plan and optimization is required in order to minimize the overall costs.
To this end, first we will define the models of the electrical networks, fuel cells, batteries, etc. present in the system. To define the total costs of the system, it is necessary to indicate some profiles about the future energy needs, production capability of renewable energy sources, and electricity price during the next few hours. In this project, uncertainties in the model and prediction profiles will be considered explicitly. Today, there are several methods in robust MPC literature that can deal with these uncertainties [1] and we aim to propose a new robust MPC that is applicable in the CaPP framework.
In addition, the combination of continuous dynamics (e.g. currents and voltages) and discrete-event behavior (e.g. switching the appliances or power sources on and off, changing the type of energy sources, and activating a certain type of energy conversion) indicates that the system is hybrid in nature. In recent years, it has been shown that the MPC can efficiently control a wide variety of hybrid systems [2]. Hence, the goal of this project is to develop a new robust hybrid MPC approach based on time-instant optimization that can determine the charge/discharge plan of the fuel cell cars.

3 Challenges

We consider a hybrid system that contains uncertainties in the model and in the prediction profiles. Therefore, it is necessary to develop a new robust MPC approach that can also deal with the hybrid nature of the system. Moreover, in real-time control, it is necessary to use fast and efficient numerical algorithms in the controller and this feature should also be considered in the development of the new robust hybrid MPC approach.

Acknowledgment

Research supported by the the NWO-URSES project “Car as Power Plant”, which is financed by the Netherlands Organisation for Scientific Research (NWO).

References

[1] M. N. Zeilinger, M. Morari, and C. N. Jones. Soft constrained model predictive control with robust stability guarantees. *IEEE Transactions on Automatic Control*, 59(5):1190–1202, May 2014.

[2] H. van Ekeren, R.R. Negenborn, P.J. van Overloop, and B. De Schutter. Time-instant optimization for hybrid model predictive control of the Rhine-Meuse Delta. *Journal of Hydroinformatics*, 15(2):271–292, 2013.

Cartesian constrained time-optimal point-to-point motion planning for robots: the waiter problem

Niels van Duijkeren, Frederik Debrouwere, Goele Pipeleers, Jan Swevers
KU Leuven, B-3001 Heverlee, Belgium
Department of Mechanical Engineering, Division PMA
Niels.vanDuijkeren@mech.kuleuven.be

1 Introduction

Time-optimal point-to-point motion is of significant importance for maximizing the productivity of robot systems. This type of motion planning for robots is however a complex problem and is therefore often solved in two phases. First, a high level planner determines a geometric path ignoring the system dynamics but taking into account geometric path constraints. Second, an optimal trajectory along the geometric path is determined taking into account system dynamics and limitations. Since the dynamics along a geometric path can be described in terms of a scalar path coordinate s and its time derivatives [1], the decoupled approach simplifies the motion planning problem to great extent. In recent work it was shown for a simplified robotic manipulator that the path following problem with Cartesian acceleration constraints can be cast as a convex optimization problem [2], which allows for the highly efficient computation of the global optimum.

In this work we explore ways to solve the motion planning problem in application to the waiter problem. The waiter problem considers moving a non-fixed object time-optimally from an initial pose to a final pose while preventing the object to slide, lift or tip over. This problem is akin to a robot that transports, e.g., a pallet with a loosely stacked payload. In [2] the convex formulation of the path following problem is implemented to solve a simplified version of the waiter problem. Assuming a fixed geometric path, the optimal timing along this path $s(t)$ is determined subject to the earlier outlined criteria. This convex problem can be solved efficiently, but is still conservative. Namely, appropriate tilting of the tray allows reduce the overall motion time. We present attempts to include the shape of the path in the optimization and to implement an efficient solution technique.

2 Approach

We compare two methods to tackle the overall time-optimal trajectory planning problem. For both methods the path is parameterized as a convex combination between lower- and upper-bound paths in joint space to achieve freedom in the Cartesian trajectory [3]. In the first approach, a high-level gradient descent optimization is applied to the parametric sensitivity of the solution for each convex path following subproblem towards the shape of the path. This algorithm can be very slow due to the many convex problem solutions that are needed to compute the gradients. The second alternative is to formulate one single non-linear program for the entire time-optimal motion planning problem. And to subsequently use a state-of-art non-linear programming solver to obtain the optimal trajectory. The goal of this case study is to assess the potential performance of both techniques in a real-time solution scheme for nonlinear model predictive control. The presentation is primarily focused towards the intermediate findings for the first described gradient-descent method.

Figure 1: Experimental setup, the ABB IRB120 manipulator.

3 Example

To illustrate the results and show the experimental validity, we apply the solution methods for the waiter problem to an industrial robot. Considered here is a six-DOF ABB IRB120 serial link manipulator with an open controller for tracking the joint trajectories, see Figure 1. The time-optimal trajectory is generated off-line and applied in open-loop for the validation of the numerical results.

References

[1] J. Bobrow, S. Dubowsky, and J. Gibson, "Time-Optimal Control of Robotic Manipulators Along Specified Paths," *Int. J. Rob. Res.*, vol. 4, pp. 3–17, Sept. 1985.

[2] F. Debrouwere, W. Van Loock, G. Pipeleers, M. Diehl, J. Swevers, and J. De Schutter, "Convex time-optimal robot path following with Cartesian acceleration and inertial force and torque constraints," *Proc IMechE Part I J. Syst. Control Eng.*, vol. 227, pp. 724–732, Nov. 2013.

[3] W. Van Loock, G. Pipeleers, and J. Swevers, "Time-optimal quadrotor flight," in *2013 Eur. Control Conf.*, pp. 1788–1792, 2013.

Acknowledgements The research leading to these results has received funding from the People Programme (Marie Curie Actions) of the European Union's Seventh Framework Programme FP7/2007-2013/ under REA grant agreement n° 607957. This work also benefits from K.U.Leuven-BOF PFV/10/002 Center-of-Excellence Optimization in Engineering (OPTEC), from the Belgian Programme on Interuniversity Attraction Poles, initiated by the Belgian Federal Science Policy Office, and from K.U.Leuven's Concerted Research Action GOA/10/11 "Global real-time optimal control of autonomous robots and mechatronic systems". Goele Pipeleers is partially supported by the Research Foundation Flanders (FWO Vlaanderen).

Counterweight synthesis for time-optimal robotic path following

Frederik Debrouwere, Goele Pipeleers, Jan Swevers
KU Leuven, Mechanical Engineering, Division PMA
frederik.debrouwere@kuleuven.be

1 Introduction

Robot path following problems determine the motion of a robot along a predetermined geometric Cartesian end effector path without any preassigned timing information. Many problems in robotics can be cast as path following problems. Standard path following techniques then determine an optimal motion along the geometric path that takes the system dynamics and limitations into account. Describing the dynamics along a geometric path by a scalar path coordinate s and its time derivatives [1] simplifies the motion planning problem to great extent and renders a convex problem with linear inequality constraints for a simplified robot model. The goal of this work is to explore the potential of adding counterweights to the robot structure in order to decrease the optimal motion time for path following problems. The idea is that the torque required to move the robot links is countered by the torque of the counterweight, hence the motor can use the ecces of torque to move the link faster. This idea originates from classic examples such as elevators. The problem of optimizing both counterweights and timing along the path can be cast as a non-convex optimization problem with bilinear inequality constraints. Despite the non-convexity of this problem, it can still be solved efficiently, rendering a relevant solution that can be used in practice.

2 Approach

Path following decouples the timing and path parameters by defining a path coordinate s going from 0 to 1 and by projecting the dynamics onto the path. Hence for a given path, the timing can be found easily. The approach here extends this idea. Since both timing and dynamic parameters of the counterweights need to be found and the path is given, we decouple the timing, path kinematics and dynamic parameters in the system model. For an n dof robot the motor torques $\tau \in \mathbb{R}^n$ are then given by

$$\tau(s) = f(A(s)\rho x(s), B(s)\mu x(s)),$$

where $A(s)$ and $B(s)$ project the dynamics onto the path for the link and counterweights respectively, $x(s)$ captures the timing along the path and ρ and μ represents the dynamic parameters of the links and counterweights respectively. Torque constraints $\tau_- \leq \tau(s) \leq \tau_+$ then introduce linear terms for the links, since ρ is known, and bilinear terms $\mu x(s)$ for the counterweights in the optimization variables μ and $x(s)$. The bilinear optimization problem can be solved in three ways: **1.** solving the non-convex problem using non-convex solvers, **2.** decomposing the bi-linearities as a convex and concave part and solving the problem using Sequential Convex Programming, **3.** decoupling the optimization: high level searches μ while low level searches $x(s)$ for a given μ by solving a convex problem. A gradient search is then used to solve the total problem All three approaches are examined and compared with respect to computation time and optimality.

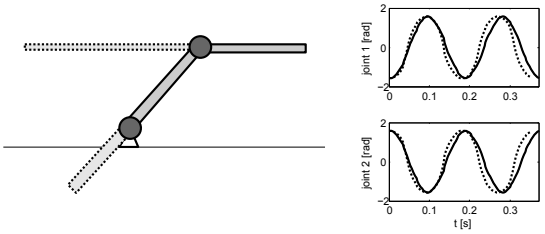

Figure 1: Right: planar robot (full) with optimal counterweights (dashed). Left: joint paths for two periods with (dashed) and without (full) optimal counterweight.

3 Example

We illustrate the practicality of the method here by considering a planar 2 dof robot in the gravitational field, shown in Figure 1. We consider a periodic task of moving the end effector up and down while keeping it parallel to the horizontal plane. The links are modelled as rods, with length 0.25 m and radius 0.01 m, while the counterweights are considered to be rod extensions of the links. Figure 1 shows the robot, the optimized counterweights and the robot motion. In this case, the optimal counterweights, with lengths 0.197, 0.409 m and radii 0.0126, 0.0068 m respectively for both links, reduce the motion time for one period with 4.4%. Future research will consider counterweight synthesis for 6 dof robots.

References

[1] D. Verscheure, B. Demeulenaere, J. Swevers, J. De Schutter, and M. Diehl. Time-optimal path tracking for robots: A convex optimization approach. *Automatic Control, IEEE Transactions on*, 54(10):2318 –2327, oct. 2009.

Acknowledgement This work benefits from K.U.Leuven-BOF PFV/10/002 Center-of-Excellence Optimization in Engineering (OPTEC), the Belgian Programme on Interuniversity Attraction Poles, initiated by the Belgian Federal Science Policy Office (DYSCO) and K.U.Leuven's Concerted Research Action GOA/10/11. Goele Pipeleers is a Postdoctoral Fellow of the Research Foundation - Flanders (FWO - Vlaanderen).

Approximate Bisimulation Relations for Linear Systems

Noorma Yulia Megawati
Jan C. Willems Center for Systems and Control
University of Groningen
P.O.Box 407, 9700 AK Groningen
n.y.megawati@rug.nl

Arjan van der Schaft
Jan C. Willems Center for Systems and Control
University of Groningen
P.O.Box 407, 9700 AK Groningen
a.j.van.der.schaft@rug.nl

1 Introduction

The notion of bisimulation relation for linear input - state - output systems is defined in [3]. Geometric control theory is used to derive a characterization of bisimulation relation and an algorithm for computing the maximal bisimulation relation. This relation unifies the concept of state space equivalent and state space reduction. This relation requires that the output of the system are and remain the same or equivalently their transfer functions are the same.

Meanwhile the notion of approximate bisimulation relation is defined in [2]. This notion allows the distance between two outputs remain bounded by some parameter. This notion is characterized as level sets called bisimulation function. This function is a function bounding the distance between the outputs of two systems.

In this paper we defined the notion of approximate bisimulation relation which allows the transfer functions which has some *moment matching*. The *moment matching* method are class of model reduction method which based on the notion of *moment* of a transfer function of linear system [1]. The idea is to equalize a spesific number of the leading coefficients of the Laurent series expansion of the transfer function.

In this paper, we concentrated on *Krylov methods* in particular *Two-sided Lanczos method* preserving the first $2k$ Markov parameters of the transfer function are the same. We introduced the notion of approximate bisimulation relation between a system and the reduced system using *Two sided Lanczos method*. Then we generalized the notion of approximate bisimulation relation for two systems.

2 Results

Consider two systems given by

$$\Sigma_i : \begin{array}{rcll} \dot{x}_i(t) & = & A_i x_i(t) + B_i u(t) & x_i \in \mathscr{X}_i, u_i \in \mathscr{U} \\ y_i(t) & = & C_i x_i(t) & y_i \in \mathscr{Y} \end{array} \quad (1)$$

with $\mathscr{X}_i, \mathscr{U}, \mathscr{Y}$ are finite dimensional linear spaces and $A_i \in \mathbb{R}^{n\times n}, B_i, C_i^T \in \mathbb{R}^n$ for $i = 1,2$. The notion of approximate bisimulation relation can be defined as follows.

Definition 1. *Two subspaces $\mathscr{P}, \mathscr{Q} \subset \mathscr{X}_1 \times \mathscr{X}_2$ are approximate bisimulation relations between Σ_1 and Σ_2 if*

1. $$\mathscr{P} \subset \mathscr{Q} \quad (2)$$
2. $$\begin{bmatrix} A_1 & 0 \\ 0 & A_2 \end{bmatrix} \mathscr{P} \subset \mathscr{Q} \quad (3)$$
3. $$\mathrm{im} \begin{bmatrix} B_1 \\ B_2 \end{bmatrix} \subset \mathscr{P} \quad (4)$$
4. $$\mathscr{Q} \subset \ker \begin{bmatrix} C_1 & -C_2 \end{bmatrix} \quad (5)$$

The existence of approximate bisimulation relations can be characterized in the following theorem.

Theorem 1. *The first $2k$ Markov parameters of Σ_1 and Σ_2 are equal, that is*

$$C_1 A_1^{j-1} B_1 = C_2 A_2^{j-1} B_2, j = 1, ..., 2k \quad (6)$$

if and only if there exists two subspaces $\mathscr{P}$ and $\mathscr{Q}$ given by

$$\begin{array}{rcl} \mathscr{P} & = & \mathrm{im} \begin{bmatrix} B_1 & A_1B_1 & ... & A_1^{k-1}B_1 \\ B_2 & A_2B_2 & ... & A_2^{k-1}B_2 \end{bmatrix} \\ \mathscr{Q} & = & \ker \begin{bmatrix} C_1 & -C_2 \\ C_1A_1 & -C_2A_2 \\ \vdots & \vdots \\ C_1A_1^{k-1} & -C_2A_2^{k-1} \end{bmatrix} \end{array} \quad (7)$$

which define an approximate bisimulation relation between Σ_1 and Σ_2.

References

[1] A.C. Antoulas, "Approximation of large-scale dynamical systems", Advances in Design and Control, vol. DC-06SIAM, Philadelphia, 2005.

[2] A. Girard and G. J. Pappas, "Approximate bisimulations for constrained linear systems", in Proc. 44th IEEE Conference on Decision and Control and European Control Conference, December 2005.

[3] A.J. van der Schaft, "Equivalence of dynamical systems by bisimulation", IEEE Transactions on Automatic Control, vol.49, pp. 2160–2172, 2004.

Global asymptotic stability of multi-agent systems with undamped nodes

Filip Koerts
University of Groningen
f.j.koerts@rug.nl

prof. dr. Arjan van der Schaft
University of Groningen
a.j.van.der.schaft@rug.nl

prof. dr. Claudio de Persis
University of Groningen
c.de.persis@rug.nl

dr. Mathias Buerger
University of Stuttgart
mathias.buerger@ist.uni-stuttgart.de

Problem formulation

We consider a linear multi-agent system defined on a graph $G = (V, E)$ with agents defined on the nodes and controllers defined on the edges. The dynamics of the agents are given by the second order differential equation $M\ddot{s} = -R\dot{s} - BDB^T s + c$ and can also be described as an interconnection of linear systems by introducing agent states $p := M\dot{s}$ and controller states $q := B^T s$. Then, the dynamics of the agents is given by $\dot{p} = -Rv - Bf + c$ with output $v = M^{-1}p$. The controller dynamics reads as $\dot{q} = B^T v$ where $(q(0) \in \mathrm{im}(B^T))$ and has output $f = Dq$.

B the incidence matrix, c a constant external input, M and D are positive definite diagonal matrices, whereas R is a semi-positive diagonal matrix.

We ask ourselves if every steady-state solution shows total output agreement, i.e. if $p \in span\{\mathbb{1}\}$ holds for $t \to \infty$. This is always the case if all nodes have strictly positive damping, in which case $R > 0$. However, when some nodes have zero resistance, convergence of p to an agreement state is not guaranteed for all initial conditions. In that case, some components might show oscillatory behavior. The problem is to decide for any configuration of B, R, M, D and c, if the agent state $p(t)$ reaches total output agreement at $t \to \infty$ for every initial condition of p and $q \in \mathrm{im}(B^T)$.

Results

To find necessary and sufficient conditions for global convergence to total output agreement, it is shown first that the the above system has a unique equilibrium. An incremental model can be introduced, whose unique equilibrium point is located in the origin. Analysis of eigenvalues of the Jacobian matrix appearing in the state-space representation of the system, yields necessary and sufficient conditions for global convergence through the Jordan normal decomposition. With Lyapunov analysis, it is shown that the elements of p corresponding to the damped nodes always converge to zero. Also, it shown that for $t \to \infty$, the solution of $p(t)$ lives in the unobservable subspace of a linear time-invariant system obtained from B, R, M and D. In fact, it is shown that this subspace is precisely the space of possible oscillations in steady-state. Therefore, we have global convergence if and only if this subspace only contains the origin.

Alternatively, global convergence can be identified through the part of M associated with the undamped nodes, together with the Laplacian matrix of the original graph G and the Laplacian matrix of the reduced graph obtained from G by performing a Kron reduction in which the damped nodes are eliminated.

A sufficient condition for global convergence can be given which only regards the topology of G. To this end, the damped nodes of the graph are colored black and the undamped nodes are colored white. Then we iteratively apply the node coloring rule: if there exists a black node which has exactly one white neighbor, then we color this neighbor black. If we can color all nodes black in this way, global convergence is guaranteed. In that case, we say that the original black nodes form a zero forcing set. The idea is that damped nodes are guaranteed to converge (from Lyapunov analysis) and if some node that is guaranteed to converge has only one neighbor whose convergence is not guaranteed, then this neighbor has to converge as well in order to ensure a constant net force exerted by the springs on the converging nodes.

References

[1] F. Koerts, C. de Persis, A.J. van der Schaft, M. Buerger. "Global asymptotic stability in multi-agent systems", *2015 (under construction)*,

Predicting on-line opinion dynamics using consensus models

Corentin Vande Kerckhove
Université catholique de Louvain - ICTEAM
corentin.vandekerckhove@uclouvain.be

Samuel Martin
Université de Lorraine - CRAN
samuel.martin@univ-lorraine.fr

1 Introduction

The modern information and communication technologies provide a new potential to design systems able to harness collective intelligence. These social systems incorporate collective decision processes resulting from opinion dynamics. Yet, predicting opinion dynamics in the context of social influence largely remains an open problem [1]. The present work provides a new step in this direction.

2 Crowdsourcing games

We carried out online experiments where participants had to estimate some quantities while receiving information regarding opinions from other players. Our research is based on an experimental website that we built, which received participants from a *crowdsourcing* platform.

When a participant took part in an experiment, he/she joined a group of participants for a series of games. During the first round, each of the players provided his/her estimation, independently of the other players. During the second and third round, each player got to know all other opinions from the first round in an anonymous fashion and provided his/her estimation again.

3 Social consensus

We use a *consensus model* [2] to capture the way individual opinions evolve during a collective decision process. Our model assumes that when an individual sees a set of opinions, his/her opinion changes linearly in the distance between his/her opinion and the mean of the group opinions. In mathematical terms, we denote $x_i(t)$ the opinion of individual i at time t and describe its evolution as

$$x_i(t+1) = x_i(t) + \alpha_i \cdot \beta_i^t \cdot (\bar{x}(t) - x_i(t)) \; + \; \eta_i(t), \qquad (1)$$

where $\bar{x}(t)$ is the mean opinion of the group at time t, $\eta_i(t)$ represents the model noises and the linear factors $\alpha_i \cdot \beta_i^t$ are called the *influencability* of the individuals. It represents the strength of attraction of an opinion toward the mean opinion.

To fit the consensus model (1) to the data, the influencability factors $\alpha_i \cdot \beta_i^t$ are estimated using two complementary methods. The log-likelihood maximization (*LLM*) is applied to estimate the influencability of each single participant independently. The Expectation-Maximization algorithm (*EM*) performs classification to cope with situations where the training set size is small.

4 Prediction efficiency

The model is assessed via crossvalidation on its ability to predict the final opinions of individuals during round 3 based on initial opinions only. A subset of the games – the training set – is used to estimate the model parameters, and the rest of the games serves to compute the root mean square error (*RMSE*) between the observed data and predictions.

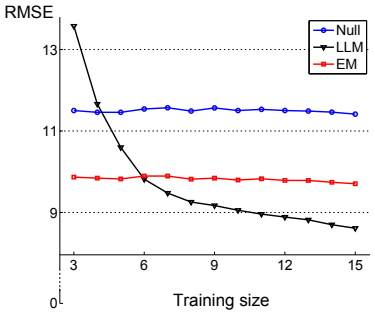

Figure 1: Comparing the prediction efficiency of LLM and EM methods for a training set size from 3 to 15 games.

LLM and EM methods are compared for various training sizes to a null model, assuming constant opinion with no influence, i.e., $\alpha_i = 0$ (Figure 1). The LLM method is sentitive to training set size : it performs better than the null model when the number of games used for training is higher than 4 but its predictions become poorer otherwise, due to overfitting. The last method always performs better than the null model and outweights the LLM when training set size is smaller than 6 games.

References

[1] M. J. Salganik, P. S. Dodds, and D. J. Watts. Experimental study of inequality and unpredictability in an artificial cultural market. Science, 311(5762):854–856, 2006.

[2] R. Olfati-Saber, J. A. Fax, and R. M. Murray. Consensus and cooperation in networked multi-agent systems. Proceedings of the IEEE, 95(1):215–233, 2007.

Acknowledgements

Research supported by the Belgian Interuniversity Attraction Poles, and the Concerted Research Actions of the French Community of Belgium. C.V. is a FRIA Fellow. S.M. is with Université de Lorraine, CRAN.

Stability Analysis For Repeated Snowdrift Games

Pouria Ramazi and Ming Cao
ENTEG, University of Groningen, The Netherlands. Email: p.ramazi, m.cao@rug.nl

1 Introduction

We focus on a special class of anti-coordination evolutionary games, *repeated snowdrift games*, to carry out some rigorous stability analysis for the evolutionary dynamics for the competition of three typical decision-making strategies.

2 Framework

2.1 Base game

The finite symmetric two-player snowdrift game in a normal form with the payoff matrix is considered to be a *base game* G.

$$\begin{array}{cc} & \begin{array}{cc} C & D \end{array} \\ \begin{array}{c} C \\ D \end{array} & \begin{pmatrix} R & S \\ T & P \end{pmatrix}, \end{array} \qquad T>R>S>P \tag{1}$$

2.2 Repeated game

A *repeated game* G^m with *reactive strategies* is constructed from the base game G by repeating it for $m \geq 2$ rounds, and limiting players' choice of strategies in a round to be based on the opponent's choice in the previous round. Three reactive strategies are considered in this paper:

- the *always cooperate (ALLC) strategy* under which the player always cooperates;
- the *tit-for-tat (TFT) strategy* under which the player cooperates in the first round, and then does the same as what her opponent did in the previous round;
- the *suspicious tit-for-tat (STFT) strategy* under which the player defects in the first round, and then does the same as what her opponent did in the previous round.

It can be easily shown that the repeated game G^m can be viewed as a normal, symmetric two-player game with a 3×3 payoff matrix A and with the pure-strategy set $\mathscr{K} = \{ALLC, TFT, STFT\}$.

2.3 Replicator dynamics

Let $x_C(t)$, $x_T(t)$ and $x_{ST}(t)$ denote the population shares of individuals playing pure strategies $ALLC$, TFT and $STFT$ respectively at time t. Then, define the associated *population state* vector as $x(t) = x_C(t)e^1 + x_T(t)e^2 + x_{ST}(t)e^3$ where e^i is the unit column-vector whose ith element is 1. The replicator dynamics describing the evolution over time of each individual's population share are given by

$$\dot{x}_i(t) = [e^i \cdot Ax(t) - x(t)\cdot Ax(t)]x_i(t). \tag{2}$$

3 Triple-wise comparison of the strategies

Theorem 3.1 *Let $\xi(t,x^0)$ be the solution to the replicator dynamics (2) at time t under the initial condition x^0. Assume $x^0 \in \text{int}(\Delta)$ where Δ is the 3-dimensional simplex spanned by e^1, e^2 and e^3 and $m = 2n, n \geq 1$. Then, it holds that*

- *if* $R < \dfrac{T+S}{2}$,
$$\lim_{t\to\infty} \xi(t,x^0) = x^2; \tag{3}$$
- *if* $R = \dfrac{T+S}{2}$,
$$\lim_{t\to\infty} \xi(t,x^0) = s_T; \tag{4}$$
- *if* $\dfrac{T+S}{2} < R < \dfrac{nT+(n-1)S}{2n-1}$,
$$\exists x^* \in \Phi^{2n} \cup \{s_T\} : \lim_{t\to\infty} \xi(t,x^0) = x^*; \tag{5}$$
- *if* $R = \dfrac{nT+(n-1)S}{2n-1}$,
$$\lim_{t\to\infty} \xi(t,x^0) = \begin{cases} g^3(x^0) & \dfrac{x^0_C}{x^0_T} \leq \dfrac{R-S}{T-R} \\ g^2(x^0) & \dfrac{x^0_C}{x^0_T} > \dfrac{R-S}{T-R} \end{cases}, \tag{6}$$
and the corresponding phase orbits consist of straight lines passing through s_{ST};
- *if* $R > \dfrac{nT+(n-1)S}{2n-1}$,
$$\exists x^* \in \Phi^{2n} \cup \{x^1\} : \lim_{t\to\infty} \xi(t,x^0) = x^* \tag{7}$$
and
$$x^0 \in \text{int}(\Delta - \mathscr{D}) \quad \Rightarrow \quad \lim_{t\to\infty} \xi(t,x^0) = x^1 \tag{8}$$

where x^2, s_T and x^1 are equilibrium points, Φ^{2n} is a set of equilibria, g^3 and g^2 are functions and

$$\mathscr{D} = \{x \,|\, x \in \Delta,\ (T-R)x_C + (\lceil \tfrac{m}{2} \rceil T + \lfloor \tfrac{m}{2} \rfloor S - mR)x_T \leq 0\}.$$

References

[1] J. W. Weibull, *Evolutionary Game Theory*. Boston: MIT press, 1997.

Local mean field analysis of the linear threshold model

Wilbert Samuel Rossi
Department of Applied Mathematics
University of Twente; 7522 NB Enschede, The Netherlands
w.s.rossi@utwente.nl

Giacomo Como
Department of Automatic Control
Lund University; 22363 Lund, Sweden
giacomo.como@control.lth.se

Fabio Fagnani
Department of Mathematical Sciences
Politecnico di Torino; 10129, Torino, Italy
fabio.fagnani@polito.it

1 The Linear Threshold Model

The spread of new behaviors may exhibit cascading effects in social, economic and technological networks [1]. These phenomena generally depend on the topology of the network as well as on the nature of the local agents' dynamics. Here we consider the (unweighted) Linear Threshold Model (LTM) on directed random graphs, of which we wish to approximate the dynamic and identify control heuristics.

The LTM is an activation process with neighborhood effects. Consider a directed graph $G=(V,E)$ of finite size n where each agent $v\in V$ has *out*-degree d_v and *in*-degree k_v. To each agent is associated a sequence of integer parameters $r_v[t]$ called *activation thresholds*, with $0\le r_v\le d_v+1$. Agents are endowed with binary states $x_v[t]\in\{0,1\}$ meaning $\{\text{inactive},\text{active}\}$ respectively. A direct link $(v,w)\in E$ means that v can access the state of its *out*-neighbor w. In the LTM dynamics agents activate if the number of active *out*-neighbors is at least as their current activation threshold, otherwise they deactivate.

$$x_v[t+1]=\begin{cases}1 & \text{if} \quad \sum_{w:(v,w)\in E} x_w[t]\ge r_v[t]\\ 0 & \text{otherwise}\end{cases} \tag{1}$$

The local deterministic rule (1) is applied synchronously by all the agents, that can switch state multiple time.

2 Analysis on Large Networks

We analyze the LTM on the directed configuration model, a large directed random network with heterogeneous agents [3]. Our aim is to describe the evolution of fraction of active agents $a[t]=n^{-1}\sum_{v\in V}x_v[t]$.

The graph ensemble is described by the fraction of nodes with given *out*/*in*-degrees, $p_{d,k}=n^{-1}\,|\{v\in V: d_v=d, k_v=k\}|$ and by the conditional statistics about the thresholds at time t: $p_{r|d,k}[t]=(n\,p_{d,k})^{-1}\,|\{v\in V: d_v=d, k_v=k, r_v[t]=r\}|$. A random permutation gives the specific wiring of the graph [4, p. 70]. This network is locally a tree: starting from a node, for depths of order $\log n$ the neighborhood is a tree with high probability. Such property allows to approximate efficiently $a[t]$ with a sequence $\nu[t]$ representing high probability predictions of the behavior of the fraction of active agents. The sequence $\nu[t]$ is the output of the *local mean field dynamic* (LMF-Dyn), the following discrete-time system with scalar state $\mu[t]$[1]:

$$\begin{array}{ll}\mu[t+1] & =\sum_{d,k,r}\frac{k\,p_{d,k}}{\bar{k}}\,p_{r|d,k}[t]\,f_{d,r}(\mu[t])\\ \nu[t+1] & =\sum_{d,k,r}p_{d,k}\,p_{r|d,k}[t]\,f_{d,r}(\mu[t])\end{array} \tag{2}$$

where $f_{d,r}(x)=\mathbb{P}\,(\mathrm{Bin}(d,x)\ge r)=\sum_{i=r}^{d}\binom{d}{i}x^i(1-x)^{d-i}$, $\bar{k}$ is the average *in*-degree and the initial conditions are $\nu[0]=a[0]$ and $\nu[0]=|E|^{-1}\sum_{v\in V}k_v\,x_v[0]$. The system (2) describes the expected activation process on an infinite tree with the same statistical properties of the original graph and hence is exact on for infinite networks. For finite networks we proved a concentration theorem: the activation process on a generic instance random graph is close to the LMF-Dyn with probability converging to one exponentially fast in the network size.

3 Control and Conclusions

Remarkably, the LMF-Dyn and the concentration theorem hold for variable thresholds too, making the approach amendable to the design of control strategies. Currently we are working on heuristics to address an optimal control problem when thresholds can be increased of one unit. Some results can be extended to the permanent activation model on directed and undirected random networks [5].

References

[1] D. Easley and J. Kleinberg, *Networks, Crowds, and Markets: Reasoning About a Highly Connected World*, Cambridge University Press, 2010.

[2] E.M. Adam, M.A. Dahleh and A. Ozdaglar, *On the behavior of threshold models over finite networks*, 51st IEEE Conference on Decision and Control, pp 2672-2677, 2012.

[3] H. Amini, R. Cont and A. Minca, Resilience to Contagion in Financial Networks, in *Mathematical finance*, 2013.

[4] R. Durrett, *Random Graph Dynamics* , Cambridge UP, 2006.

[5] H. Amini, M. Draief and M. Lelarge, *Marketing in a Random Network*, in Net. Control & Optim., pp 17-25, 2009.

[1] Due to space limitations, we skip the precise $\mu[t]$ and $\nu[t]$ definitions.

New Applications of Tensors to Graphs

Paul Smyth[1]
paul.smyth@esat.kuleuven.be

Johan Suykens[1]
johan.suykens@esat.kuleuven.be

Lieven De Lathauwer[1,2]
lieven.delathauwer@kuleuven-kulak.be

[1]KU Leuven, Department of Electrical Engineering (ESAT),
STADIUS Center for Dynamical Systems, Signal Processing and Data Analytics,
and iMinds Medical IT,
Kasteelpark Arenberg 10 box 2446, 3001 Leuven, Belgium

[2]KU Leuven - Kulak - Group Science, Engineering and Technology,
E. Sabbelaan 53, 8500 Kortrijk, Belgium

1 Abstract

Networks are ubiquitous. From physical systems such as energy and transport networks, biological networks of metabolic pathways and gene regulation, to online social and information networks. This small snapshot of an ever-growing list shows the far-reaching applications of network theory [1, 2]. The mathematical description of networks, or graphs, has a long history dating back to Euler's study of the bridges of Königsberg in the 18th century. The classical approach to studying a graph is to encode the connections between its vertices in a matrix. In the simplest case, each vertex is assigned a row and a column in a symmetric matrix, the *adjacency matrix*. An entry of the adjacency matrix is non-zero when the two corresponding vertices are connected. This elegant and powerful mathematical translation of the graph structure has led to many remarkable insights.

In the modern era the classical matrix approach to networks starts to show its limitations. For instance, one might want to consider a network of webpages by studying both which pages are connected and via what hyperlinks [3] i.e. a latent semantic analysis of the World Wide Web. Other examples are time-evolving networks or situations where one needs to consider different kinds of connections, such as the different levels of interaction in a social network that exists between friends, family and colleagues. The natural language with which to consider these more general questions uses tensors - multilinear extensions of matrices (see [4, 5, 6] and references therein). A 3rd order tensor can be used to capture information in a graph that is changing in time, for example, whereby the tensor is a time-evolved adjacency matrix. Here each frontal slice of the tensor is the adjacency matrix of the graph a fixed point in time.

In this talk, we will consider a different application of tensors to graphs. Rather than using tensors to capture the different 'levels' of a network or time-evolution, we shall use the higher-order nature of tensors to capture higher-order information about connections between vertices in the graph. As a concrete example, we shall describe a particular tensorization of the adjacency matrix which captures connections between triples of vertices. Such a shape is called a *3-clique* in network theory and is known to play an important role in identifying communities, or clusters, of vertices. We shall describe how the tensor capturing the 3-cliques in a graph can be used to identify clusters in real networks and then discuss further possible tensorizations which could have interesting future applications.

References

[1] M. E. J. Newman. The structure and function of complex networks. *SIAM review*, 45(2):167–256, 2003.

[2] M. E. J. Newman. *Networks: an introduction*. Oxford University Press, 2010.

[3] T. G. Kolda, B. W. Bader, and J. P. Kenny. Higher-order web link analysis using multilinear algebra. In *Data Mining, Fifth IEEE International Conference on*, pages 8–pp. IEEE, 2005.

[4] S. Boccaletti, G. Bianconi, R. Criado, C.I. Del Genio, J. Gómez-Gardeñes, M Romance, I Sendiña-Nadal, Z Wang, and M Zanin. The structure and dynamics of multilayer networks. *Physics Reports*, 544(1):1–122, 2014.

[5] T. G. Kolda and B. W. Bader. Tensor decompositions and applications. *SIAM review*, 51(3):455–500, 2009.

[6] A. Cichocki, D. Mandic, A.H. Phan, C. Caiafa, G. Zhou, Q. Zhao, and L. De Lathauwer. Tensor decompositions for signal processing applications from two-way to multiway component analysis. *Accepted for publication in IEEE Signal Processing Magazine*, March 2015.

Iterative Feedforward Control with Application to a Wafer Stage

Lennart Blanken[1], Frank Boeren[1], Dennis Bruijnen[2], Tom Oomen[1]
[1]Eindhoven University of Technology, Dept. of Mechanical Engineering, Control Systems Technology, The Netherlands
[2]Philips Innovation Services, Mechatronics Technologies, Eindhoven, The Netherlands
l.l.g.blanken@student.tue.nl

Introduction

Feedforward control enables high performance in industrial motion systems. The key performance enhancement is in general obtained by using feedforward with respect to the reference trajectory. In existing methods, typically a trade-off exists between the attainable performance and the required robustness to changes in the reference. Through new developments in feedforward control it is aimed to attain high performance for a class of reference signals.

Iterative feedforward control with a rational basis

Iterative feedforward control can attain high performance for a class of reference signals [1]. To achieve this, measured data from previous tasks is exploited in conjunction with a suitable parametrization for the feedforward controller $C_{ff}(\theta)$. The need for an approximate model of the system, as is common in ILC [2], is eliminated by formulating the approach as an instrumental variable-based estimation problem as in [3]. The corresponding control configuration is depicted in Fig. 1. The parameters θ^{j+1} in the $(j+1)^{\text{th}}$ task result from an optimization problem based on measured data from the j^{th} task.

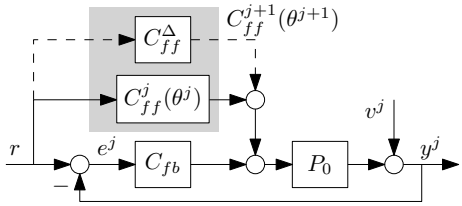

Figure 1: Control configuration for iterative feedforward control.

Existing approaches focus on a polynomial parametrization of C_{ff}, see e.g. [1], [4]. However, in [2] it is shown that for a rational system P_0, a rational parametrization is required for C_{ff} to attain high performance for a class of reference signals. The present research aims to introduce such a parametrization in iterative feedforward control using system identification techniques.

A system identification approach to iterative feedforward control

The present research consists of three main aspects. First, a framework is presented for iterative feedforward control with a rational parametrization. This approach is based on instrumental variables, as in [3], [5]. Second, the limits of accuracy are investigated and an iterative algorithm is proposed that obtains parameter estimates θ^{j+1} with optimal accuracy in terms of variance. Third, an experimental validation of the proposed methodology is presented.

Experimental results

The proposed approach is implemented on a wafer stage. The experimental results in Fig. 2 and 3 illustrate that superior servo performance is achieved with the proposed rational parametrization for C_{ff}.

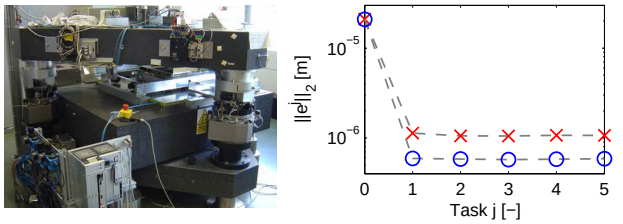

Figure 2: Wafer stage (left) and experimental results (right): superior performance is achieved with a rational parametrization (○) compared to a polynomial parametrization (×).

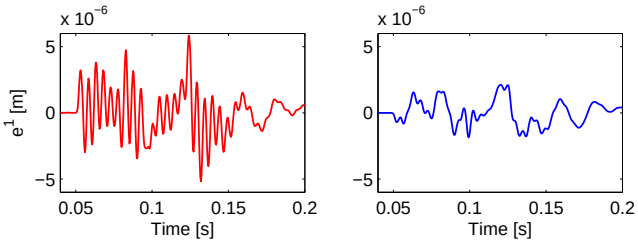

Figure 3: Time domain plot of measured error signal e^1 in the first task. Left: polynomial parametrization, right: rational parametrization.

Ongoing research

Current work is aimed at generalizing the proposed approach to multivariable systems, extensions to position-dependent behavior, and trajectory design.

References

[1] S. van der Meulen and R. Tousain and O. Bosgra, Fixed Structure Feedforward Controller Design exploiting Iterative Trials: Application to a Wafer Stage and a Desktop Printer, *Journal of Dynamic Systems, Measurement, and Control*, 130(5):0510061-05100616, 2008.

[2] J. Bolder and T. Oomen, Rational basis functions in iterative learning control - With experimental verification on a motion system, *IEEE Transactions on Control Systems Technology*, 23(22):722-729, 2015.

[3] T. Söderström and P. Stoica, Instrumental Variable Methods for System Identification, ser. LNCIS, vol. 57, Springer-Verlag, Germany, Berlin, 1983.

[4] F. Boeren, and T. Oomen and M. Steinbuch, Iterative motion feedforward tuning: A data-driven approach based on instrumental variable identification, *Control Engineering Practice*, vol. 37, 11-19, 2015.

[5] M. Gilson, H. Garnier, P. Young and P. Van den Hof, Optimal instrumental variable method for closed-loop identification. *IET Control Theory & Applications*, 5(10):1147-1154, 2011.

This research is supported by Philips Innovation Services.

Hybrid Potential Bacterial Foraging Optimization Algorithm with Robot Swarm Obstacle Avoidance

Thoa Mac Thi[1,2], Cosmin Copot[1], Robin De Keyser [1], and Trung Tran Duc [2]

[1]Department of Electrical energy Systems and Automation, Ghent University, Sint-Pietersnieuwstraat 41, B-9000 Gent, Belgium.
[2]School of Mechanical Engineering, Hanoi University of Science and Technology, Dai Co Viet street 1, Hanoi Vietnam.
{Thoa.MacThi,Cosmin.Copot,Robain.DeKeyser}@UGent.be and Trung.tranduc@hust.edu.vn

1 Introduction

Bacterial foraging optimization is a heuristic algorithm inspired from foraging behavior based on swarm algorithms which have been successfully applied for optimization problems and robot swarm navigation [1]. A robot swarm is simply a group of robots that move in some cohesive way in order to perform some tasks. In moving from one position to another, robots must avoid certain obstacles that appear in their workspace. In this paper, we consider the hybrid potential bacterial foraging method to find the optimal path for cooperative robot swarm. To solve this problem, the obstacle and goal functions are combined into a cost function. The swarm of robots is engaged in a social foraging by cost functions, which are viewed as a nutrient profile. The basic foraging strategy is made adaptive through a potential scheme in order to find the global optimal solution.

2 Hybrid potential bacterial foraging optimization.

In the basic bacterial foraging, the robot is represented as an object under the influence of a potential field U, which is the cost function defined as:

$$U = U_{att} + U_{rep} \tag{1}$$

The attraction U_{att} influence tends to pull the robot toward the target position, while the repulsion U_{rep} tends to push the robot away from the obstacles. In the applied hybrid potential bacterial foraging method, we modify the cost function in order to avoid trap situations due to local minimum solutions. We propose the following attraction and repulsion potential formulas:

$$U_{att} = \left\{ \begin{array}{ll} \beta_1 |\xi - \xi_a|^2, & d \leq d_0 \\ \beta_2 |\xi - \xi_a|^2, & d \geq d_0 \end{array} \right\} \tag{2}$$

$$U_{rep} = \eta \left\{ \sum_{i=1}^{n} max(exp(-\gamma(\xi - \xi_0)^2)) \right\} (\xi - \xi_a)^2 \tag{3}$$

where: η, β_1,β_2, γ are adjustment constants, n is the number of obstacles, ξ is the current position of the robot, ξ_a is the position of the end point, $d = |\xi - \xi_0|$, ξ_0 is the obstacle position, d_0 is the influence distance of the attraction force.

3 Simulations

To test the efficiency of the proposed method, different simulations are conducted in Matlab. The number of robots in swarm is 10, each robot has its own initial position nearby the start point (5,5). Their task is to find the optimal path to the target point (30,30) and avoid all obstacles which appear on their way. Robot to robot interactions considered are of the "attract-repel" type. The simulation on Figure 1 (left side) shows that every agent in swarm can perform a successful navigation and that the trajectories of the robot swarm converge to the optimal path. Figure 1 (right side) describes the position of each agent in the x direction and y direction.

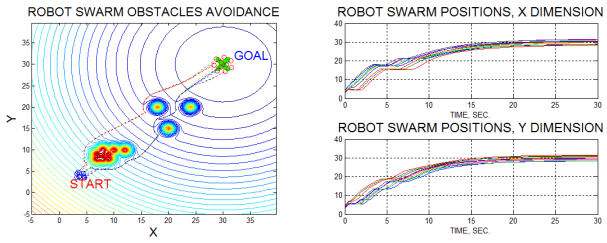

Figure 1: Robot Swarm Obstacle Avoidance

4 Conclusion

This research presents a new algorithm for cooperative robot swarm obstacle avoidance. A combination of the potential method and bacterial foraging is applied to determine the shortest feasible path to move from the current position to the target in an environment with a number of obstacles.

References

[1] M.A.Hossain, I.Ferdous, Autonomous robot path planning in dynamic environment using a new optimization technique inspired by bacterial foraging technique, 64 (2015) 137-141, Robotics and Autonomous Systems.

An experimental comparison of control architectures for bilateral teleoperation

Ruud Beerens[1], Dennis Heck[2], Henk Nijmeijer[3]
Dynamics and Control
Eindhoven University of Technology
P.O. Box 513, 5600 MB Eindhoven
the Netherlands
[1]r.beerens@student.tue.nl
{ [2]d.j.f.heck, [3]h.nijmeijer } @tue.nl

1 Introduction

Many different control strategies for bilateral teleoperation under the influence of communication delays have been proposed as described in e.g. [1]. Despite several (scattered) theoretical and experimental studies, a clear comparison of different controllers on a wide range of performance metrics is missing. Related to remote handling applications in nuclear fusion reactors, we present the development of a comparative analysis, including clear representative performance metrics, and focus on several architectures that range from motion synchronization to a combination of motion and explicit force control.

2 Experiments

Four of the selected eight control architectures are: PD-control, wave variable control (W), four-channel control (4C) and four-channel control with wave variables (4CW). Two series of experiments on a one degree of freedom teleoperation setup are designed to test and compare these architectures on motion synchronization, physical operator load, force reflection and stiffness perception. The first series consists of experiments where the system's performance in free motion is investigated. To achieve consistency in the results, a modelled operator is used to eliminate inter-experimental variations caused by a real operator. This model includes an "operator-intended trajectory" that encompasses a realistic range of frequencies of a human input. The second series consists of experiments where the slave is in contact with a stiff environment. Here, an operator torque profile is recorded from the experimental setup, which is played back on the master device during each in-contact experiment.

For both series of experiments, the controllers are first evaluated for situations with zero delay, from which the results can be interpreted as benchmarks. Subsequently, the experiments are performed for increasing values of the communication delay. Based on existing theoretical stability results, damping is injected accordingly where needed to guarantee stability for the specific delay value.

3 Results

A small selection of the results, namely position tracking and stiffness reflection, is presented in Figure 1. A lower value of the metric indicates better performance. Our main conclusions are that the use of force sensors, especially at the slave side, is beneficial for force reflection and stiffness perception, especially for large values of the communication delay. For delays up to 10 ms, a 4C controller performs best in terms of position tracking and stiffness perception. For larger delays, using wave variables in combination with a 4C architecture (4CW) results in the best overall performance. For large values of the delay, position-based architectures are not recommended due to poor motion tracking and high operator effort.

References

[1] P.F. Hokayem, M.W. Spong, "Bilateral teleoperation: a historical survey", in *Automatica*. vol. 42, pp. 2035-2057, 2006

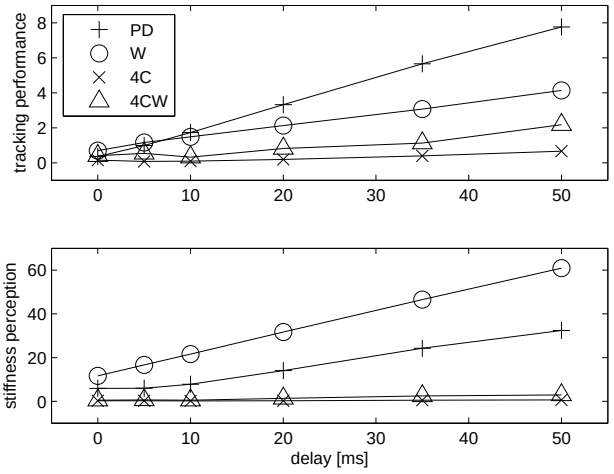

Figure 1: RMS values indicating tracking performance and stiffness perception for a selection of control architectures.

A waterbed effect in disturbance feedforward control with application to a vibration isolator

M.A. Beijen, M.F. Heertjes, H. Butler and M. Steinbuch
Eindhoven University of Technology, PO Box 513, 5600 MB Eindhoven (NL), E-mail: M.A.Beijen@tue.nl

1 Introduction

Disturbance feedforward control (DFC) is used in many applications, such as active noise/vibration control and stage synchronization [1]. In this paper, which summarizes our work in [2], DFC is implemented on an active vibration isolator to demonstrate the waterbed effect that exists for DFC systems.

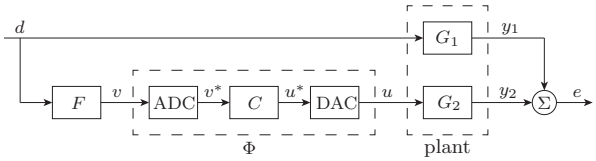

Figure 1: General block scheme configuration for a DFC system.

The general block scheme for DFC in Figure 1 shows an input disturbance d transmitted through a primary path G_1 leading to output y_1. A secondary path from d to y_2 is formed by sensor filter F, an analog-to-digital converter (ADC), digital feedforward controller C, a digital-to-analog converter (DAC) and plant dynamics G_2. The error $e = y_1 + y_2$ should ideally be zero for maximum disturbance rejection. However, performance is shown to be limited by sensor dynamics and filtering, sampling delays and non-perfect plant inversion in the controller design.

2 The waterbed effect

Performance of DFC systems is limited by the feedforward sensitivity integral [1]:

$$\int_0^\infty \log|S_{ff}(j\omega)|\, d\omega = \pi \sum_i \{z_i\}, \qquad (1)$$

in which z_i are the right-half-plane zeros of the feedforward sensitivity function S_{ff}, defined as

$$S_{ff}(s) = G_1(s) - G_2(s)\Phi(s)F(s), \qquad (2)$$

and with describing function Φ representing the behavior of $\mathcal{H}$, C and $\mathcal{S}$ as an LTI system in the Laplace domain. The RHP zeros in S_{ff} have the same role as the RHP poles in the Bode sensitivity integral for feedback systems. Note that (1) only holds in case S_{ff} has two more poles than zeros, a property that is easily satisfied for mechanical systems. In view of (1), DFC systems have the performance properties of a feedback system, but the stability properties of a feedforward control system. The latter follows from the fact that the poles of the plant G_1, G_2 are not affected by C, thus destabilizing the loop by controller C is not possible.

3 Results and Conclusions

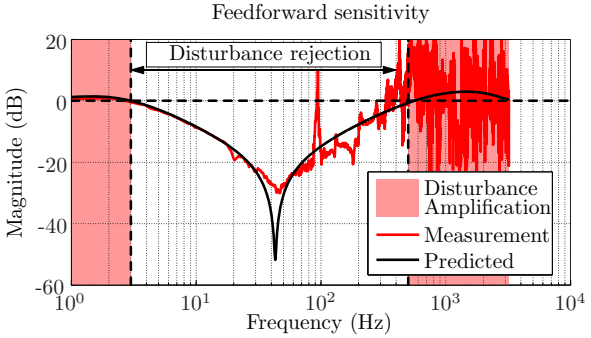

Figure 2: Predicted and measured disturbance rejection on an active vibration isolator [3]. The plots are shown up to the Nyquist frequency (3.2 kHz).

To demonstrate the waterbed effect, DFC is added to an active vibration isolator [3] to suppress platform motions due to floor vibrations. Figure 2 shows the predicted and measured S_{ff}. For the predicted S_{ff}, the behavior of the ADC and DAC is modeled as a half-sample time-delay, $C = G_2^{-1}G_1$, and F is a band-pass filter with frequency band 2-3000 Hz plus a low-pass filter at 800 Hz. The measured S_{ff} is obtained by exciting the vibration isolator in vertical direction and applying DFC using a 6.4 kHz sampling frequency.

Both the predicted and experimental results illustrate the waterbed effect, in the sense that disturbance rejection at mid-frequencies leads to amplification at low and high frequencies. Further research focuses on developing a feedforward loop shaping method, taking into account the trade-off imposed by the waterbed effect.

4 Acknowledgement

The authors gratefully acknowledge the Mechanical Automation and Mechatronics group at the University of Twente for facilitating the experimental setup.

References

[1] M.F. Heertjes et al., *Self-tuning in master-slave synchronization of high-precision stage systems*. Control Engineering Practice, vol. 21, no. 12, 2013.

[2] M.A. Beijen et al., *Performance trade-offs in disturbance feedforward compensation systems with application to an active hard mount vibration isolator*. Submitted to *the American Control Conference (2015)*, Chicago, Illinois.

[3] D. Tjepkema, *Active hard mount vibration isolation for precision equipment*, PhD thesis, University of Twente, Enschede, The Netherlands, 2012.

Iterative Learning Control for Varying Tasks

Jurgen van Zundert[1], Joost Bolder[1], Sjirk Koekebakker[2], Tom Oomen[1]
[1]Eindhoven University of Technology, Department of Mechanical Engineering, Control Systems Technology group, The Netherlands
[2]Océ Technologies, P.O. Box 101, 5900 MA Venlo, The Netherlands

1 Background

Iterative Learning Control (ILC) [1] can significantly enhance the performance of systems that perform repeating tasks. However, small variations in the task often lead to a large performance deterioration. This leads to a trade-off between high performance and extrapolation properties, i.e., the ability to cope with reference variations. The goal of this research is to improve this trade-off in ILC.

2 Iterative Learning Control

Consider the control setup in Figure 1 with trial number j. Given old measurement data e_j, f_j, the goal in ILC is to determine f_{j+1} such that $J_{j+1} = \|e_{j+1}\|_2^2$ is minimized.

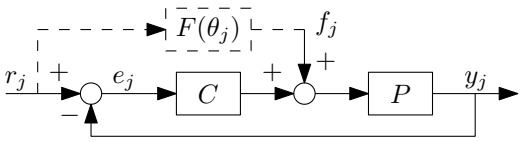

Figure 1: Control setup: the goal is to minimize error e_j by iteratively updating feedforward f_j.

ILC is known to achieve excellent performance for systems operating repetitively ($r_j = r, \forall j$). However, for varying reference signals there is significant performance deterioration.

3 Basis functions

To enhance extrapolation properties, ILC is extended with basis functions by using $f_j = F(\theta_j)r$, with $F(\theta_j)$ a parameterized filter. Examples include polynomial basis functions [2] of the form $F(\theta_j) = A(\theta_j)$ and more recently rational basis functions [4] of the form $F(\theta_j) = \frac{A(\theta_j)}{B(\theta_j)}$, where $A(\theta_j), B(\theta_j)$ are affine.

An analytic solution to the optimization problem is available for polynomial basis functions and rational basis functions with fixed poles. However, this requires a careful selection of poles and typically limits the achievable performance. In this work [3], rational basis functions are proposed where both poles and zeros are not pre-specified but optimized. In pre-existing work [4] an iterative approach based on Steiglitz-McBride identification is presented, which from related system identification algorithms is known to generally yield non-optimal results. The new approach, which has strong connections to instrumental variable system identification, does yield optimal results in the sense that it converges to a minimum [5]. The solution takes the standard ILC form $\theta_{j+1}^{\langle q \rangle *} = Q^{\langle q \rangle} f_j + L^{\langle q \rangle} e_j$, with $Q^{\langle q \rangle}, L^{\langle q \rangle}$ based on approximate models of C and P.

4 Simulations

Simulations with various ILC approaches for the y-direction of the printing system in Figure 2 are executed. The reference signal is varied over the trials: r^a is active at trial $j = 0,1,2$, r^b at $j = 3,4,5$, and r^c at $j = 6,7,8$. The results are shown in Figure 3. The figure indicates that the performance of standard ILC deteriorates significantly after a change in reference signal, whereas the influence on the performance of ILC with basis functions is negligible. The results also indicate the enhanced performance of ILC with rational basis functions using the proposed approach compared to the pre-existing approach.

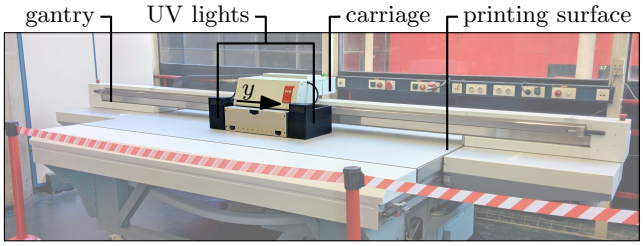

Figure 2: Océ Arizona 550 GT at TU/e CST Motion Lab.

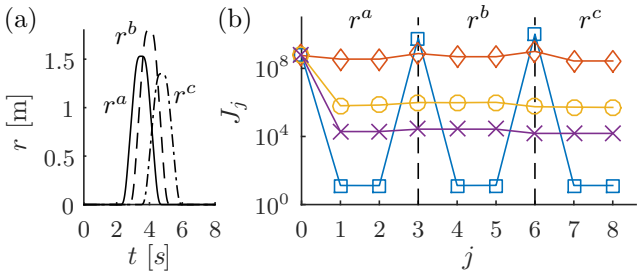

Figure 3: (a) trial varying reference signal; (b) performance criterion J_j for standard ILC (□), polynomial basis functions (◇), and rational basis functions using the pre-existing approach (○) and proposed approach (×).

References

[1] D. A. Bristow, M. Tharayil, and A. G. Alleyne, "A Survey of Iterative Learning Control - a learning-based method for high-performance tracking control," *Control Systems, IEEE*, vol. 26, no. 3, pp. 96-114, 2006.

[2] J. van de Wijdeven and O. Bosgra, "Using basis functions in iterative learning control: analysis and design theory," *International Journal of Control*, vol. 83, no. 4, pp. 661-675, 2010.

[3] Jurgen van Zundert, Joost Bolder, and Tom Oomen. "Iterative learning control for varying tasks: Achieving optimality for rational basis", *In Proceedings of the 2015 American Control Conference*, 2015.

[4] Joost Bolder and Tom Oomen, "Rational Basis Functions in Iterative Learning Control - With Experimental Verification on a Motion System," *IEEE Transactions on Control Systems Technology*, vol. 23, no. 2, pp. 722-729, 2014.

[5] Marion Gilson, Hugues Garnier, Peter Young, Paul Van den Hof. "Optimal instrumental variable method for closed-loop identification," *IET Control Theory and Application*, 2011, vol. 5, no. 10, pp. 1147-1154, 2011.

Woofer-tweeter adaptive optics for EUV lithography

Michel Habets[1], Ruben Merks[1,2], Siep Weiland[1], Wim Coene[1,2]
[1]Department of Electrical Engineering, Eindhoven University of Technology
P.O. Box 513, 5600 MB Eindhoven, The Netherlands
[2]ASML Netherlands B.V., De Run 6501, 5504 DR Veldhoven
P.O. Box 324, 5500 AH Veldhoven, The Netherlands
Email: m.b.i.habets@tue.nl

1 Mirror heating in EUV lithography

In EUV lithography, light with a wavelength of 13.5 [nm] is used. EUV light is primarily being absorbed by: (1) the illuminator (2) the reticle and (3) the so-called projection optics box (POB). Coupled to the roadmap for EUV lithography, the EUV source power will increase in order to enable higher wafer throughputs. The POB consists of six mirrors, by which the light is reflected and focused. The mirrors are heated by the absorption of the EUV light during normal use of the scanner, leading to thermally induced deformations.

The criterion which is often used for the maximum allowable rms wavefront error (rms-WFE) in lithography is $\lambda/20 = 0.675$ [nm] [1]. In order to meet this requirement for the heated POB we adopt a wavefront correction strategy that mitigates the thermally induced wavefront aberrations.

2 Multiphysics mirror heating model

We simulate the decrease in imaging performance with a fully coupled opto-thermo-mechanical model of the POB. The heat load on each mirror is dominated by diffraction of the structures on the mask and by the illumination settings. Using diffraction physics and geometrical optics the heat load on each mirror is determined. The thermo-mechanical behavior of the mirrors is modeled using FEM. The resulting optical aberrations are determined by means of ray tracing.

3 Wavefront correction

To reduce the optical aberrations caused by mirror heating we employ adaptive optics for EUV lithography. Adaptive optics is a well-established technology that is being used in: astronomy, vision science and microscopy to reduce the impact of optical aberrations. The three main components of any adaptive optics system are: a wavefront sensor to measure distortion, a deformable mirror to compensate for the distortion and a control system to calculate the required correction to apply to the deformable mirror.

We make use of a so-called woofer-tweeter configuration. The low frequency distortions are corrected by alignment of the mirrors, reticle and wafer using their individual 6 DOF (woofer). A piezoelectric deformable mirror is included into the optical path to correct for the high frequency distortions (tweeter).

4 Results

We have used the 6-mirror POB of [2], the closed-loop simulation results for a Y-dipole illumination profile are shown in Figure 1. The rms-WFE of the cold system (a) refers to the intrinsic aberrations of the POB. The hot system (b) has a 5 times larger rms-WFE. Figures (c) and (d) show the rms-WFE after the woofer, respectively the woofer+tweeter have been enabled.

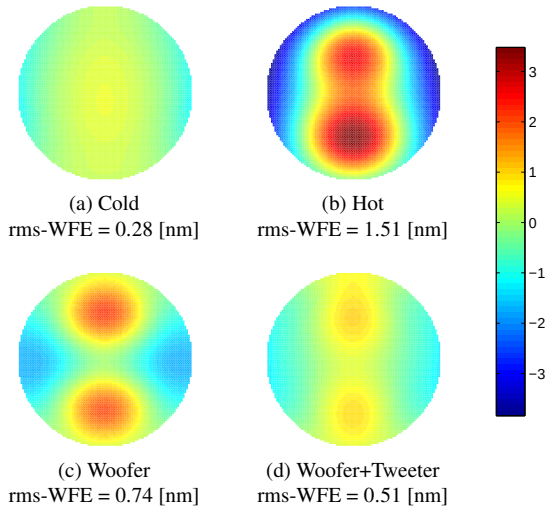

(a) Cold
rms-WFE = 0.28 [nm]

(b) Hot
rms-WFE = 1.51 [nm]

(c) Woofer
rms-WFE = 0.74 [nm]

(d) Woofer+Tweeter
rms-WFE = 0.51 [nm]

Figure 1: WFE for one field point in [nm]

References

[1] R. Saathof, "Adaptive optics to counteract thermal aberrations: System design for euv-lithography with sub-nm precision," Ph.D. dissertation, Delft University of Technology, 2013.

[2] R. Hudyma, "High numerical aperture ring field projection system for extreme ultraviolet lithography," U.S. Patent 6 033 079, Mar. 7, 2000.

RF identification and filter synthesis: a happy marriage?

Evi Van Nechel Yves Rolain
Evi.Van.Nechel@vub.ac.be Yves.Rolain@vub.ac.be
Vrije Universiteit Brussel

1 State of the art

Currently, filters at RF frequencies are designed using brute force optimization. The drawback hereof is the lack of physical insight in and sensitivity knowledge about the obtained design. On the other hand, classical filter synthesis methods [1] fall short to accurately realize the transmission line based filters that are needed at RF frequencies.

In this work, we will try to bridge the gap between these approaches. We propose a two-step procedure. First, a geometry dependent model set for an elementary transmission line structure is identified. This model allows for an improved realization of the filter. In a second phase, the model structure is incorporated in the approximation of the filter template. Hence, the filter synthesis becomes technology aware.

2 A test case: the defective ground plane resonator filter

In a first phase, a demonstrator of the framework is aimed at. We select the defective ground plane resonator filter as an example because it is straightforward to slice it in elementary sections. Such a section is shown in Figure 1.

Figure 1: Elementary section of a defective ground plane resonator filter. Left: cross-section. Right: top-view.

In the identification phase, we seek a scalable model for this section, based on electromagnetic (EM) simulations. The goal of this modeling is two-fold. On the one hand, it provides for a simulation model that is cheap to evaluate. On the other hand, it enables to obtain physical insight in the operation of the elementary section. This is crucial to determine the class of rational approximants describing the set of realizable resonators. Remember that this is the knowledge we want to feedback to the initial rational approximation process.

To ease this understanding, we propose to extract a lumped-element equivalent circuit model for the elementary section. To this end, the topology proposed in the literature [2] is extended to improve the model accuracy. First, an equivalent circuit is extracted to model the first resonance of the slot (Figure 2). The same topology can be used to model the harmonics. In order to obtain a wideband model, these structures at different resonances are simply cascaded.

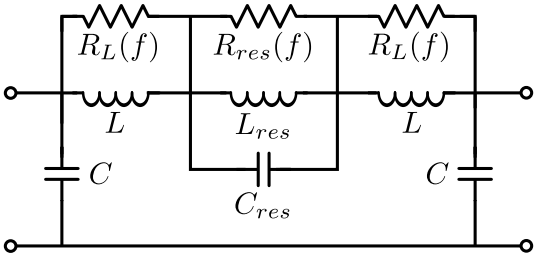

Figure 2: Equivalent circuit for one slot resonance.

The model is very accurate at the excited resonances (error at -35 dB). Therefore, the estimated model is usable in a design context. At the non-excited resonances, however, the model is less accurate (error at -20 dB). To deliver a first-time-right realization, it is clear that the model needs some fine-tuning at the non-excited resonances.

3 Conclusion

A first step is taken in the identification-aware synthesis of microwave filters. A proof of concept is started for defective ground plane structures. Initial results show the potential of the proposed approach.

Acknowledgments: This work was supported in part by FWO-Vlaanderen, the Methusalem grant of the Flemish Government (METH-1), the Belgian Government through the Inter university Poles of Attraction IAP VII/19 DYSCO program, and the ERC advanced grant SNLSID, under contract 320378.

References

[1] J. C. Richard, M. K. Chandra, and R. M. Raafat, *"Microwave filters for communication systems: Fundamentals, Design, and Applications"*, John Wiley & Sons, 2007

[2] C. Caloz, H. Okabe, T. Iwai, and T. Itoh, *"A simple and accurate model for microstrip structures with slotted ground plane"*, IEEE MWCL, Vol 14, No.4, pp. 133-135, April 2004

Tensor-based reduced order adjoints for water flooding optimization

Edwin Insuasty
Eindhoven University of Technology
e.g.insuasty.moreno@tue.nl

Paul Van den Hof
Eindhoven University of Technology
p.m.j.vandenhof@tue.nl

Siep Weiland
Eindhoven University of Technology
s.weiland@tue.nl

Jan Dirk Jansen
Delft University of Technology
j.d.jansen@tudelft.nl

1 Introduction

Large-scale models for oil reservoirs are at the core of current methods for reservoir management. These model-based techniques aim to counteract the effects of subsurface uncertainty on production, by applying a systematic approach consisting of the use of state and parameter estimation, prediction and economic optimization. Reservoir models are simulated numerically, and the evaluation of any stage of the management scheme is a computationally expensive task, hence there is a potential to use reduced-order modeling for accelerating these procedures. In this work, we focus on reducing the computational complexity of economic optimization by using a tensor-oriented approach for reduced-order modeling.

2 Production optimization

The purpose of model-based production optimization is to determine a production strategy that maximize profits based on large-scale numerical models for the multi-phase flow through porous media. Traditionally, the financial measure used to describe performance along the life cycle of the reservoir is the Net Present Value (NPV), which, in a simplified form, is a measure of the net earnings of oil production minus the costs associated with water injection and production. The problem of maximizing NPV can be formulated as a dynamical optimization problem constrained by the models for multiphase flow. From an optimal control perspective, the adjoint system of equations can be derived from the conditions of optimality, and it can be used for the computation of a search direction to a local optimum [1]. A step evaluation of the optimization procedure is computationally expensive, as it requires one set of flow and adjoint simulations. The use of reduced-order models may therefore reduce the computational burden of performing water flooding optimization.

3 Tensor-based empirical projection spaces

Proper Orthogonal Decomposition (POD)-based techniques generate projection spaces from simulations data, and can be used for reducing the computational complexity of reservoir models [2]. In reservoir engineering, classical POD has not succeeded due to its inability to capture correlations from highly nonlinear dynamics, and the resulting reduced order models turned out to be either unstable or inaccurate. In this work, we exploit the spatial-temporal correlations from simulations by computing the projection spaces using tensor decompositions as presented in [3]. Snapshots of the oil saturation are stacked in multidimensional arrays and novel techniques for tensor decompositions are used to find tensor based empirical projection spaces [4].

4 Reduced order adjoints

Classical Galerkin projection of the flow and adjoint models onto tensor-based projection spaces is performed to obtain reduced-order models. Gradient-based optimal production strategies for water flooding are determined by using POD reduced-order models, as introduced by [5], and tensor-based reduced order models, as proposed in [3]. For the application case, the tensor strategy shows a better financial performance compared to the POD strategy and it is close to the optimal strategy for the full order model.

5 Acknowledgements

The authors acknowledge financial support from the Recovery Factory program sponsored by Shell Global Solutions International.

References

[1] J.D Jansen, O.H. Bosgra, and P.M.J. Van den Hof. Model-based control of multiphase flow in subsurface oil reservoirs. *Journal of Process Control*, 18(9), 846–855, 2008.

[2] R. Markovinovic, and J.D Jansen. Accelerating iterative solution methods using reduced-order models as solution predictors. *International Journal for Numerical Methods in Engineering*, 68(5), 525–541, 2006.

[3] E. Insuasty, P.M.J. Van den Hof, S. Weiland, and J.D. Jansen. Tensor-based reduced order modeling in reservoir engineering: An application to production optimization. *Submitted to the 2nd IFAC Workshop on Automatic Control in Offshore Oil and Gas Production.* Florianopolis, Brazil, 2015.

[4] H. Shekhawat, and S. Weiland. On the problem of low rank approximation of tensors. Groningen, The Netherlands, 2014.

[5] J.F.M. van Doren, R. Markovinovic, and J.D. Jansen. Reduced-order optimal control of water flooding using POD. *Computational Geosciences*, 10(1), 137–158, 2006.

Identifying a Multi-tapped Lossless Transmission Line

Maral Zyari Yves Rolain
Maral.Zyari@vub.ac.be Yves.Rolain@vub.ac.be
Vrije Universiteit Brussel

1 Introduction and Approach

The goal of this work is to model a transmission line that is tapped by lumped impedances, where only the input and the output of the lines are accessible as shown in Figure 1. Any discontinuity in the lines or mismatches in the impedances of the lines causes a reflection in the travelling waves. [1] This results in an impulse response that is a sum of delayed lumped responses.
The following model is introduced to model the mixed distributed-lumped nature of the system:

$$B(t) = \sum_{i=1}^{n_\tau} h_i(t-\tau_i) * A(t) \quad (1)$$

$$B(\omega) = \sum_{i=1}^{n_\tau} e^{-j\omega\tau_i} H_i(\omega) A(\omega) \quad (2)$$

Where n_τ is the number of the delays to be estimated, $B(t)$ and $A(t)$ are respectively output and input signals, τ_i represents the delay that each transmission line introduces and h_i is the damped exponential impulse response (Figure 1).

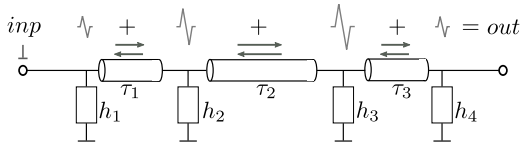

Figure 1: Cascade of transmission lines and lumped impedances where an impulse is applied to the system.

We identify both the discontinuities $h_i(t)$ in the transmission line and the delays τ_i.

2 Challenge

To be able to identify the introduced model, initial values are needed for the delays and the impulse responses in (1). Obtaining them is very hard as the estimator is nonlinear in the parameters, hence the optimization is non-convex.
To obtain the initial values, a linearized model is used. A sum of Cisoids is shown to be a good candidate. A Cisoid is a complex damped exponential. [1]
This linearized model yields the initial values for the delays that are used to start up the nonlinear least squares estimator.

3 Results and conclusion

As an application of a tapped line, an impedance tuner is measured and identified. The measured impulse response of the tuner is shown in Figure 2.
The impulse response is estimated with a common denominator rational model for $H_i(\omega)$. The order of the model is set to 2 for both numerator and the denominator. The number of delays to be estimated is 4. The initial delay values and coefficients of the rational model for $H_i(\omega)$ are provided by the Cisoids approach and plugged into the model. A least squares estimate is obtained next.

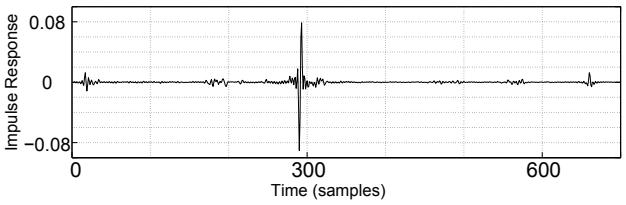

Figure 2: Measured impulse response of the system

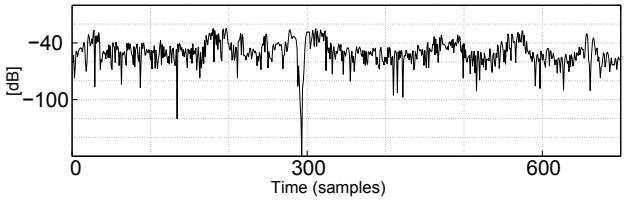

Figure 3: Relative estimation error in dB as a function of time

The difference between the estimated response and the measured data, is shown in Figure 3.
A multi-delay linear time-invariant model has been successfully identified for a tapped transmission line. The level of the error is below $-30\,dB$ at all t which proves the very good quality of the model as is shown in Figure 3.

Acknowledgments: This work was supported in part by the Fund for Scientific Research (FWO-Vlaanderen), the Methusalem grant of the Flemish Government (METH-1), by the Belgian Government through the Inter university Poles of Attraction IAP VII/19 DYSCO program, and the ERC advanced grant SNLSID, under contract 320378.

References

[1] Hugo Van Hamme, *High Resolution Frequency Domain Reflectometry by Estimation of Modulated Superimposed Complex Sinusoids*. IEEE Transactions on instrumentation and measurements, Vol 41, No.6 , Dec 1992

Two different approaches to dynamic modeling of hot-melt extrusion processes

J. Grimard, L. Dewasme, A. Vande Wouwer

Service d'Automatique, Université de Mons, Bd. Dolez 31, 7000 Mons - Belgique

jonathan.grimard@umons.ac.be, laurent.dewasme@umons.ac.be, alain.vandewouwer@umons.ac.be

1 Introduction

Industrial hot-melt extrusion processes are increasingly applied in the pharmaceutical field. While "classical" drug production processes require several combined methods (sifting, mixing, granulation, drying, ...) and the corresponding pieces of equipment to provide the final products, only one unit is required in drug delivery using hot-melt extrusion, in turn saving space, energy and reducing waste.

In this work, an extruder is modelled as a MIMO distributed parameter system (three inputs: screw rotation, feed flow rate and heat exchange energy / three outputs: filling ratio, pressure and temperature) in order to study and eventually improve product quality. A first approach to dynamic modeling consists in discretizing the extruder in tanks in series [1], [2], as it is done classically for tubular chemical reactors. A second appealing approach is the formulation of partial differential equation (PDE) systems, as for instance in [3] where a one-dimensional PDE system of the extrusion process is developed.

In this study, the two approaches are followed and compared, based on simulation codes written within the MATLAB environment.

2 Model derivation and numerical simulation

In both methods, a complete description of the extruder can be obtained applying mass, momentum, and energy balances. Mass balances allow the determination of the spatial material distribution while energy balances lead to the determination of the temperature field. Some simplifying assumptions allows the derivation of algebraic equations for the pressures in the system, depending on the material distribution.

In the tank-in-series approach [2], the extruder can be discretized using a certain number of tanks N, and forward and backward flow rates coexist between tanks. In the PDE model formulation, diffusive terms account for mass and heat diffusion. The advantage of the PDE formulation is that it uncouples the mathematical model derivation from the numerical method used to achieve the simulation. In this study, we use the method of lines with finite difference schemes (of adjustable accuracy) and ordinary differential equation solvers from the Matlab ODE suite. In the tank-in-series approach however the two issues are intrinsically linked, since the elementary tanks are equivalent to cells in a first-order finite volume method. The accuracy of the approach is therefore limited.

3 Preliminary results

Simulation results are computed for various inputs, including steps and multi-sines. Both models show comparable steady state results while dynamic responses to multi-sine signals show the low-order accuracy of the tanks-in-series approach. The PDE approach is definitely more flexible and accurate. Figure 1 shows a sample of these results.

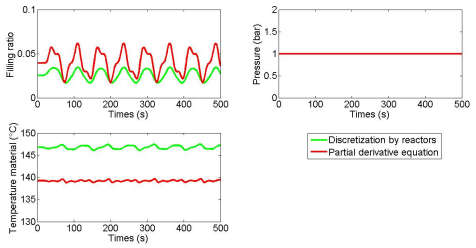

Figure 1: Dynamic responses of both models to a multi-sine input

4 Acknowledgments

The authors acknowledge the support of the WBgreen MYCOMELT project, achieved in collaboration with the University of Liege (ULg). The scientific responsibility rests with its author(s).

References

[1] K.J. Ganzeveld, J.E. Capel, D.J. Van Der Wal, and L.P.B.M. Janssen. The modelling of counter-rotating twin screw extruders as reactors for single-component reactions. Chemical Engineering Sciences, Volume 49, No 10, 1994, pages 1639-1649

[2] S. Choulak, F. Couenne, Y. Le Gorrec, C. Jallut, P. Cassagnau, A. Michel *Generic dynamic model for simulation and control of reactive extrusion*, Ind. Eng. Chem. Res., 43 (2004), pages 7373-7382

[3] C.H. Li. Modelling Extrusion Cooking. Food and Bioproducts Processing, Volume 77, Issue 1, March 1999, pages 55-63

Identification of a static LPV differential equation in the continuous time and frequency domain

Jan Goos jan.goos@vub.ac.be
John Lataire john.lataire@vub.ac.be
Rik Pintelon rik.pintelon@vub.ac.be
ELEC, Vrije Universiteit Brussel, Pleinlaan 2 1050 Brussel

1 Context

We are studying the class of Linear Parameter-Varying (LPV) systems, which is closely related to the class of Linear Time-Varying (LTV) systems. The difference is that the model dynamics depend on an external signal $p(t)$ (which we assume to be known), instead of having an unknown dependency on the (continuous) time t.

2 Approach

We will build on the LTV framework of [1], where a time-varying block structure is identified. The underlying model is a differential equation, where the coefficients change over time. In the LPV framework, these model coefficients are functions of the scheduling parameter $p(t)$. In the time and Laplace domain, the differential equation then reads respectively

$$\sum_{i=0}^{n_a} a_i(p(t))y^{(i)}(t) = \sum_{i=0}^{n_b} b_i(p(t))u^{(i)}(t) \tag{1}$$

$$\sum_{i=0}^{n_a} A_i(p(s)) * \left(s^i Y(s)\right) = \sum_{i=0}^{n_b} B_i(p(s)) * \left(s^i U(s)\right) \tag{2}$$

Note that the scheduling parameter $p(t)$ is not simply another input to the model, but directly affects the system dynamics.

Both the time and frequency domain have their own merits. The multiplication of the two time-varying signals is easier in the the time domain, but the derivative can be computed more easily in the frequency domain. Therefore, in the block structured approach of [1], a hybrid approach is used, as shown in Figure 1.

The model coefficient functions $a_i(p(t))$ and $b_i(p(t))$ are modelled as static (non-linear) functions of the scheduling signal $p(t)$, which are approximated by a user selected basis $\Phi_j(p(t))$.

$$a_i(p(t)) = \sum_{j=0} a_{i,j}\Phi_j(p(t)) \tag{3}$$

In the framework of [1], it is possible to handle arbitrary (non-periodic) excitation signals $u(t)$, but also arbitrary scheduling signals $p(t)$. The resulting output spectrum can be modeled exactly in the frequency domain. Even more, the measurements of the input and output singals $u(t)$ and $y(t)$ can be perturbed by colored Gaussian noise, and we will still obtain a consistent estimate, by minimizing

$$\hat{\theta}_{\text{WNLS}} = \arg\min_\theta \ \varepsilon(\theta)^H C_e^{-1} \varepsilon(\theta) \tag{4}$$

where θ represents the model coefficients (3), $\varepsilon(\theta)$ is the residual of (1), and C_e is the covariance of the residual $\varepsilon(\theta)$.

3 Acknowledgement

This work was supported in part by the Fund for Scientific Research (FWO-Vlaanderen), by the Flemish Government (Methusalem Fund, METH1), and by the Belgian Federal Government (IUAP VII, DYSCO).

References

[1] J. Lataire and R. Pintelon, "Frequency domain weighted nonlinear least squares estimation of continuous-time, time-varying systems," *IET Control Theory & Applications*, vol. 5, no. 7, pp. 923–933, 2011.

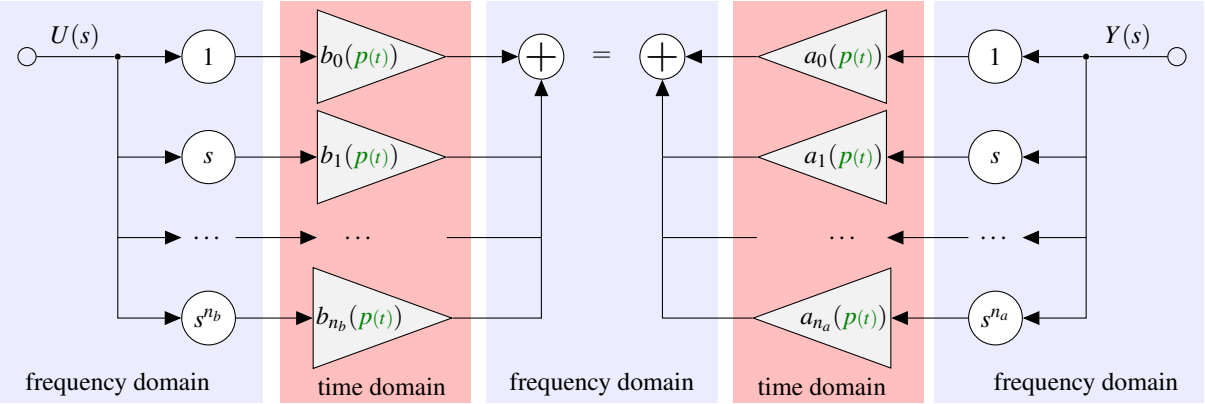

Figure 1. Block structure for an LPV IO model. All the coefficients appear linearly in this representation.

Parametric estimation of LPV partial differential equation

Julien Schorsch
Université Libre de Bruxelles (ULB),
Departement of Control Engineering and System Analysis
julien.schorsch@ulb.ac.be

1 Partial differential equation

Partial differential equations (PDE) also called distributed parameter systems (DPS) describe a wide range of physical behaviors with many applications in various fields as for example the state-of-health in advanced batteries [1]. The main characteristics of PDE with respect to the usually considered ordinary differential equations (ODE) is the introduction of partial derivatives along different dimensions, mostly depicting the time and space components of the considered system.

PDE models are most of the time derived from physical laws and therefore expressed in continuous time-space (CTS). To solve the identification problem of PDE systems, three main approaches can be distinguished:

- methods where optimization techniques are used to directly estimate the PDE model parameters;
- methods which aim at approximating the DPS by a continuous-time or a discrete-time lumped parameter system or by a discrete time-space system;
- methods which transform the partial differential equation to an algebraic equation. This usually includes the use of a preprocessing method to generate some measures of the process signals and their time-derivatives. This family of methods is therefore similar or very close to the approaches available for ODE model estimation.

In the usual ODE linear system case, one of the main limitations of indirect approaches, i.e. discrete-time approaches, is the impossibility to deal with non-regularly sampled data. In the presented PDE case, while it is fair to assume a regular time-sampling, the spatial-sampling is directly bounded to a physical sensor implantation and hence limited by cost and physicaly possible positioning. Consequently, in practice, indirect identification of PDE systems might often not be applicable. In order to cope with these limitations, direct approaches aim at directly identifying the physical CTS parameters, with the inherent difficulty to approximate partial derivatives from sampled noisy signals. This difficulty is commonly solved by a low pass filtering of the data. Nevertheless, it was only recently that the noise modeling problem with respect to these filters was addressed for direct identification of PDE systems [2].

2 Linear parameter varying system

Another statement is that the PDE considered for system identification are mostly linear time and space invariant. However, in practice most of the physical behaviors have a nonlinear or time-space varying nature. Consider for example a pollutant transport along a river. From a conceptual reasoning, it clearly appears that the transport speed directly depends on the river flow or the river profile for example. This directly leads to the concept of Linear Parameter Varying (LPV) models for which the parameters of a linear model are allowed to depend on a external so-called scheduling variable. Consequently, LPV-PDE system identification is studied.

3 Least squares and instrumental variable based methods

Regarding direct identification of continuous time LPV models, only a few methods are available in the ODE case [3], and to the best of author knowledge, there is no specific work in the PDE case. Consequently, the abstract is here focused on CTS-LPV-PDE system identification from sampled data under some realistic noise conditions. Because of the nature of the parameters which are dependent on a scheduling variable, a system reformulation has been proposed in [3] in order to apply the linear time invariant system theory to the LPV identification problem. This reformulation is here extended to the PDE case, allowing the use of an iterative least squares method [4] which provides efficient estimates for output-error type of noise in the prediction error minimization sense. However, as it will be shown in a numerical example, in the situation where the output is corrupted by an additive colored noise, this method delivers biased estimates. The second approach is then based on the simplified refined instrumental variable (SRIV) method. An advantage of the SRIV algorithm is to make use of a filter which reduces the noise influence on the estimated parameters [5].

References

[1] S. J. Moura, N. A. Chaturvedi, and M. Krstić, "PDE estimation techniques for advanced battery management systems - Part I: SOC estimation", *Proceedings of the American Control Conference*, Montreal (QC), pp: 559 - 565, 2012.

[2] J. Schorsch, H. Garnier, M. Gilson and P. C. Young, "Instrumental variable methods for identifying partial differential equation models", *International Journal of Control vol. 86(12)*, pp: 2325-2335, 2013.

[3] V. Laurain, R. Tóth, M. Gilson and H. Garnier, " Direct identification of continuous-time linear parameter-varying input/output models", *IET Control Theory & Applications*, vol. 5(7), pp: 878-888, 2011.

[4] K. Steiglitz and L. E. McBride, "A technique for the identification of linear systems", *IEEE Transactions on Automatic Control, vol. 10*, pp: 46-464, 1965.

[5] P.C. Young, *Recursive Estimation and Time-series Analysis: An Introduction for the Student and Practitioner*, second ed., Berlin: Springer-Verlag, 2011.

Estimation of LPV-SS Models with Static Dependency*

P. B. Cox, R. Tóth, and P. M. J. Van den Hof
Control Systems Group
Eindhoven University of Technology
P.O. Box 513, 5600 MB Eindhoven
The Netherlands
p.b.cox@tue.nl

1 Introduction

Numerous physical or chemical processes exhibit parameter variations due to non-stationary or nonlinear behaviour, often depending on measurable exogenous variables or measurable endogenous process states. These nonlinear parameter variations can be captured in the *linear parameter-varying* (LPV) modeling paradigm, which originates from the need of finding model structures, that are linear and low in complexity, but still allow to represent the nonlinear aspects of systems during control design. Similarly to *linear time-invariant* systems, the LPV model class assumes a linear relation between the inputs and outputs of the system, however the parameters of this relation are functions of a measurable, time-varying signal, the *scheduling variable* $p : \mathbb{Z} \to \mathbb{P}$, with $\mathbb{P} \subseteq \mathbb{R}^{n_\mathrm{P}}$. The resulting p-dependent parameter variation makes it possible to embed both non-stationary and nonlinear behaviour of the underlying physical or chemical process.

2 Identification of LPV-SS Models

Data-driven modeling approaches can be used to reveal the underlying dynamics of the LPV system, which can be represented in various representations. For control purposes, LPV *state-space* (SS) models are preferable, particularly with static and affine dependence on the scheduling signal. These LPV-SS models can be parsimoniously parameterized in the *multi-input multi-output* (MIMO) case compared to LPV *input-output* (IO) models. However, a realization from an LPV-IO model is computational expensive and will generally result in rational dependence in the scheduling variable or in a non-minimal realization. Hence, despite LPV-IO identification is advanced, it cannot support control synthesis well. Identification of LPV-SS models in the *prediction error minimization* (PEM) framework is a nonlinear optimization problem with a high computational load and it is very prone to local minima. Additionally, current *subspace identification* approaches suffer heavily from the curse of dimensionality, making estimation of moderate sized LPV-SS models computational infeasible. The interesting objective is how to achieve a computational efficient fusion of the advanced LPV-IO model identification and the available results of direct state-space model estimation.

3 Three-Step Approach

To tackle the computational complexity and perform rapid identification of LPV-SS models, a three-step approach is presented, which combines the attractive properties of PEM LPV-IO identification with the usefulness of the LPV-SS models. The three steps are: 1) the estimation of the impulse response coefficients, also known as Markov coefficients, 2) an exact LPV-SS realization scheme based on these estimated Markov coefficients, and 3) an LPV-SS nonlinear optimization based refinement step. In the first step we present two possible methods: i) correlation analysis and ii) MIMO finite impulse response estimation with ridge regularization. The second step is a basis reduced, deterministic Ho-Kalman like LPV-SS realization scheme based upon [1], which uses the estimated Markov coefficients of the first step. Finally, a third step is executed as a refinement step to reach the maximum likelihood estimate, for which two methods are considered i) an iterative LPV-SS expectation-maximization method [2] and ii) an extension of the enhanced Gauss-Newton method [3].

* This work was supported by the Netherlands Organization for Scientific Research (NWO, grant no.: 639.021.127).

References

[1] R. Tóth, H. S. Abbas, and H. Werner. On the state-space realization of LPV input-output models: practical approaches. *IEEE Trans. on Control Systems Technology*, 20(1):139–153, Jan. 2012.

[2] A. Wills and B. Ninness. System identification of linear parameter varying state-space models. In *Linear parameter-varying system identification: new developments and trends*, chapter 11, pages 295–316. 2011.

[3] A. Wills and B. Ninness. On gradient-based search for multivariable system estimates. *IEEE Trans. on Automatic Control*, 53(1):298–306, Feb. 2008.

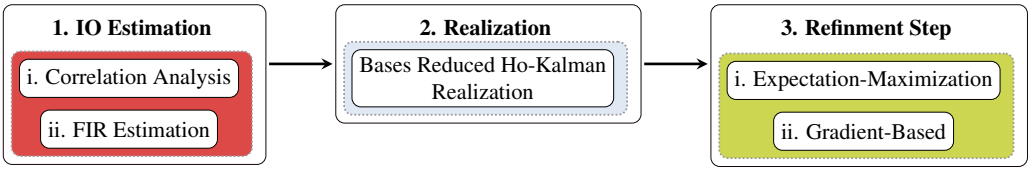

A combined global and local identification approach for LPV systems

Dora Turk, Goele Pipeleers and Jan Swevers
Department of Mechanical Engineering, KU Leuven, Belgium
Email: dora.turk@mech.kuleuven.be

1 Introduction

Linear parameter-varying (LPV) systems are nonlinear systems described by a linear model coefficients of which vary as a function of the so called *scheduling parameters*. The literature on LPV system identification typically distinguishes between two different identification approaches - global and local. Global techniques directly identify an LPV model based on data obtained from an experiment where both the input signal and the scheduling parameters are continuously changing. Local identification techniques typically consist of two steps. In the first step, several LTI models are identified based on input-output data for various fixed values of the scheduling parameter. In the second step, the LTI models are interpolated yielding a parameter varying model.
The global approach may offer high accuracy in predicting the system behavior under changing scheduling parameter conditions, in exhange for involved experiment design related to ensuring persistancy of the excitation. What goes in its favour is also the fact that *dynamic scheduling dependency*, i.e. system's dependency on time-shifted instances of the scheduling parameters, can only be detected through a global identification experiment. The local approach, on the other hand, can accurately identify only systems with *static scheduling dependency* - dependency on the instantaneous time values of the scheduling parameters, but can to a large extent rely on the well-studied linear time-invariant (LTI) identification methods.

2 Methodology

Although different, data originating from global and local experiments both provide valuable information that, when put together, gives a more complete picture of the system at hand. Our research is currently focused on the possibility of combining the two approaches. We consider the nonlinear least-squares identification framework for LPV systems [1], convenient for several reasons: it easily combines data originating from different experiments, the data it engages can be in the time and/or the frequency domain, it allows to emphasize particular experiments by simply employing weighting matrices, and the solution can be efficiently found by the well-known Levenberg-Marquardt algorithm. In this way, it is possible to balance between the importance of the system's behavior under changing scheduling parameter conditions, and the behavior for fixed operating conditions.

Table 1: Mean squared error of the identified LPV model calculated with respect to the global validation data - first row, local identification data - second row, and local validation data - third row; averaged over 100 identification proceedings.

$\alpha = 0.005$	$\alpha = 0.5$	$\alpha = 0.995$
$2.876 \cdot 10^{-1}$	$5.478 \cdot 10^{-2}$	$4.127 \cdot 10^{-2}$
$4.697 \cdot 10^{-4}$	$7.247 \cdot 10^{-3}$	$8.543 \cdot 10^{-3}$
$4.901 \cdot 10^{-4}$	$4.017 \cdot 10^{-3}$	$4.505 \cdot 10^{-3}$

3 Simulation example

Assume a single-input single-output discrete time LPV system of second order, with one scheduling parameter. We combine data from a global time domain experiment and local data: five frequency response functions each obtained for a different fixed value of the scheduling parameter. The total number of data samples in the local experiments equals the total number of data samples in the global experiment. To balance between the global and local behavior, we introduce weighting scalars α and β for the global and local data respectively, with $\alpha + \beta = 1$, $\alpha > 0$, $\beta > 0$. As the initial guess for the LPV identification, the LTI model identified for the scheduling value in the middle of the operating range is taken.

The results given in Table 1 clearly show that putting emphasis on one approach gives better results in the context interesting for that approach. Nevertheless, a compromise between the two seemingly exclusive objectives ($\alpha = 0.5$) is also achievable.

Acknowledgement

This research is sponsored by the Fund for Scientific Research (FWO-Vlaanderen) through project G.0002.11, by the KU Leuven-BOF PFV/10/002 Center-of-Excellence Optimization in Engineering (OPTEC), and by the Belgian Program on Interuniversity Poles of Attraction, initiated by the Belgian State, Prime Ministers Office, Science Policy programming (IAP VII, DYSCO).

References

[1] V. Verdult, "Non Linear System Identification: A State-space Approach." N.p., 2002.

Description of the cyclostationary processes in Linear Periodically Time-Varying (LPTV) systems

Vladimir Lazov , Ebrahim Louarroudi and Gerd Vandersteen
Dept. ELEC, Vrije Universiteit Brussel, Pleinlaan 2, 1050 Brussels, Belgium
e-mail : vladimir.lazov@vub.ac.be

1 Introduction

Various circuit blocks in telecommunication systems such as frequency converters, samplers and oscillators have a periodically time varying nature. Noise generated and processed by them therefore needs to be described using periodically time varying statistics [1]. Most signal processing methods assume stationary noise, implying that they have statistical parameters that do not vary with time. The stationarity assumption is not always applicable to signals in manmade systems encountered in different areas as e.g. communication systems.
Cyclostationary (CS) processes are much more than a trivial variation of stationary processes. Cyclostationarity can generally be exploited to enhance the accuracy and reliability of information collected from data sets such as measurements of corrupted signals. In communication systems, the statistical parameters of signals usually vary periodically with time. Our goal is to grow the awareness by recognizing and exploiting CS in the design and modeling process rather than ignoring it by treating signals as if they were stationary.We therefore need to extend and generalize the essential theorems for stationary and nonstationary processes to cyclostationary ones.

2 Framework and Problem overeview

As opposed to stationary signals, cyclostationary signals contain extra information due to their 'hidden' periodicity. In the time domain, the auto-correlation function carries the additional information which can be observed by the variation in its statistics. In the frequency domain, there are also correlations between spectral components that are spaced apart by specific frequencies, known as cyclic frequencies. The objective of all cyclic spectral analysis applications is to exploit signals spectral redundancy to improve the accuracy and reliability of information extracted from the measurements of corrupted signals [2]. Our current work aims to provide a complete description of the cyclostationary processes when a CS noise is processed by a linear periodically time-varying (LPTV) system. Moreover, we aim to extend the identification of LPTV systems using Local Polynomial Method (LPM) by including the cyclostationarity of the noise. This method should be able to suppress the leakage error by estimating the nonparametric frequency response function (FRF) and the leakage error over a small frequency range [3].
Another important issue is to find and check the assumptions under which the CS process becomes a stationary one. CS noise is for instance present at the output of a mixer when the noise is periodically modulated. However, figure 1 shows two configurations which transform CS noise into stationary noise: a cascade of two mixers at the top, and a cascade of single mixer and low pass filter (LPF) at the bottom. At the end, multiple simulations will help us determining the frequency response functions at the output of the both systems presented below.

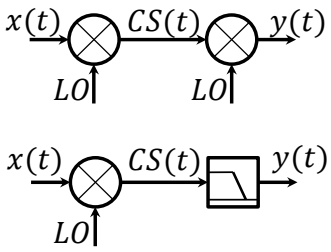

Figure 1: Top: A cascade of two mixers. Bottom: A cascade of a mixer and a low pass filter (LPF) and the signals used for both scenarios denoted as: input signals x (t), output signals y (t) and cyclostationary signals CS (t).

3 Acknowledgement

This work is supported by Strategic Research Program (SRP-19) Center for model-based system improvement: From Computer-Aided Engineering to Model-Aided Engineering.

References

[1] M.T Terrovitis, *The cyclostationary noise in radio-frequency communication systems,* Circuits and Systems I: Fundamental Theory and Applications, IEEE Transactions.

[2] A.W. Gardner,*Cyclostationarity: Half a century of research,* Signal Processing Volume 86, Issue 4, April 2006, Pages 639-697.

[3] M. Gevers, R. Pintelon,J. Schoukens *The Local Polynomial Method for nonparametric system identification: improvements and experimentation,* Decision and Control and European Control Conference (CDC-ECC), 2011 .

Time-Delay Pre-Filter Design for Periodic Signal Tracking of Lightly-Damped Multivariable Systems

Rick van der Maas
Dept. of Mechanical Engineering
Eindhoven University of Technology
Eindhoven, The Netherlands
r.j.r.v.d.maas@tue.nl

Tarunraj Singh
Dept. of Mechanical and Aerospace Engineering
State University of New York at Buffalo
Buffalo, New York, USA
tsingh@buffalo.edu

1 Introduction

Modern trends in mechatronic positioning systems require faster movements and increased accuracy. Lightweight system design is motivated by the desire to achieve higher accelerations, but this is at the cost of a shift of flexible dynamical behavior to a lower frequency region. Dealing with the imposed contradiction typically requires advanced control strategies. Input-shaping or time-delay filtering (TDF), are proven methods for the reduction of undesired motion induced dynamical effects [3], however typically limited to point-to-point motions, this in contrast to feedback procedures [1]. The main aim of this work is the introduction of a time-delay filter design which enables zero-phase error tracking for periodic reference signals according to the structure depicted in Fig. 1.

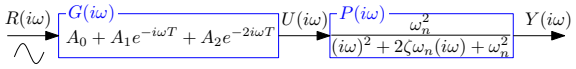

Figure 1: Open-loop TDF structure of a second-order system

2 Time-Delay Filtering for Periodic Movements

The fundamental idea behind input-shaping is the cancellation of the systems poles by exploiting the zeros of the filter. Periodic signals can be denoted by,

$$r(t) = \sum_{k=1}^{n} a_k \sin(\hat{\omega}_k), \quad \forall \omega \in \Omega_r, \tag{1}$$

with n the total number of harmonics and Ω_r the set of all $\hat{\omega}_k$. For zero-phase tracking of signals described by (1), the following constraints should be satisfied.

Design Requirements:

1. $G(s = p_j) = 0 \quad \forall p_j$, with p_j the poles of $P(s)$,
2. $|G(s = i\omega)| = |P(s = i\omega)|^{-1}$,
3. $\angle G(s = i\omega) + \angle P(s = i\omega) = \begin{cases} 0 & \text{if} \quad \omega < \omega_n \\ \pi & \text{if} \quad \omega > \omega_n \end{cases}$,

$\forall \omega \in \Omega_r$. A time-delay filter parametrization is proposed of the form,

$$G(s) = \sum_{k=1}^{L} A_k e^{-skT}, \tag{2}$$

with L depending on the number of poles of the system and the number of harmonics in (1). In Fig. 2, the results for a fourth-order system and three harmonics are illustrated. It can be observed that the proposed TDF enforces $|H(i\omega)| = |G(i\omega)P(i\omega)| = 1$ and $\angle H(i\omega) = 0 \ \forall \omega \in \Omega_r$, leading to perfect tracking.

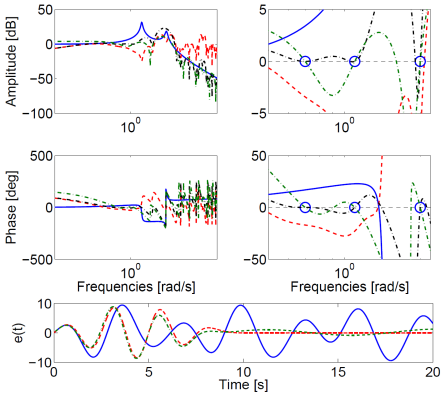

Figure 2: Frequency- and time domain results of $H(i\omega)$ for various TDF designs; uncontrolled (blue); normal TDF (red); harmonic TDF (green); robust harmonic TDF (green). All $\omega \in \Omega_r$ are indicated by blue circles.

3 Extensions for Robustness and Multivariable Systems

Robustness is key for successful application of the method which is for parameter variations extensively discussed in literature, see, *e.g.*, [3]. Variations in $\omega \in \Omega_r$ require an additional constraint that leads to the robust result in Fig. 2,

$$\left.\frac{dH(s)}{d\omega}\right|_{s=i\omega} = 0 \quad \forall \omega \in \Omega_r. \tag{3}$$

The method is also applicable for multivariable systems, based on the work in [2].

Acknowledgements

The research leading to these results has received funding from the Dutch ministry of Economic affairs and is part of the joint TU/e and Philips Healthcare MIxR Project.

References

[1] M. Steinbuch, S. Weiland, and T. Singh, "Design of noise and period-time robust high-order repetitive control, with application to optical storage," Automatica, 43(12):2086-2095, 2007. Addison Wesley, 1994.

[2] D. de Roover, F.B. Sperling, and O.H. Bosgra, "Point-to-point Control of a MIMO Servomechanism," Proc. Amer. Ctrl. Conf., 1998.

[3] T. Singh, "Optimal Reference Shaping for Dynamical Systems: Theory and Applications," Taylor & Francis, 2009.

Output agreement problem with unmatched disturbances

Nima Monshizadeh Claudio De Persis

Smart Manufacturing Systems Group, Engineering and Technology Institute Groningen, University of Groningen, The Netherlands
{n.monshizadeh@rug.nl,c.de.persis@rug.nl}

1 Introduction

Output agreement has evolved as one of the most important control objectives in cooperative control, see e.g. [1]. Output agreement roughly means that agents agree on a certain quantity of interest. This is typically done through communications via an interconnection structure given by a graph $G = (V,E)$. Depending on the context, agents may have identical (homogenous networks) or nonidentical (heterogeneous networks) dynamics. Moreover, the coupling imposed by the interconnection structure may be static or dynamic. In certain applications, the network dynamics is subjected to unknown disturbances. Output agreement with disturbance rejection/attenuation, therefore, has been studied in the literature, see e.g [2]. In this talk, we consider agents with nonindentical nonlinear port-Hamiltonian dynamics. The edge dynamics is assumed to be single integrator, yet with a nonlinear output map. Our objective is to achieve output agreement on a prescribed set point, and despite the presence of constant disturbances which are affecting the nodal dynamics. The key contribution of our results is that we cover the *unmatched control-disturbance* scheme, meaning that control signals and disturbances may be applied to different subset of nodes. An application of our results is balancing demand and supply in heterogenous power networks, where power generated at synchronous generators corresponds to the control inputs, and power demand at loads corresponds to disturbances.

2 Main Results

Consider systems at the edges and nodes

$$\dot{\eta}_k = v_k \tag{1}$$
$$\lambda_k = \nabla H_{e,k}(\eta_k) \qquad k = 1,2,\dots,M \tag{2}$$
$$\dot{x}_i = -R_i \nabla H_{n,i}(x_i) + \sigma_i + u_i + w_i, \qquad i \in I_1 \tag{3}$$
$$\dot{x}_i = -R_i \nabla H_{n,i}(x_i) + \sigma_i + w_i, \qquad i \in I_2 \tag{4}$$
$$y_i = \nabla H_{n,i}(x_i), \tag{5}$$

with $V = I_1 \cup I_2$ and $I_1 \cap I_2 = \varnothing$, interconnected via

$$v = B^T y, \quad \sigma = -B\lambda \tag{6}$$

to give the compact representation

$$\dot{\eta} = B^T \nabla H_n(x) \tag{7}$$
$$\lambda = \nabla H_e(\eta) \tag{8}$$
$$\dot{x}^{(1)} = -R^{(1)} \nabla H_n^{(1)}(x) - B^{(1)} \nabla H_e(\eta) + u^{(1)} + w^{(1)} \tag{9}$$
$$\dot{x}^{(2)} = -R^{(2)} \nabla H_n^{(2)}(x) - B^{(2)} \nabla H_e(\eta) + w^{(2)} \tag{10}$$
$$y = \nabla H_n(x). \tag{11}$$

For the sake of simplicity, we consider here constant disturbances w, i.e. $\dot{w} = \mathbf{0}$.

Notice that the interconnection (6) can be interpreted as a *physical* coupling among the systems. The absence of control in part of the node dynamics embodies possible failures in the actuators.
We are interested in an output agreement problem characterized as follows. There exists a unique constant vector $\bar{x}$ such that

$$\nabla H_{n,i}(\bar{x}_i) = \nabla H_{n,j}(\bar{x}_j), \quad \forall i,j \in I.$$

Under certain feasibility conditions, the controller

$$\dot{\theta} = -L_{comm}\theta - Q^{-1}[\nabla H_n^{(1)}(x) - \nabla H_n^{(1)}(\bar{x})] \tag{12}$$
$$u^{(1)} = Q^{-1}\theta \tag{13}$$

guarantees $x(t) \to \bar{x}, \quad \theta(t) \to \overline{\theta}, \quad u(t) \to \bar{u}$, where $\bar{u}$ is the minimizer of the cost function

$$C(u) = \frac{1}{2} u^T Q u$$

subject to

$$\dot{\overline{\eta}} = \mathbf{0} \tag{14}$$
$$\mathbf{0} = -R^{(1)} \nabla H_n^{(1)}(\bar{x}) - B^{(1)} \nabla H_e(\overline{\eta}) + \bar{u}^{(1)} + w^{(1)} \tag{15}$$
$$\mathbf{0} = -R^{(2)} \nabla H_n^{(2)}(\bar{x}) - B^{(2)} \nabla H_e(\overline{\eta}) + w^{(2)}. \tag{16}$$
$$\tag{17}$$

The analysis rests on the incremental total energy

References

[1] R. Olfati-Saber, J. A. Fax, and R. M. Murray. "Consensus and cooperation in networked multi-agent systems.", *Proceedings of the IEEE*, 95(1): 215-233, 2007.

[2] C.D.Persis and B.Jayawardhana, "On the internal model principle in the coordination of nonlinear systems", *IEEE Transactions on Control of Network Systems*, 1(3): 272-282, 2014.

Asynchronous Event-Triggered Implementation with a Lower Bound for Global Event Intervals

Anqi Fu, Manuel Mazo Jr.
Delft Center for Systems and Control, Delft University of Technology
Mekelweg 2, Delft, The Netherlands
Email:{A.Fu-1, M.Mazo}@tudelft.nl

1 Introduction

Network control systems (NCS) are control systems that have their components, sensors, controllers, actuators and coordinate nodes connected via a communication network. One of the promising research directions is to replace time-triggered controllers by event-triggered controllers, in order to save bandwidth.

In an event-triggered control implementation, the measurements from the sensors are sent to the controllers aperiodically. The times of update depend on the satisfaction of some predesigned conditions. As a result, the measurements are only sent when it is necessary. These conditions are often some relations between current measurements and the last sent measurements.

Let h represent such a triggering condition function, the event time in an event-triggered implementation is given by:

$$t_{k+1} = \min\{t > t_k | h(x(t), x(t_k)) > 0\}$$

The present work is a coordination of the work of [1]. In that paper, Mazo and Cao present an asynchronous event-triggered implementation, which makes the event triggering mechanism distributed in the sensors. In this case, for some local triggering functions h_i, the transmission times for each sensor i is given by:

$$t^i_{k+1} = \min\{t > t^i_k | h_i(x_i(t), x_i(t^i_k)) > 0\}, i \in \{1, \cdots, n\}, x \in \mathbb{R}^n$$

If there is an event in one of the sensors, only its measurement is used in the update of the next control action. This strategy was proposed to reduce sensors' listening time, which consequently reduces their energy consumption.

According to [1], there is a lower bound between transmissions of the same sensors:

$$t^i_{k+1} - t^i_k > \tau^i$$

where τ^i is the bound. However, this implementation cannot guarantee a lower bound between transmissions of different sensors, i.e. $\forall i \neq j$, there is no τ^d satisfying:

$$t^i_{k_i} - t^j_{k_j} > \tau^d$$

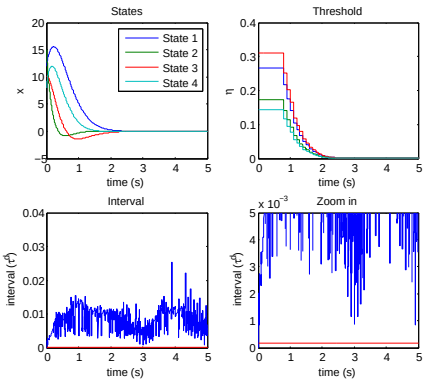

Figure 1: Simulation result, $\tau^d = 0.00017s$

Without this τ^d, a controller may calculate and send inputs to the actuators more than once in a very short time, which will cause a high instantaneous bit-rate.

In the present paper, we solve this problem by introducing an improved triggering strategy. This strategy requires the controllers to check the measurements of other sensors when there is an event. If another event can be expected in the future τ^d, the controller updates those sensor measurements by current measurements at the same time before calculating the inputs, thus a lower bound τ^d is achieved.

2 Linear case and Example

Fig.1 shows a simulation result of one system using our new asynchronous event-triggered implementation with lower bound guarantees for global event intervals. The system is a 4 dimensional linear system. The results show that the new strategy can guarantee asymptotic stability of the closed-loop as well as a lower bound for global event intervals.

References

[1] Manuel Mazo Jr. and Ming Cao. Asynchronous decentralized event-triggered control. *Automatica*, (0):–, 2014.

Energy Dissipation in Preisach and Duhem Hysteresis Models for Damage Estimation

J.J. Barradas-Berglind[1], B. Jayawardhana[2], R. Wisniewski[1]

[1]Automation and Control, Dept. of Electronic Systems, Aalborg University
Fredrik Bajers Vej 7, 9220 Aalborg, Denmark. {jjb,raf}@es.aau.dk.
[2]Discrete Technology and Production Automation, University of Groningen
Nijenborgh 4, 9747AG Groningen, The Netherlands. b.jayawardhana@rug.nl.

1 Motivation and Introduction

Fatigue damage is regarded as a critical factor in structures where it is essential to guarantee a certain life span for operating conditions in turbulent or coarse environments. These conditions might lead to irregular loads, which decrease the life expectancy of such structures. For example, this is the case for wind turbines, and structures in contact with waves and uneven roads. Fatigue is a phenomenon that occurs in a microscopic scale, manifesting itself as damage [1]. The most popular and widely spread measure of fatigue damage is the so-called rainflow counting (RFC) method, whose name comes from an analogy with roofs collecting rainwater. Despite its widespread usage, the RFC method has a complex non-linear algorithmic character that limits it as a post-processing tool primarily.

As mentioned in [2], the purpose of the RFC method is to identify the closed hysteresis loops in stress signals. In [3] an equivalence between RFC and a particular hysteresis operator is provided, allowing to incorporate a fatigue estimator online within the control loop, in contrast to the RFC case; a sketch of this idea is depicted in Figure 1. However, the inclusion of hysteretic elements in the control loop is not straightforward, since hysteresis operators involve discontinuities and non-smooth nonlinearities, and in the case of the Preisach hysteresis model, infinite dimensional memory [3].

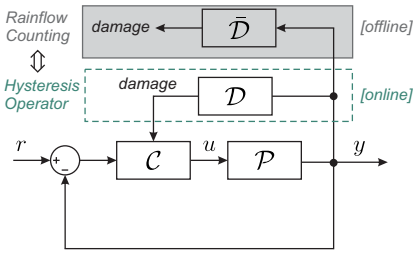

Figure 1: Damage calculation comparison between RFC ($\bar{D}$) and Hysteresis operator (D) in a control loop.

2 Proposed Approach

In this work, we relate the variations of certain Preisach hysteresis operator to its dissipated energy [4, 5]; with this equivalence we show the connection between damage as understood by Brokate in [3] and dissipated energy. Consequently, we transport the notion of damage to the Duhem hysteresis framework [6], where the aim is to use the dissipated energy [7, 8] as a measure or proxy for accumulated damage. Lastly, we include the aforementioned proxy in the cost functional of a model predictive control problem, where we illustrate the applicability of the proposed strategy.

The main advantage of the presented approach is that control of complex physical systems can be achieved, since the Duhem model can be explicitly written as a semi-linear differential equation [9], facilitating its inclusion in the control problem. Lastly, this damage estimation can be used in a wider set of applications, ranging from magnetics to mechanics, which are well described in the Duhem hysteresis framework.

References

[1] W. Schütz, "A history of fatigue," *Engineering Fracture Mechanics*, vol. 54, no. 2, pp. 263–300, 1996.

[2] S. Downing and D. Socie, "Simple rainflow counting algorithms," *International Journal of Fatigue*, vol. 4, no. 1, pp. 31–40, 1982.

[3] M. Brokate and J. Sprekels, *Hysteresis and phase transitions, volume 121 of Applied Mathematical Sciences*. Springer-Verlag, New York, 1996.

[4] R. B. Gorbet, K. A. Morris, and D. W. Wang, "Passivity-based stability and control of hysteresis in smart actuators," *Control Systems Technology, IEEE Trans. on*, vol. 9, no. 1, pp. 5–16, 2001.

[5] I. D. Mayergoyz, *Mathematical Models of Hysteresis*. Springer-Verlag, 1991.

[6] A. Visintin, *Differential models of hysteresis*. Springer Berlin, 1994, vol. 1.

[7] R. Ouyang, V. Andrieu, and B. Jayawardhana, "On the characterization of the Duhem hysteresis operator with clockwise input–output dynamics," *Systems & Control Letters*, vol. 62, no. 3, pp. 286–293, 2013.

[8] B. Jayawardhana, R. Ouyang, and V. Andrieu, "Stability of systems with the Duhem hysteresis operator: The dissipativity approach," *Automatica*, vol. 48, no. 10, pp. 2657–2662, 2012.

[9] J. Oh and D. S. Bernstein, "Semilinear duhem model for rate-independent and rate-dependent hysteresis," *Aut. Control, IEEE Trans. on*, vol. 50, no. 5, pp. 631–645, 2005.

Distributed control design for nonlinear output agreement in convergent systems

Erik Weitenberg
Rijksuniversiteit Groningen
e.r.a.weitenberg@rug.nl

Claudio De Persis
Rijksuniversiteit Groningen
c.de.persis@rug.nl

1 Abstract

This work studies the problem of output agreement in homogeneous networks of nonlinear dynamical systems under time-varying disturbances using controllers placed at the nodes of the networks. For the class of contractive systems, necessary and sufficient conditions for output agreement are derived, and these conditions relate the eigenvalues of the network Laplacian and the node dynamics.

2 Motivation

This result builds upon the method of [1], in which the output agreement problem is solved for the class of incrementally passive systems using dynamic couplings.

Previous results [2] study the problem of output *regulation*, and propose a solution using similar methods. However, such approaches are in general of limited use in large-scale networks, as conditions derived depend on the entire Laplacian matrix of the graph, and the resulting control strategy needs to be computed in a centralized manner.

3 Setting

We study networks of n systems

$$\begin{aligned}\dot{w}_i &= s_i w_i\\ \dot{x}_i &= f(x_i) + u_i + p_i w_i\\ y_i &= C x_i\end{aligned}$$

Here, s_i is assumed to be skew-symmetric. The stacked version of the interconnected system is denoted by $\bar{x}, \bar{u}, \bar{w}$ along with $\bar{f}, \bar{s}$ and $\bar{h}$.

When these are placed on the nodes of a graph $\mathscr{G}$, we denote the adjacency matrix by B and the Laplacian matrix by $\mathscr{L}$.

To achieve output agreement, we place controllers at the nodes of the form

$$\begin{aligned}\dot{\xi}_i &= p_i^T Q x_i + s_i \xi_i + H \sum_{j \in \mathscr{N}_i} (\xi_j - \xi_i),\\ u_i &= -p_i \xi_i.\end{aligned}$$

The objective is then to design H, Q and p_i such that $y_i - y_j \to 0$ as $t \to \infty$ for all pairs of nodes.

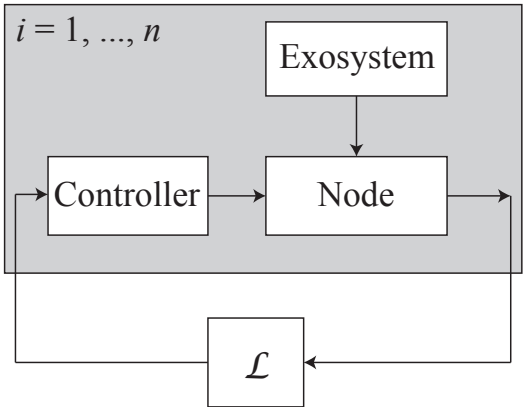

4 Approach

If the Jacobian of the entire system is quadratically stable, we achieve output agreement trivially. However, we aim to show that it's possible to achieve the same result by satisfying a simpler condition on the node systems for each eigenvalue of $\mathscr{L}$: we require instead that an expression of the form

$$f'(x) + \lambda_i H \tag{1}$$

be quadratically stable.

This result extends to dynamic controllers positioned at the nodes. In the case of scalar systems, this condition guarantees state synchronization; for the case of non-scalar systems, we have output synchronization.

References

[1] M. Bürger and C. De Persis. Dynamic coupling design for nonlinear output agreement and time-varying flow control. *Automatica*, 51:210–222, 2015.

[2] A. Pavlov, N. van de Wouw, and H. Nijmeijer. Global nonlinear output regulation: Convergence-based controller design. *Automatica*, 43(3):456–463, Mar 2007.

[3] M. Arcak. Certifying spatially uniform behavior in reaction-diffusion PDE and compartmental ODE Systems. *Automatica*, 47(6):1219–1229, Jun 2011.

[4] H. Bai and S. Y. Shafi. Output synchronization of nonlinear systems under input disturbances. *Under review*, arXiv:1312.6421, 2013.

Constrained proportional integral control of dynamical distribution networks with state constraints

Jieqiang Wei, Arjan van der Schaft
JBI, University of Groningen, PO Box 407,9700AK Groningen, the Netherlands
Email: J.Wei@rug.nl, A.J.van.der.Schaft@rug.nl

1 Abstract

In this paper we continue our study of the dynamics of distribution networks. Identifying the network with a directed graph we associate with every vertex of the graph a state variable x corresponding to *storage*, and with every edge a control input variable μ corresponding to *flow*, possibly subject to constraints. More precisely, on the vertices of graph we have

$$\begin{aligned} \dot{x} &= -B\mu + E\bar{d}, \quad x \in \mathbb{R}^n, \quad \mu \in \mathbb{R}^m \quad d \in \mathbb{R}^k \\ y &= \frac{\partial H}{\partial x}(x), \quad y \in \mathbb{R}^n, \end{aligned} \tag{1}$$

where $H : \mathbb{R}^n \to \mathbb{R}$ is a differentiable function, B is the incidence matrix of the network and $E\bar{d}$ is a vector of constant but unknown disturbances. In this paper we consider the case when the controller is defined on the edges to provide the flow variables. As explained in [1] a proportional-integral (PI) controller which is given as

$$\begin{aligned} \dot{\eta} &= \zeta, \quad \eta, \zeta \in \mathbb{R}^m, \\ \mu &= R\zeta + \frac{\partial H_c}{\partial \eta}(\eta) \end{aligned} \tag{2}$$

where η_i is state variable associated to i^{th} edge, R is a diagonal matrix with strictly positive diagonal elements $r_1, r_2, \ldots, r_m$, and H_c the Hamiltonian function corresponding to the controller, is sufficient to reach output agreement. Here the controller is driven by the relative output of the systems (1) on vertices, i.e.,

$$\zeta = B^T y \tag{3}$$

In many cases of practical interest it is natural to require that the state variables of the distribution network will remain larger than a given minimal value, e.g. zero. On the other hand, PI controller introduces oscillatory behavior which may cause the state variables x become smaller than some given lower bounds. In this paper we aim at regulating the system to consensus, while the storage variables remain greater or equal than a given lower bound γ. The problem is solved by using a distributed PI controller structure with constraints which vary in time. The closed-loop is given as

$$\begin{aligned} \dot{x} &= -B\,\mathrm{sat}(\mu(t), -\phi^+(t), \phi^+(t)), \\ \dot{\eta} &= B^T \frac{\partial H}{\partial x}(x). \end{aligned} \tag{4}$$

It is shown the constraints $\phi^+(t)$ can be obtained as the solution of an optimization problem.

In fact, for each time t and each vertex v_i, the edges adjacent to it can be divided into two sets

$$\begin{aligned} f^{in}_{v_i}(t) &= \{e_j \in \mathscr{E} \mid B_{ij}\mu_j < 0\} \\ f^{out}_{v_i}(t) &= \{e_j \in \mathscr{E} \mid B_{ij}\mu_j > 0\}. \end{aligned} \tag{5}$$

The vertices of the network can be divided into the following subsets, referred to as *gray and black*

$$\begin{aligned} \mathscr{V}^G(t) &= \{v_i \in \mathscr{V} \mid x_i(t) = \gamma_i\} \\ \mathscr{V}^{B1}(t) &= \{v_i \in \mathscr{V}^G \mid B(i,:)\mu(t) > 0\} \\ \mathscr{V}^{B2}(t) &= \{v_i \in \mathscr{V}^G \mid \exists v_j \in \mathscr{V}^{B1} \text{ s.t. } f^{in}_{v_i}(t) \cap f^{out}_{v_j}(t) \neq \emptyset\} \end{aligned}$$

where $B(i,:)$ is the ith row of B. Furthermore, we denote $\mathscr{V}^B(t) = \mathscr{V}^{B1}(t) \cup \mathscr{V}^{B2}(t)$. Let us denote the set of outgoing edges of all vertices in $\mathscr{V}^B(t)$, i.e., $\cup_{v_i \in \mathscr{V}^B(t)} f^{out}_{v_i}$, as $\mathscr{E}^B_{out}(t)$. By taking $\phi^+(t)$ as the solution of the following optimization problem

$$\begin{aligned} \min_{\phi} \; & \sum_{e_j \in \mathscr{E}^B_{out}(t)} \frac{1}{2|\mu_j(t)|}\Big(\big(\phi_j - \mu_j(t)\big)^2 + \phi_j^2\Big) \\ \text{s.t. } & B(i,:)\phi = 0, \forall v_i \in \mathscr{V}^B(t), \\ & \phi_k = \mu_k(t), \text{ if } e_k \in \mathscr{E} \setminus \mathscr{E}^B_{out}(t). \end{aligned} \tag{6}$$

we have the following result.

Theorem 1. *Consider the system (4) on the graph $\mathscr{G}$ in closed loop with the saturation bounds as solution of (6). Assume that $H = \sum_{i=1}^n H_i(x_i) \in \mathbb{C}^2$ and $H_c \in \mathbb{C}^1$ are positive definitive and radially unbounded. Furthermore H_i are strictly convex with* $\arg\min_{x \in \mathbb{R}^n} H(x) = \gamma \in \mathbb{R}^n$. *Then*

(i) $x(t) \geqslant \gamma$ for all $t > 0$ if $x(0) \geq \gamma$;

(ii) the trajectories of the closed-loop system (4) will converge to an element of the load balancing set

$$\mathscr{E}_{\text{tot}} = \{(x,\eta) \mid \frac{\partial H}{\partial x}(x) = \alpha \mathbb{1}, \alpha \in \mathbb{R}^+, B\frac{\partial H_c}{\partial \eta}(\eta) = 0\}.$$

if and only if $\mathscr{G}$ is weakly connected.

The proof is based on the Filippov solution of (4).

References

[1] J. Wei and A.J. van der Schaft, "Load balancing of dynamical distribution networks with flow constraints and unknown in/outflows," *Systems & Control Letters*, vol. 62(11), pp. 1001–1008, 2013.

Average consensus over unreliable networks: an improved compensation method

Francesco Acciani
Department of
Applied Mathematics
University of Twente
Enschede, The Netherlands
f.acciani@utwente.nl

Geert Heijenk
Department of
Computer Science
University of Twente
Enschede, The Netherlands
geert.heijenk@utwente.nl

Paolo Frasca
Department of
Applied Mathematics
University of Twente
Enschede, The Netherlands
p.frasca@utwente.nl

1 Introduction

We consider in the present work the average consensus problem over fully connected networks, with transmitter-based stochastic communication losses. Each node has an initial state, and the aim of the nodes is to reach consensus at the average value of the initial states of the nodes.
As the attention to multi agent control systems has grown, distributed consensus has been widely studied in the last decade, however the assumption that the network topology is static, i.e. the links are reliable and fixed, is not realistic, as in a wireless based network messages can be lost due to packet collision or interference on the channel. If the topology of the network changes dynamically, the consensus might not be achieved, therefore compensation methods must be introduced to make the network converge. It should be noticed, however, that the consensus value it is not necessarily be the average value of the initial states [1].
In the present work a solution to achieve convergence to the *exact* average value of the initial states is presented.

2 Consensus and compensation

An efficient distributed algorithm to solve the problem of averaging over a number N of nodes, is the dynamic system

$$x_i(t+1) = \sum_{j=1}^{N} P_{ij} x_j(t) \tag{1}$$

where P is a matrix such that $P_{ij} = 0$ if the nodes i and j are not connected. Moreover, it can be proved that if P is *doubly stochastic*, (i.e $P_{ij} \geq 0 \, \forall i, j$, $P\mathbb{1} = \mathbb{1}$ and $\mathbb{1}^T P = \mathbb{1}^T$) then P solves the average consensus problem.
Clearly, if the communication between two nodes can fail, the matrix P will not be constant over time, and then could be not stochastic for the whole time necessary to the system (1) to converge to consensus. In [1] two consensus strategies are proposed to compensate the information lost due to packet drop and be able to reach consensus: the *biased compensation method* and the *balanced compensation method* which both modify the matrix P if a communication failure happens. It should be noticed that the both compensation algorithms do not guarantee *average* consensus, but only consensus, which means that all the nodes will reach the same value which will not be the average of the initial states, but will differ by a quantity dependent on P.

3 Proposed solution

In the present work the biased method proposed in [1] is improved. Assume that the probability for a node to fail the communication with his neighbours is p and define $L(t) = diag(l_1, l_2, ...l_N)$, where $l_i = 0$ if the node i was not able to communicate at time t, 1 otherwise, and $\mathbb{P}[l_i = 0] = p$
Clearly, the $P(t)$ matrix will be $P(t) = \bar{P}L(t)$, where $\bar{P}$ is the matrix without failures. Applying the biased compensation method, the update matrix is

$$P_B(t) = P(t) + diag(\mathbb{1} - P(t)\mathbb{1}) \tag{2}$$

which is stochastic, but not double stochastic. It is however possible to define the matrix

$$G(t) = L(t)\bar{P}L(t) + I - L(t) \tag{3}$$

and then use the matrix

$$P_I(t) = G(t) + \frac{(\mathbb{1} - G(t)\mathbb{1})(\mathbb{1}^T - \mathbb{1}^T G(t))}{(\mathbb{1}^T - \mathbb{1}^T G(t))\mathbb{1}} \tag{4}$$

which is doubly stochastic, and then achieves the average consensus. However, the second term in (4) is in general a full matrix. Hence, this compensation method may not be suitable when the network is not fully connected

4 Conclusion

A novel approach to deal with packet losses over wireless networks was proposed. The method is capable to achieve average consensus even over unreliable networks. Other algorithms are capable to achieve consensus, but not average consensus. Current work is focusing on extending this compensation method to more general network topologies.

References

[1] F. Fagnani, S. Zampieri "Average consensus with packet drop communications", Journal of Control Optimisation, vol 48, No. 1, pp. 102-133, 2009.

Properties of feedback Nash equilibria in scalar LQ differential games

Jacob Engwerda
Tilburg University, The Netherlands, P.O. Box 90153, 5000 LE Tilburg
engwerda@uvt.nl

1 Abstract

In this note we study linear feedback Nash equilibria of the scalar linear quadratic N-player differential game. We present a complete characterization of the solution structure of this game using a geometric approach. Furthermore we investigate the effect on this solution structure of some characteristics of the game, i.e.: the number of players; the entrance of new players; and the level of asymmetry. For that purpose we distinguish three types of the game: the economic game; the regulator game and the mixed game. The analysis is restricted to the case the involved cost depend only on the output and control variables.

We consider the problem where N players try to minimize their individual quadratic performance criterion. Each player controls a different set of inputs to a single system. The system dynamics are described by the scalar differential equation

$$\dot{x}(t) = ax(t) + \sum_{i=1}^{N} b_i u_i(t),\ x(0) = x_0, \qquad (1)$$

Here x is the state of the system, u_i is a (control) variable player i can manipulate, x_0 is the arbitrarily chosen initial state of the system, a (the state feedback parameter) and $b_i,\ i \in \mathbf{N} := \{1,..,N\}$, are constant system parameters, and $\dot{x}$ denotes the time derivative of x. All variables are scalar.
The performance criterion player $i \in \mathbf{N}$ aims to minimize is:

$$J_i(u_1,\cdots,u_N) := \frac{1}{2}\int_0^\infty \{q_i x^2(t) + r_i u_i^2(t)\}dt, \qquad (2)$$

where r_i are positive and both b_i and q_i differ from zero.
We will assume that the players use time invariant feedback strategies, $u_i(t) = f_i x(t)$, to control the system. Although the players act in principle non-cooperatively we assume that there is some form of cooperation between the players in the sense that they agree to choose their strategies such that the closed-loop system will be stable. That is, we restrict the set of strategies to $\mathscr{F}_N := \{(f_1,\cdots,f_N) | a + \sum_{i=1}^N b_i f_i < 0\}$.

For this game we distinguish three cases. The case that $q_i < 0,\ i \in \mathbf{N}$, (the *economic game*); the case that $q_i > 0,\ i \in \mathbf{N}$ (the *regulator game*); and the case that for some indices q_i is negative and for other indices this parameter is positive (the *mixed game*).

For all three games we characterize geometrically the set of feedback Nash equilibria (FNE).

For the symmetric game (i.e. all players have the same cost function) we characterize how the set of system parameters where there exists a unique equilibrium depends on the number of involved players. It turns out that this set increases for the regulator game and decreases for the economic game.
Furthermore it is shown that if an economic player enters a regulator game, the area where a unique equilibrium exists decreases. Whereas an opposite reaction occurs if a regulator player enters an economic game. In such a case the area where a unique equilibrium exists increases.

For the two-player game we discuss how asymmetry between both cost functions impacts the area where a unique equilibrium exists. This area increases the more asymmetric the game is. More in particular we show that this growth is approximately a factor $\sqrt{3}$ larger in the regulator game than in the economic game.

Keywords: Linear quadratic differential games; linear feedback Nash equilibria; analysis solution structure;

References

[1] J.C. Engwerda, 2015. Properties of feedback Nash equilibria in scalar LQ differential games. Internal report. Tilburg University.

Consensus and Automata [1]

Pierre-Yves Chevalier, Julien M. Hendrickx, Raphaël M. Jungers[2]
ICTEAM
Université catholique de Louvain
Belgium
{pierre-yves.chevalier, julien.hendrickx,
raphael.jungers}@uclouvain.be

1 Consensus Systems

A consensus system represents a group of agents trying to agree with each other on some common value. These systems, and in particular linear ones, have attracted an important research attention because they are commonly used in a variety of distributed computation schemes. Possible applications range from coordination of autonomous platoons of vehicles to data fusion in systems with distributed measurements, distributed optimization or coordination of multi-agent systems.

We consider here the following discrete-time consensus system:

$$x(t) = A_{\sigma(t)}x(t-1). \quad (1)$$

The state vector represents the values of the agents: $x_i(t)$ is the value of agent i at time t. The index $\sigma(t)$ represents how the transition matrix is chosen in a set $S = \{A_1, \dots, A_m\}$ (representing all possible configurations of the system) at each time t. The matrices of S are (row) stochastic, representing agents computing their new values as weighted averages of values of other agents.

We are interested in convergence to consensus, that is, a state in which all agents have the same value. More specifically, we would like to know if it is possible to pick the sequence σ in such a way that System (1) converges to consensus.

2 Method

We first prove that the existence of a sequence such that System (1) converges to consensus is equivalent to the existence of a product P of matrices from the set S that has a positive column. We call such a product a *synchronising* product. We call a *synchronising word* the sequence of indices corresponding to a synchronising product.

In particular, if w is a synchronising word, then $www\dots$ is a sequence such that System (1) converges to consensus.

We notice that the problem of the existence of a synchonising word is very similar to the problem of synchronisability of automata. An automata is a set of stochastic matrices with *binary* entries. An automaton is said to be synchronisable if there is a product of matrices from the automaton that has a positive column.

The second step of our approach is to extend a couple of results from automata theory (see [2] for a survey) to sets of stochastic matrices to obtain results on our original consensus system.

3 Results

We obtain the following results: if there is a synchronising word, the shortest one is shorter than $\frac{n^3-n}{6}$. It can be check in polynomial time if a synchronising word exists but it is NP-hard to find the shortest one.

Theorem 1 (Short Synchronising Word) *Let S be a set of stochastic matrices. If S has a synchronising word, then it has a synchronising word of length smaller than $\frac{n^3-n}{6}$.*

Theorem 2 (Polynomial Time Decision Algorithm) *Let S be a set of stochastic matrices. There is an algorithm that decides in time $O(n^2)$ if the set S has a synchronising word.*

Theorem 3 (NP-hardness) *Let S be a set of stochastic matrices and $l \in \mathbb{N}$. The problem of the existence of a synchronising word of length smaller than l is NP-hard. The problem remains NP-hard when restricted to sets of matrices with positive diagonal.*

References

[1] P.-Y. Chevalier, J. M. Hendrickx and R. M. Jungers, *Efficient Algorithms for the Consensus Decision Problem*, Submitted, 2014.

[2] M. Volkov, *Synchronizing automata and the Černý conjecture*, in LATA 2008.

[1] This text presents research results of the Belgian Network DYSCO, funded by the Interuniversity Attraction Poles Program, initiated by the Belgian Science Policy Office. The research is also supported by the Concerted Research Action (ARC) of the French Community of Belgium.

[2] Raphaël Jungers is a FNRS research associate.

Robustness Issues with Directed Formations

Hector G. de Marina, M. Cao and B. Jayawardhana
University of Groningen
h.j.de.marina@rug.nl

Miguel Martinez
University of Alcala
miguel.martinez@depeca.uah.es

1 Introduction

Recently some robustness issues on formation control based on the gradient of potential energy have been identified [1]. These issues have been studied for rigid formations where the underlying graph describing the sensing topology is undirected. More specifically, the gradient-based controllers are not robust when a pair of neighboring robots measure differently about the relative position between each other. The effects of this discrepancy for formations in the plane are a distortion of the final shape of the formation with respect to the desired one and an undesired circular motion of the agents. Some work has been done addressing such issues in [2].

In this work we turn our attention to the formations where the sensing topology is directed. Therefore by construction there cannot exist discrepancies in the measured relative positions between neighbors since only one agent of any neighboring pair is measuring, but the effects of having a distorted shape and an undesired motion of the agents show up again when we discretize the dynamics of the agents and add zero-mean noise to the sensor readings. The surprise comes when one should expect a randomly perturbed movement of the formation due to the random noise in the measurement, but we will show that for the directed triangular formation, the dominating undesired movement is in fact a circular one whose mean angular velocity can be calculated. This effect can also be extrapolated to bigger directed rigid formations consisting of more than three agents.

2 Directed triangular formation as a case study

Consider the control law presented in [3] and discretize it by applying Euler's method

$$x_i(k+1) = x_i(k) - T z_i(k) e_i(k), \qquad (1)$$

where $i \in \{1,2,3\}$ is the label of the agent, k is the time index, $T \in \mathbb{R}$ is the sampling period, $x_i \in \mathbb{R}^2$ is the position of agent i, $z_i = x_i - x_{[i+1]}$ is the relative position between neighbors, $[\,]$ is the $mod(3)$ operation and $e_i(k) = ||z_i(k)||^2 - d_i^2$ is the error between the squares of the actual and the desired relative distance d_i.

We first show that the error system is self contained and stable, i.e. $\sum_i (e_i(k+1)^2 - e_i(k)^2) = f(e_i(k), T, d_i) \leq 0$ for some initial conditions $||e(0)|| \leq \rho > 0$ and for some sufficiently small sample time T. This implies that the shape of the desired triangle is robust against perturbations on the measurements. However, in the Cartesian space we can translate and rotate the triangular shape without affecting the error at all. That means that if a perturbation in the position of the agents causes a rotation or a translation of the whole formation at the same time, then the control law (1) will not necessarily be able to counter react such perturbation. We will show that such perturbation happens when we simply add a zero-mean Gaussian noise $v_i(k)$ to the measurement of the relative position, i.e. $y_i(k) = z_i(k) + v_i(k)$, and we replace $z_i(k)$ by $y_i(k)$ in (1).

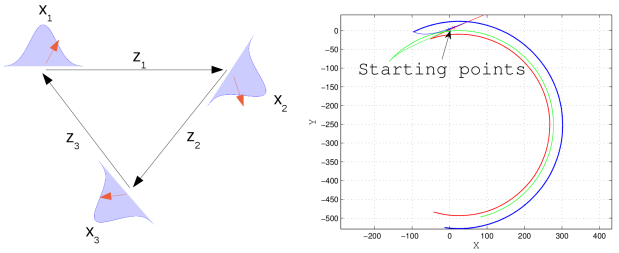

Figure 1: On the left the black arrows indicate the sensing topology. Sensing is corrupted by Gaussian noise, therefore the exact position of the neighboring agent is unknown. When the agents are close to the equilibrium, this uncertainty in the control law (1) causes a non-zero mean velocity represented by the orange arrow. On the right a numerical simulation of the agents' trajectory following (1) with noise in their measurements. We can see clearly how they describe a circular motion.

The argument for showing that there is a circular motion of the formation is based on the analysis of having two agents with an unknown position close to the equilibrium point. We can show that there exists a non-zero mean velocity component for each agent, and the resultant expected velocity for the whole formation is also non-zero. This circular motion is shown in the simulation on the right of Figure 1.

References

[1] S. Mou, A.S. Morse, A. Belabbas and B. Anderson,"Undirected Rigid Formations are Problematic", 53rd IEEE Conference on Decision and Control, pp 637–642, 2014.

[2] H.G. de Marina, M. Cao and B. Jayawardhana,"Controlling Rigid Formations of Mobile Agents Under Inconsistent Measurements", IEEE Transactions on Robotics, 2014, to be published.

[3] M. Cao, A.S. Morse, C. Yu, B. Anderson and S. Dasgupta,"Maintaining a directed, triangular formation of mobile autonomous agents", Communications in Information and Systems, Vol. 11, No. 1, pp. 1-16, 2011.

Model Inversion-based Iterative Learning Control: Optimal Performance Trade-offs

Tong Duy Son, Goele Pipeleers and Jan Swevers
Division PMA, Department of Mechanical Engineering,
Katholieke Universiteit Leuven, Celestijnenlaan 300B, B-3001 Heverlee, Belgium
Email: tong.duyson@mech.kuleuven.be

1 Introduction

Iterative learning control (ILC) is widely used in control applications to improve performance of repetitive processes [1]. The key idea of ILC is to update the control signal iteratively based on measured data from previous trials, such that the output converges to the given reference trajectory. Model-inversion based ILC uses the system model as a basis for the learning algorithm. Since system models are never perfect in practice, accounting for model uncertainty in the model inversion-based ILC analyses and designs needs to be addressed.

This work first discusses the robust monotonic convergence and tracking performance conditions of model inversion-based ILC. Next, the learning gain $\mathbf{Q}$ is designed such that the corresponding ILC controller realizes an optimal trade-off between the converged tracking performance $\mathbf{e}_\infty$ and the convergence speed. The design is reformulated as a convex optimization problem. Finally, the proposed model-inversion based ILC design is validated through a numerical example.

2 System Representation

We consider an LTI, single-input single-output (SISO) system that is subject to unstructured multiplicative uncertainty, $P_\Delta(q) = \hat{P}(q)(1+W(q)\Delta(q))$ and $\Delta(q) \in \mathscr{B}_\Delta = \{\Delta(q) = \text{stable, causal LTI system} : \|\Delta(q)\|_\infty \leq 1\}$. $\hat{P}(q)$ is the nominal plant model and the weight $W(q)$ determines the size of the uncertainty. $\hat{P}(q)$, $W(q)$, and $\Delta(q)$ are stable transfer functions. The ILC design is formulated in the trial domain, relying on the lifted system representation. The system is then represented by: $\mathbf{P}_\mathbf{\Delta} = \hat{\mathbf{P}}(\mathbf{I}+\mathbf{\Delta W})$, where $\hat{\mathbf{P}}, \mathbf{W}$ and $\mathbf{\Delta}$ are lower triangular Toeplitz matrices.

In ILC, the updated control signal is generally computed from the following learning algorithm:

$$\mathbf{u}_{j+1} = \mathbf{Q}(\mathbf{u}_j + \mathbf{L}\mathbf{e}_j), \tag{1}$$

where $\mathbf{e}_j = \mathbf{y}_\mathrm{d} - \mathbf{P}_\mathbf{\Delta}\mathbf{u}_j$ is the j-th trial tracking error, and $(\mathbf{Q}, \mathbf{L})$ are the designed learning matrices. The ILC algorithm is robust monotonic convergent if $\|\mathbf{Q}(\mathbf{I}-\mathbf{L}\mathbf{P}_\mathbf{\Delta})\| < 1$, $\forall \mathbf{\Delta} \in \mathscr{B}_\Delta$, and the converged tracking error is obtained as $\mathbf{e}_\infty = \left[\mathbf{I} - \mathbf{P}_\mathbf{\Delta}[\mathbf{I} - \mathbf{Q}(\mathbf{I}-\mathbf{L}\mathbf{P}_\mathbf{\Delta})]^{-1}\mathbf{Q}\mathbf{L}\right]\mathbf{y}_\mathrm{d}$.

In model inversion-based ILC, the learning gain $\mathbf{L}$ is selected as the inversion of the system model $\hat{\mathbf{P}}$, i.e. $\mathbf{L} = \hat{\mathbf{P}}^{-1}$. If the system is non-minimum phase or ill-conditioned, this learning gain is modified as the pseudo-inverse of the system model, i.e. $\mathbf{L} = \hat{\mathbf{P}}^\dagger$.

3 Analysis and Design

First, in order to obtain a tractable reformulation of the proposed ILC analyses, the set $\mathscr{B}_\Delta$ is replaced by an outer approximation: $\mathscr{B}^\mathrm{o}_\mathbf{\Delta} = \left\{\mathbf{\Delta} \in \mathbb{R}^{N\times N} : \|\mathbf{\Delta}\| \leq 1\right\}$. Then the ILC algorithm (1) is robust monotonic convergent if:

$$\|\mathbf{QW}\| < 1, \tag{2}$$

and the smaller $\|\mathbf{QW}\|$, the faster convergence speed. Moreover, the robust tracking performance condition is given by

$$\|\mathbf{W}_\mathrm{p}(\mathbf{I}+\mathbf{P}_\mathbf{\Delta}\mathbf{C})^{-1}\| \leq 1. \tag{3}$$

where $\mathbf{W}_\mathrm{p}$ is the performance weight and $\mathbf{C} = (\mathbf{I}-\mathbf{Q})^{-1}\mathbf{Q}\mathbf{L}$. This condition is equivalent to a bilinear matrix inequality.

In the ILC design, the objective is to optimize both the tracking error and the convergence speed as a multi-objective problem, yielding the following optimization problem

$$\begin{aligned} \underset{\mathbf{Q}}{\text{minimize}} \quad & \|\mathbf{W}_\mathrm{p}(\mathbf{I}+\hat{\mathbf{P}}\mathbf{C})^{-1}\|^2 \\ \text{subject to} \quad & \|\mathbf{QW}\|^2 < \gamma. \end{aligned} \tag{4}$$

The weight γ quantifies the relative importance of converged tracking error and convergence speed. This problem is reformulated as a convex optimization problem in the variable $\mathbf{Q}$. We then analyze the optimal trade-off design by solving (4) for different values of $\gamma < 1$.

Acknowledgements

This work was supported by the European Commission under the EU Framework 7 funded Marie Curie Initial Training Network (ITN) IMESCON (grant no. 264672). This work also benefits from KU Leuven-BOF PFV/10/002 Cente of Excellence: Optimization in Engineering (OPTEC), and from the Belgian Network Dynamical Systems, Control and Optimization (DYSCO), initiated by the Belgian Science Policy Office. Goele Pipeleers is partially supported by the Research Foundation Flanders (FWO Vlaanderen).

References

[1] D.A. Bristow, M. Tharayil, and A.G. Alleyne, "A survey of iterative learning control: A learning-based method for high-performance tracking control", *IEEE Control Systems Magazine*, vol. 26, no. 3, pp. 96–114, 2006.

Optimal Control of Uncertain Switched Systems Based on Model Reference Adaptive Control

Shuai Yuan, Simone Baldi, and Bart De Schutter
Delft Center for Systems and Control
Delft University of Technology
2628 CD, Delft, The Netherlands
s.yuan-1@tudelft.nl

1 Introduction

Switched systems are an important subclass of hybrid systems that consists of subsystems with continuous dynamics and a rule to regulate the switching behavior between them. Switched systems appear in a wide range of applications, such as intelligent transportation systems and smart energy systems. Due to the desire to drive switched systems toward optimal behavior, e.g. maximization of traffic flow in traffic networks, minimization of energy consumption in energy systems, optimal control of switched systems has attracted a lot of attention. Solution of the Hamilton-Jacobi-Bellman (HJB) equation via Dynamic Programming has been proposed to address optimal control for switched systems. This, however, gives rise to the 'curse of the dimensionality'. Recently, adaptive dynamic programming (ADP) has been adopted to solve optimal control problems for switched systems. ADP algorithms are capable of avoiding the 'curse of the dimensionality' and approximating the optimal control law via recursive relationships and soft computation technologies, like neural networks. Lu and Ferrari [1] train neural networks to approximate the optimal value function in a forward fashion. The weights are updated online by recursive relationships involving the objective function and its gradient with respect to the switching modes. Heydari and Balakrishnan [2] adopt ADP to obtain the optimal switching sequence and switching instants. A batch training algorithm is applied to update weights of the neural networks in a backward fashion.

2 Problem formulation and methodology

Approaches developed in literature for optimal control of switched systems require to some extent the knowledge of the system dynamics. For example, the knowledge of the system dynamics in a neighborhood set of the continuous system state trajectory is a prerequisite condition of the approach of [1]. The algorithm of [2] is based on known dynamics of the switched system and can be only implemented offline. In light of this, we propose to adopt a model reference adaptive control (MRAC) scheme to solve optimal control problems of uncertain LTI switched systems. MRAC is an adaptive scheme to obtain a control law that drives the output of an unknown system to track the response of a reference model. The unknown dynamics of switched systems can be expressed as

$$\dot{x}(t) = A_{i(t)}x(t) + B_{i(t)}u(t) + d(t)$$
$$y(t) = C_{i(t)}x(t)$$

where x, u, y and i are the state vector, the continuous control law, the output and the switching sequence respectively; d is a bounded disturbance. For every mode i, the matrices A_i, B_i and C_i are unknown. A family of reference models, one for each mode, is also defined: the reference models have input r, state $\hat{x}$ and output $\hat{y}$. Moreover, the retrospective cost function considering the past output difference is needed. Instead of solving the HJB equation, the inputs and objective function of switched systems are optimized based on asymptotically diminishing the difference online between the expected output of the reference models and the closed-loop output. Additionally, a family of Lyapunov functions, one for each subsystem, is considered to determine the corresponding switching actions. The stability of the switched systems will be guaranteed by optimizing the switching sequence so that the values of the Lyapunov function at switch-in points of one subsystem are smaller than those of previous switch-in points.

3 Conclusions and future work

To date, the optimal control problem of uncertain switched systems has not been solved satisfactorily. Every method proposed in literature, to the best of the authors' knowledge, requires to some extent the knowledge of the system dynamics. In this work, we propose a new optimal control scheme for unknown switched systems based on model reference adaptive control.

References

[1] W. J. Lu and S. Ferrari, "An Approximate Dynamic Programming Approach for Model-free Control of Switch Systems", in *Proc. 52nd IEEE Conference on Decision and Control*, pp. 3937–3844, 2013.

[2] A. Heydari and S. N. Balakrishnan, "Approximate Feedback Solution to Optimal Switching Problems with Switching Cost", *IEEE Trans. on Neural Networks and Learning Systems*, vol. 25, no. 6, pp. 1106–1117, 2014.

An Adaptive Online Game-theoretic Approach for Complete Vehicle Energy Management

H. Chen, J.T.B.A. Kessels, and S. Weiland
Control System group, Dept. of Electrical Engineering, TU/e
Email: h.chen2@tue.nl

1 Introduction

Complete Vehicle Energy Management (CVEM) is proposed in [2]. A single-leader multi-follower game-theoretic framework is developed in [1] for CVEM. In this approach, the likelihood of driving behaviour is characterized by a probability distribution function, G, in terms of the requested torque and speed over a drive-cycle. Up to now, using one G function in the game-theoretic setting has been explored. On the other hand, it should be noted that G functions may vary significantly for different drive-cycles and drivers. Consequently, the use of only one G function in the optimization criterion for an energy management system may not produce robust results when varying over different drive-cycles and different drivers. In this paper, the possibility of adapting the game-theoretic approach to improve the robustness over different drive-cycles is explored.

2 The adaptive approach

The adaptive approach can be structured in the following three steps:

1.: N_w representative drive-cycles are selected and a corresponding probability distribution function G_j is constructed, $j = 1,2,...,N_w$ for each of them.

2.: Next, we cast the problem into a game-theoretic framework by defining the driver as the leader and each auxiliary as a follower. The cost function J_j involving G_j is designed for the leader and the cost fucntion J_{ij} is designed for the ith follower. The leader makes its decision first. With the knowledge of the leader's decision, the ith follower chooses the optimal response. The optimal game-theoretic strategy of the ith follower corresponding to the jth leader is then stored in a look-up-table for all $j = 1,2,...,N_w$.

3.: An online function $G_{ol}(w,t_k)$ is constructed by using the recorded driving data in the sliding window with length t_w and evolves with time in a receding horizon framework (see Figure 1). After every time interval t_{pd}, (1) classifies G_{ol} into one of N_w classes of drive patterns represented by G_j.

$$\min_{j\in\{1,2,...,N_w\}} \sum_{\omega} \left(\frac{\bar{\tau}_j(\omega) - \bar{\tau}_{ol}(\omega)}{\tau_{max}} \right)^2 \cdot G_{ol}((\bar{\tau}_{ol}(\omega),\omega),t_k), \tag{1}$$

where τ and ω are the requested torque and speed, respective; $\bar{\tau}_j(\omega) = \arg\max_\tau G_j((\tau,\omega))$ and $\bar{\tau}_{ol}(\omega) = \arg\max_\tau G_{ol}((\tau,\omega),t_k)$. Consequently, all followers adopt the game-theoretic strategies corresponding to the identified drive pattern and seek the equilibrium solution as described in [1] until the next time instance of the classification.

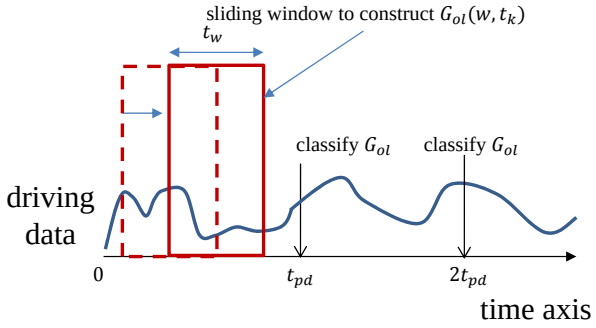

Figure 1: Online classification of the driving history

Multiple strategies are simulated on a model of a hybrid truck with additional auxiliaries. The results are compared in terms of fuel economy over different drive-cycles. In the simulation, the adaptive approach shows an up to 14.7% performance improvement compared to the non-adaptive one.

References

[1] H. Chen, J.T.B.A. Kessels, M.C.F. Donkers, and S. Weiland. Game-theoretic approach for complete vehicle energy management. In *Vehicle Power and Propulsion Conference (VPPC)*, Coimbra, Portugal, October 2014.

[2] J.T.B.A. Kessels, J.H.M. Martens, P.P.J. Van den Bosch, and W.H.A. Hendrix. Smart vehicle powernet enabling complete vehicle energy management. In *Vehicle Power and Propulsion Conference (VPPC), 2012 IEEE*, pages 938–943, Seoul, Korea, Oct 2012.

Wave form replication using combined Adaptive and Iterative Learning Control

Sikandar Moten, Goele Pipeleers, Wim Desmet and Jan Swevers
Department of Mechanical Engineering, KU Leuven
Celestijnenlaan 300 - bus 2420, 3001 Leuven, Belgium
sikandar.moten@kuleuven.be

1 Abstract

In the automotive industry, durability testing is a crucial step in the design and development cycle. The goal of these tests is to replicate or track real operating conditions in lab environment typically on a multi-axis vibration test rig. The wave forms that have to be tracked are repeated sequentially for a certain number of cycles or until failure occurs. Existing techniques to replicate these sequences consist of fixed position controllers for the actuators with feedforward approaches; for instance the current state of the art Time Wave Replication (TWR) process. The TWR process consists of two phases [2]: Identification of non-parametric frequency domain model and its inverse followed by off-line iterative learning control (ILC) phase. Although TWR is a slow off-line process for finding the appropriate drive signals, it allows to control systems with delays and non-minimum phase, which is typical for hydraulic test rigs. This research proposes an online technique that can also handle systems with delays and non-minimum phase by investigating a combined use of adaptive inverse control (AIC) and ILC . As a result, this will help to accelerate the drive signal generation process.

2 Approach

AIC makes use of adaptive digital filters. Such filters use the input signal, the output signal and the corresponding error signal to adapt the parameters of the filter. For current study, we limit ourselves to Finite Impulse Response (FIR) Filters and make use of recursive least squares to adapt the parameters of the FIR filters, see [1]. First, the AIC algorithm learns itself how to control a specific system and creates the first feedforward drive signal. Next, the use of ILC helps to improve the performance. The steps for the wave form replication in real-time are as follows:
(a) Identify the plant P and controller dynamics P^{-1} using adaptive algorithm.
(b) Use the identified FIR model of P^{-1} in order to generate the first drive in real-time.
(c) Use the identified P^{-1}, previous drive u_j and error signals e_j for generating the new drive signal u_{j+1} using classical ILC i.e. $u_{j+1}(k) = u_j(k) + gain \times P^{-1} e_j(k)$, see [2].
(d) Keep iterating using step (c) and monitor convergence. Stop iteration as per the terminating condition.

3 Validation

The presentation will discuss a first validation of this approach through simulation on a SISO discrete-time system:

$$P(z) = \frac{z^2 + 1.6z}{z^2 - z + 0.65}$$

$P(z)$ is the non-minimum phase stable system which implies its inverse $P^{-1}(z)$ will be unstable. The goal is to replicate a multi-sine reference target with a spectral content between 5 and 50 Hz. The mean squared error (MSE) for the first drive is found to be 2.6×10^{-4} Units. After 15 iterations, the MSE is reduced to 2.5×10^{-5} Units. Figure 1 depicts this reduction in the MSE. In conclusion, an online technique for the wave form replication is proposed in which ILC uses the first drive and FIR model of inverse plant dynamics provided by adaptive algorithm to find the subsequent drives till convergence.

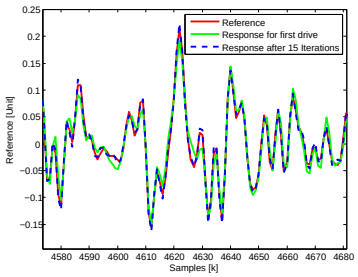

Figure 1: Response signals in comparison with reference target

4 Acknowledgement

The research of S. Moten is funded by an Early Stage Researcher grant within the European Project IMESCON Marie Curie Initial Training Network (GA 264672). This work also benefits from the KU Leuven Optimization in Engineering Center (OPTEC) and Belgian Programme on Interuniversity Attraction Poles, initiated by the Belgian Federal Science Policy Office (DYSCO). Goele Pipeleers is Postdoctoral Fellow of the Research Foundation Flanders (FWO).

References

[1] G. L. Plett. Efficient linear MIMO adaptive inverse control. *Proceedings of 2001 IFAC Workshop on Adaptation and Learning in Control and Signal Processing*, pg. 89-94, 2001.

[2] J. De Cuyper. Linear feedback control for durability test rigs in the automotive industry. *PhD Thesis*, Katholieke Universiteit Leuven, 2006.

Combustion Control with Multiple Fuel Injections for Clean and Fuel Efficient Diesel Engines

Xi Luo
Control Systems Technology
Technische Universiteit Eindhoven
P.O. Box 513, 5600 MB EINDHOVEN
The Netherlands
Email: X.Luo@tue.nl

Frank Willems
Control Systems Technology
Technische Universiteit Eindhoven
P.O. Box 513, 5600 MB EINDHOVEN
The Netherlands
Email: F.P.T.Willems@tue.nl

1 Introduction

The combustion phase and load for diesel engines may differ from the optimal one due to practical disturbances, such as the change of ambient conditions, fuel quality and engine component ageing. This deviation downgrades diesel engine's performance, including higher fuel consumption engine-out emission level and possibly higher noise level. Using the multiple-pulse fuel injection profile instead of a single pulse, larger flexibility is introduced to shape the combustion phase. A feedback controller at the combustion level can be designed to manipulate the timing of each fuel injection pulse such that the optimal engine performance is achieved with the presence of various disturbances.

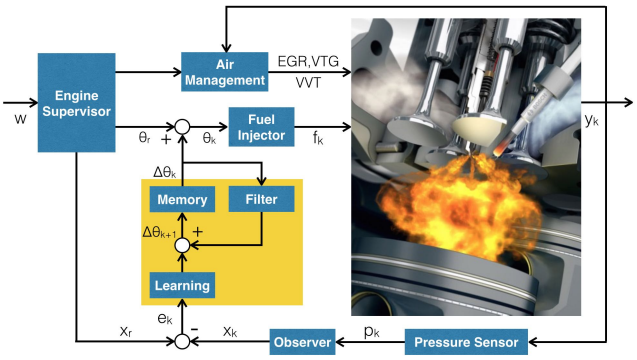

Figure 1: Block diagram for combustion phase control.

2 Approach

The cylinder pressure signal is the key enabler for closed-loop control of the combustion phase in diesel engines. Several metrics are extracted from the cylinder pressure signal and used to describe the combustion phase, e.g. the crank angle degree reaching 50% accumulated heat release (CA50) and indicated mean effective pressure (IMEP). Given the reference value of these combustion phase and load metrics, which leads to optimal engine performance, the difference between the reference signal and the measured one from the previous combustion cycle is regarded as the feedback. It is used to computed the control signal in the next combustion cycle, such that the combustion phase deviation eventually converges to zero. As the block diagram shown in Figure 1, the error signal is learned iteratively and used to update the control signal, which is regarded as the Iterative Learning Controller (ILC) and also known as the cycle to cycle control scheme [1].

3 Results

A feedback learning controller was designed to manipulate the two-pulses fuel injection profile with disturbed injection timing parameters. Based on measured combustion phase and load metrics and the reference signal, the controller updates the fuel injection timing parameters for the next combustion cycle. The simulation results were computed using TNO's engine package DYNAMO+. Judging from the results as plotted in Figure 2, the measured combustion phase metrics, as well as the engine performance, converge to the nominal values rapidly with the presence of disturbances. Therefore, it can be concluded that the designed controller manages to reject the disturbances at stationary operation condition such that the engine performance becomes robust.

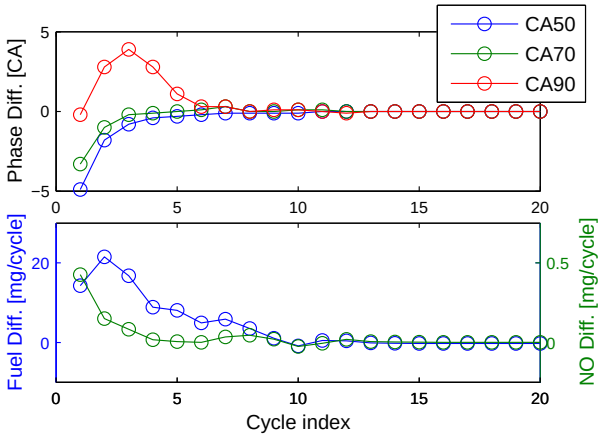

Figure 2: Controlled converging combustion phase and engine performance with disturbed fuel injection timing.

References

[1] Luo X., Jager B., and Willems F. Emission constrained multiple-pulse fuel injection optimisation and control for fuel efficient diesel engines. In *European Control Conference (ECC)*, 2015.

Initial estimates for Wiener-Hammerstein dynamics using phase-coupled multisines

Koen Tiels, Maarten Schoukens, and Johan Schoukens
Department ELEC, Vrije Universiteit Brussel, B-1050 Brussels, Belgium
koen.tiels@vub.ac.be

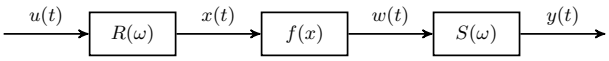

Figure 1: A Wiener-Hammerstein model (*R* and *S* are linear dynamic systems and *f* is a nonlinear static system).

1 Introduction

Even if nonlinear distortions are often present, many dynamical systems can be approximated by a linear model. When the nonlinear distortions are too large, a linear model is insufficient, and a nonlinear model is needed. One possibility is to use block-oriented models, which consist of linear dynamic and nonlinear static sub-blocks. This work proposes a method to generate initial values for the linear dynamic subsystems in a Wiener-Hammerstein model (see Figure 1).

2 Problem statement

The identification of a Wiener-Hammerstein model is nonlinear in its parameters (e.g. polynomial coefficients of *f* and transfer function coefficients of *R* and *S*). Good starting values are thus required. An estimate of the product of the two linear dynamic sub-blocks can be easily obtained using the best linear approximation (BLA) [1] of the system for a Gaussian excitation. It is more difficult, however, to split these global dynamics over the individual sub-blocks.

3 Proposed method

In [2], we propose a well-designed multisine excitation with pairwise coupled random phases. Next, we estimate a modified BLA on a shifted frequency grid. It is shown that the input dynamics shift over a user-specified frequency offset in this shifted BLA, while the output dynamics remain fixed (see Figure 2 for an example). The transfer function of the shifted BLA, which has complex coefficients due to the frequency shift, is estimated with a modified frequency domain estimation method. The identified poles and zeros can be assigned to either the input or output dynamics, depending on whether they shift or remain fixed.

The method is generalized in [3] from a cubic nonlinearity to a polynomial nonlinearity of arbitrary degree, and is illustrated on experimental data obtained from the Wiener-Hammerstein benchmark system [4].

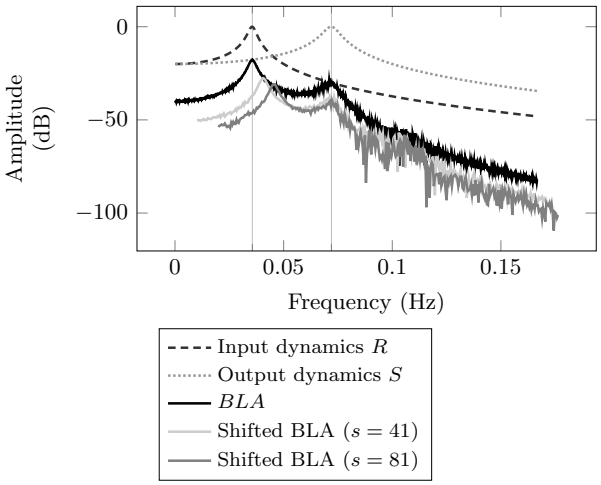

Figure 2: The BLA of a Wiener-Hammerstein model excited by a Gaussian input is proportional to the product of the two linear dynamic sub-blocks. When using the proposed phase-coupled multisine excitation, the input dynamics shift over a user-specified frequency offset *s* (in frequency bins), while the output dynamics remain fixed.

Acknowledgments

This work was supported in part by the Fund for Scientific Research (FWO-Vlaanderen), by the Flemish Government (Methusalem), by the Belgian Federal Government (IAP DYSCO VII/19), and by the ERC advanced grant SNLSID, under contract 320378.

References

[1] R. Pintelon and J. Schoukens, "System Identification: A Frequency Domain Approach," Wiley-IEEE Press, 2012.

[2] J. Schoukens, K. Tiels, and M. Schoukens, "Generating initial estimates for Wiener-Hammerstein systems using phase coupled multisines," In 19^{th} IFAC World Congress, Cape Town, South Africa, August 24–29, 2014.

[3] K. Tiels, J. Schoukens, and M. Schoukens, "Initial estimates for Wiener-Hammerstein models using phase-coupled multisines," Internal note VUB-ELEC-Tiels, 2014.

[4] J. Schoukens, J. Suykens, and L. Ljung, "Wiener-Hammerstein benchmark," In 15^{th} IFAC Symposium on System identification, Saint Malo, France, July 6–8, 2009.

Dynamic berth and quay crane allocation for complex berthing process in container terminals

R. T. Cahyono[1,2], E. J. Flonk[1] and B. Jayawardhana[1]
[1]Faculty of Mathematics and Natural Sciences, Rijksuniversiteit Groningen
Nijenborgh 4 9747 AG, Groningen, the Netherlands
[2]Faculty of Industrial Technology, Institut Teknologi Bandung
Jalan Ganesha 10, Bandung, 40132, Indonesia
{r.tri.cahyono, b.jayawardhana}@rug.nl[1], rully@ti.itb.ac.id[2]

1 Introduction

The modeling of berth and quay crane (QC) allocation is usually in a static setting, as reviewed in [1]. We discuss a dynamical model that describes the operation of berthing process with multiple discrete berthing positions and multiple QCs. The allocation strategy is based on model predictive control (MPC) paradigm. This work is based on [2].

2 Contribution

In this paper, we develop a dynamical model of the berthing process that improves the one used in the dynamic berth allocation problem (DBAP) as in [3]. We include set dynamics describing the ships arrival and the dynamics of the berthing process with multiple berthing positions and multiple QCs. Based on the proposed model, we propose a dynamic allocation strategy of both the berth and quay cranes allocation, simultaneously, using model predictive control (MPC) and propose a novel heuristic, so-called N-level FCFS, which combines the FCFS and exhaustive search strategy to solve the MPC problem.

3 Simulation results

We use a data set where there are 2 berth positions, 7 QCs, and 29 incoming ships. We first use the commonly adopted method first come first served (FCFS) and density-based quay crane allocation (DBQA). Secondly, we use a N-level FCFS method to solve the MPC problem. The simulation results is shown in Table 1. The results for both strategies can be seen in Figure 1. It can be seen from this figure that at the berthing step 2, the ship "Sejahtera" is given a priority to the ship "Meratus I", which arrives earlier, for berthing. The MPC with with a horizon of 8 can already decrease the total cost of 20.56% compared with the traditional FCFS and DBQA methods.

Table 1: Simulation result of the berth and quay crane allocation for multiple berth positions and multiple QCs.

N	*Allocation Strategy*	*Total cost*	*Ave. Calc. time per step (s)*
1	FCFS & DBQA	3,921,923	0.0958
2	MPC	3,828,642	0.3634
3	MPC	3,642,352	1.2493
4	MPC	3,547,157	4.4727
5	MPC	3,364,535	12.8840
6	MPC	3,230,941	29.7830
7	MPC	3,162,912	70.5480
8	MPC	3,115,403	155.9200

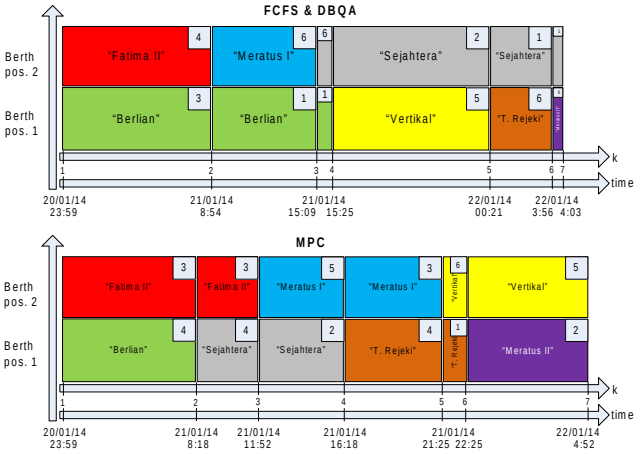

Figure 1: The resulting berth and QC allocation for the first 7 berthing steps. The MPC-based strategy is with $N = 8$. The berth positions are shown in the vertical axis and the time (and the berthing step) is shown in the horizontal axis. The number on the top-right corner of every box gives the allocated QCs.

References

[1] C. Bierwirth and F. Meisel, "A survey of berth allocation and quay crane scheduling problems in container terminals," Eur. J. Oper. Res., vol. 202, pp. 615–627, 2010.

[2] R. T. Cahyono, E. J. Flonk, and B. Jayawardhana, "Dynamic berth and quay crane allocation for multiple berth positions and quay cranes," Preprint submitted.

[3] A. Imai, E. Nishimura, and S. Papadimitriou, "The dynamic berth allocation problem for a container port," Transp. Res. Part B, vol. 35, pp. 401–417, 2001.

Filter interpretation of the cost function in regularized FIR modeling

Anna Marconato and Johan Schoukens
Department ELEC
Vrije Universiteit Brussel
Pleinlaan 2, 1050 Brussels
Belgium
anna.marconato@vub.ac.be

1 Introduction

We consider the estimation of FIR models by means of Bayesian regularization techniques. The regularization approach allows one to obtain solutions characterized by a reduced variance, at the price of slightly increasing the bias term. This is done by embedding in the problem prior information about the underlying linear dynamic system, by designing a suitable kernel matrix, see e.g. [1]. In this work, we look at the same problem from a different perspective, focusing on the cost function interpretation, rather than on the kernel definition.

2 Regularized FIR models

The regularized estimate of the impulse response θ is:

$$\hat{\theta}_{reg} = \arg\min_{\theta} \|Y - K\theta\|^2 + \theta^T R\theta = (K^T K + R)^{-1} KY \quad (1)$$

where Y is a vector of length N that contains all output values, $K \in \mathbb{R}^{N\times n}$ is the regressor matrix that contains shifted instances of the input sequence, and R is the *regularization matrix*. Using a Bayesian framework, one has $R = \sigma^2 P_n^{-1}$, where σ^2 is the output noise variance, and P_n is the prior covariance matrix (*kernel*) of the FIR model parameters. P_n is defined to include the assumptions that the impulse response of the system is smooth, and that it exponentially decays to zero. Examples of such a matrix are given by the DC and TC kernels, see [1] for more details. In the following we will focus on the TC kernel, characterized by hyperparameters c and α [1]:

$$P_n(k,j) = c\min(\alpha^k, \alpha^j). \quad (2)$$

3 A cost function interpretation

In this work, we consider the same regularized FIR modeling problem, but we study it from a different angle. Instead of focusing directly on the kernel matrix P_n, and on how the information about the covariance of the parameters is encoded in such a matrix, we address its inverse, the regularization matrix R (up to a constant factor), and we look more closely at how the parameters θ are penalized through the regularization term in the cost function in (1).

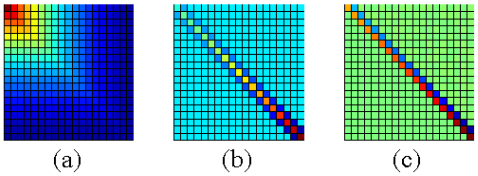

Figure 1: Regularized FIR models: (a) kernel matrix (TC); (b) regularization matrix R; (c) Cholesky decomposition of regularization matrix.

We observe that the inverse R of the (structured) TC kernel (Figure 1a) is a tridiagonal symmetric matrix (Figure 1b), which is derived in closed-form [2]. Inspired by a *random walk kernel*, we recognize in the cost function, due to the structure of R, a squared differences minimization. By computing the Cholesky decomposition of R, $R = U^T U$, we obtain a bidiagonal matrix U (Figure 1c), also derived analytically. This matrix U acts as a prefiltering operation for the parameters, before they enter the cost function. The study of this Cholesky matrix reveals the high-pass nature of the obtained filter, with an increasing gain associated to the parameters at the tail of the impulse response.

These results give more insight into the regularized FIR modeling approach, but they also confirm what we already knew about the TC kernel: we aim at constructing a solution which is smooth (i.e. the high frequency components are suppressed), and which decays to zero (i.e. the parameters at the tail are more heavily penalized). Moreover, this new insight from the cost function perspective could open up possibilities to design the regularization matrix directly, based on the user's specifications.

References

[1] T. Chen, H. Ohlsson and L. Ljung, "On the estimation of transfer functions, regularizations and Gaussian processes - Revisited", Automatica, vol. 48, no. 8, pp. 1525-1535, 2012.

[2] A. Marconato, M. Ishteva and J. Schoukens, "On the asymptotic performance of regularized FIR models", Internal Report VUB-ELEC Marconato 2014.

Towards an assistive drug delivery system for general anesthesia

Dana Copot, Clara Ionescu, Robin De Keyser
Department of Electrical energy, Systems and Automation
Ghent University, Sint-Pietersnieuwstraat 41, 9000, Gent, Belgium
{Dana.Copot,ClaraMihaela.Ionescu,Robain.DeKeyser}@UGent.be

1 Introduction

General anesthesia plays an important role in surgery and intensive care unit (ICU) and requires critical assessment of induced quantities of drugs into the patient [1]. It is characterized by unconsciousness through the action of anesthetics, but also by loss of the ability to perceive pain through the action of analgesics. Analgesia is a key feature of general anesthesia, but there is no available sensor to measure pain relief during general anesthesia. Therefore, in clinical practice, the anesthesiologist has to provide specific care during surgery for neuromuscular blockade, hypnosis and analgesia.

2 Modeling

Pharmacokinetic/pharmacodynamics (PK-PD) modeling brought a significant contribution to anesthesia. PK-PD models are a set of mathematical equations used to predict the drug effect in time. PK models describe what the body does to the drug while PD modeling describe what the drug does to the body. Compartmental modeling approach is widely used in the specialized fields of pharmacokinetics and pharmacology. Compartmental analysis is based on mathematical models represented by a set of differential equations that are widely used to characterize the uptake, distribution and elimination of a drug into the body. From patient-individualized control point of view, PD models are the most challenging part of the patient model and pose most challenges for control (i.e. highly nonlinear characteristic).

3 Control

When inducing and maintaining anaesthesia, anaesthesiologists select initial doses based on a variety of considerations, they observe the results, and then make adjustments based on several factors, at irregularly varying intervals. In control engineering terminology, this constitutes a closed loop control system, due to the feedback present in the observations and interventions of the anesthesiologist. The purpose of computer-controlled closed-loop systems is to formalize the process of observation and intervention as to provide better and more accurate control. A short summary of the control techniques used in anesthesia are presented in figure 1. The proposed closed loop control scheme consists of: the syringe pump, as the actuator; the patient, as the system to be controlled; the monitoring device, which can be considered as the measurable representation of the system to be controlled; the controller, which in represented by the anesthesiologist in figure 2 left and by the computer in figure 2 right.

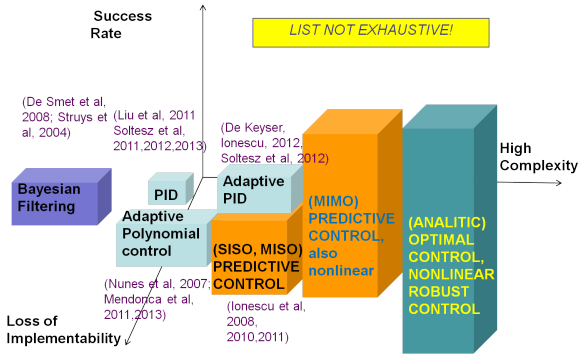

Figure 1: Control methods applied in anesthesia.

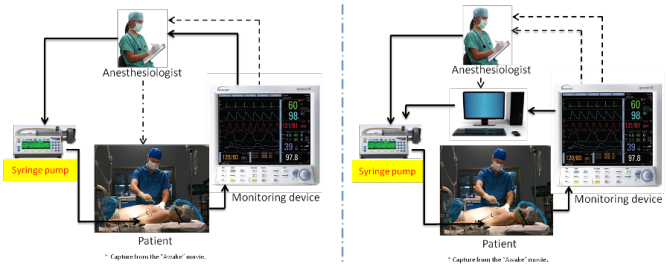

Figure 2: Left: Current state of use in anesthesia. Right: State of the art .

4 Conclusion

General anesthesia is difficult to interpret due to the fact that the physiological signals and responses are time-variant. Standard dosing guidelines often result in an inappropriate under - or over-sedation leading to increased morbidity and mortality.

References

[1] Dumont G, Martinez A, Ansermino M., Robust control of depth of anaesthesia, International Journal of Adaptive Control Signal Processing, 23, 435-454, 2009.

Nonconvex Sorted ℓ_1 Minimization for Compressed Sensing

Xiaolin Huang
ESAT-STADIUS
KU Leuven
3001, Leuven, Belgium
xiaolin.huang@esat.kuleuven.be

Lei Shi
School of Mathematical Sciences
Fudan University
200433, Shanghai, P.R. China
leishi@fudan.edu.cn

Johan A.K. Suykens
ESAT-STADIUS
KU Leuven
3001, Leuven, Belgium
johan.suykens@esat.kuleuven.be

1 Introduction

As an efficient convex relaxation for the ℓ_0 minimization, the ℓ_1 norm has been widely and successfully applied. For problems with fewer samplings, one needs to enhance the sparsity via non-convex methods, e.g., the iteratively reweighted ℓ_1 minimization. It assigns large weights on small components in magnitude and small weights on large components in magnitude, which enhances sparsity but brings nonconvexity. In this study, we consider a new kind of nonconvex penalties, of which the weights are set based on sorting the magnitude. On the one hand, the sorted ℓ_1-norm can enhance the sparsity, due to its non-convexity, and on the other hand it enjoys good convergence behavior, due to its piecewise convexity. Accordingly, we established iteratively reweighted method and iterative sorted thresholding and then prove the convergence to a local optimum. In numerical experiments, the sorted ℓ_1-norm shows better performance in sparse signal recovery than weighting methods based on component values.

2 Nonconvex Sorted ℓ_1 Minimization

Compressed sensing can acquire and reconstruct a signal from relatively fewer measurements than the classical Nyquist sampling. Random linear projections are used to sub-sample the analogue signal and get the digital measurements. The sampling can be formulated in a discrete form as $b=\Phi x$, where $\Phi\in\mathbf{R}^{m\times n}$ is the sampling matrix, $x\in\mathbf{R}^n$ is the signal, and $b\in\mathbf{R}^m$ represents the compressive measurements. We have $m<n$ and x is a sparse signal. To recover a sparse signal, the following method has been well studied,

$$\min_x \quad \|x\|_{\ell_1} \quad \text{s.t. } \Phi x=b,$$

and the corresponding regularization problem is

$$\min_x \quad \|b-\Phi x\|_{\ell_2}^2+2\tau\|x\|_{\ell_1}.$$

Minimizing the ℓ_1-norm is an efficient relaxation for ℓ_0-norm, but for some applications, the result of the ℓ_1 minimization is not sparse enough and the original signals cannot be recovered. To enhance the sparsity, we in this paper will establish a new penalty, which can enhance the sparsity and is equal to a linear function in a large region. The key property of this new penalty is that the weights are related to the sorted order, not the componential values. Specifically, let λ be a nondecreasing sequence of nonnegative numbers,

$$0\le\lambda_1\le\lambda_2\le\cdots\le\lambda_n,$$

with $\lambda_n>0$. The nonconvex sorted ℓ_1 [1] is defined as

$$L_\lambda(x)=\lambda_1|x|_{[1]}+\lambda_2|x|_{[2]}+\cdots+\lambda_n|x|_{[n]}, \qquad (1)$$

where $|x|_{[1]}\ge|x|_{[2]}\ge\cdots\ge|x|_{[n]}$ are the absolute values ranked in decreasing order.

3 Main Result

Iteratively reweighted ℓ_1 minimization for

$$\min_x \quad L_\lambda(x) \quad \text{s.t. } \Phi x=b$$

is essentially the same for other nonconvex penalties. But the set of all the weights is fixed and each reweighting is just a permutation of the weights. This is different from classical iteratively reweighted ℓ_1 minimization methods [2], where each weight is updated independently from the corresponding component of the previous result. This key property allows us to prove the convergence of the iteratively reweighted ℓ_1 minimization for the proposed nonconvex sorted ℓ_1.

We also proved the convergence for iterative sorted soft thresholding for

$$\min_x \quad \|b-\Phi x\|_{\ell_2}^2+2\tau L_\lambda(x).$$

Notice that for other nonconvex regularization problems, the convergence of soft thresholding cannot be guaranteed.

acknowledgement

This works was supported by GOA/10/09 MaNet, CoE PFV/10/002(OPTEC), FWO: G.0377.12, G.088114N, BIL12/11T, IUAP P7/19 (DYSCO, 2012-2017), ERC AdG A-DATADRIVE-B.

References

[1] X. Huang, Y. Liu, S. Lei, S. Van Huffel, J.A.K. Suykens, "Two-level ℓ_1 Minimization for Compressed Sensing," *Signal Processing*, 108:459-475, 2015.

[2] E. J. Candès, M. B. Wakin, S. P. Boyd, "Enhancing sparsity by reweighted ℓ_1 minimization," *Journal of Fourier Analysis and Applications*, 14: 877–905, 2008.

Cayley-Hamilton and Hilbert's function for nD-systems

Antoine Vandermeersch
Department of Electrical Engineering (ESAT)-STADIUS, KU Leuven, 3001 Leuven, Belgium
antoine.vandermeersch@esat.kuleuven.be

Bart De Moor
Department of Electrical Engineering (ESAT)-STADIUS, KU Leuven, 3001 Leuven, Belgium
bart.demoor@esat.kuleuven.be

1 abstract

Similar to the 1D case, there is a strong link between computational algebra and nD realization theory. In 1D realization theory, the link is symbolized using the Cayley-Hamilton theorem. In nD systems theory, systems of multivariate polynomials now form the natural extension that allow us to model nD systems. We utilize a linear algebra framework to establish model orders based on rank properties of large structured matrices that involve the equation coefficients. We provide an intuitive definition of the Cayley-Hamilton theorem for nD systems and illustrate its role in nD realization algorithms. Finally, we show how this Cayley-Hamilton theorem is closely intertwined to the transition from Hilbert function to Hilbert polynomial through the index of regularity in the algebra setting.

Economic impact of sensor and actuator degradation in offices using model based heating and cooling control

Joachim Verhelst, Energyville, KULeuven, Mechanical Engineering Department
Joachim.Verhelst@kuleuven.be,
Van Ham, G., KULeuven, Electrical Engineering Department
Geert.Van.Ham@kuleuven.be,
Saelens D., KULeuven, Building Physics Section
Dirk.Saelens@kuleuven.be
Helsen, L., KULeuven, Mechanical Engineering Department
Lieve.Helsen@kuleuven.be,

The HVAC-installation sector is a highly competitive and demand-driven industry, resulting in many innovations, but also leading to the implementation of some non-standardized control options, which are not equally fault-resilient. Since control components in buildings are prone to degradation during their lifetime, this can have an important economic consequence.

Degradation faults typically reside in HVAC systems unchecked for long periods [Roth et al, 2005][1]. In hydronically heated and cooled offices, degradation of water supply flow actuators, zone air temperature sensors and supply water temperature sensors can have a detrimental impact on energy usage and thermal comfort [Dexter et al, 2004[2]].

In this paper, the economic effects of degradation faults (described above) on the control performance of multiple model-based (MB) controllers are investigated through monte-carlo simulations over a reference year, using an emulator model of a hydronically heated and cooled office. Three controllers are compared, both in fault free and fault present periods, together with their lower performance bound (PB) (free floating indoor air temperature) and upper PB (net energy demand required to realise thermal comfort): (A) an open loop controller with weather compensated temperature control and clock-controlled flow-rate, (B) a PID-controller with dead-band for supply water temperature control and flow-rate control and (C) a receding horizon (RH) controller using a grey-box model.

As an evaluation metric, the averaged yearly net present value (NPV) over 10 years [€/y/m^2] is determined as described in equation 1[3]. Per controller, all related monetized costs are summed, weighted by the expected frequency of occurrence ($freq_{i,j}$) of a specific degradation type (i) and severity level (j). This monetized cost of degradation faults is calculated for each MB controller separately: The (direct) yearly energy cost for heating and cooling C_{Coo} and C_{Hea} are a direct output of the simulations. The (indirect) yearly economic impact of office worker productivity decrease due to thermal discomfort is calculated using the thermal discomfort metric [K^{2}h average/y/zone].

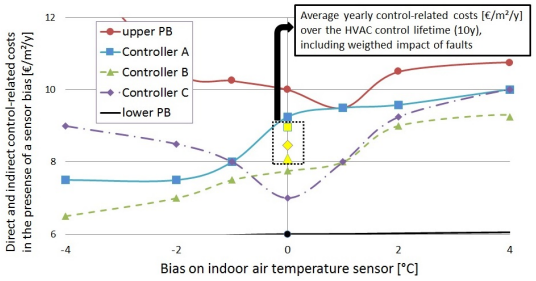

Figure 1: Graphical paper abstract: Each dot represents the emulated direct and indirect economic impact for different model based controllers, evaluated at different levels of sensor bias. The central (yellow) markers enclosed by the dotted line, show the average yearly cost for each MB controller, including occurrence-weighted degradation effects. Note that the data shown here is random!

$$NPV_{MBC,yearly} = \sum_{i:FType} \sum_{j:FSeverity} [(C_{Hea} + C_{Coo} + C_{Disc}) * freq_{i,j}] \quad (1)$$

The simulation results are summarized in graphical overviews (see figure 1) per degradation type and subsequently discussed. These results show the economic impact of sensor and actuator degradation through degraded control performance. This leads to insights on preferential controllers for economic heating and cooling control for offices similar to the studied case. Also, advisable accuracy levels for sensors and actuators are derived.

[1] Roth, K., Westphalen, D., & Feng, M. (2005). Energy impact of commercial building controls and performance diagnostics: market characterization, energy impact of building faults and energy savings potential. Prepared by TAIX LLC. Appendix B

[2] Liao, Z., & Dexter, A. (2004). The potential for energy saving in heating systems through improving boiler controls. Energy and Buildings, 36(3), p 261â“271

[3] Note that this equation is somewhat simplified, since inflation and energy cost increase are also taken into account in the actual NPV calculation.

Controllability and input selection for interconnected systems: a graph theoretic point of view

Jacob van der Woude
Delft Institute of Applied Mathematics
Faculty of Electrical Engineering, Mathematics and Computer Science
Delft University of Technology
Mekelweg 4
2628 CD Delft
The Netherlands
Email: J.W.vanderWoude@tudelft.nl

1 Abstract

In this talk we consider controllability aspects of linear systems. We assume that only the interconnection structure of such systems is available. The systems can then be studied using directed graphs. We recall some well-known graph theoretic criteria for the generic controllability of such structured systems. Also we discuss some of the great challenges that exist in relation to these systems. For instance, how to select the inputs, their type and their (minimal) number, when an autonomous system is required to be made generically controllable.

2 Introduction

In the nowadays society interconnected systems play an important role. For instance, think of complex networks as the internet and the social media, interconnected computer networks, but also networks of chemical or biological processes, and so on. Clearly, the ability to influence or control of such networks is an issue of great importance.

The structured systems in this talk are a special kind of network systems based on linear difference or differential equations with constant coefficients in which the interconnection structure can be exploited. For structured systems statements concerning properties like connectability, controllability, observability, etc. can be derived from the interconnection structure.

3 Structured systems and generic controllability

Consider the linear system $\Sigma : \dot{x} = Ax + Bu$ with A an $n \times n$ matrix and B an $n \times m$ matrix. Assume that only the zero/nonzero structure of the matrices is known and that the nonzeros are so-called algebraically independent. The system Σ can then be represented by the directed graph $G = (V, E)$. The vertex set V of the graph is given by $U \cup X$ with $U = \{u_1, \ldots, u_m\}$ the input vertices, $X = \{x_1, \ldots, x_n\}$ the state vertices. Denoting (v, v') for a directed edge from the vertex $v \in V$ to the vertex $v' \in V$, the edge set E of the graph is described by $E_A \cup E_B$ with $E_A = \{(x_j, x_i) | A_{ij} \neq 0\}$, $E_B = \{(u_j, x_i) | B_{ij} \neq 0\}$. In the latter, for instance $A_{ij} \neq 0$ means that the (i, j)-th entry of the matrix A is a nonzero.

We say that there exists a U-rooted path in G if there is an integer t and a vertex $v \in U$ and distinct vertices $w_1, \ldots, w_t \in X$ such that $(v, w_1) \in E$ and $(w_{i-1}, w_i) \in E$ for $i = 2, \ldots t$. Similarly, there exists an X-circuit in G if there is an integer t and distinct vertices $w_1, \ldots, w_t \in X$ such that $(w_t, w_1) \in E$ and $(w_{i-1}, w_i) \in E$ for $i = 2, \ldots t$. We say that a collection of U-rooted paths and X-circuits is disjoint if every two U-rooted paths and/or X-circuits have no vertex in common. If the collection contains all vertices of X, it is said to cover X. The following result is well-known (in one form or the other, cf. [1], [2])

Theorem *The structured system Σ is generically controllable if and only if every state vertex is on a U-rooted path and there is a collection of U-rooted paths and X-circuits that is disjoint and that covers X.*

4 Input vertex selection

In this talk we want to discuss the problem of making an autonomous structured system, i.e., a system without input vertices, generically controllable by adding a number of input vertices. Questions that will be addressed are where to put these input vertices, of what type do they have to be (one input to one state vertex, one input to many state vertices,...), what is their minimal number, and so on.
This talk is inspired by [3], [4].

References

[1] C.T. LIN, *Structural controllability*, IEEE Trans. Automat. Control, AC-19 (1974), pp. 201–208.

[2] K.J. REINSCHKE, *Multivariable Control, A Graph-theoretic Approach*, Springer-Verlag, New York, 1988.

[3] Y.Y. LIU, J.J. SLOTINE, A.L. BARABASI, *Controllability of complex networks*, Nature, 473, (2011), pp. 167-173.

[4] C. COMMAULT, J.M. DION, *Input addition and leader selection for the controllability of graph based systems*, Automatica, (2013), pp. 3322–3328.

Stability analysis of switching systems with constrained switching sequences.[1]

Matthew Philippe, Raphaël M. Jungers
Institute of Information and Communication Technologies, Electronics and Applied Mathematics
Université catholique de Louvain, Belgium
{matthew.philippe, raphael.jungers}@uclouvain.be

1 Introduction

Discrete-time linear switching systems have appeared in many applications (such as networked control systems, viral mitigation, congestion control, etc...). This work presents a new framework for the stability analysis of such systems.

As a switching system evolves, its dynamics switch between *modes*. For a discrete-time linear switching system, the mode at a given time t, written $\sigma(t)$, is associated to a matrix in a finite set $\mathbf{A} \subset \mathbb{R}^{n\times n}$ of N matrices. The dynamics of such a system are given by

$$x_{t+1} = A_{\sigma(t)} x_t,$$

with $x_0 \in \mathbb{R}^n$ and $A_{\sigma(t)} \in \mathbf{A}$.

The sequence of modes, $\sigma(0), \sigma(1), \ldots$, is called the *switching sequence* of the system. These sequences are often assumed to be non-deterministic. Depending on the application, switching sequences may be subject to logical constraints. To represent these constraints, we use a *finite automaton*. It takes the form of a graph $\mathbf{G}(V,E)$, with V the set of nodes, and E a set of directed, labeled edges. An edge is represented by a triplet $e = (v_i, v_j, \sigma) \in E$, with $v_i, v_j \in V$, and $\sigma \in \{1,\ldots,N\}$ is the label of the edge. A given switching sequence is accepted if there is a path in the graph that generates the sequence with its labels (see example on Figure 1).

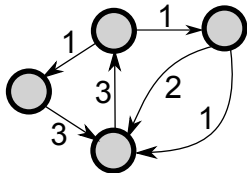

Figure 1: The sequence "1, 2, 2" is forbidden here.

A *constrained switching system* is defined by a set of matrices $\mathbf{A}$ and an automaton $\mathbf{G}$, and is denoted $S(\mathbf{G},\mathbf{A})$. A system is (asymptotically) stable if, for any initial condition and switching sequence, $\lim_{t\to\infty} x_t = 0$.

[1]Research supported by the Belgian Interuniversity Attraction Poles, and the Concerted Research Actions of the French Community of Belgium.
M.P. is a FRIA (F.R.S.-FNRS) Fellow.
R.J. is a FNRS Research Associate.

The results presented here are generalizations of existing results on arbitrary switching systems [1] (i.e. without constraints). We will highlight three questions.

Question 1. *If a system is stable, does it admit a Lyapunov function?*

Interestingly enough, for a stable system, there might not be any Lyapunov function (a positive definite function decreasing along the trajectories) depending solely on x_t. This even holds in the scalar case. However, it can be shown [2] that a *multiple* Lyapunov function, associating a different *vector norm* per node in V, satisfying a contractivity condition along the edges of E, always exists for stable systems.

Question 2. *Can we estimate the exponential growth rate of a system with arbitrary accuracy in finite time?*

We present [2] a scheme based on quadratic approximations of the above mentioned multiple Lyapunov functions. We can estimate the exponential growth rate of a system, with arbitrary accuracy, in finite-time.

Question 3. *When does a marginally unstable system remain bounded?*

Marginally unstable systems are those with a unitary exponential growth rate. Knowing whether the trajectories of such systems remain bounded is a difficult question. For arbitrary switching systems, the irreducibility of the set of matrices ensures boundedness. We present [3] a generalization of the concept of irreducibility for constrained switching systems, taking into account properties of both $\mathbf{G}$ and $\mathbf{A}$.

References

[1] R. Jungers, "The joint spectral radius," *Lecture Notes in Control and Information Sciences*, vol. 385, 2009.

[2] M. Philippe and R. Jungers, "Converse Lyapunov theorems for discrete-time linear switching systems with regular switching sequences," *arXiv preprint: "http://arxiv.org/abs/1410.7197"*, 2014.

[3] M. Philippe and R. Jungers, "A sufficient condition for the boundedness of matrix product accepted by an automaton," To appear in *Proceedings of Hybrid Systems: Computation and Control*, 2015.

A geometric approach to fault detection and isolation for a class of bimodal piecewise-linear systems

A.R.F. Everts[♭], P. Rapisarda[♯] and M.K. Camlibel[♭]

[♭]JBI for Mathematics and Computer Science, University of Groningen, The Netherlands

[♯]CSPC group, School of Electronics and Computer Science, University of Southampton, United Kingdom

a.r.f.everts@rug.nl, pr3@ecs.soton.ac.uk, m.k.camlibel@rug.nl

1 Abstract

In this work we study the fault detection and isolation problem for continuous bimodal piecewise-linear systems. Geometric techniques are used to design observers that generate residual signals which detect and identify faults.

2 Introduction

Fault detection and isolation (FDI) is an active area of research in control theory, due to the essential requirement of high reliability for many applications of control systems. Various types of FDI techniques have been proposed for linear systems and for some classes of nonlinear ones, see e.g. [1]. On the other hand, research on FDI for hybrid and switched systems, and in particular for piecewise linear systems, has been less intensive and fruitful (see [3, 4]).

In this paper, we use the classical geometric control theory framework to investigate the problem of fault detection and isolation for piecewise linear systems. Our approach is inspired by the geometric approach-based ideas pioneered in [2], where several formulations of the fault detection and isolation problem were stated and solved.

3 Problem Statement

We consider the fault detection and isolation (FDI) problem for continuous piecewise-linear systems with two modes. Such systems are given by

$$\frac{d}{dt}x = \begin{cases} A_1x(t)+Bu(t)+\sum_{i=1}^k F_im_i(t) & \text{if } c^\mathsf{T}x(t)\leqslant 0 \\ A_2x(t)+Bu(t)+\sum_{i=1}^k F_im_i(t) & \text{if } c^\mathsf{T}x(t)\geqslant 0 \end{cases} \tag{1a}$$

$$y = Cx, \tag{1b}$$

with state $x\in\mathbb{R}^n$, input $u\in\mathbb{R}^m$, output $y\in\mathbb{R}^p$, fault modes $m_i\in\mathbb{R}^{f_i}$ for $i=1,2,\ldots,k$, vector c and matrices A_1, A_2, B, C and F_i of appriopiate sizes. We assume that the right-hand side of (1a) is continuous in x, which is equivalent to saying that A_1 and A_2 satisfy

$$A_1-A_2 = hc^\mathsf{T}$$

for some $h\in\mathbb{R}^n$. Furthermore, we assume that $\ker C\subseteq \ker c^\mathsf{T}$.

Similar to the FDI problem for linear systems [2], we aim at designing a Luenberger-type observer that produces residual signals. These residuals provide information about the presence and the nature of failures. The dynamics of the to-be-designed observer are

$$\begin{aligned} \frac{d}{dt}\widehat{x}(t) &= \begin{cases} A_1\widehat{x}(t)+Bu(t)-L(y(t)-\widehat{y}(t)) & \text{if } c^\mathsf{T}\widehat{x}(t)\leqslant 0 \\ A_2\widehat{x}(t)+Bu(t)-L(y(t)-\widehat{y}(t)) & \text{if } c^\mathsf{T}\widehat{x}(t)\geqslant 0 \end{cases} \\ \widehat{y} &= C\widehat{x}(t) \\ r_i(t) &= D_i(y(t)-\hat{y}(t)), \qquad i=1,2,\ldots,k, \end{aligned} \tag{2}$$

where r_i is the ith residual and $L\in\mathbb{R}^{n\times p}$ and $D_i\in\mathbb{R}^{q_i\times p}$ are design parameters.

We call observer (2) a *fault detector* for system (1) if the following holds whenever $x(0)=\hat{x}(0)$: $r_i(t)=0$ for all $t\geqslant 0$ if and only if $m_i(t)=0$ for almost all $t\geqslant 0$.

In this talk, we give a sufficient condition for the existence of a fault detector for system (1).

References

[1] I. Hwang, S. Kim, Y. Kim and C.E. Seah, *A Survey of Fault Detection, Isolation, and Reconfiguration Methods*, IEEE Trans. Contr. Syst. Techn. 18(3): 636–653, 2010.

[2] M.-A. Massoumnia, *A geometric approach to the synthesis of failure detection filters*, IEEE Trans. Aut. Contr. 31(9):839–846, 1986.

[3] S. Narasimhan, G. Biswas, G. Karsai, T. Pasternak and F. Zhao, *Building observers to address fault isolation and control problems in hybrid dynamic systems*, Systems, Man, and Cybernetics, IEEE International Conference on:4, p. 2393–2398, 2000.

[4] D. Wang, W. Wang and P. Shi, *Robust fault detection for switched linear systems with state delays*, Systems, Man, and Cybernetics, Part B: Cybernetics, IEEE Transactions on, 39(3):800–805, 2009.

State feedback control for systems pre-compensated by input shapers

Dan Pilbauer, Wim Michiels
Department of Computer Science
Katholieke Universiteit Leuven
3001 Heverlee
Belgium
dan.pilbauer@cs.kuleuven.be

Tomas Vyhlidal
Department of Instrumentation and Control Engineering
Czech Technical University in Prague
160 00 Prague
Czech Republic
tomas.vyhlidal@fs.cvut.cz

1 Abstract

The objective of this work is to investigate the applicability of spectral methods for designing feedback controller for a closed loop system with an input shaper with time delays proposed in [8] and described by equation $v(t) = aw(t) + (1-a)\int_0^T w(t-\eta)dh(\eta)$, where w and v are the shaper input and output.

The primary objective of including such a shaper into to feedback loop is to pre-compensate the low-damped oscillatory modes of a flexible subsystem, which is attached to the controlled main body of the system.

As shown earlier by the authors, inverted distributed delay shaper serves the best for this purpose. However, after inserting a shaper into the feedback loop, the closed loop dynamics becomes infinite dimensional.

A robust controller design then requires guaranteeing that all the poles of the closed loop system will safely be located in the left half of the complex plane. Besides, the closed loop dynamics needs to be sufficiently fast in order to take over and keep filtering properties of the input shaper.

For the spectral design of the controller, the recently developed pole placement method for interconnected time delay systems is applied[3]. By this methodology, the rightmost roots of the closed loop infinite spectrum will be optimized over the controller parameter space to achieve both the above mentioned stability and filtering objectives.

The presented methods are tested on a case study example, which is a multi-degree of freedom mechanical system.

References

[1] Bhat S. P., Miu D. K. (1990), Precise Point-to-Point Positioning Control of Flexible Structures, *ASME Journal of Dynamic Systems, Measurement, and Control*, vol. 112, no. 4, p. 667-674.

[2] Hyde J. M., Seering W. P., (1991), Using Input Command Pre-Shaping to Suppress Multiple Mode Vibration, *IEEE Int.Conf. on Robotics and Automation*, Sacramento, CA, pp. 2604-2609.

[3] Michiels W., Gumussoy S., (2014) Eigenvalue based algorithms and software for the design of fixed-order stabilizing controllers for interconnected systems with time delays, Vyhlidal T., Lafay J.-F., Sipahi R. (editors), Delay systems-from theory to numerics and applications, *Advances in Delays and Dynamics*, Vol. 1, Springer, Cham, p. 243-256

[4] Park J., Chang P. H., Park H. S., Lee E., (2006), Design of Learning Input Shaping Technique for Residual Vibration Suppression in an Industrial Robot, *IEEE/ASME Transaction on mechatronics*, VOL. 11, NO. 1.

[5] Singer N.C., Seering W.P. (1990), Preshaping command input to reduce system vibration, *Journal of Dynamics, System, Measure and Control*, vol 112., pp 76-82.

[6] Singhose W.E., Eloundou R., Lawrence J. (2010). Command Generation for Flexible Systems by Input Shaping and Command Smoothing. *AIAA J. of Guidance, Control, and Dynamics*, 33(6), 1697-1707.

[7] Staehlin U., Singh T. (2003), Design of closed-loop input shaping controllers, in *American Control Conference*, Denver, Co, pp. 51675172.

[8] Vyhlidal T., Kucera V., Hromcik M., (2013), Zero vibration shapers with distributed delays of various types, 52^{nd} *Conference on Decision and Control*, Firenze, Italy, December 10-13, p. 940-945

[9] Vyhlidal T., Kucera V., Hromcik M, (2013), Signal shapers with distributed delays: spectral analysis and design, *Automatica*, Vol. 49, Issue 11, pp. 3484-3489

[10] Vyhlidal T., Hromcik M. (2014) Parameterization of zero vibration shapers with delays of various distribution, submitted to *Automatica*.

Positive stabilization of a discretized diffusion system

Jonathan N. Dehaye, Joseph J. Winkin
Namur Center for Complex Systems (naXys) and Department of Mathematics
University of Namur, 8 Rempart de la Vierge, B-5000 Namur, Belgium
Email: jonathan.dehaye@unamur.be, joseph.winkin@unamur.be

1 Framework

The positive stabilization problem is studied for the class of linear time-invariant (LTI) single-input positive systems that are described by the equation $\dot{x} = Ax + bu$ where A is a Metzler (nonnegative off-diagonal) matrix and b is nonnegative and has only one non-null entry. A feedback (row) matrix k is said to be positively stabilizing for such system if the resulting closed-loop system is positive and internally (exponentially) stable. It is reported that for any system in this class, it is possible to characterize all its positively stabilizing feedbacks by means of a parameterization. The analysis involves positive control theory [1],[2] and linear programming techniques [3].

2 Main result

We have applied this result to an approximate finite difference model of the pure diffusion system described by the parabolic partial differential equation

$$\frac{\partial x}{\partial t} = D_a \frac{\partial^2 x}{\partial z^2}$$

with Neumann boundary conditions

$$\begin{cases} \frac{\partial x}{\partial z}(t,0) &= u \\ \frac{\partial x}{\partial z}(t,L) &= 0 \end{cases}$$

where D_a is the axial dispersion coefficient, L is the domain length and u is the input. Discretizing the system by using finite differences (with n discretization points z_i, $i = 1,...,n$) leads to a finite-dimensional positive system, A being Metzler and b being nonnegative, that falls in the particular class of systems we described above. Clearly, A is not exponentially stable, zero being in its spectrum. Our main result is the fact that we can parameterize the set of all (infinitely many) feedbacks that positively stabilize this diffusion system.

3 Numerical Simulations

This parameterization has been coded in MATLAB as an algorithm that provides the user with a positively stabilizing feedback. The numerical results are dependent upon the choice of parameter values. For example, considering $L = 1$, $D_a = 1$ and $n = 11$ and choosing the all-ones eigenvector corresponding to the Frobenius unstable eigenvalue $\lambda = 0$ as initial condition yielded the state trajectories

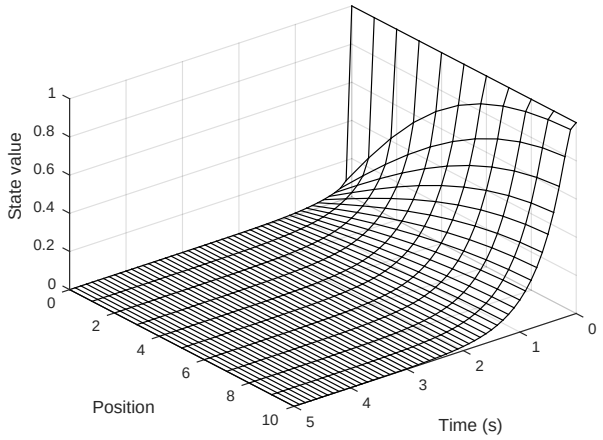

Figure 1: State trajectories in closed-loop

which illustrate as expected the fact that the closed-loop system is positive and that it is stable unlike the open-loop system.

4 Perspectives

The next steps in this work will be notably to optimize the choice of a positively stabilizing feedback, and to analyze the convergence of the algorithm when the discretization step becomes small (i.e. $n \to \infty$) in order to extend the results to infinite-dimensional systems. These questions are currently under investigation.

Acknowledgement: This abstract presents research results of the Belgian Network DYSCO (Dynamical Systems, Control, and Optimization), funded by the Interuniversity Attraction Poles Programme initiated by the Belgian Science Policy Office.

References

[1] B. Roszak and E. J. Davison, Necessary and sufficient conditions for stabilizability of positive LTI systems, *Systems & Control Letters*, Vol. 58, 2009, pp. 474-481.

[2] J. N. Dehaye, *Stabilisation positive de systemes differentiels lineaires : theorie et application aux reacteurs tubulaires*, Master thesis, University of Namur, Belgium, 2011.

[3] A. Schrijver, *Theory of Linear and Integer Programming*, John Wiley & Sons, 1998.

Fault Classification in Batch Processes: Contribution Plots versus Process Data

S. Wuyts, G. Gins, P. Van den Kerkhof and J.F.M. Van Impe
BioTeC, Department of Chemical Engineering, KU Leuven
W. de Croylaan 46 PB 2423, B-3001 Heverlee (Leuven), Belgium
{sam.wuyts, geert.gins, jan.vanimpe}@cit.kuleuven.be

1 Introduction

Batch processes are indispensable for the (bio)chemical industry, especially in the production of high added value products such as pharmaceuticals or specialty chemicals. The inherent dynamic nature of a batch process and the scarcity of online product quality measurements limit its controllability. Therefore, monitoring, fault detection and fault diagnosis in batch processes is not straightforward.

Statistical Process Control (SPC) is generally applied to solve this problem. Chemical plants typically store all available online measurements of a large set of process variables in large historical databases. These databases provide a lot of information which is efficiently exploited by SPC to establish a fast and reliable monitoring and fault detection procedure.

2 Problem statement

After the detection of a process upset, the root cause still needs identification to enable a timely remediation. In SPC, experts and operators typically evaluate abnormal events based on contribution plots [2], because these do not require prior knowledge about underlying process disturbances. However, contribution plots that unequivocally reveal the underlying variable(s) causing the fault are rare and expert interpretation of the contribution pattern is hence still required for accurate fault diagnosis.

When all possible fault classes are known, the root cause of the detected process fault can be determined via an automated classifier trained on faulty data. This substantially reduces the time between fault detection and remediation because the expert interpretation of the contribution plot is bypassed. Misclassification of faults is however still possible due to the so-called *fault smearing effect*, which negatively impacts the accuracy of the contributions [3, 4].

Providing alternative data patterns (i.e., patterns not subject to fault smearing) to the classifier might therefore ameliorate automatic classification performance. This paper compares the classification accuracy for two different classifier input patterns: the first contains the variables' contributions while the second consists of the raw or pretreated process data.

3 Results

Simulation of the benchmark penicillin fermentation process `Pensim` in `RAYMOND` [1] yields data to test the classification accuracy for both fault classification approaches. To maximize the performance, both the variables' contributions and the process data are pretreated in different ways depending on the characteristics of the occurring faults. These pretreatments are found to have a major influence on the classification. Furthermore, the negative influence of fault smearing on the contributions is confirmed. The conclusion is that better automatic classification performance is achieved by using the pretreated process measurements rather than the variables' contributions as classifier input patterns.

Acknowledgements. Work supported in part by Project PFV/10/002 (OPTEC Optimization in Engineering Center) of the Research Council of the KU Leuven, KU Leuven Knowledge Platform SCORES4CHEM (www.scores4chem.be), and the Belgian Program on Interuniversity Poles of Attraction initiated by the Belgian Federal Science Policy Office. The authors assume scientific responsibility.

References

[1] G. Gins, J. Vanlaer, P. Van den Kerkhof and J.F.M. Van Impe. The RAYMOND simulation package – Generating RAYpresentative MONitoring Data to develop advanced process monitoring and control algorithms. *Computers & Chemical Engineering*, 69:110–118, 2014.

[2] P. Nomikos. Detection and diagnosis of abnormal batch operations based on multi-way principal component analysis, World Batch Forum, Toronto, May 1996. *ISA Transactions*, 37(1):41–59, 1996

[3] P. Van den Kerkhof, J. Vanlaer, G. Gins and J. F. Van Impe. Analysis of smearing-out in contribution plot based fault isolation for Statistical Process Control. *Chemical Engineering Science*, 104:285–293, 2013.

[4] J. A. Westerhuis and S. P. Gurden and A. K. Smilde. Generalized contribution plots in multivariate statistical process monitoring. *Chemometrics and Intelligent Laboratory Systems*, 51(1):95–114, 2000.

Dynamic Event-triggered Control: Guaranteed $\mathscr{L}_p$-gain Performance and Zeno-freeness

V.S. Dolk D.P. Borgers W.P.M.H. Heemels
Department of Mechanical Engineering, Eindhoven University of Technology, The Netherlands
Email: {v.s.dolk, d.p.borgers, w.p.m.h.heemels}@tue.nl

1 Introduction

In most networked control system (NCS) applications, the communication resources are often limited and possibly shared with other tasks. Hence, efficient use of the network is desired in the sense that the number of transmission instants should be limited. In traditional digital control schemes, these transmission instants are determined in a time-triggered fashion according to a fixed sample period. In event-triggered control (ETC) systems, transmission instants are determined online, using well-designed event conditions based on, *e.g.*, state measurements of the system. As such, ETC aims to reduce the communication utilization with respect to time-triggered schemes by only transmitting data when needed to maintain desired stability and control performance. One of the main difficulties in ETC is to design an event-triggering mechanism (ETM) which ensures the existence of a minimum inter-event time (MIET), especially in the presence of disturbances. This positive MIET is an essential property to exclude Zeno behavior (the occurence of an infinite number of events in finite time), and to enable practical implementation of the ETC system. As in many applications disturbances are present, it is also desired to guarantee a finite $\mathscr{L}_p$-gain that represents the level of disturbance attenuation when constructing the ETM. In this work, a novel event-triggered control (ETC) strategy is proposed that can simultaneously guarantee a finite $\mathscr{L}_p$-gain and a strictly positive lower bound on the inter-event times. See [3] for more details.

2 ETC method

To guarantee a robust MIET, most recent works on ETC employ time-regularization, at which the trigger condition is only being monitored after a specific time duration τ_{miet} since the last transmission event, to enforce a positive lower-bound on the inter-event times. The majority of these works consider *static* ETMs, at which the next transmission instant t_{k+1} is determined by a condition of the form

$$t_{k+1} := \inf\{t > t_k + \tau_{miet} \mid \Psi(x,e) < 0\},$$

where x is the state vector and e the transmission error. However, such an ETC scheme reduces to approximately time-triggered periodic communication when the state is close to the origin. For this reason, we consider a *dynamic* ETM of the form

$$\dot{\eta} = \Psi(x,e,\eta),\ \eta^+ = \eta_0(e)$$
$$t_{k+1} := \inf\{t > t_k + \tau_{miet} \mid \eta(t) < 0\},$$

see also [4] and [5]. In this paper we present a systematic approach to find Ψ, η_0 and τ_{miet}, which is inspired by [1] and [2] that provide time-based specifications for NCS are provided, in terms of a maximum allowable transmission interval τ_{mati}, such that a finite $\mathscr{L}_p$-gain is guaranteed. In fact, the ETM proposed here guarantees a τ_{miet}, which is slightly smaller than the τ_{mati} bound for time-based NCS.

3 Numerical Example

The plots below show that the proposed *dynamic* ETM does not converge to a time-triggered solution in contrast to static ETMs employing time-regularization. Moreover, the proposed dynamic ETC schemes yield average transmission intervals, which are significantly larger than the MATI bounds derived in [1] and [2].

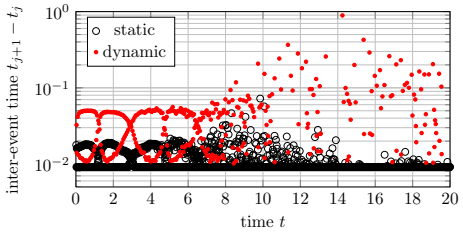

Figure 1: Inter-event times corresponding to $\mathscr{L}_2$-gain $\theta = 4$

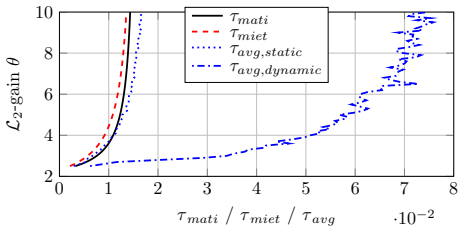

Figure 2: Tradeoff curves between $\mathscr{L}_2$-gain and minimum and average transmission intervals

This work is supported by the Dutch Technology Foundation (STW) through the project Integrated design approach for safety-critical real-time automotive systems (No. 12698), and the VICI grant Wireless control systems: A new frontier in automation (No. 11382).

References

[1] D. Carnevale, A.R. Teel, D. Nešić, A Lyapunov Proof of an Improved Maximum Allowable Transfer Interval for Networked Control Systems, TAC, 2007.

[2] W.P.M.H. Heemels, A.R. Teel, N. van de Wouw, Nešić, Networked control systems with communication constraints: Tradeoffs between transmission intervals, delays and performance, TAC, 2010.

[3] V.S. Dolk, D.P. Borgers and W.P.M.H. Heemels, Dynamic Event-triggered Control: Tradeoffs Between Transmission Intervals and Performance, Proc. 53rd IEEE Conf. Decision and Control, 2014.

[4] R. Postoyan, P. Tabuada, D. Nešić, A. Adolfo, Event-triggered and self-triggered stabilization of distributed networked control systems, Proc. 50th IEEE Conf. Decision and Control, 2011.

[5] A. Girard, Dynamic triggering mechanisms for event-triggered control, TAC, 2014.

Distributed Sensor Fault Detection and Isolation over Sensor Network

Jingjing Hao and Michel Kinnaert
Department of Control Engineering and System Analysis
Université libre de Bruxelles (ULB)
Email: Jingjing.Hao@ulb.ac.be, Michel.Kinnaert@ulb.ac.be

1 Introduction

Wireless sensor networks (WSN) can be used in a wide range of applications including environment monitoring and structural health monitoring. For many applications, sensor nodes are exposed directly in inaccessible or extreme environment. The external environment could have influence on the sensing components of the sensor nodes or even destroy them. In order to provide reliable measurements, one should make sure that the measurements are fault free before using the measurements recorded by the WSN. Model-based approaches such as parity equations and observer-based methods have been widely used for sensor fault detection and isolation (FDI). As the traditional centralized solution to FDI would be complex and would consume a large amount of energy for a large scale system, distributed methods have drawn significant attention recently. The aim of this work is to design and implement distributed monitoring algorithm requiring limited computational resources while being robust with respect to environmental and operational changes.

2 Distributed system model

The considered dynamic system is described by the following state equation:

$$x(k+1) = Ax(k) + B_u u(k) + B_v v(k)$$

where $x(k)$ is the system state, $u(k)$ is the system input and $v(k)$ is the process noise.

At the i^{th} node of the network, measurement $y_i(k)$ as given by the following equation is recorded:

$$y_i(k) = C_i x(k) + D_{u,i} u(k) + f_i(k) + \varepsilon_i(k)$$

where $f_i(k)$ is the fault vector at node i and $\varepsilon_i(k)$ is the measurement noise. $v(k)$ and $\varepsilon_i(k)$ are zero mean uncorrelated white noise sequences. The network is made of M nodes and it is characterized by its adjacency matrix W, a $M \times M$ matrix with Boolean entries. If nodes i and j are connected, the $(i,j)^{th}$ entry is equal to 1 otherwise, the entry is equal to 0.

3 Distributed sensor fault detection and isolation system

Based on the above model, a FDI system is designed at each node. It combines a residual generator based on the parity space approach and a statistical change detection and isolation algorithm. An iterative systematic approach is developed to ensure that a desired fault detection performance is achieved at each node, when possible, while limiting the exchange of information with neighboring nodes. The performance is characterized in terms of a lower bound on the probability of correct detection, and an upper bound on the probability of false detection. The methodology relies on the Kullback-Leibler divergence between the probability density function of the residual in faulty and fault free modes to select the data to be exchanged between different nodes. Simulations on a simple example illustrate the effectiveness of the method.

References

[1] Daniel Eriksson and Erik Frisk and Mattias Krysander. A method for quantitative fault diagnosability analysis of stochastic linear descriptor models, Automatica 49 (2013), pp. 1591-1600.

[2] Michele Basseville and Igor V. Nikiforov, Detection of Abrupt Changes (Prentice-Hall, 1993).

Plenary Lectures

Plenary: P1 **Les Arcades**

PID: Past, present and perspectives

Tore Hägglund

Chair: Clara Ionescu **Tuesday, 11.30–12.30**

Except for the on/off controller, the PID controller is the simplest controller one can imagine. It is also by far the most common controller in industry. The presentation will start with a discussion about the function of the PID controller, how it has been developed over the years, and how it is used in industry today.

The focus of the presentation will be on PID controller tuning. There are numerous methods to tune the parameters of the controller proposed and published in the literature. In spite of this, most PID controllers are badly tuned or even not tuned at all.

There are several aspects that should be taken into account when tuning a PID controller. The closed-loop system should behave well with respect to setpoint changes, load disturbances, and measurement noise. It must also be robust to process variations, since most processes are nonlinear. Very few design methods take all these aspects into account, especially not simple ones. The many aspects and the fact that the specifications vary from case to case make the PID controller tuning a trade-off problem, that can be seen as a constrained optimization problem. The trade-off trade-off has to be made by the engineers, either manually or computer based.

Measurement noise has only recently been taken into account in PID controller tuning. This may be one reason why the derivative part is so seldom used in practice. It is difficult to take the noise into account without knowledge of the noise characteristics, but it is suggested that the filter in the PID controller is tuned so that it is as effective as possible in reducing the control signal variations due to noise, but with a limited reduction of the control performance at load disturbances.

Finally, it should be remarked that even a good design method will not solve the problem that the engineers have very limited time to spend on the controller tuning. Therefore, the presentation ends with a discussion about automatic tuning procedures, and how these should be developed to meet the demands and be accepted and used more extensively in industry.

PID: Past, Present and Perspectives

Tore Hägglund

Dept. of Automatic Control
Lund University

PID: Past, Present and Perspectives

1. What is a PID controller?
2. How is it used?
3. The basic feedback loop
4. PID controller design
5. Common tuning rules
6. Design of noise filter
7. Automatic tuning

PID: Past, Present and Perspectives

The textbook version:

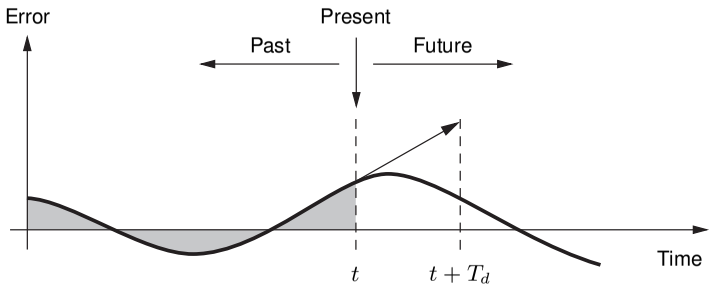

$$u = K\left(e + \frac{1}{T_i}\int e(t)dt + T_d\frac{de}{dt}\right)$$

Parallel form

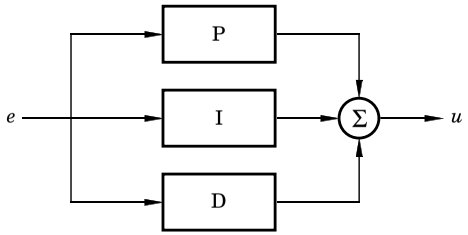

$$u = K\left(e + \frac{1}{T_i}\int e(t)dt + T_d\frac{de}{dt}\right)$$

Series form

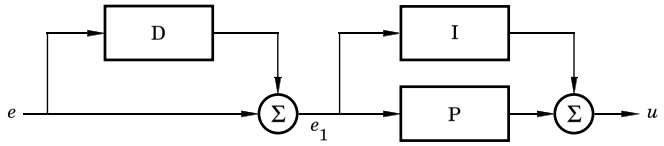

$$e_1 = e + T_d' \frac{de}{dt}$$

$$u = K' \left(e_1 + \frac{1}{T_i'} \int e_1(t)dt \right)$$

Integral action - classical implementation

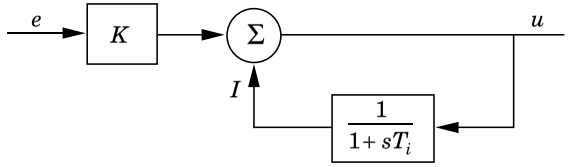

$$u = Ke + I = T_i \frac{dI}{dt} + I.$$

$$T_i \frac{dI}{dt} = Ke,$$

$$u = K \left(e + \frac{1}{T_i} \int e(\tau)d\tau \right),$$

Derivative action - classical implementation

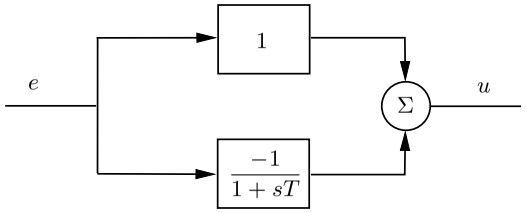

$$U(s) = \left(1 - \frac{1}{1+sT}\right) E(s) = \frac{sT}{1+sT} E(s)$$

Two PID controllers

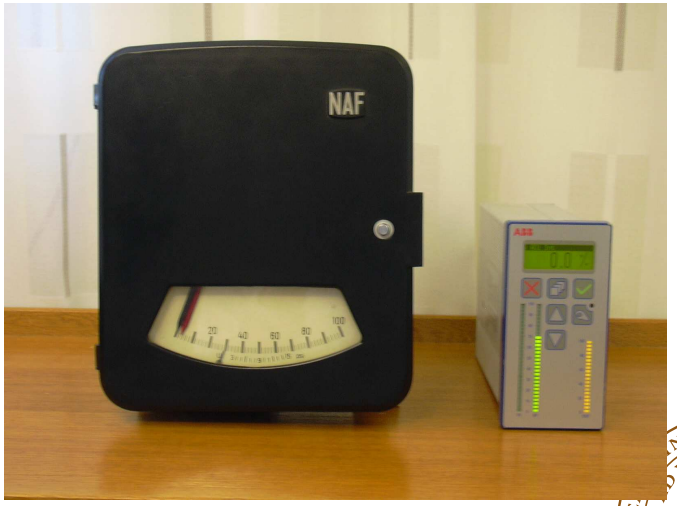

Pneumatic PID controller

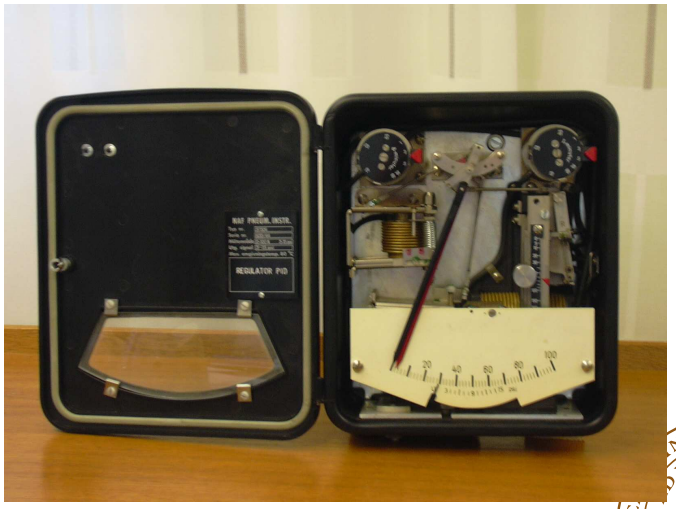

Computer-based PID controller

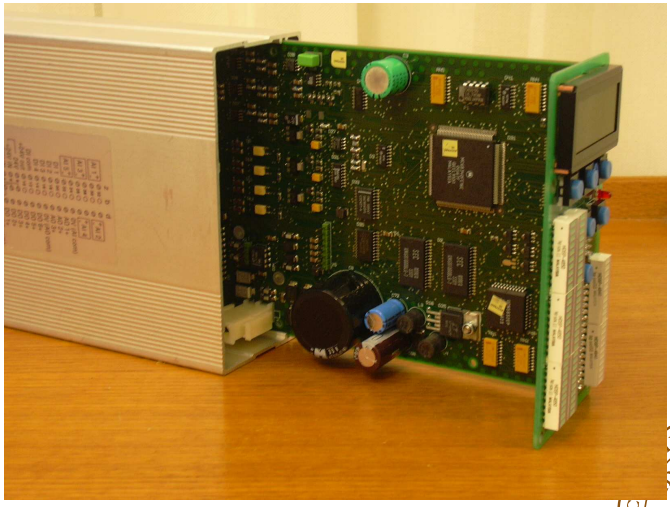

PID: Past, Present and Perspectives

1. What is a PID controller?
2. How is it used?
3. The basic feedback loop
4. PID controller design
5. Common tuning rules
6. Design of noise filter
7. Automatic tuning

Process Control

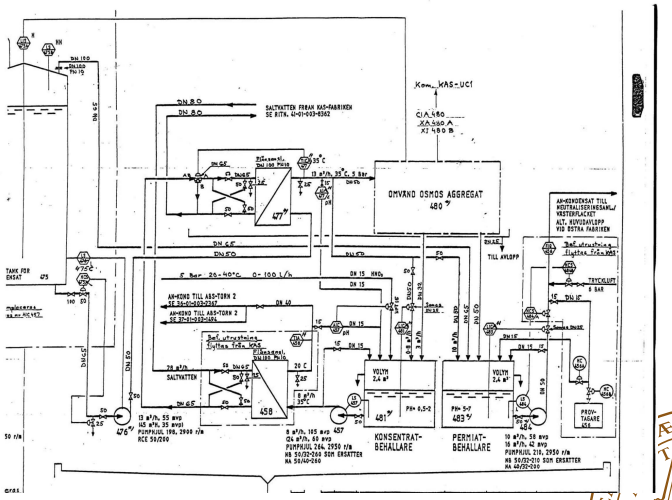

Process Control

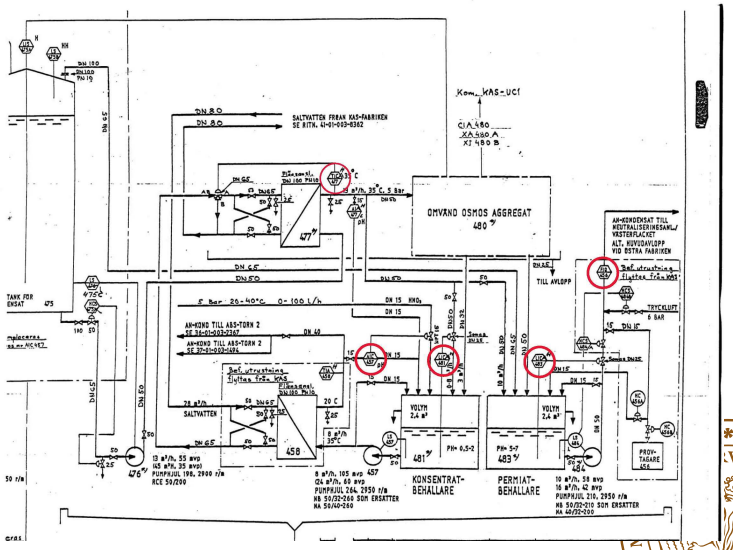

Tore Hägglund: PID: Past, Present and Perspectives

Automation history

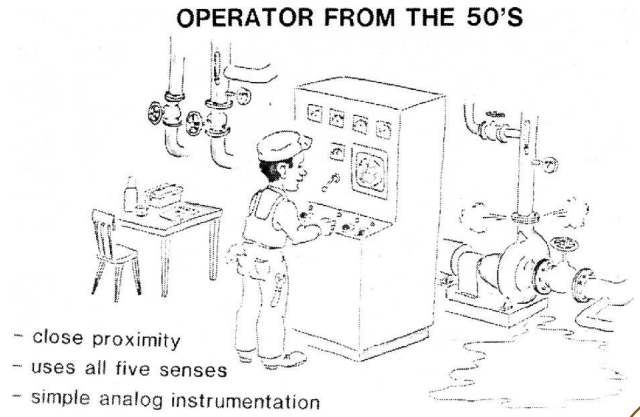

Tore Hägglund: PID: Past, Present and Perspectives

Automation history

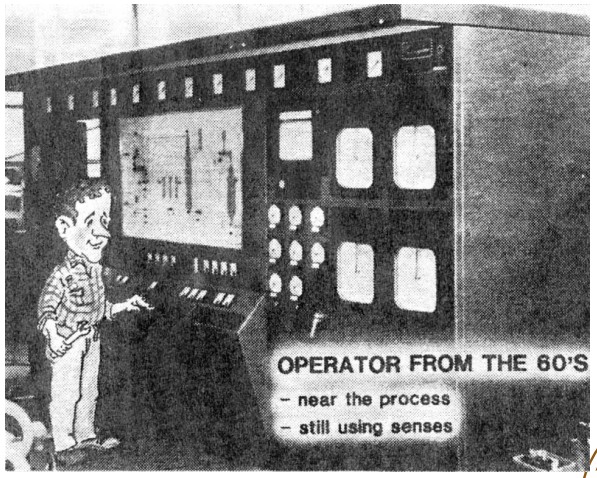

Tore Hägglund: PID: Past, Present and Perspectives

Automation history

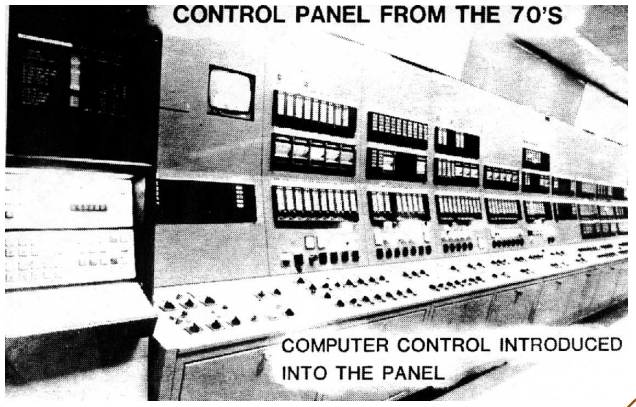

Tore Hägglund: PID: Past, Present and Perspectives

Automation history

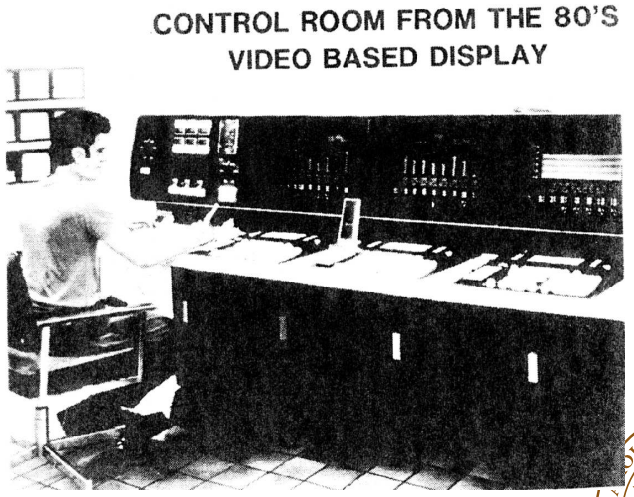

Automation history

The automation trend

- Fewer operators
- More to supervise
- Control rooms ⇒ sight, hearing, smelling are not used anymore
- Operators don't know the process as before
- More complicated processes
- Higher quality demands

PID: Past, Present and Perspectives

1. What is a PID controller?
2. How is it used?
3. The basic feedback loop
4. PID controller design
5. Common tuning rules
6. Design of noise filter
7. Automatic tuning

The basic feedback loop

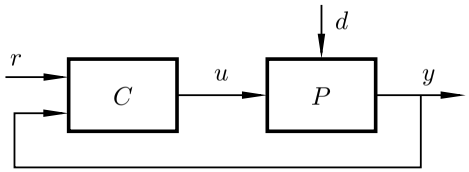

The basic feedback loop

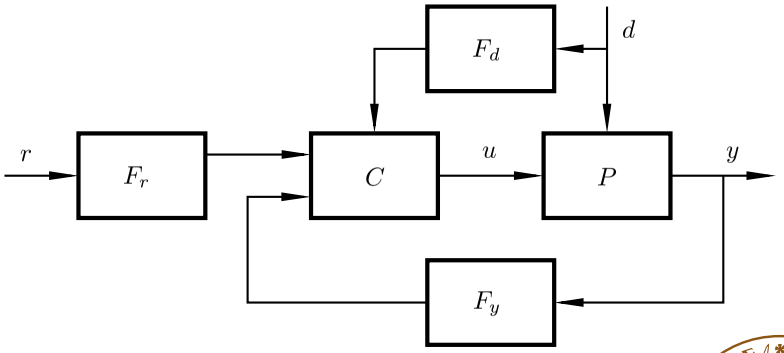

Controller with filters

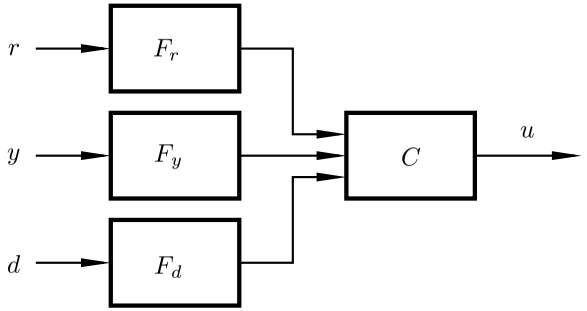

Setpoint filter F_r

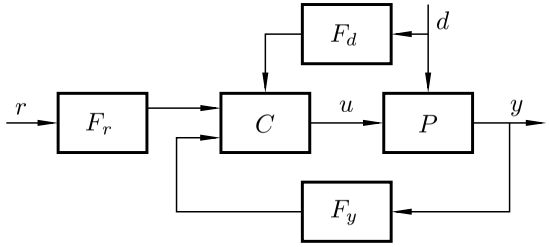

- Utilize the two degrees of freedom
- Remove undesired components in r

Process output filter F_y

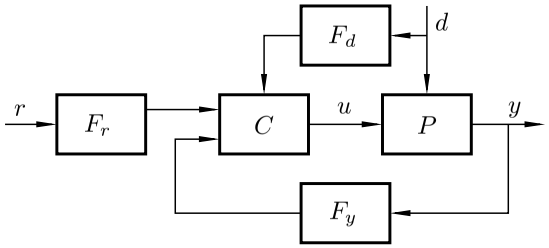

- Noise filtering
- Dynamics compensation

Disturbance filter F_d

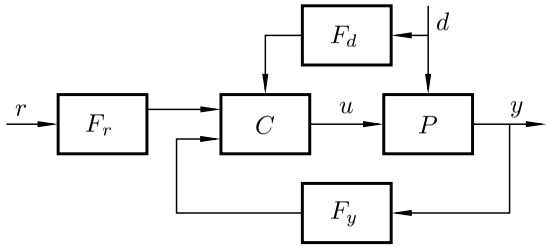

- Feedforward control

Summary

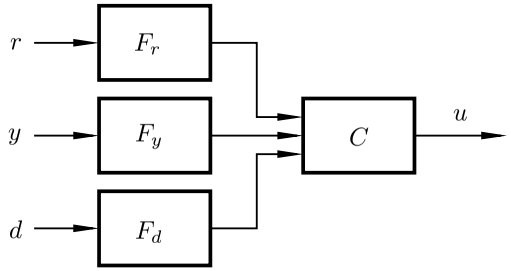

F_r: Separate setpoint and load handling.
Remove undesired components in r.

F_y: Modify the process dynamics.
Remove undesired components in y.

F_d : Feed information about d forward.

PID: Past, Present and Perspectives

1. What is a PID controller?
2. How is it used?
3. The basic feedback loop
4. PID controller design
5. Common tuning rules
6. Design of noise filter
7. Automatic tuning

Process Control today

- Never tuned – Automatic mode (default settings)
- Never tuned – Manual mode
- Manual tuning – PI only!
- Automatic tuning

Why?

Specifications

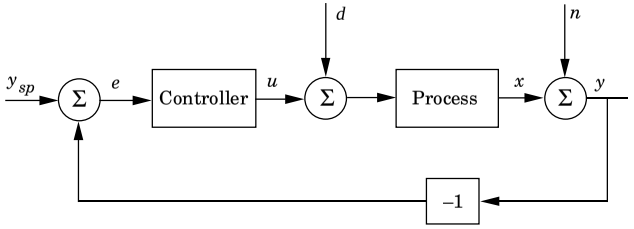

- Setpoint following
- Load disturbance rejection
- Measurement noise amplification
- Robustness with respect to process variations

Two degrees of freedom

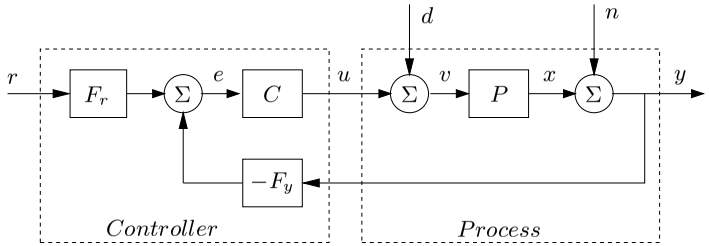

We can forget setpoint following in the controller design.

Performance at load disturbances

Common design criteria:

Minimize

$$IAE = \int |e(\tau)| d\tau$$

$$ISE = \int e(\tau)^2 d\tau$$

$$IE = \int e(\tau) d\tau = \frac{T_i}{K} = \frac{1}{k_i}$$

at step changes in the load.

Robustness

Sensitivity functions:

$$S(i\omega) = \frac{1}{1 + P(i\omega)C(i\omega)}, \quad T(i\omega) = \frac{P(i\omega)C(i\omega)}{1 + P(i\omega)C(i\omega)}$$

Useful measures:

$$M_s = \max_\omega(|S(i\omega)|)$$
$$M_t = \max_\omega(|T(i\omega)|)$$
$$M_{st} = \max_\omega(|S(i\omega)|, |T(i\omega)|)$$

Suitable values: $1.2 \leq M \leq 2$

Robustness

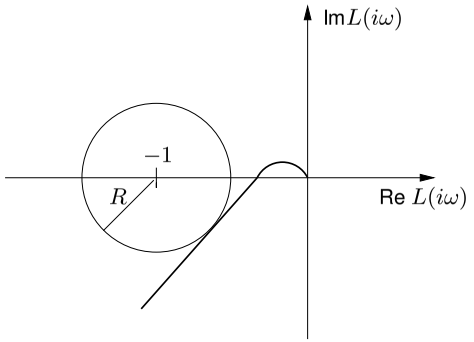

$$R = 1/M_s$$

Noise sensitivity

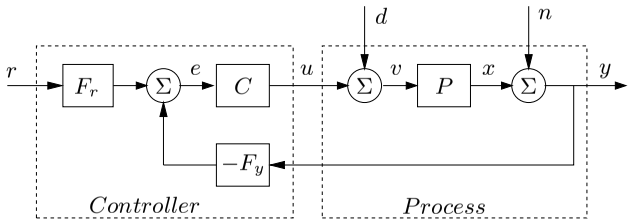

$$U = -\frac{CF_y}{1 + PCF_y}N \approx CF_y$$

Standard deviation of u, when n is white noise:

$$\text{SDU} = \sigma_{uw} = \sqrt{\int_{-\infty}^{\infty} |G_{un}(i\omega)|^2 \Phi_0 d\omega} = ||G_{un}||_2.$$

The normalized time delay

Process model:

$$P(s) = \frac{K_p}{1 + sT}e^{-sL}$$

The normalized time delay

$$\tau = \frac{L}{L + T}$$

Lag dominant	$0 \leq \tau \leq 0.2$
Balanced	$0.2 < \tau < 0.7$
Delay dominant	$0.7 \leq \tau \leq 1$

Three process models

$$P_1(s) = \frac{1}{(s+1)(0.1s+1)(0.01s+1)(0.001s+1)} \qquad \tau = 0.067$$

$$P_2(s) = \frac{1}{(s+1)^4} \qquad \tau = 0.33$$

$$P_3(s) = \frac{1}{(1+0.05s)^2} e^{-s} \qquad \tau = 0.92$$

Normalized time delay

$$\tau = \frac{L}{L+T}$$

Trade-off plots

P_1 - Lag-dominant dynamics

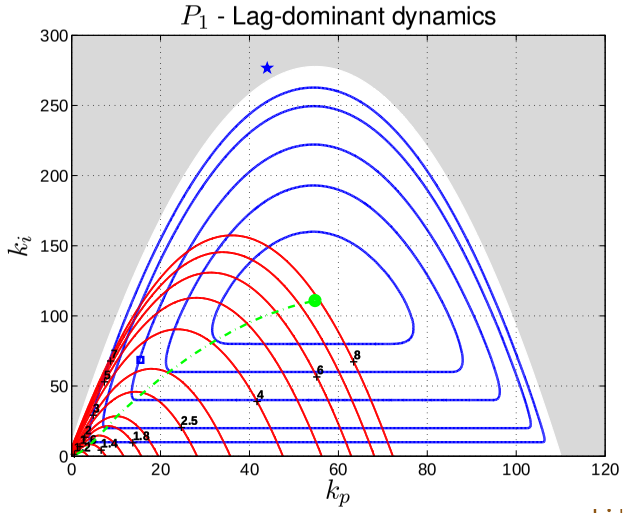

Trade-off plots

P_1 - Lag-dominant dynamics

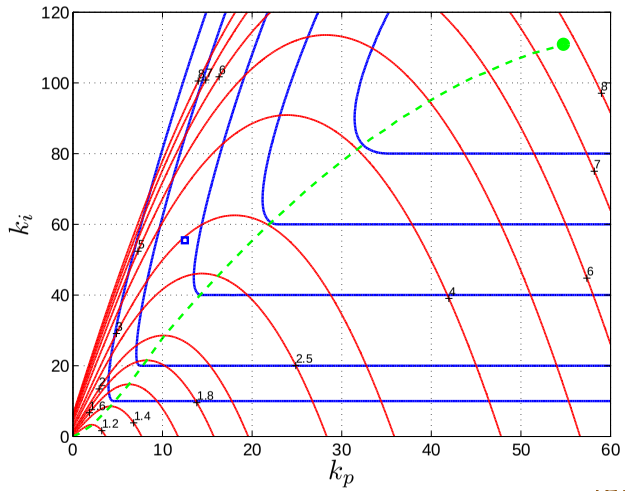

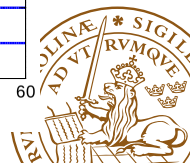

Trade-off plots

P_2 - Balanced dynamics

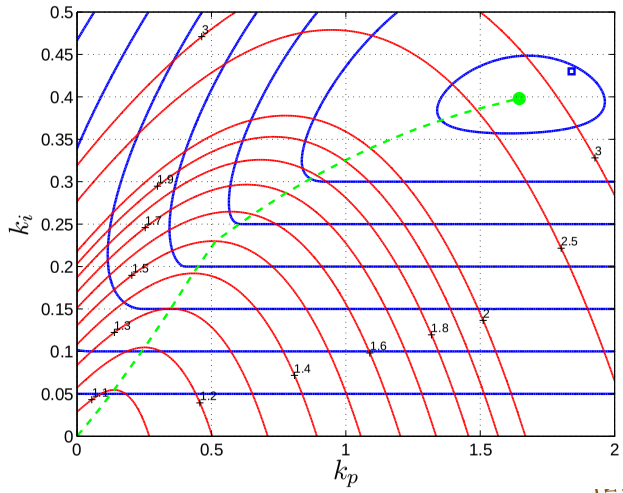

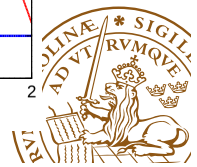

Trade-off plots

P_3 - Delay-dominant dynamics

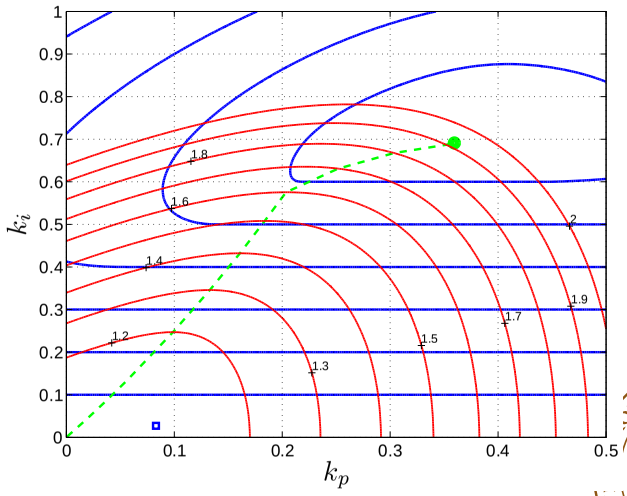

PID: Past, Present and Perspectives

1. What is a PID controller?
2. How is it used?
3. The basic feedback loop
4. PID controller design
5. Common tuning rules
6. Design of noise filter
7. Automatic tuning

Ziegler-Nichols' step response method

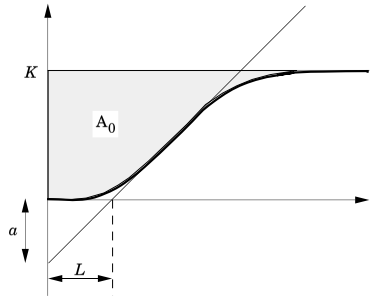

Design criterion: Decay ratio 0.25

Two parameters: a and L

Ziegler-Nichols' step response method

Controller	K	T_i	T_d
P	$1/a$		
PI	$0.9/a$	$3L$	
PID	$1.2/a$	$2L$	$0.5L$

The Lambda Method

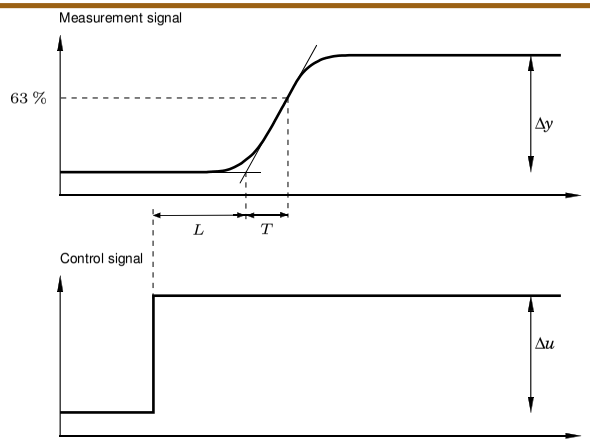

$$K_P = \frac{\Delta y}{\Delta u}$$

The Lambda Method

Process:

$$P(s) = \frac{K_p}{1+sT}e^{-sL}$$

Desired closed-loop transfer function ($r \rightarrow y$)

$$G(s) = \frac{1}{1+s\lambda}e^{-sL}$$

The Lambda method

PI control

$$K = \frac{1}{K_p}\frac{T}{L+\lambda}$$
$$T_i = T$$

$$\lambda = \begin{cases} T & \text{"Aggressive" control} \\ 2T & \text{"Secure" control} \\ 3T & \text{"Robust" control} \\ \max(T, 3L) & \text{Process with long time delay} \end{cases}$$

The Lambda method

PID control, series form

$$K' = \frac{1}{K_p}\frac{T}{L/2+\lambda}$$
$$T_i' = T$$
$$T_d' = \frac{L}{2}$$

Skogestad's SIMC

Modification of the Lambda method

$$K = \frac{1}{K_p}\frac{T}{L+\lambda}$$
$$T_i = \min(T, 4(\lambda + L))$$

$$\lambda = \begin{cases} L & \text{Primary choice} \\ > L & \text{More robust control} \end{cases}$$

Skogestad's SIMC+

Modification for delay-dominant systems

$$K = \frac{1}{K_p}\frac{T + L/3}{L+\lambda}$$
$$T_i = \min(T + L/3, 4(\lambda + L))$$

The Amigo tuning rules

1. Considered a batch of 134 process models.
2. Tuned PI and PID controllers based on M-constrained Integral Gain Optimization.
3. Found FOTD approximations of all models.
4. Found relations between the FOTD models and the controller parameters.

AMIGO – PI

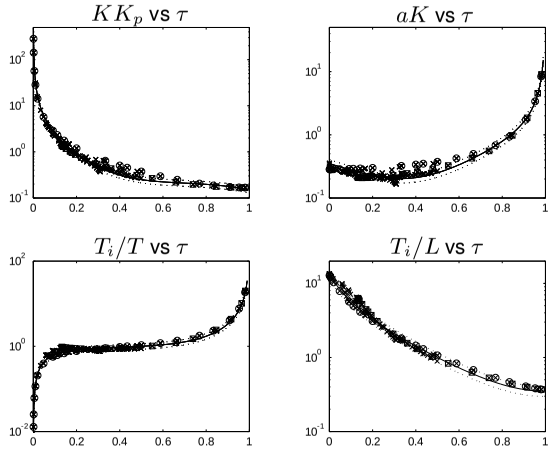

AMIGO – PI

$$K = \frac{0.15}{K_p} + \left(0.35 - \frac{LT}{(L+T)^2}\right)\frac{T}{K_p L}$$

$$T_i = 0.35L + \frac{13LT^2}{T^2 + 12LT + 7L^2}$$

AMIGO – PID

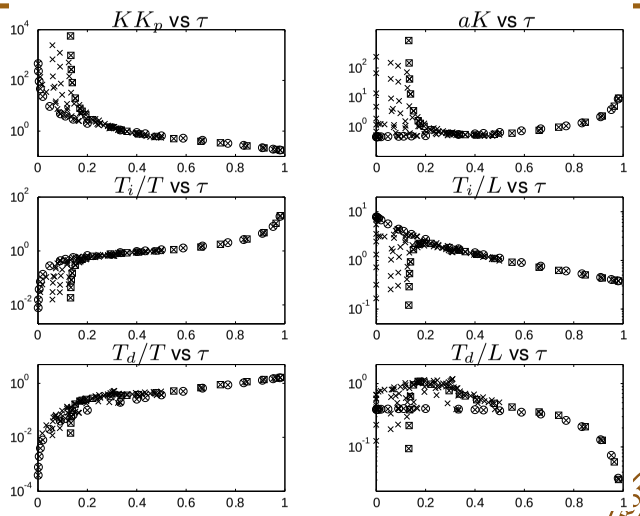

AMIGO – PID

Conservative tuning rules:

$$K = \frac{1}{K_p}\left(0.2 + 0.45\frac{T}{L}\right)$$

$$T_i = \frac{0.4L + 0.8T}{L + 0.1T}L$$

$$T_d = \frac{0.5LT}{0.3L + T}$$

Efficient for $\tau > 0.2$

Conservative for $\tau < 0.2$

Trade-off plots

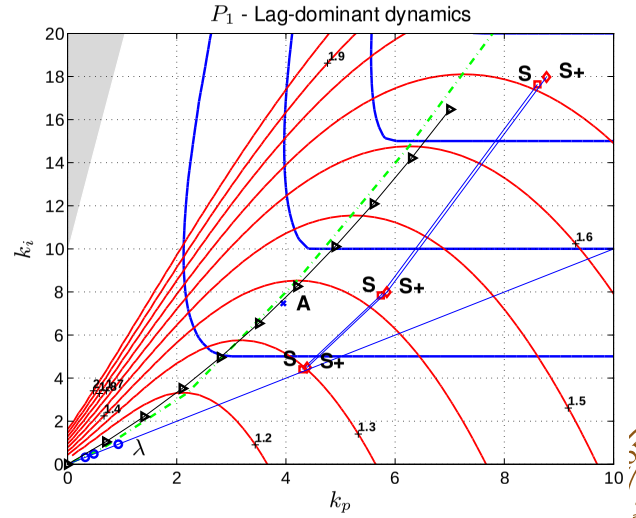

Trade-off plots

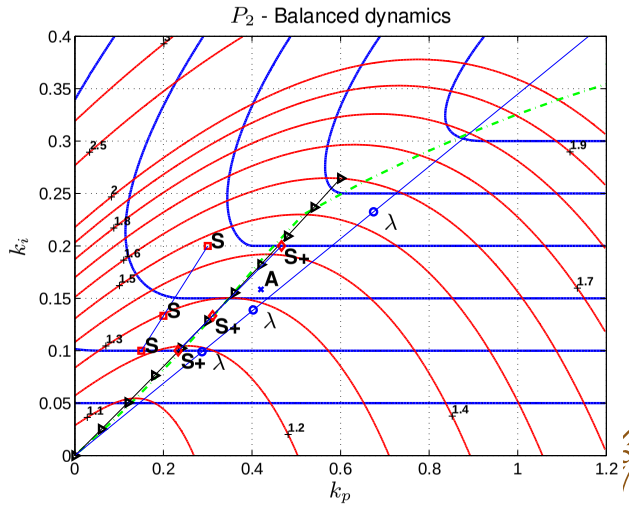

Trade-off plots

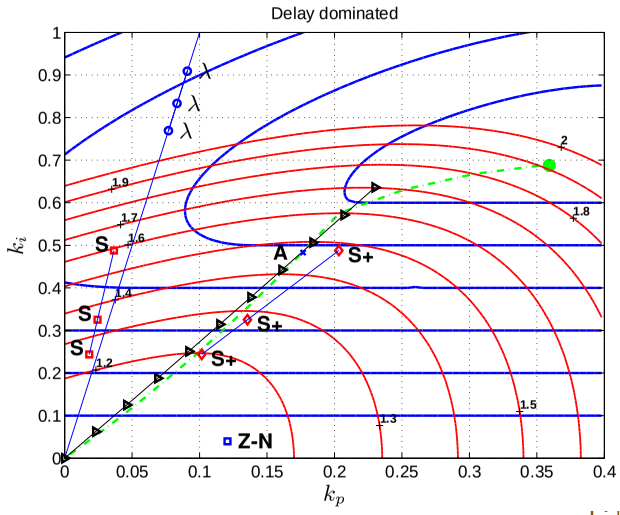

PID: Past, Present and Perspectives

1. What is a PID controller?
2. How is it used?
3. The basic feedback loop
4. PID controller design
5. Common tuning rules
6. Design of noise filter
7. Automatic tuning

Noise filtering in PID controllers

Traditional solutions:

$$C = K\left(1 + \frac{1}{sT_i} + \frac{sT_d}{1 + sT_d/N}\right)$$

$$C = K\left(1 + \frac{1}{sT_i}\right)\left(1 + \frac{sT_d}{1 + sT_d/N}\right)$$

$$C = K\left(1 + \frac{1}{sT_i}\right)\left(\frac{1 + sT_d}{1 + sT_d/N}\right)$$

$N \approx 10$

Noise filtering in PID controllers

Proposed solution:

$$C = K\left(1 + \frac{1}{sT_i} + sT_d\right)$$

$$C = K\left(1 + \frac{1}{sT_i}\right)(1 + sT_d)$$

and

$$F_y = \frac{1}{1 + sT_f} \quad \text{or} \quad F_y = \frac{1}{1 + sT_f + s^2T_f^2/2}$$

Use at least first order filter for PI and second order for PID

Process output filter F_y

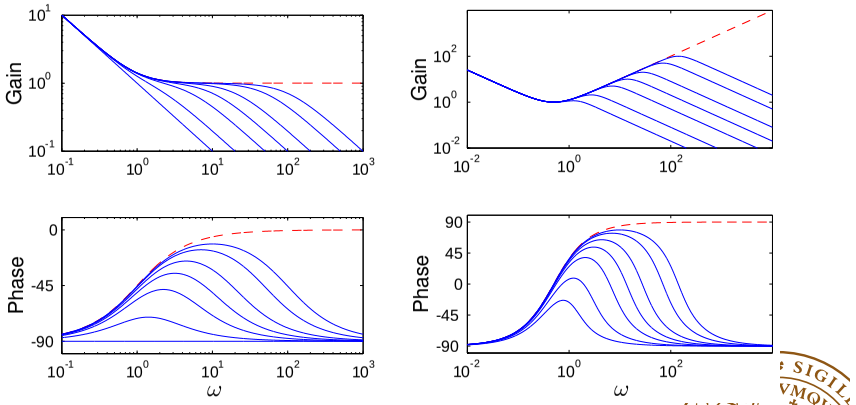

Process output filter F_y

In most cases, the filter will influence the performance.

The filter design should be included in the PID controller design.

The trade-off

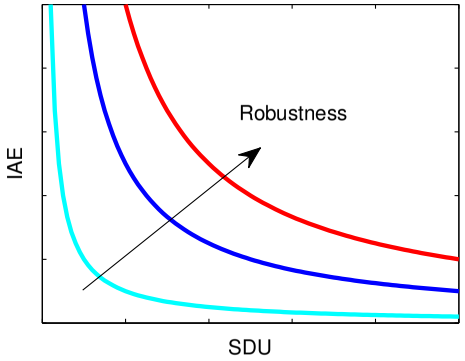

The trade-off

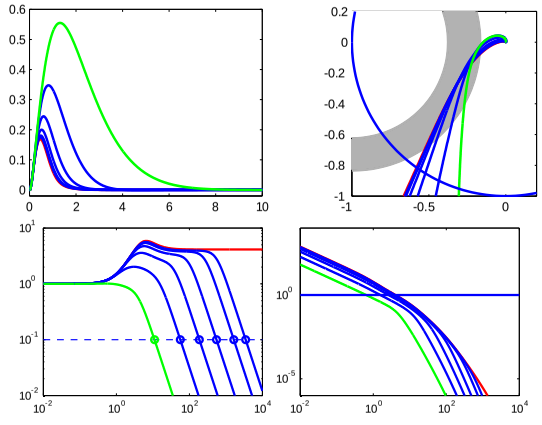

Design principle

Choose T_f as large as possible, keeping robustness and not reducing performance too much.

Filter design PI

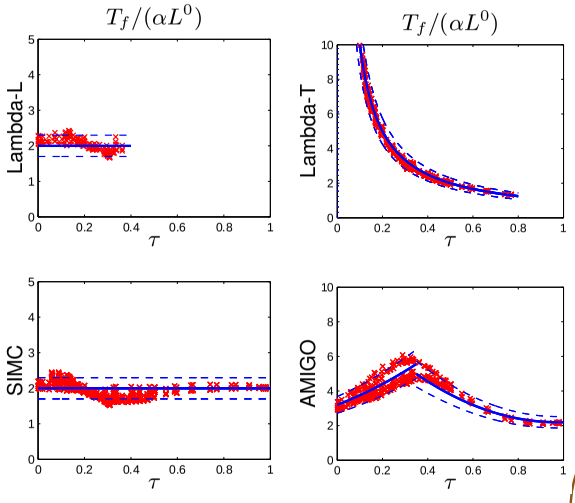

Filter design PID

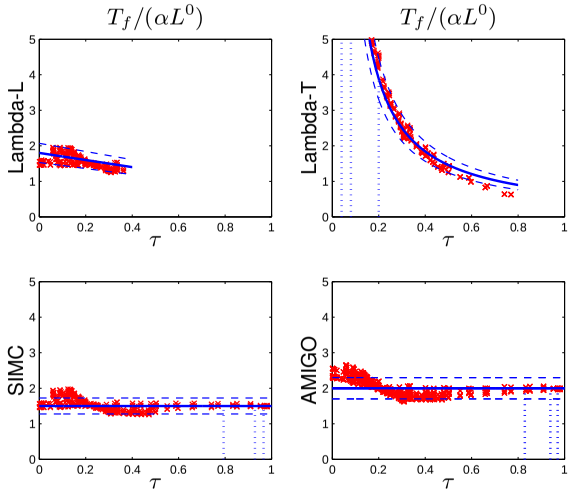

Tuning rules

PI Control			
	T_{cl}	$T_f/(\alpha L^0)$	Remark
Lambda	L T	2 $1/\tau$	no integrating processes
SIMC	L	2	whole Test Batch
AMIGO		$5\tau^2 + 5\tau + 3.2$, for $\tau < 0.35$ $7.2\tau^2 - 14\tau + 9$, for $\tau \geq 0.35$	whole Test Batch

PID Control			
	T_{cl}	$T_f/(\alpha L^0)$	Remark
Lambda	L T	$1.8 - \tau$ $0.7/(\tau - 0.02)$	no integrating processes
SIMC	$L/2$	1.5	no integrating processes
AMIGO		2	whole Test Batch

Added dynamics

$$P_f(s) = \frac{K}{1 + s(T + T_a)} e^{-s(L+L_a)}$$

$$L_a = (1 - 0.65\tau^8)T_f, \qquad T_a = 1.1\tau^8 T_f$$

The complete procedure

1. Determine an FOTD model
2. Determine T_f
3. Update the FOTD model by adding filter dynamics
4. Usa a tuning rule to find K, T_i, and T_d

PID: Past, Present and Perspectives

1. What is a PID controller?
2. How is it used?
3. The basic feedback loop
4. PID controller design
5. Common tuning rules
6. Design of noise filter
7. Automatic tuning

Automatic tuning

When a controller is to be tuned, the following tasks are performed:

1. Disturb the process.
2. Derive a process model.
3. Determine controller parameters based on the model.

Automatic tuning:

An aid where these tasks are performed automatically.

Automatic tuning

Many methods were developed and implemented in the 80ies, when the controllers went computer based.

Developed with the computation power and the knowledge about PID controller design available at that time.

Automatic tuning - Step response approaches

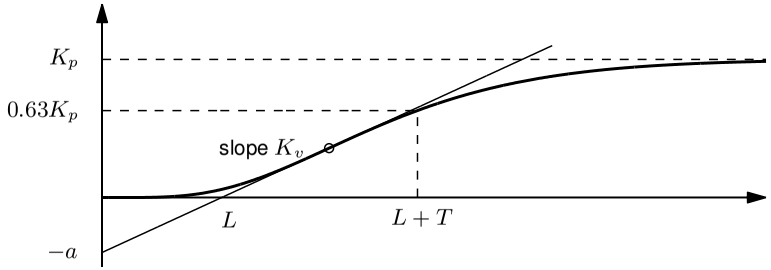

Problem: How large step in u? How long should we wait?

The relay method

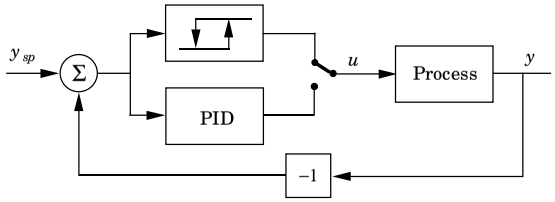

The relay method – symmetric relay

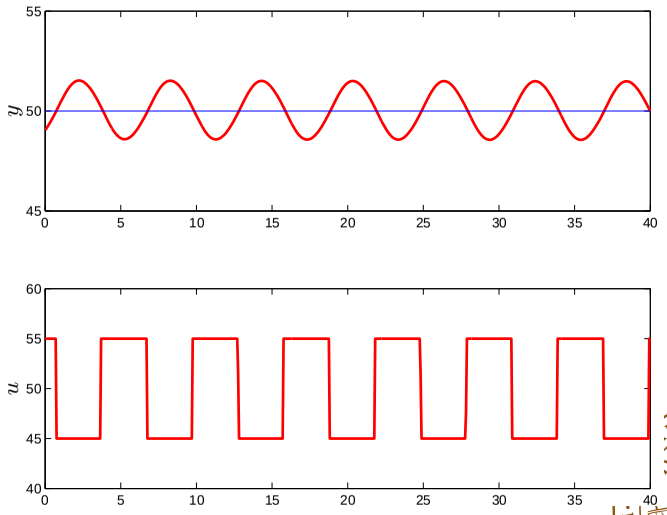

The relay method

Problem: Gives only one frequency point, corresponding to two parameters.

We need three parameters (e.g. K_p, L, T) to tune a PI controller, and would like to have four parameters to tune a PID.

The relay method – unsymmetric relay

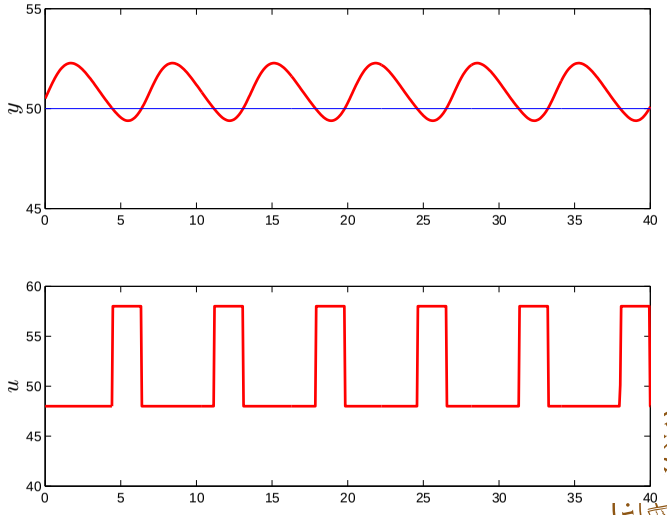

Conclusions

- PID is the basic component in process control.
- Tuning a PID controller is complicated. There are many aspects to take into account.
- We are close to design procedures that take all aspects into account and that finds K, T_i, T_d, and T_f.
- Automatic tuning is the final solution.

Plenary: P2 **Les Arcades**

Dynamics and control of particulate processes

Achim Kienle

Chair: Filip Logist **Wednesday, 11.30–12.30**

Particulate products like crystals, granules, powders play a major role in process industries. Typical examples are pharmaceuticals, detergents, pigments, polymers etc. They represent about 60% of the produced value in the chemical industry. Typical production processes comprise crystallization, granulation, polymerization etc. Function and effectiveness of particulate products often depend on particle properties - such as size, porosity, morphology or composition. Main objective of our research in this field of application is to devise new methods and tools for modeling and control of particulate processes aiming at adjustment of desired product properties.

This is a challenging issue due to nonuniformity of particle systems, where particles differ with respect to individual properties, and product properties are represented by the collective behavior of the particle population. From the theoretical point of view particulate processes belong to a special class of distributed parameter systems, so called population balance systems. They are described by nonlinear partial differential equations often coupled to integro differential equations describing the surrounding medium.

The talk will address main challenges for modeling and control of particulate processes and present some solution approaches developed in our group in recent years. Theoretical concepts will be illustrated with practical application examples including crystallization and granulation processes.

Plenary: P3 **Les Arcades**

System identification in dynamic networks

Paul M.J. Van den Hof

Chair: Ivan Markovsky **Thursday, 11.30–12.30**

In current day systems and control research, as well as in technology development, distributed (control) systems play an important role. The systems to be controlled are no longer characterized by a single or multiple control loop, but a network structure underlies the dynamical interaction between several subsystems. In system identification the classical configuration is to consider open-loop or closed-loop systems. In this work we are going to explore the extensions of these configurations towards linear dynamic network structures, and we will discuss the several questions that this step yields. We generalize the classical closed-loop identification methods to deal with identification problems of particular modules in a network, and use tools from graph theory to verify the structural conditions. We discuss options of input/sensor selection, and assess the problems of introducing measurement noise in measured variables, handling the so-called errors-in-variables problem. In a dynamic network setting this latter problem will appear to be more easily solvable than in the classical closed-loop configuration. Finally we discuss options for identifying the structure/topology of a dynamic network.

List of Participants

Francesco Acciani
UTwente
Netherlands
f.acciani@gmx.com

Oscar Mauricio Agudelo
KU Leuven
Belgium
mauricio.agudelo@esat.kuleuven.be

Farid Alavi
TU Delft
Netherlands
f.alavi@tudelft.nl

Desti Alkano
Rijksuniversiteit Groningen
Netherlands
d.alkano@rug.nl

Duarte Antunes
TU Eindhoven
Netherlands
d.antunes@tue.nl

Behnam Asadi Khashooei
TU Eindhoven
Netherlands
B.Asadi.Khashooei@tue.nl

Nikolaos Athanasopoulos
Université catholique de Louvain
Belgium
nikolaos.athanasopoulos@uclouvain.be

Ahmad Alrianes Bachnas
TU Eindhoven
Netherlands
a.a.bachnas@tue.nl

Ruud Beerens
TU Eindhoven
Netherlands
r.beerens@student.tue.nl

Michiel Beijen
TU Eindhoven
Netherlands
M.A.Beijen@tue.nl

Benjamin Biemond
KU Leuven
Belgium
benjamin.biemond@cs.kuleuven.be

Georgios Birpoutsoukis
Vrije Universiteit Brussel
Belgium
Georgios.Birpoutsoukis@vub.ac.be

Lennart Blanken
TU Eindhoven
Netherlands
l.l.g.blanken@student.tue.nl

Thomas Blanken
TU Eindhoven
Netherlands
t.c.blanken@tue.nl

Ruxandra Valentina Bobiti
TU Eindhoven
Netherlands
r.v.bobiti@tue.nl

Jan Bontsema
Wageningen UR
Netherlands
jan.bontsema@wur.nl

Niek Borgers
TU Eindhoven
Netherlands
d.p.borgers@tue.nl

Martijn Boussé
KU Leuven
Belgium
martijn.bousse@esat.kuleuven.be

Piet Bronders
Vrije Universiteit Brussel
Belgium
pbronder@vub.ac.be

Rully Cahyono
Rijksuniversiteit Groningen
Netherlands
r.tri.cahyono@rug.nl

Isaac Topiltzin Castanedo Guerra
TU Eindhoven
Netherlands
i.t.castanedo.guerra@tue.nl

Luis Daniel Cauto
Université Libre de Bruxelles
Belgium
luis.daniel.couto.mendonca@ulb.ac.be

Handian Chen
TU Eindhoven
Netherlands
h.chen2@tue.nl

Xiaodong Cheng
Rijksuniversiteit Groningen
Netherlands
x.cheng@rug.nl

Amelie Chevalier
Ghent University
Belgium
amelie.chevalier@ugent.be

Pierre-Yves Chevalier
Université catholique de Louvain
Belgium
pierre-yves.chevalier@uclouvain.be

Adam Cooman
Vrije Universiteit Brussel
Belgium
acooman@vub.ac.be

Cosmin Copot
Ghent University
Belgium
cosmin.copot@ugent.be

Dana Copot
Ghent University
Belgium
dana.copot@ugent.be

Pepijn Cox
TU Eindhoven
Netherlands
p.b.cox@tue.nl

Péter Zoltán Csurcsia
Vrije Universiteit Brussel
Belgium
pcsurcsi@vub.ac.be

Alexander De Cock
Vrije Universiteit Brussel
Belgium
adecock@vub.ac.be

Robin De Keyser
Ghent University
Belgium
Robain.DeKeyser@UGent.be

Bart De Moor
KU Leuven
Belgium
bart.demoor@esat.kuleuven.be

Otto Debals
KU Leuven Kulak
Belgium
otto.debals@esat.kuleuven.be

Frederik Debrouwere
KU Leuven
Belgium
frederik.debrouwere@kuleuven.be

Adeline Decuyper
Université catholique de Louvain
Belgium
adeline.decuyper@uclouvain.be

Jeremy Dehaye
UNamur
Belgium
jeremy.dehaye@unamur.be

Jonathan Dehaye
UNamur
Belgium
jonathan.dehaye@unamur.be

Jean-Charles Delvenne
Université catholique de Louvain
Belgium
jean-charles.delvenne@uclouvain.be

Mamadou Aliou Diallo
Université Libre de Bruxelles
Belgium
mamadoualiou.diallo27@yahoo.com

Alina Doban
TU Eindhoven
Netherlands
a.i.doban@tue.nl

Victor Dolk
TU Eindhoven
Netherlands
V.S.Dolk@tue.nl

Tijs Donkers
TU Eindhoven
Netherlands
m.c.f.donkers@tue.nl

Martijn Dresscher
Rijksuniversiteit Groningen
Netherlands
m.dresscher@rug.nl

Jacob Engwerda
Tilburg University
Netherlands
engwerda@uvt.nl

Anneroos Everts
Rijksuniversiteit Groningen
Netherlands
a.r.f.everts@rug.nl

Alireza Fakhrizadeh Esfahani
Vrije Universiteit Brussel
Belgium
alireza.fakhrizadeh.esfahani@vub.ac.be

Federico Felici
TU Eindhoven
Netherlands
f.felici@tue.nl

Shuai Feng
Rijksuniversiteit Groningen
Netherlands
s.feng@rug.nl

Sofia Fernandes de Sousa
UMons
Belgium
sofia.afonsofernandes@umons.ac.be

Paolo Frasca
UTwente
Netherlands
p.frasca@utwente.nl

Anqi Fu
TU Delft
Netherlands
A.Fu-1@tudelft.nl

Rolf Gaasbeek
TU Eindhoven
Netherlands
R.I.Gaasbeek@tue.nl

Hector Garcia de Marina
Rijksuniversiteit Groningen
Netherlands
hgdemarina@gmail.com

Emanuele Garone
Université Libre de Bruxelles
Belgium
egarone@ulb.ac.be

Egon Geerardyn
Vrije Universiteit Brussel
Belgium
egon.geerardyn@vub.ac.be

Matthieu Genicot
Université catholique de Louvain
Belgium
matthieu.genicot@uclouvain.be

Balazs Gerencser
Université catholique de Louvain
Belgium
balazs.gerencser@uclouvain.be

Geert Gins
KU Leuven
Belgium
geert.gins@cit.kuleuven.be

Giannina Giovannini
UMons
Belgium
giannina.giovannini@gmail.com

François Gonze
Université catholique de Louvain
Belgium
francois.gonze@uclouvain.be

Jan Goos
Vrije Universiteit Brussel
Belgium
jan.goos@vub.ac.be

Jonathan Grimard
UMons
Belgium
Jonathan.GRIMARD@umons.ac.be

Martin Gueuning
UNamur & Université catholique de Louvain
Belgium
martin.gueuning@unamur.be

Michel Habets
TU Eindhoven
Netherlands
m.b.i.habets@tue.nl

Sofie Haesaert
TU Eindhoven
Netherlands
s.haesaert@tue.nl

Tore Hägglund
Lund University
Sweden
tore@control.lth.se

Jurre Hanema
TU Eindhoven
Netherlands
j.hanema@tue.nl

Jingjing Hao
Université Libre de Bruxelles
Belgium
jinghao@ulb.ac.be

Maurice Heemels
TU Eindhoven
Netherlands
m.heemels@tue.nl

Hans Hellendoorn
TU Delft
Netherlands
j.hellendoorn@tudelft.nl

Julien Hendrickx
Université catholique de Louvain
Belgium
julien.hendrickx@uclouvain.be

Gabriel Hollander
Vrije Universiteit Brussel
Belgium
gabriel.hollander@vub.ac.be

Romain Hollanders
Université catholique de Louvain
Belgium
romain.hollanders@uclouvain.be

Jie Huang
Rijksuniversiteit Groningen
Netherlands
autohuangjie@gmail.com

Wen Huang
Université catholique de Louvain
Belgium
wen.huang@uclouvain.be

Edwin Insuasty
TU Eindhoven
Netherlands
e.g.insuasty.moreno@tue.nl

Clara Ionescu
Ghent University
Belgium
claramihaela.ionescu@ugent.be

Franck Iutzeler
Université catholique de Louvain
Belgium
franck.iutzeler@uclouvain.be

Bayu Jayawardhana
Rijksuniversiteit Groningen
Netherlands
b.jayawardhana@rug.nl

Hidde-Jan Jongsma
Rijksuniversiteit Groningen
Netherlands
h.jongsma@rug.nl

Monika Jozsa
Rijksuniversiteit Groningen
Netherlands
m.jozsa@rug.nl

Raphael Jungers
Université catholique de Louvain
Belgium
raphael.jungers@uclouvain.be

Iurii Kapitaniuk
Rijksuniversiteit Groningen
Netherlands
i.kapitaniuk@rug.nl

Yanin Kasemsinsup
TU Eindhoven
Netherlands
y.kasemsinsup@tue.nl

Achim Kienle
Otto von Guericke University Magdeburg
Germany
achim.kienle@ovgu.de

Michel Kinnaert
Université Libre de Bruxelles
Belgium
pascale.lathouwers@ulb.ac.be

Nikolaos Kontaras
TU Eindhoven
Netherlands
n.kontaras@tue.nl

John Lataire
Vrije Universiteit Brussel
Belgium
jlataire@vub.ac.be

Vladimir Lazov
Vrije Universiteit Brussel
Belgium
vladimir.lazov@vub.ac.be

Filip Logist
KU Leuven
Belgium
filip.logist@cit.kuleuven.be

Xi Luo
TU Eindhoven
Netherlands
x.luo@tue.nl

Thoa Mac
Ghent University
Belgium
Thoa.MacThi@UGent.be

Hannes Maes
Vrije Universiteit Brussel
Belgium
hlmaes@vub.ac.be

Anna Marconato
Vrije Universiteit Brussel
Belgium
anna.marconato@vub.ac.be

Ivan Markovsky
Vrije Universiteit Brussel
Belgium
ivan.markovsky@vub.ac.be

Mayank Mayank
Vrije Universiteit Brussel
Belgium
mayank@vub.ac.be

Noorma Yulia Megawati
Rijksuniversiteit Groningen
Netherlands
n.y.megawati@rug.nl

Tim Mercy
KU Leuven
Belgium
tim.mercy@kuleuven.be

Ruben Merks
TU Eindhoven
Netherlands
r.w.h.merks@student.tue.nl

Khadija Mhallem Gziri
Université Libre de Bruxelles
Belgium
kmhallem@ulb.ac.be

Wim Michiels
KU Leuven
Belgium
Wim.Michiels@cs.kuleuven.be

Nima Monshizadeh
Rijksuniversiteit Groningen
Netherlands
n.monshizadeh@rug.nl

Pooya Monshizadeh
Rijksuniversiteit Groningen
Netherlands
p.monshizadeh@rug.nl

Sikandar Moten
KU Leuven
Belgium
sikandar.moten@kuleuven.be

D.B. Nguyen
Rijksuniversiteit Groningen
Netherlands
d.b.nguyen@rug.nl

Le Ha Vy Nguyen
UNamur
Belgium
le-ha-vy.nguyen@unamur.be

Tam Nguyen
Université Libre de Bruxelles
Belgium
tam.nguyen@ulb.ac.be

Marco Nicotra
Université Libre de Bruxelles
Belgium
marco.maria.nicotra@ulb.ac.be

Jean-Philippe Noel
Vrije Universiteit Brussel
Belgium
jp.noel@ulg.ac.be

Tom Oomen
TU Eindhoven
Netherlands
t.a.e.oomen@tue.nl

Leyla Ozkan
TU Eindhoven
Netherlands
l.ozkan@tue.nl

Matthew Philippe
Université catholique de Louvain
Belgium
matthew.philippe@uclouvain.be

Dan Pilbauer
KU Leuven
Belgium
dan.pilbauer@cs.kuleuven.be

Rik Pintelon
Vrije Universiteit Brussel
Belgium
Rik.Pintelon@vub.ac.be

Goele Pipeleers
KU Leuven
Belgium
goele.pipeleers@kuleuven.be

Anton Proskurnikov
Rijksuniversiteit Groningen
Netherlands
avp1982@gmail.com

Yiwen Qi
Rijksuniversiteit Groningen
Netherlands
y.qi@rug.nl

Pouria Ramazi
Rijksuniversiteit Groningen
Netherlands
p.ramazi@gmail.com

Rishi Relan
Vrije Universiteit Brussel
Belgium
rishi.relan@vub.ac.be

Emilie Renard
Université catholique de Louvain
Belgium
emilie.renard@uclouvain.be

Michel Reniers
TU Eindhoven
Netherlands
M.A.Reniers@tue.nl

Rodolfo Reyes Baez
Rijksuniversiteit Groningen
Netherlands
r.reyes-baez@rug.nl

Anne Richelle
Université Libre de Bruxelles
Belgium
arichell@ulb.ac.be

James Riehl
Rijksuniversiteit Groningen
Netherlands
j.r.riehl@rug.nl

Mark Rijnen
TU Eindhoven
Netherlands
m.w.l.m.rijnen@tue.nl

Muhammad Zakiyullah Romdlony
Rijksuniversiteit Groningen
Netherlands
m.z.romdlony@rug.nl

Constantijn Romijn
TU Eindhoven
Netherlands
t.c.j.romijn@tue.nl

Wilbert Samuel Rossi
UTwente
Netherlands
w.s.rossi@utwente.nl

Alessandro Saccon
TU Eindhoven
Netherlands
a.saccon@tue.nl

Bahadir Saltik
TU Eindhoven
Netherlands
m.b.saltik@tue.nl

Michael Schaub
Université catholique de Louvain
Belgium
michael.schaub@uclouvain.be

Jacquelien Scherpen
Rijksuniversiteit Groningen
Netherlands
j.m.a.scherpen@rug.nl

Tjardo Scholten
Rijksuniversiteit Groningen
Netherlands
t.w.scholten@rug.nl

Julien Schorsch
Université Libre de Bruxelles
Belgium
julien.schorsch@ulb.ac.be

Johan Schoukens
Vrije Universiteit Brussel
Belgium
johan.schoukens@vub.ac.be

Daniel Senejohnny
Rijksuniversiteit Groningen
Netherlands
d.senejohnny@gmail.com

Muhammad Mohsin Siraj
TU Eindhoven
Netherlands
m.m.siraj@tue.nl

Paul Smyth
KU Leuven
Belgium
paul.smyth@esat.kuleuven.be

Tong Duy Son
KU Leuven
Belgium
tong.duyson@kuleuven.be

Maarten Steinbuch
TU Eindhoven
Netherlands
m.steinbuch@tue.nl

Armin Steinhauser
KU Leuven
Belgium
jan.swevers@kuleuven.be

Julian Stoev
Flanders Make
Belgium
julian.stoev@flandersmake.be

Zhou Su
TU Delft
Netherlands
z.su-1@tudelft.nl

Jan Swevers
KU Leuven
Belgium
jan.swevers@mech.kuleuven.be

Hadi Taghvafard
Rijksuniversiteit Groningen
Netherlands
taghvafard@gmail.com

Adrien Taylor
Université catholique de Louvain
Belgium
adrien.taylor@uclouvain.be

Koen Tiels
Vrije Universiteit Brussel
Belgium
koen.tiels@vub.ac.be

Roland Tóth
TU Eindhoven
Netherlands
r.toth@tue.nl

Maguy Trefois
Université catholique de Louvain
Belgium
maguy.trefois@uclouvain.be

Sebastian Trip
Rijksuniversiteit Groningen
Netherlands
s.trip@rug.nl

Dora Turk
KU Leuven
Belgium
dora.turk@mech.kuleuven.be

Mark Vaes
Vrije Universiteit Brussel
Belgium
mark.vaes@vub.ac.be

Peter van Beveren
Wageningen UR
Netherlands
peter.vanbeveren@wur.nl

Tobias Van Damme
Rijksuniversiteit Groningen
Netherlands
t.van.damme@rug.nl

Paul Van den Hof
TU Eindhoven
Netherlands
p.m.j.vandenhof@tue.nl

Rick van der Maas
TU Eindhoven
Netherlands
R.J.R.v.d.Maas@tue.nl

Paul Van Dooren
Université catholique de Louvain
Belgium
paul.vandooren@uclouvain.be

Niels van Duijkeren
KU Leuven
Belgium
niels.vanduijkeren@kuleuven.be

Frederik Van Eeghem
KU Leuven Kulak
Belgium
frederik.vaneeghem@kuleuven.be

Eelco van Horssen
TU Eindhoven
Netherlands
e.p.v.horssen@tue.nl

Wannes Van Loock
KU Leuven
Belgium
wannes.vanloock@kuleuven.be

Evi Van Nechel
Vrije Universiteit Brussel
Belgium
evi.van.nechel@vub.ac.be

Ruben Van Parys
KU Leuven
Belgium
ruben.vanparys@kuleuven.be

L. Gerard van Willigenburg
Wageningen UR
Netherlands
gerard.vanwilligenburg@wur.nl

Jurgen van Zundert
TU Eindhoven
Netherlands
j.c.d.v.zundert@tue.nl

Corentin Vande Kerckove
Université catholique de Louvain
Belgium
corentin.vandekerckhove@uclouvain.be

Antoine Vandermeersch
KU Leuven
Belgium
Antoine.Vandermeersch@esat.kuleuven.be

Maarten Verbandt
KU Leuven
Belgium
maarten.verbandt@kuleuven.be

Dieter Verbeke
Vrije Universiteit Brussel
Belgium
dieter.verbeke@vub.ac.be

Joachim Verhelst
KU Leuven R&D
Belgium
joachim.verhelst@kuleuven.be

Koen Verkerk
TU Eindhoven
Netherlands
k.w.verkerk@tue.nl

Robbert Voorhoeve
TU Eindhoven
Netherlands
r.j.voorhoeve@tue.nl

Xin Wang
KU Leuven
Belgium
xin.wang@mech.kuleuven.be

Harm Weerts
TU Eindhoven
Netherlands
h.h.m.weerts@tue.nl

Jieqiang Wei
Rijksuniversiteit Groningen
Netherlands
jieqiang.wei@gmail.com

Erik Weitenberg
Rijksuniversiteit Groningen
Netherlands
e.r.a.weitenberg@rug.nl

Joseph Winkin
UNamur
Belgium
joseph.winkin@unamur.be

Sam Wuyts
KU Leuven
Belgium
sam.wuyts@cit.kuleuven.be

Quan Xu
Rijksuniversiteit Groningen
Netherlands
xuquan223@hotmail.com

Hitoshi Yanami
Fujitsu Ltd.
Japan
yanami@jp.fujitsu.com

Shuai Yuan
TU Delft
Netherlands
s.yuan-1@tudelft.nl

Maral Zyari
Vrije Universiteit Brussel
Belgium
mzyari@vub.ac.be

Organizational Comments

Welcome

The Organizing Committee has the pleasure of welcoming you to the *34^{th} Benelux Meeting on Systems and Control*, at Center Parcs De Vossemeren in Lommel, Belgium.

Aim

The aim of the Benelux Meeting is to promote research activities and to enhance cooperation between researchers in Systems and Control. This is the thirty-fourth in a series of annual conferences that are held alternately in Belgium and The Netherlands.

Scientific Program Overview

1. Plenary lecture by *Tore Hägglund* (Lund University, Sweden) on **PID: Past, present and perspectives**.
2. Plenary lecture by *Achim Kienle* (Max Planck Institute for Dynamics of Complex Technical Systems, Germany) on **Dynamics and control of particulate processes**.
3. Plenary lecture by *Paul Van den Hof* (Eindhoven University of Technology, The Netherlands) on **System identification in dynamic networks**.
4. Contributed short lectures. See the list of sessions for the titles and authors of these lectures.
5. Meet-the-Experts sessions, providing an informal atmosphere where early-stage PhD students can interact with experts who will give their undivided attention for research advice and networking.

Directions for speakers

For a contributed lecture, the available time is 25 minutes. Please leave a few minutes for discussion and room changes, and adhere to the indicated schedule. In each room beamers are available. *When using a beamer, you have to provide a notebook yourself and you have to start your lecture with the notebook up and running and the external video port switched on.*

Registration

The Benelux Meeting registration desk, located in the foyer of the business center, will be open on Tuesday, March 24, from 09:00 to 12:30. Late registrations can be made at the Benelux Meeting registration desk, when space is still available. The on-site fee schedule is:

Arrangement	Price (EUR)
hotel room	580
2-room cottage	550
3-room cottage	520
meals only	500
one day	350

The registration fees include:

- Admission to all sessions.
- A copy of the Conference Booklet.
- Coffee, tea and water during the breaks.
- In the case of a three days arrangement: lunch and dinner on Tuesday; breakfast, lunch, and dinner on Wednesday; and breakfast and lunch on Thursday.
- In the case of a one day arrangement: lunch and dinner on Tuesday or Wednesday, or lunch on Thursday.
- Free use of a wireless internet connection (WiFi) in each cottage.

The registration fee does *not* include:

- Cost of phone calls
- Special ordered drinks during breakfast, lunch, dinner, in the evening, etc.

Organization

The Organizing Committee of the 34^{th} Benelux Meeting consists of

O.M. Agudelo Manozca
KU Leuven
E-mail: mauricio.agudelo@esat.kuleuven.be

A. Chevalier
Universiteit Gent
E-mail: amelie.chevalier@ugent.be

B. De Moor
KU Leuven
Email: bart.demoor@esat.kuleuven.be

G. Gins
KU Leuven
Email: geert.gins@cit.kuleuven.be

C. Ionescu
Universiteit Gent
E-mail: claramihaela.ionescu@ugent.be

F. Logist
KU Leuven
filip.logist@cit.kuleuven.be

I. Markovsky
Vrije Universiteit Brussel
ivan.markovsky@vub.ac.be

W. Michiels
KU Leuven
wim.michiels@cs.kuleuven.be

G. Pipeleers
KU Leuven
goele.pipeleers@kuleuven.be

W. Van Loock
KU Leuven
wannes.vanloock@kuleuven.be

Sponsor

The meeting is supported by the Research Foundation Flanders (FWO).

Conference location

The lecture rooms of Center Parcs De Vossemeren are situated on the ground floor. Consult the map at the end of this booklet to locate rooms. During the breaks, coffee and tea will be served in the foyer. Announcements and personal messages will be posted near the main conference room. Accommodation is provided in the conference center and in the cottages. Room/Cottage keys can be picked up at lunch time on the first day and need to be returned before 10:00 on the day of departure. Parking is free of charge.

The address of Center Parcs De Vossemeren is

Elzen 145
3920 Lommel
Belgium
T +32 (0)11 54 82 00

Facilities

The facilities at the center include a restaurant, bar, and recreation/sports facilities. You can refer to the reception desk of the center for detailed information about the use of these facilities.

Breakfast will be served in the "Evergreenz Restaurant", from 7:00 until 9:00. Lunches take place in the "Evergreenz Restaurant", from 12:30 until 14:00. The dinner on Tuesday takes place in the "Evergreenz Restaurant", from 19:00 until 21:00. The dinner on Wednesday takes place in the "Fuego Restaurant", from 19:00 until 21:00.

Best junior presentation award

Continuing a tradition that started in 1996, the 34^{th} Benelux Meeting will close with the announcement of the winner of the Best Junior Presentation Award. This award is given for the best presentation, given by a junior researcher, and it consists of a trophy that may be kept for one year and a certificate. The award is specifically given for quality of presentation rather than quality of research, which is judged in a different way. At the meeting, the chairs of sessions will ask three volunteers in the audience to fill out an evaluation form. After the session, the evaluation forms will be collected by the Prize Commissioners who will then compute a ranking. The winner will be announced on Thursday, March 26, in room Les Arcades, at 14:20. The winner is the candidate with the highest evaluation score among all candidates present at the prize ceremony. He or she will be presented the award, which consists of a trophy that may be kept for one year, and also a certificate. He or she will give the winning presentation once more at the end of the ceremony. The evaluation forms of each presentation will be returned to the junior researcher who gave the presentation. The Prize Commissioners are Jean-Charles Delvenne (Université catholique de Louvain), Paolo Frasca (University of Twente) and John Lataire (Vrije Universiteit Brussel).

The organizing committee counts on the cooperation of the participants to make this contest a success.

DISC certificates and best thesis award

The ceremony for the distribution of the DISC certificates and for the Best Thesis Award will be held on Thursday, March 26, room Les Arcades, 14:00–14:20.

Website

An *electronic version* of the Book of Abstracts can be downloaded from the Benelux Meeting web site.

Tuesday March 24, 2014

11:25 – 11:30	P0 Les Arcades *Welcome and Opening*			
11:30 – 12:30	P1 Les Arcades *PID: Past, present and perspectives* Tore Hägglund			
12:30 – 14:00	Lunch			
Room	Les Arcades *Optimization I*	Emanuel *Mechanical Engineering I*	Impressario *Identification I*	Bloemen *Model Reduction*
14:00 – 14:25	Taylor	Romdlony	Verbeke	Jongsma
14:25 – 14:50	Huang	Chevalier	Darwish	Verkerk
14:50 – 15:15	Trefois	Trip	Hollander	Schaub
15:15 – 15:40	Iutzeler	Couto	Weerts	Giovannini
15:40 – 16:05	Telsang	Kapitaniuk	Noël	van Mourik
16:05 – 16:30	Break			
Room	Les Arcades *Games & Agents I*	Emanuel *Biochemical Engineering*	Impressario *Identification II*	Bloemen *Control I*
16:30 – 16:55	Senejohnny	Richelle	Csurcsia	Doban
16:55 – 17:20	Gueuning	Fernandes	Voorhoeve	Proskurnikov
17:20 – 17:45	Su	Gziri	Vaes	Biemond
17:45 – 18:10	Gonze	Nimmegeers	Nguyen	Borgers
18:10 – 18:35	Riehl	Taghvafard	Boussé	Bobiti
18:35 – 19:00	Les Arcades *Meet the Experts: Session I* Tore Hägglund, Achim Kienle, Jaqueline Scherpen, Robain De Keyser, Julien Hendrickx, Pierre-Antoine Absil, Rik Pintelon, Johan Schoukens, Maarten Steinbuch			
19:00 – 21:00	Dinner			

Wednesday March 25, 2014

Room	Les Arcades *Optimization II*	Emanuel *MPC*	Impressario *Identification III*	Bloemen *Systems Theory I*	Seaside *Control Applications I*
09:00 – 09:25	Hollanders	Bachnas	Guerra	Van Eeghem	Alkano
09:25 – 09:50	Gerencsér	Rostampour	De Cock	Markovsky	Siraj
09:50 – 10:15	Feng	Nguyen	Van Loock	Debals	Van Parys
10:15 – 10:40	Van Willigenburg	Wang	Scholten	Potters	Yanami
10:40 – 11:05	Mehrkanoon	Hanema	Esfahani	Potters	Fernandes
11:30 – 12:30	P2 Les Arcades *Dynamics and control of particulate processes* Achim Kienle				
12:30 – 14:00	Lunch				
Room	Les Arcades *Control over Networks*	Emanuel *Optimal Control*	Impressario *Identification IV*	Bloemen *Identification V*	Seaside *Control Applications II*
14:00 – 14:25	Haesaert	Verbandt	Merks	Geerardyn	van Beveren
14:25 – 14:50	Romijn	Stoev	Bronders	Relan	Alavi
14:50 – 15:15	Saltik	Rijnen	Blanken	Gaasbeek	van Duijkeren
15:15 – 15:40	van Horssen	Mercy	Birpoutsoukis	Maes	Debrouwere
15:40 – 16:05	Khashooei	Nicotra	Stoev	Cooman	Megawati
16:05 – 16:30	Break				
Room	Les Arcades *Games & Agents II*	Emanuel *Mechanical Engineering II*	Impressario *Identification VI*	Bloemen *LPV*	Seaside *Nonlinear Control*
16:30 – 16:55	Koerts	Blanken	Habets	Goos	van der Maas
16:55 – 17:20	Vande Kerckhove	Mac Thi	Van Nechel	Schorsch	Monshizadeh
17:20 – 17:45	Ramazi	Beerens	Insuasty	Cox	Fu
17:45 – 18:10	Rossi	Beijen	Zyari	Turk	Barradas-Berglind
18:10 – 18:35	Smyth	van Zundert	Grimard	Lazov	Weitenberg
18:35 – 19:00	Les Arcades *Meet the Experts: Session II* Tore Hägglund, Achim Kienle, Paul Van den Hof, Michel Kinnaert, Julien Hendrickx, Paul Van Dooren, Pierre-Antoine Absil, Rik Pintelon, Johan Schoukens, Maarten Steinbuch				
19:00 – 21:00	Dinner				

Thursday March 26, 2014

Room	Les Arcades *Games & Agents III*	Emanuel *ILC & Adaptive Control*	Impressario *Identification VII*	Bloemen *Systems Theory II*	Seaside *Control II*
09:00 – 09:25	Wei	Tong Duy	Tiels	Vandermeersch	Pilbauer
09:25 – 09:50	Acciani	Yuan	Cahyono	Verhelst	Dehaye
09:50 – 10:15	Engwerda	Chen	Marconato	van der Woude	Wuyts
10:15 – 10:40	Chevalier	Moten	Copot	Philippe	Dolk
10:40 – 11:05	Garcia de Marina	Luo	Huang	Everts	Hao
11:30 – 12:30	P3 Les Arcades *System identification in dynamic networks* Paul M.J. Van den Hof				
12:30 – 14:00	Lunch				
14:00 – 14:20	Les Arcades *DISC Award Ceremony*				
14:20 – 14:55	Les Arcades *Best Junior Presentation Award*				

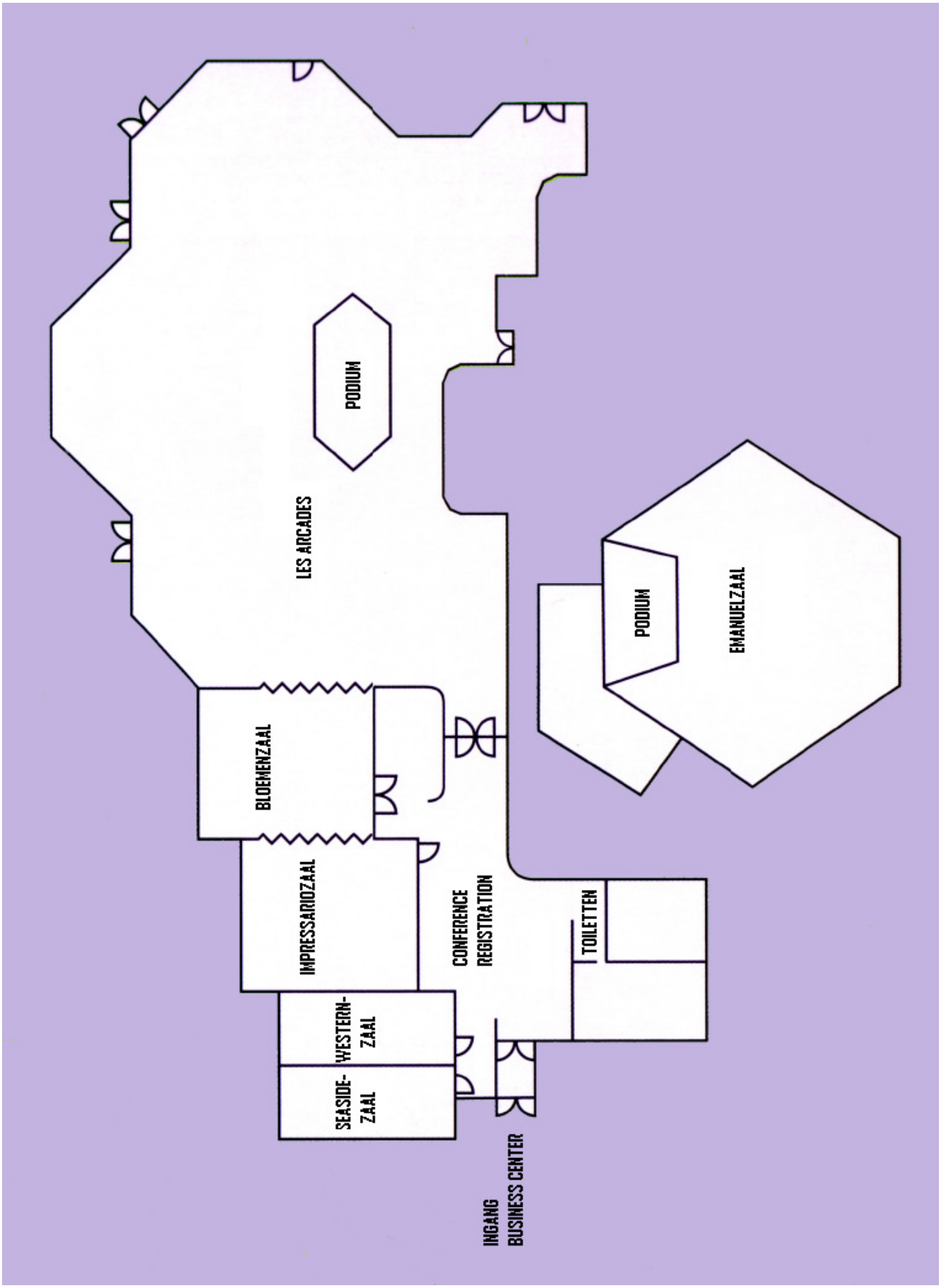
PODIUM
LES ARCADES
PODIUM
EMANUELZAAL
BLOEMENZAAL
IMPRESSARIOZAAL
CONFERENCE REGISTRATION
TOILETTEN
WESTERN-ZAAL
SEASIDE-ZAAL
INGANG BUSINESS CENTER